Terms and Conditions of Use of Digitised Theses from Trinity College Library Dublin

Copyright statement

All material supplied by Trinity College Library is protected by copyright (under the Copyright and Related Rights Act, 2000 as amended) and other relevant Intellectual Property Rights. By accessing and using a Digitised Thesis from Trinity College Library you acknowledge that all Intellectual Property Rights in any Works supplied are the sole and exclusive property of the copyright and/or other IPR holder. Specific copyright holders may not be explicitly identified. Use of materials from other sources within a thesis should not be construed as a claim over them.

A non-exclusive, non-transferable licence is hereby granted to those using or reproducing, in whole or in part, the material for valid purposes, providing the copyright owners are acknowledged using the normal conventions. Where specific permission to use material is required, this is identified and such permission must be sought from the copyright holder or agency cited.

Liability statement

By using a Digitised Thesis, I accept that Trinity College Dublin bears no legal responsibility for the accuracy, legality or comprehensiveness of materials contained within the thesis, and that Trinity College Dublin accepts no liability for indirect, consequential, or incidental, damages or losses arising from use of the thesis for whatever reason. Information located in a thesis may be subject to specific use constraints, details of which may not be explicitly described. It is the responsibility of potential and actual users to be aware of such constraints and to abide by them. By making use of material from a digitised thesis, you accept these copyright and disclaimer provisions. Where it is brought to the attention of Trinity College Library that there may be a breach of copyright or other restraint, it is the policy to withdraw or take down access to a thesis while the issue is being resolved.

Access Agreement

By using a Digitised Thesis from Trinity College Library you are bound by the following Terms & Conditions. Please read them carefully.

I have read and I understand the following statement: All material supplied via a Digitised Thesis from Trinity College Library is protected by copyright and other intellectual property rights, and duplication or sale of all or part of any of a thesis is not permitted, except that material may be duplicated by you for your research use or for educational purposes in electronic or print form providing the copyright owners are acknowledged using the normal conventions. You must obtain permission for any other use. Electronic or print copies may not be offered, whether for sale or otherwise to anyone. This copy has been supplied on the understanding that it is copyright material and that no quotation from the thesis may be published without proper acknowledgement.

Identification of *Schistosoma mansoni* adult male worm excretome-secretome and production of recombinant proteins with immunomodulatory potential

by

Julia Silveira Fahel

A Thesis Submitted to Trinity College Dublin in Partial Fulfilment of the Requirements for the Degree of Doctor in Philosophy in Clinical Medicine

Dublin, Ireland

2012

Declaration

I declare that the present work has not been submitted to Trinity College Dublin or any other institution as an exercise for a degree and it is entirely comprised of my own work except where references indicate otherwise. Trinity College Library may lend or copy this thesis upon request.

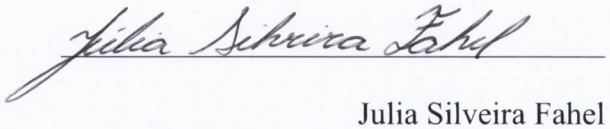

Julia Silveira Fahel

4th May, 2012

Acknowledgments

First and foremost, I am heartily thankful to my supervisor, Prof. Padraic Fallon, for his guidance and expert help throughout my Ph.D.

My deepest gratitude to Dr. Poom Adisakwatanna for all the practical advice and for sharing his own perspective on this work.

My sincerest gratitude to Dr. Antonio Alcami Pertejo and members of his group, in particular, Dr. Soledad Blanco Chapinal and Ms. Rocio Martin Hernandez, for their assistance during my training in the Centro de Biologia Molecular Severo Ochoa, Madrid – Spain.

I am very grateful to Dr. Henry Windle and Dr. William McCormac for kindly providing assistance whenever requested.

Many thanks to all the members, past and present, of the Fallon group, with whom I have had the pleasure to work.

My sincerest gratitude to my work colleagues and friends; Dr. Aoife Smyth, Dr. Caoimhe Fahy, Ms. Denise Triglia, Dr. Hendrik Nel, Dr. Marlies Fischer and Dr. Sylvie Amu for their encouragement and support throughout the course of this project.

Finally, I would like to thank my parents and my sisters, who are my greatest supporters in life.

Julia Silveira Fahel

Summary

Over two billion people worldwide are infected with helminth parasites. Helminths strongly modulate the host's immune response in order to establish a balanced parasite-host dynamic. This helminth-derived immunomodulatory response does not only favour the parasite and host survival but also interferes with non related diseases that may occur to the host during the infection (*1*). Molecules released by the worm into the host's blood circulation are the mostly likely to interact with immune cells therefoby mediating the immunomodulatory response. The aim of my Ph.D. is to identify and characterise immunomodulatory helminth-derived proteins. In this study, the human parasite *Schistosoma mansoni* was used as a model of a parasitic helminth that is a potent modulator of the immune system. It has been shown that single-sex infection with male schistosome, as opposed to bisex infection, protects mice from developing airway hyperresponsiveness and dextran sodim sulphate (DSS)-induced colitis (*2, 3*). Therefore, I have focused my work on the identification of adult male worm excreted-secreted (WES) molecules. Firstly, *S. mansoni* male worms were incubated *in vitro* for isolation of WES molecules. Subsequently, WES proteins were resolved by high-resolution two-dimensional electrophoresis and identified by mass spectrometry. Potential immunomodulatory candidates were selected based on sequence similarity with molecules of known modulatory activity. For characterization of the immunomodulatory candidates, recombinant proteins were generated in *E. coli* and baculovirus-insect cell system. Candidate proteins are currently being screened for immunomodulation and the molecules that have proven to be immunosuppressive will be further tested as novel immunotherapeutics in mouse models of inflammatory diseases.

Table of Contents

Chapter 1 - Introduction

Chapter 2 - Materials and Methods

Chapter 3 - Proteomic Analysis of *Schistosoma mansoni* Male Adult Worm Excretory-secretory Molecules

Chapter 4 - Cloning, Expression and Purification of *Schistosoma mansoni* Peroxiredoxin 1 and *Schistosoma mansoni* Thioredoxin

Chapter 5 - Cloning, Expression and Purification of *Schistosoma mansoni* Cyclophilin and *Schistosoma mansoni* Cyclophilin B

List of Figures

List of Tables

1 - Introduction

1.1 - Schistosome: a helminth parasite

Schistosomes are helminths of the genus *Schistosoma* (Phylum Platyhelminthes, Class Trematoda) that causes a parasitosis known as schistosomiasis, bilharzia or snail fever. The disease transmission requires contact with water contaminated by excreta and the presence of specific freshwater snails. Natural water reservoirs such as lakes and rivers, and man made reservoirs, such as irrigation systems, facilitate the spread of the disease (*1*). Poor communities without adequate sanitation and potable water are the most vulnerable to infections (*2*). The World Health Organization (WHO) considers schistosomiasis as a major public health problem. It strategically works on schistosomiasis as part of an integrated approach to the control of neglected tropical diseases (*3*).

The adult schistosomes have a cylindrical body 7 to 20 mm long with two terminal suckers. Unlike other trematodes, they are digenetic. The male's body forms a groove, named gynaecophoric channel, which holds the thinner and longer female (Figure 1.1). Schistosomes feed on blood and globulin through anaerobic glycolysis and regurgitate the debris back into the host's blood (*1*).

Figure 1.1: **Electron microscope image of male and female *S. mansoni.*** (Source: Davies, S J. July 4, 2005. Davies Laboratory - Uniformed Services University of the Health Sciences – Bethesda – MD. Retrieved August 30, 2011 from http://www.usuhs.mil/mic/Davies/Research.html).

1.1.1 - Global burden of schistosomiasis and human-infecting species

Schistosomiasis is endemic in 76 tropical and subtropical countries and territories worldwide (Figure 1.2). There are more than 207 million people infected and an estimated 779 million are at the risk of infection. Regarding the number of infected people and those at risk of infection, schistosomiasis ranks second among parasitic diseases, only behind malaria. The highest prevalence is in Africa which houses 97% of all infected individuals and 85% of the population is at risk of infection (*4*).

The human infecting schistosomes of greatest medical relevance are *S. haematobium, S. intercalatum, S. japonicum, S. mansoni* and *S. mekongi*. The *S. haematobium* adult worm populates the perivesicular veins of the host causing genitourinary schistosomiasis. The other species populate the host mesenteric veins causing hepatointestinal schistosomiasis. The geographical distribution of these species depends on the ecological niche of the freshwater snails they require for completion of the life cycle (Table 1.1) (*1, 5*).

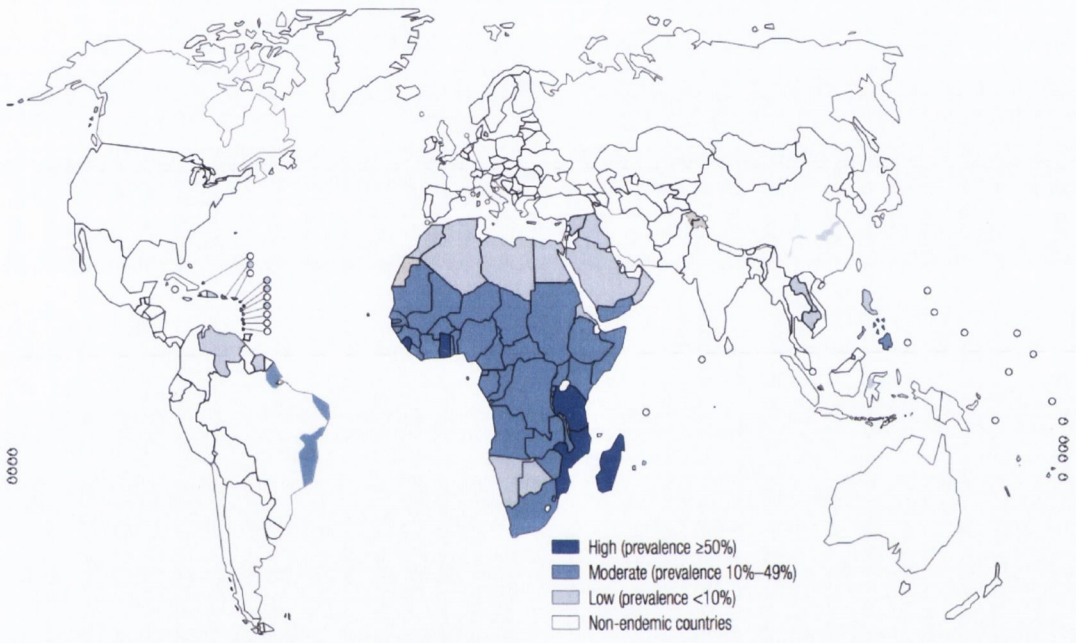

Figure 1.2: **Prevalence of schistosomiasis worldwide in 2009.** (Source: World Health Organization. 2010. Working to overcome the global impact of neglected tropical diseases. Retrieved August 30, 2011 from http://whqlibdoc.who.int/publications /2010/9789241564090_eng.pdf)

Geographical distribution of main human-infecting schistosomes and their freshwater snail hosts

Disease form	Schistosome species	Freshwater snail hosts	Geographical distribution
Hepatointestinal schistosomiasis	*Schistosoma mansoni*	*Biomphalaria spp.*	Africa, the Middle East, the Caribbean, Brazil, Venezuela, Suriname
	Schistosoma japonicum	*Oncomelania spp.*	China, Indonesia, the Philippines
	Schistosoma mekongi	*Neotricula spp.*	Several districts of Cambodia and the Lao People's Democratic Republic
	*Schistosoma intercalatum**	*Bulinus spp.*	Rain forest areas of central Africa
Genitourinary schistosomiasis	*Schistosoma haematobium*	*Bulinus spp.*	Africa, the Middle East

Table 1.1: **Geographical distribution of main human-infecting schistosomes and their freshwater snail hosts.** * *S. intercalatum* infection induces only mild intestinal disease. (Adapted from World Health Organization. February, 2010. Schistosomiasis Fact sheet N° 115. Retrieved August 30, 2011 from http://www.who.int/mediacentre/factsheets/fs115/en/index.html)

1.1.2 - Schistosome life cycle

Schistosomes have a complex life cycle (Figure 1.3). The cercarial larva is the infecting form. It has a characteristic bifurcated tail and actively penetrates the skin or mucosal surfaces of mammals (definitive hosts). This process and the subsequent migration into the host tissue are facilitated by the release of proteolytic enzymes from cercaria's glands (*6, 7*). During and after penetration, the larvae go through several morphological and biochemical alterations such as tail loss and development of acidic compartments. The resulting larvae, named schistosomulae, migrate through the host's subcutaneous tissue entering the blood vessels from where they are pushed by blood flow to the lungs (*8-10*).

From the lungs, the schistosomulae migrate, against the blood flow, to the portal vein. During 4 to 6 weeks they maturate into male or female adult worms and mate. As permanently embraced couples, they migrate into the perivesicular (*S. haematobium*) or mesenteric (other species) veins and initiate the sexual reproduction (*11*).

An adult schistosome lives 3-5 years in average. Depending on the species, the female can produce hundreds to thousands of eggs per day (*1*). A *S. mansoni* female worm, for example, lays approximately 400 eggs a day. The eggs are laid in the subcutaneous layer of capillaries and venules. Some of the eggs migrate through the bladder and ureteral wall (*S. haematobium*) or intestinal wall (other species) and are excreted in the urine or faeces (*11*). Each ovum carries a ciliated miracidium larva. Through the egg shell, the miracidium secretes proteolytic enzymes that assist in the transmigration process, which is also facilitated by a periovular inflammatory reaction mediated by host's immune response (*12*). The eggs that are not released to the exterior remain attached to the intestinal mucosa or are pushed by blood flow to other host organs causing damage.

If released into water reservoirs with intense light, high temperatures and oxygenation, the eggs hatch and release the miracidia. The miracidia, guided by light and chemical stimuli, penetrate the tegument of freshwater snails (intermediate host) and initiate the asexual reproduction. Each miracidium develops into a multicellular sporocyte and later into cercarial larvae. 4 to 6 weeks after infection, cercariae are released through vesicles that bud from the snail's tegument. The cercariae swim freely in the water for up to 72 hours or until they find a suitable host to penetrate (*1*).

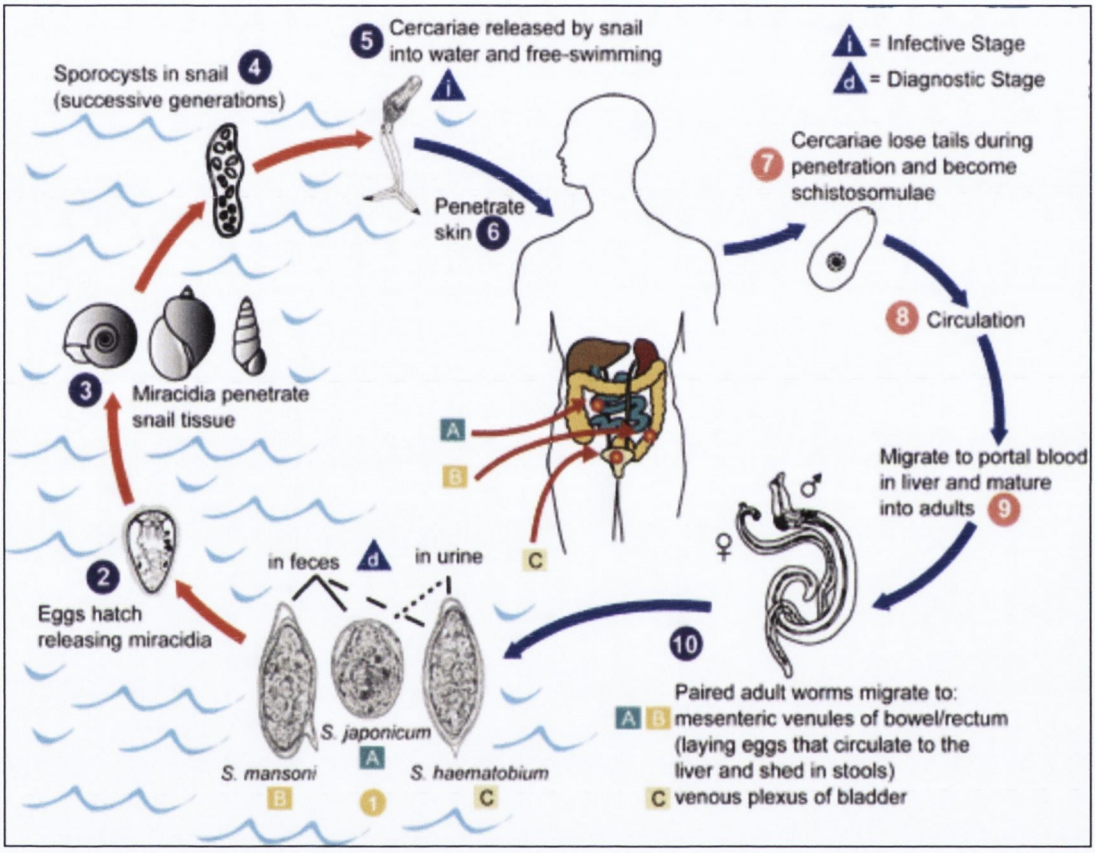

Figure 1.3: ***S. mansoni, S. japonicum and S. haematobium*** **life cycle**. (Adapted from Centers for disease control and prevention. Image Library – Schistosomiasis. Retrieved August 30, 2011 from http://www.dpd.cdc.gov/dpdx/HTML/ImageLibrary/Schistosomiasis_il.htm)

1.1.3 - Clinical manifestations of schistosomiasis

1.1.3.1 – Acute pathology

Schistosomiasis clinical manifestations follow the development of the parasite in the host. Cercaria penetration into the skin provokes a local and temporary allergic reaction known as cercarial dermatitis (CD). This symptom may persist for several days. After cercaria penetration, the migration of the schistosomula and the initial egg deposition induce a systemic hypersensitive reaction, known as Katayama fever or Katayama syndrome. The Katayama Fever is characterized by a rapid onset of fever, fatigue, myalgia, malaise, headache, a nonproductive cough, eosinophilia and patchy infiltrates visible on pulmonary radiography. After schistosomula maturation into juvenile worms, the migration of paired schistosomes may lead to abdominal pain and discomfort. Taken together, these symptoms constitute the acute pathology of schistosomiasis (*13-15*).

Acute schistosomiasis is extremely rare in endemic populations probably due to in-utero sensitization or infection at an early age (*16, 17*). However, it is extremely common among tourists and migrants, i.e. people first exposed to the parasite with no immunity, after primary infections and can lead to a more serious disease with weight loss, dyspnoea, diarrhea and toxemia among other symptoms (*15*) . However, *S. japonicum* infections, as opposed to the other schistosome species, can induce Katayama Fever in endemic populations with a history of previous infections (*13, 18*).

1.1.3.2 – Chronic pathology

In established infections the constant deposition of eggs in tissue is the main cause of damage to the host. The eggs that are not excreted stay trapped in the host tissue during perivesical or per-intestinal migration causing an inflammatory reaction, known as periovular granuloma. The schistosomotic granuloma results from the host's immune response to lytic and antigenic molecules secreted through the eggshell micro pores. Endothelial cells, eosinophils, macrophages and $CD4^+$ T cells are the main cell types in the granuloma. The inflammatory infiltrate is tissue-dependent, may vary with time and is gradually replaced by fibrotic deposits (*5, 19*).

In *S. haematobium* infections, the deposition of eggs in the walls of the bladder and ureters induces fibrosis that in turn leads to calcification. Partial blockage of urine excretion causes renal colic, hydroureter (distention of the ureter with fluid) and hydronephrosis (swelling of the kidneys). Secondary bacterial infections are very common. In extreme cases, renal failure may occur (*1, 20*).

Eggs can also be lodged in the vulva, vagina and cervix where granulomas generate ulcerative lesions. If uterus, fallopian tubes and ovaries are affected, infertility may occur as a result of fibrotic scarring. In males, granulomas can occur in the epididymis, testicles and spermatic cord. Haematospermia (blood in semen) is the main symptom. Genitourinary schistosomiasis has been associated with the outcome of bladder carcinoma (*21-23*).

Regarding the other human-infecting schistosomes, *S. mansoni*, *S. japonicum*, *S. mekongi* and *S. intercalatum*, the perintestinal migration of eggs causes intermittent abdominal pain and discomfort, loss of appetite, diarrhoea and superficial bleeding (*1, 24*). *S. mansoni*, *S. japonicum* and *S. mekongi* also induce hepatointestinal schistosomiasis, as opposed to *S. intercalatum* infection that is restricted to mild intestinal disease. Eggs

pushed by the portal vein blood flow get trapped in the small pre-sinuisodal vessels in the liver and escape to hepatic tissue causing granulomas. The granuloma is gradually replaced by fibrotic deposits which block blood circulation generating portal hypertension and subsequent hepatomegaly (*5, 24, 25*).

In extreme cases, there is an additional deposition of collagen in the periportal spaces, know as Symmer's pipestem fibrosis. The gradual occlusion of portal veins leads to splenomegaly and porto-systemic collateral circulation, mainly oesophageal varices, from where bleeding may occur (*26*). Progression to chronic disease is faster and more severe in *S. japonicum* infections (*1*).

Chronic schistosomiasis may be further complicated by the development of pulmonary schistosomiasis. As a result of the advance of the portal-systemic collateral circulation, schistosome eggs can leak into the lungs causing portopulmonary hypertension and consequent cardiopulmonary abnormalities (*27*) . Schistosome eggs can also reach the nervous tissue leading to nerve damage. *S mansoni* and *S haematobium* eggs usually affect the spinal cord, whereas *S japonicum* causes cerebral lesions (*28*).

1.1.4 – Diagnosis and treatment of schistosomiasis

The most common diagnostic method is the microscopic examination of excreta (urine/stool). Schistosome eggs can be easily identified due to their characteristic size and shape. They have a typical lateral or terminal spine and in fresh samples the living miracidium can be seen. However, for detection of light infections, the eggs must be concentrated from urine or faeces specimens, by sedimentation, filtration or centrifugation, prior to microscopic examination. In patients with typical clinical manifestations but no detectable eggs in the urine or faeces, a biopsy of bladder or rectal mucosa may be considered (*29*).

Antibody-based assays against parasite antigens are useful for diagnosis of infection in tourists and migrants. Routine techniques detect IgG, IgM or IgE against soluble worm or eggs antigens by enzyme-linked immunosorbent assay (ELISA), indirect haemagglutination, or immunofluorescence. Nevertheless, they are not applicable under field conditions, as they cannot distinguish history of exposure from active infection (*1*).

Imaging techniques, such as ultrasonography or radiography, can assess the extent of the pathology. Pelvic radiography or ultrasound allows visualization of bladder, ureteral and renal pathology. Abdominal ultrasound can determine the extend of liver and spleen pathology and the portal vein distention or gastro-oesophageal varices can be visualized by contrast radiography (*1, 29*).

Praziquantel (PQZ) is the drug of choice for treatment of schistosomiasis. PQZ is safe and effective and it is used in one single oral dose. It is active against all schistosome species. The drug damages the schistosome tegument paralyzing the worms, however, its precise molecular action is unknown. PQZ has few side effects. The most common side effects are a transient nausea, dizziness, rash and pruritus. Those effects are thought to be associated with the consequences of worm death rather than the drug itself (*29*).

1.1.5 - The search for an anti-schistosomal vaccine

Thus far, several antigens have been tested in animal models as potential candidates to develop an anti-schistosomal vaccine. However, the infection with radiation-attenuated (RA) cercaria, which was extensively tested during the late 1970s, is still the most effective strategy and induces protective levels up to 70-80% in mice. Unfortunately, the RA larva is not considered a safe vaccine. There is a risk that the parasite could recover its infectious ability (*30, 31*).

In the 1990s, WHO selected the 6 most promising vaccine candidates from *S.*

mansoni and initiated an independent pre-clinical trial. The antigens selected were: Glutathione-S-transferase 28 kDa (Sm28GST), Triose phosphate isomerase (TPI), Paramyosin (Sm97), 23 kDa integral membrane tetraspanin protein (Sm23), Myosin heavy chain (IrV5) and 14 kDa fatty acid binding protein (Sm14). These antigens were selected based mainly on their recognition by protective antibodies or their high immunogenicity. They were tested in mice models by independently contracted laboratories. However, they failed to induce protection above 40% (*32*).

Until now, only one schistosome antigen has been tested in clinical trials, the *S. haematobium* 28 kDa Glutathione-S-transferase (Sh28-GST). The recombinant Sh28-GST has been taken through phase I and II clinical trials and is now entering phase III in Europe and West Africa (*33*). Other antigens have undergone preclinical studies with success. Sm-p80, a DNA vaccine encoding the large subunit of *S. mansoni* Calpain, was tested in baboons and provided levels of protection as high as immunization with irradiated cercaria (*34*).

One of the WHO's vaccine candidates, Sm14, is at present, at the stage of planning for a clinical trial. Sm14 also induces protection against *Fasciola hepatica*, a trematode that causes human and veterinary fascioliasis (*35*). More recently other prospective vaccine candidates have been tested. For instance, Sm-TSP-2, the second extracellular domain of *S. mansoni* Tetraspanin, has been shown to provide a high level (87%) of protection in mice. Sm-TSP-2 is a strong vaccine candidate, as putatively resistant individuals living in endemic areas have elevated antibody response to Sm-TSP-2 as compared to chronically infected individuals from the same area (*36*). Another *S. mansoni* protein that induces protection is the antigen Sm21.7. Mice immunized with Sm21.7 exhibit 51% and 22.5% decrease in adult worm burden and hepatic eggs, respectively (*37*).

1.2 – Immunology of helminth infections

1.2.1 – The host-parasite balance

Helminths are extremely diverse parasites and undergo distinct and complex life cycles. Humans can be infected via the oral route (*Ascaris lumbricoides, Fasciola hepatica*), through skin penetration (schistosome species) or fly bites (*Onchocerca voulvulus*). Once inside the host, they exist as eggs, larvae or adult worms and affect different organs such as colon, small intestines, lymphatics, lungs and liver. Although some individuals may develop severe disease, most helminth infections are usually asymptomatic or subclinical chronic diseases. The parasite persistence results from a notable balance between host immune defence and parasite immune evasion. In addition, helminths have the ability to modulate host immune response through several mechanisms leading to a tolerizing regulatory response. This multifactorial equilibrium, shaped by long-term evolution, provides parasite and host survival (*38-40*).

1.2.1.1 - Host protective immune response

Host protective immune defence against helminth parasites includes a variety of mechanisms. Trematode larval stages (*Schistosoma sp., Fasciola sp*) or nematodes migrate through tissue and can be immobilized by eosinophils, neutrophils, macrophages and platelets. This mechanism is known as antibody dependent cellular cytotoxicity (ADCC). Antibodies IgE, IgG or IgA bound to the helminth surface interact with the Fc fragment receptors (Fcr) on the membrane of these cells. The binding results in cell activation and the release of toxic products, such as major basic protein, eosinophil cationic protein, eosinophil-derived neurotoxin and reactive nitrogen intermediates (*41*). Toxic products are

also released by interferon-gamma (IFN-γ) and tumor necrosis factor-alpha (TNF-α) activated macrophages during the acute or early phase of trematode infection (*Schistosoma sp., Fasciola sp.)* (*42*).

Another protective mechanism is the formation of a granuloma that can occur around the parasite. Granulomas have been well investigated in *S. mansoni* infections. Eggs trapped in hepatic tissue or intestinal wall are surrounded by eosinophils, macrophages and lymphocytes. As the granuloma matures, there is increasing fibrosis, which resolves after the eggs die. In the intestinal wall, inflammation ceases after egg expulsion in feces (*24, 43*).

1.2.1.2 - Parasite immune evasion

Helminths have developed several strategies to escape the host's immune response. One of the first described escape strategies is the acquisition of host's immunoglobulins (Igs) into the worm surface (*44, 45*). Human IgG1, IgG3 and IgM were detected on the *S. mansoni* tegument (*46*). These host Igs bind to Fc receptors in the parasite surface and are believed to prevent parasite recognition by masking worm antigens. These surface immunoglobulins do not activate the complement cascade, as they do not exhibit the Fc domain (*47*). Apart from masking worm molecules, host-derived Igs may also inhibit eosinophil adhesion to the worm surface thus evading the ADCC (*38*).

A range of helminth secreted products have been shown to have an immune evasion function. *F. hepatica*, for instance, secretes cathepsin L-protease that cleaves IgE and IgG inactivating the ADCC (*48, 49*). The hookworm *Necator americanus* secretes metalloproteases that specifically cleave eotaxin, an eosinophilic chemotatic factor (*50*). Moreover, release of antioxidant enzymes such as superoxide dismutase and glutathione-s-transferase has been described in several proteomics studies of worm's secretome. These

enzymes are believed to neutralize the toxic radicals released by host's immune cells (*51, 52*). The neutralization of host molecules by parasite-derived products has also been described in schistosome eggs. *S. mansoni* eggs secrete a chemokine binding protein (smCKBP) that protects the parasite from an inflammatory reaction. smCKBP has been shown to block IL-8 induced neutrophil migration and inhibit pulmonary neutrophilic inflammation in a hypersensitivity contact model (*53*).

1.2.1.3 – Parasite modulation of host immune response

Helminth infections typically induce a Th2 type immune response that involves; the cytokines interleukin-3 (IL-3), IL-4, IL-5, IL-9 and IL-13, mostly produced by $CD4^+$ Th2 cells; the antibody isotypes IgG1, IgG4 and IgE; and expansion of eosinophils, basophils and mast cells (*54*). IL-4 and IL-13 are key inducers of a Th2 type of immune response with the IL-4 receptor α-chain (IL- 4Rα), a component of IL-4 and IL-13 receptors, playing a major role. This adaptative Th2 cell response is believed to be initiated and amplified by non-B non-T innate immune cells. A new type of innate helper cells, named nuocytes or natural helper cells, have been recently described. Nuocytes are crucial inducers of Th2 cells as they function as an early source of IL-13 during a helminth infection (*55*).

The Th2 type immune response described above can potentially lead to severe tissue damage and fibrosis. Nonetheless, during helminth infections, tissue damage is a tightly regulated process, which results from parasite modulation of the host immune response (*40*). The initial Th2 cell proliferation is, at a later stage, inhibited by secretion of the immune suppressive cytokines interleukin-10 (IL-10) and transforming growth factor-beta (TGF-β) by antigen-presenting cells or regulatory T cells (*56*). As a result, infected individuals show a T-cell hyporesponsiveness and an unresponsive state of parasite

reactive T-cells (*57*). Another major immune suppressive cell population induced by helminth infection is the B regulatory cells (Breg). Breg cells suppress inflammation via production of IL-10 and recruitment of T regulatory cells to the site of infection, however the exact mechanism remains unclear (*58*).

An induction of alternatively activated macrophages (AAMΦs) is also observed during helminth infections. AAMΦs are elicited by IL-4 and IL-13. They modulate the immune response through secretion of IL-10, differentiation of Th2 cells and downregulation of Th1 type inflammation. AAMΦs has also been shown to contribute to fibrosis and repair of tissue damage at the site of infection, which may be of major importance during helminth infections (*59, 60*).

1.2.2 - Helminth infections and non-related disorders

The strong immunomodulation induced by helminths is not only directed to the parasites but also affects non-related diseases that may occur during the infection. The consequences of the helminth induced immunomodulatory response have been extensively investigated in several epidemiological studies in infected populations and experimental studies using mouse models. However, helminth infections have been shown to either suppress or exacerbate unrelated disorders and, thus far, it is not possible to draw a general conclusion. A combination of several factors, such as; parasite species; infection intensity; host genetic background, age and nutritional status may be the cause of the inconsistent disease outcomes (*40*).

1.2.2.1 - Helminth infections and allergies

Investigations of some endemic populations suggest a negative association between helminth infections and the prevalence of allergic diseases. The cutaneous response to common aeroallergens is suppressed in *S. mansoni*-infected individuals from an endemic area in Brazil (*61*). *S. mansoni*-infected individuals may also show amelioration of allergic disease and a reduced course of asthma was observed in infected patients (*62*). In Ethiopia, *A. lumbricoides* infection has also been shown to be protective with wheezing being less prevalent in *A. lumbricoides*-infected young children (*63*). Additionally, in a recent systematic review, a consistent protective effect was found for infection by *A. lumbricoides, Tricuris trichuria,* hookworms and schistosomes (*64*).

On the contrary, some studies have shown no association or even positive association between helminths and allergies. A study of children infected with *A. lumbricoides* in China revealed an increased sensitization to aeroallergens and an increased risk of asthma. Additionally, no association with wheeze and asthma was detected among geohelminth infected children in an endemic area of Ethiopia (*65*).

More solid evidence comes from studies in animal models. *S. mansoni* infection has been shown to efficiently suppress allergic airway inflammation and inhibit anaphylaxis (*58, 66*). *Heligmosoides poligyrus* infection also downregulates allergic airway inflammation, as well as anaphylaxis and production of allergen specific IgE in mice (*67*) (*68*). Several other helminths, such as, *Strongyloides stercoralis*, *Litomosoides sigmodontis* and *N. brasiliensis* have been shown to reduce allergic responses (*69-71*). However, some studies demonstrate a contrary effect, for example, *T. spirales* infection of mice exacerbates anaphylaxis (*72*) and infection of primates with *A. suum* increases sensitivity to aero-allergens (*73*).

1.2.2.2 - Helminth infections and autoimmune diseases

Unlike allergic diseases, autoimmune disorders are less prevalent therefore epidemiological studies regarding the influence of helminth infections in the outcome and/or course of such disorders are limited. Most of the epidemiological data rely on the fact that the global distribution of autoimmune diseases is the opposite of endemic helminth infections (*74*).

Opposingly, several studies in animal models have revealed that helminth parasites may block or reduce the severity of autoimmune disorders (*75*). *S. mansoni* infection has been shown to prevent the development of dextran sodium sulphate (DSS) induced colitis in mice and to inhibit the development of Type 1 diabetes mellitus in non-obese diabetic (NOD) mice (*76, 77*). *S. mansoni* infection also reduces induction and progression of experimental autoimmune encephalomyelitis (EAE) and the severity of collagen-induced arthritis in mice (*78, 79*). Moreover, spontaneous arthritis developed by MRL/Ipr mice is ameliorated by *N. brasiliensis* and EAE is modulated by *T. spiralis* in rats (*80*).

1.2.2.3 – Clinical use of helminths

Based on the available epidemiological and experimental evidence, helminth infections present therapeutic potential and have been considered for clinical human trials. Some helminths have already been tested and there are undergoing trials. Infection of patients with inflammatory bowel disease (IBD) with *Trichuris suis*, a pig worm, or *N. americanus* has been shown to be a safe and effective treatment (*81*) (*82*). *T. suis* have also been tested as treatment for Crohn's disease with a positive outcome and no side effects (*83*). Recently, a clinical trial of experimental *N. americanus* infection in people with allergic asthma was performed, but did not result in any significant improvement.

The use of helminths in a clinical setting has the inevitable risk of side effects. A safer approach to the treatment of allergies and autoimmune diseases would be the exploitation of helminth derived immunomodulatory molecules (*84, 85*). Some helminth molecules with anti-inflammatory activity have already been characterized and will be described in the following section.

1.3 – Helminth-derived molecules with immunomodulatory potential

The interaction between helminths and the host's immune system is mediated by molecules that are secreted or excreted by the parasite during different phases of its life cyle: adult worms, larvae or eggs. Despite the potent immunomodulatory activity of helminth parasites, relatively few immunomodulatory molecules (IMs) from parasitic worms have been characterized to-date (Table 1.2).

IM	Helminth	Modulatory activity	Ref.
Cystatin	*Onchocerca volvulus* *Acanthocheilonema viteae*	1. Induces cell hyporesponsiveness 2. Induces IL-10 derived macrophages	(*86*) (*87*)
ES-62	*Acanthocheilonema viteae*	1. Anti-inflammatory (prevents collagen induced arthritis) 2. Protects against allergic airway hyperresponsiveness and skin hypersensitivity	(*88*) (*89*)
LNFPIII	*Schistosoma mansoni*	Th2-inducing adjuvant	(*90*) (*91*)
Lyso-PC	*Schistosoma mansoni*	Stimulates IL-10 producing regulatory T cells	(*92*)
Sm16	*Schistosoma mansoni*	Suppresses cutaneous inflammation	(*93*)
SmCKBP	*Schistosoma mansoni*	Chemokine binding protein (suppresses acute inflammation)	(*53*)
Thioredoxin peroxidase	*Fasciola hepatica* *Schistosoma mansoni*	Induces alternatively-activated macrophages	(*94*) (*95*)

Table 1.2: **Examples of molecules from helminths that modulate immune responses.**

1.3.1 – *A. viteae* excretory-secretory 62 kDa protein (ES-62)

ES-62 was first discovered as a 62 kDa protein in the excretory secretory products of *Acanthocheilonema viteae*, a filarial nematode of rodent in 1989 by Harnett *et al (96)*. It was also identified in other filarial nematode species such as *Wuchereria bancrofti*, *Brugia malayi* and *Onchocerca volvulus*. ES-62 is a phosphorylcholine (PC) containing glycoprotein that has been widely investigated as an immunomodulatory molecule. The active native molecule contains phosphorylcholine (PC) moieties that are modified by post-translational processes.

ES-62 exhibits immunomodulatory effects that can lead to downregulation of immunity, as well as inducing the maturation of Th2-inducing dendritic cells (DC) with a resulting Th2 cell polarized immune response. In addition, it is broadly anti-inflammatory and mediates diverse effects on various cells of the immune system (*96*). Functional studies of ES-62 suggested that immunomodulatory activity may rely on the PC moiety (*97*). Indeed, in a recent study, PC conjugated with other carrier proteins mimics the function of native ES-62, whereas recombinant ES-62 without PC did not display immunomodulatory activity (*98*). ES-62 modulates macrophages and DCs by first binding with TLR4 on their surface (*99*). In addition to modulating macrophages and DCs, ES-62 forms a complex with TLR4 on the surface of human mast cells, triggering a downstream signal cascade (*89*). The downstream product triggered by the ES-62/TLR4 complex directly inhibits the Fc RI-related allergic response of mast cells and blocks mast cell degranulation. In terms of therapeutic potential, ES-62 reduces articular inflammation in a model of collagen-induced arthritis in the DBA-1 mouse (*88*). Moreover, ES-62 efficiently protected against hypersensitivity, mediated by mast cells in the skin and lungs of a hyperresponsive allergic mouse model (*89*). The data provides compelling evidence in

support of further research into the therapeutic potential of ES-62, or small molecule derivatives/peptides, in a variety of immunological diseases and disorders.

1.3.2 – *S. mansoni* 16.8 kDa protein (Sm16)

Previous studies suggest that *S. mansoni* larvae utilize an immunomodulatory mechanism during penetration and migration through the skin of rodent host by suppressing inflammatory responses (*93, 99*). Thus ES products from S. mansoni cercariae and schistosomula could activate production of IL-1 receptor antagonist from human keratinocytes in vitro and cercariae also stimulate mouse skin and cultured keratinocytes to produce IL-10 that is a crucial regulatory cytokine (*100*). An analysis of the bioactivity in cercariae ES products of the parasite found that a 16.8 kDa protein, designated Sm16, has partial homology with human stathmin and exerts an anti-inflammatory activity (*101*). In vitro studies support a role for Sm16 in reducing expression of IL-1 in human keratinocytes, suppressing lymphocyte proliferation and down-regulating expression of ICAM-1. Furthermore, consistent with a role in suppression of inflammation, intradermal delivery of Sm16 cDNA reduced cutaneous inflammation in mice (*102*). Sm16 efficiently binds to the lipid bilayer presented on the cell membrane of diverse cell types that probably play a crucial role during skin penetration, which may account for its modulatory activity (*103*).

1.3.3 - *S. mansoni* Chemokine Binding Protein (smCKBP)

Production and secretion of cytokine and chemokine binding proteins (CKBP) is an immune-modulation strategy widely employed by a range of viruses (*104*). SmCKBP is the first CKBP described in a parasite and is secreted solely from the eggs of *S. mansoni, S.*

heamatobium and *S. japonicum* (*53*). SmCKBP selectively binds to certain members of the chemokine subfamilies as well as the glycosaminoglycan heparan. Recombinant smCKBP suppresses inflammation induced in a mouse contact hypersensitivity model and blocked CXCL8-induced pulmonary inflammation.32 The smCKBP gene has also been cloned by Hass and colleagues and is reported to be an inducer of degranulation of basophils (*105*).

1.3.4 – Peroxiredoxin 1 (Prx1)

Peroxiredoxins (Prxs) are enzymes that protect cellular components from oxidative damage by reactive oxygen species (*106*). Prx is a ubiquitous enzyme that can be found in various organisms in the whole animal kingdom. Among helminths, Prx has been identified in both trematode, nematode and cestode species, examples of which include *Fasciola hepatica, S. mansoni, Onchocerca volvulus* and *Echinococcus granulosus (94, 107)*. Functional characterization of Prxs in helminths suggests that it plays a significant role in host-parasite interaction as an antioxidant enzyme against host ROS (*108*). Recombinant *F. hepatica* and *S. mansoni* Prxs have shown immunomodulatory activity and were demonstrated to be inducers of alternatively activated macrophages, including the recruitment of such macrophages to the peritoneum in a mouse model. Recombinant Prx directly activates a mouse macrophage cell-line to induce a polarized Th2 cell response (*94*). A recent study argues that the role of Prx on alternative activation of macrophages, is not only independent of antioxidant activity, but IL-4 and IL-13 independent as well. This suggests that helminth Prx activates macrophage as an initial step to developing a Th2 response (*95*).

1.3.5 - *Onchocerca volvulus* cystatin (Onchocystatin)

The Cystatins are ubiquitous proteinase inhibitors of cysteine proteases that regulate various biological and pathological processes by inhibition of cysteine protease activity. Cystatin is secreted by human mononuclear phagocytes and during inflammatory processes its expression is down modulated which, in turn contributes to increased cytsteine protease activity. In addition, the study of cystatin in DC maturation and MHC molecule processing suggested that cystatin plays a role in the intracellular control of invariant chain degradation and antigen presentation (*109*).

In parasites, cystatin was first described in the filarial parasite *Onchocerca volvulus*, hence termed onchocystatin, which causes river blindness (*110*). The cellular hyporeactivity induced by secreted onchocystatin when added to human peripheral blood mononuclear cells (PBMC) in vitro, is comparable to some aspects of the state of immune hyporesponsiveness seen in patients infected with *O. volvulus (86)*. In addition, onchocystatin stimulated human PBMCs to produce significant levels of IL-10 compared to unstimulated PBMCs and down-regulated the expression of HLA-DR proteins and costimulatory molecules on human monocytes (*111*). Interestingly, an in vivo study with the administration of filarial cystatin (*A. viteae*) to an allergic airway hyperresponsive mouse model supported the role of cystatin in suppression of allergic hyperreactivity by induction of IL-10-derived macrophages. Furthermore, in a chemically-induced colitis mouse model, cystatin regressed the macrophage-mediated inflammatory infiltration and epithelial damage in the colon (*87*). Immunomodulatory cystatins are present in other parasitic nematodes, which contrast with the absence of such activity in cystatins from free-living nematode *Caenorhabditis elegans (109, 112)*. Cystatin has been also identified in the blood fluke *S. mansoni*, with a potential function as a cysteine protease inhibitor (*113*). However, the immunomodulatory potential of schistosome cystatin has yet to be

fully addressed.

1.3.6 - Helminth glycans and glycolipids as IMs

Recent studies demonstrate that carbohydrate and lipid determinants within cell surface and secreted glyco- or lipo-conjugates are capable of eliciting an immunomodulatory potential (*114-116*). In parasitic helminths, several different carbohydrate and lipid molecules from the parasitic surface or ES product are potent modulators of the host immune response. The most widely investigated helminth carbohydrate IM is Lacto-N-fucopentaose III (LNFPIII) (*117*) while with respect to helminth lipid IMs, schistosomal lysophosphatidylserine (lyso-PS) is the best characterized (*92*).

1.3.6.1 - Lacto-N-fucopentaose III (LNFPIII)

Previous studies on the role of carbohydrates in schistosome eggs demonstrated that glycans in soluble egg antigen promoted an enhanced Th2 response (*90*). LNFPIII is one such glycan that is present in schistosome soluble egg antigens with potent modulatory activity. Administration of LNFPIII conjugated with carrier molecule into a mouse model demonstrated strong Th2 responses, thus functioning as a potent Th2-inducing adjuvant (*90*). In addition, LNFPIII induces in mice expansion of IL-10-producing B-1 cells (*118, 119*) a peritoneal macrophage population that can suppress CD4 T-cell (*120, 121*), evoke alternative activation of macrophages in vivo (*122*) and also induces DC to develop into a DC2 phenotype (*91, 123*). With its potent in vivo modulatory activity, it will be of interest to further evaluate the effects of LNFPIII administration in animal models of inflammatory diseases.

1.3.6.2 - Lysophosphatidylserine (Lyso-PS)

Lysophosphatidylserine (Lyso-PS) was identified in a screen for innate interactions between human DCs and different classes of lipids from schistosome worms or eggs. Human DCs treated with schistosome Lyso-PS were modulated such that they primed naive T-cells to suppress proliferation of autologous T-cells, via the production of IL-10 in a TLR2-dependent manner. The specific factor that induced IL-10-producing regulatory cells was shown to be lyso-PS (*92, 124*).

1.3.7 - Helminth Cytokine and Chemokine Homologues as IM

The host immune response to helminths is partially controlled by cytokines, as immune cell signaling molecules and chemokines, to induce cell-specific chemotaxis, in order to elicit the appropriate anti-helminthic response. Prolonged co-existence of helminths and their hosts have resulted in the parasite's developing homologues to human cytokines and chemokines that manipulate the host immune response in such a way as to prolong parasite infestation. Examples of helminth cytokine and chemokine homologues are shown in Table 1.3 and described herein.

Cytokine and chemokine Homologues	Helminth	Modulatory activity	Ref.
IFN-γ	*Trichuris muris*	Polarizes Th-1 immune response (inappropriate anti-helminthic immune response)	(*125*)
HMGB1	*Schistosoma mansoni*	Probably modulates host immune responses to promote helminth egg dissemination	(*126*)
MIF	*Trichuris muris*	Probably controls migration of immune cells to the infection site	(*127*)
TCTP	*Brugia malayi*	Antioxidant (prevents oxidative damage)	(*128*)
TGF-β	*Brugia malayi*	Binds to human TGF-β receptor (Possibility of immune modulation)	(*129*)

Table 1.3: **Helminth-derived cytokine and chemokine homologues.**

1.3.7.1 - Interferon gamma (IFN-γ)

The generation of a Th2 type immune response by the host expels infections by many helminths, thus it would be advantageous for the helminth to evoke a counter regulating type 1 response. During research on *T. muris*, a mouse model of human infecting nematode *T. trichiura*, a homologue to a type 1 immune response driving cytokine, Interferon gamma (IFN-γ), was uncovered. This protein had the capacity to bind to the mouse IFN-γ receptor with similar downstream effects as the host cytokine, including Th1 lymphocyte differentiation and function (*125*). The secretion of an IFN-γ homologue by a helminth could alter the local cytokine milieu and facilitate its survival in the host.

1.3.7.2 - High-Mobility Group Box 1 (HMGB1)

High-Mobility Group Box 1 (HMGB1) is an abundant nuclear protein released from dying mammalian cells, as well as being secreted from activated macrophages, that can induce the production of TNF-α and lead to inflammation and tissue repair (reviewed in ref. (*130*)). Homologs of HMGB1 have been identified among the schistosome species. SmHMGB1 is expressed in large quantities in adult female, or in schistosoma eggs and egg-secreted antigens, prompting speculation that the molecule plays a role in modulating host immune responses to promote helminth egg dissemination. Recombinant *S. mansoni* HMGB1 has been shown to induce the release of pro-inflammatory cytokines from macrophages *in vivo* implying a significant role for this cytokine-like molecule in eliciting host immune responses (*126*).

1.3.7.3 - Macrophage Migration Inhibition Factor (MIF)

Many helminths, such as *Trichinella spiralis, Brugia pahangi, Ancylostoma ceylanicum*, have an ortholog of the Macrophage migration inhibition factor (MIF) (*131*). MIF was one of the first cytokines discovered and has been shown to play a role in promoting inflammation through macrophage and T-cell activation as well as IgE synthesis (*132*). It has also been shown to play a central role in host protection against some helminths, specifically *Taenia crassiceps (133)*. Using recombinant helminth MIFs, it has been shown that many of these orthologs have the ability to be chemoattractant to human monocytes in vitro and thus might have the ability to control the influx of immune cells and the egress of primed antigen presenting cells from the infection site. Some heminth MIFs also have the ability to interact with the human MIF receptor (CD74), resulting in monocyte activation and their subsequent cytokine production, capable of affecting appropriate anti-helminth immune responses (*127, 134*).

1.3.7.4 - Translationally Controlled Tumor Protein (TCTP)

Translationally Controlled Tumor Protein (TCTP), also known as tumor protein, translational-controlled 1 (TPT1), is expressed in various organisms, including helminths and has broad biological activities (*135*). TCTP homologs from the human filarial parasites *W. bancrofti* and *B. malayi*, have been shown to possess both histamine-releasing function as well as calcium-binding properties in vitro. Their precise function in helminths do not seem clear, but in vivo injection of isolated helminth TCTP into mice induced the accumulation of eosinophils implying a role in the induction of host pathology as a possible survival strategy (*136*). A recent study on the Bm-TCTP homologue has implicated a role as an antioxidant protein that could provide protection against oxidative

damage brought on by a host anti-helminthic immune response (*128*).

1.3.7.5 - Transforming Growth Factor beta (TGF-β)

TGF-β homologs, or TGF-β-like protein or TGF-β-like ligand, have been observed in all subgroups of helminths. The filarial worm, *B. malayi*, secretes a TGF-β-like protein that is capable of binding to the mammalian TGF-β receptor with possible immune modulation. Several *in vivo* and *in vitro* studies have demonstrated the interaction of *S. mansoni*-derived TGF-β receptors, SmTRI, with the human TGF 1 ligand that is ultimately capable of resulting in gene specific transcription (*137, 138*). This provides evidence for a possible involvement in the regulation of early schistosome development in response to host-derived factors. In the cestode *Echinococcus multilocularis*, 2 Smad protein family members have been identified that are crucially involved in intracellular TGF-β signaling (*139*) providing further evidence for a TGF-β-like signaling cascade within helminths as a mechanism of host-parasite interaction.

2 - Materials and Methods

2.1 - *Schistosoma mansoni* life cycle maintenance

The *S. mansoni* life cycle was routinely maintained in the Institute of Molecular Medicine (Trinity Centre for Health Sciences, Trinity College Dublin). A Puerto Rican strain of *S. mansoni* was maintained by passage in BALB/c strain mice and albino *Biomphalaria glabrata* snails. All animal experiments were performed in compliance with Irish Department of Health and Children regulations and approved by the Trinity College Dublin's BioResources ethical review board.

2.1.1 - Snails maintenance

Albino *B. glabrata* snails were kept in plastic containers filled with Lepple water (Appendix 1). The snails were housed in incubators at 28°C with a 12-hour day/night cycle. Snail tanks were aerated using air pumps (RENA). The snails were fed every second day with commercially available fish food (TetraPond). The Lepple water in the plastic containers was changed weekly. For this purpose, the snails were collected in a sieve, the water was removed from the containers, the containers were scrubbed and cleaned with tap water and rinsed in Lepple water before return of the snails. Floating polystyrene rafts were placed in breeding tanks and the hermaphroditic snails laid their eggs on the underside of the rafts. Rafts with the eggs attached were transferred to separate tanks for hatching.

2.1.2 - Mice maintenance

Female BALB/c strain mice were used for egg and worm production (*140*). Mice were obtained from the Trinity College Dublin BioResources Unit. They were housed in individually ventilated and filtered cages under positive pressure (Techniplast) and maintained on an irradiated and OVA-free diet (Harlan) with food and water supplied *ad libitum*. Sentinel mice were routinely screened (Harlan; Surrey Diagnostics Ltd) to ensure the Specific Pathogen-Free status of the unit where mice were housed.

2.1.3 - Preparation of miracidia for snail infection

To prepare miracidia for infection of snails, the liver of a *S. mansoni* infected mouse was removed 49 days post infection. Mice were injected subcutaneously with 2.5 mg hydrocortisone (Sigma, Poole Dorsett) 35 days post infection. Hydrocortisone suppresses the hosts' immune response to the parasite eggs and reduces inflammation around the egg aiding its extraction from the tissue. On day 49, the animals were euthanized by an overdose of sodium pentobarbital injected intraperitoneally and the liver was removed. The tissue surrounding the egg was gently disrupted by homogenizing the liver in double-strength saline (Appendix 1) with a blender. The use of double-strength saline stops the eggs from hatching. Lepple water was then added to initiate egg hatching. The solution was placed in a conical flask wrapped in aluminium foil with the neck exposed to a light source. Following hatching of the eggs the phototropic miracidia swim towards the light source. After 30 minutes a sample of miracidia was collected from the top of the solution using a glass pipette and counted under a microscope.

2.1.4 - Snail infection

A single snail was placed in an individual well of a 24 well plate with 1 mL Lepple water containing 4-6 miracidium for a mixed male and female infection. The snails were infected for approximately 6 hours or overnight. Infected snails were placed in fresh plastic containers in incubators at 28°C with a 12-hour day/night cycle. Cercariae development takes 28-35 days.

2.1.5 - Preparation of cercaria for mice infection

Snails with patent infections were transferred into individual wells of a 24 well plate with 1 ml Lepple water and placed under a lamp for 90 minutes. Snails were examined under a microscope to ascertain they were infected and shedding cercaria. Cercariae were stained for counting using Lugol's iodine (Appendix 1) and visualized under the microscope.

2.1.6 - Mice infection

Mice were percutaneously infected with 350 cercariae. For this purpose, six to eight week-old mice were anaesthetized with 60 mg/kg sodium pentobarbital (Sagatal). Their abdomen was shaved and moistened with Lepple water. They were secured on a specially adapted infection board and a metal ring was placed with tape over their shaved abdomen. Three hundred and fifty cercariae were placed in the center of the metal ring and the mice were kept on the infection board for 25 minutes after which time they were placed on a heated mat and monitored until they recover. Upon full recovery they were returned to their cages.

2.2 - Schistosome antigen preparations

2.2.1 - Portal perfusion of infected mice for recovery of adult worms

S. mansoni adult worms were recovered by portal perfusion of infected mice (*141*). Forty-nine days infected mice were euthanized by an overdose of sodium pentobarbital injected intraperitoneally. The thoracic and peritoneal cavities were exposed and the hepatic portal vein was cut. Mice were perfused through the left heart with an injection of 20 mL of perfusion media (Appendix 1). Worms were collected in a glass beaker and immediately transferred to washing media (Appendix 1).

2.2.2 - Preparation of soluble adult worm (AW) antigens

For soluble adult worm (AW) antigen preparation, worms were washed several times in phosphate buffered saline (PBS, Appendix 1) until no debris was visible. The PBS was discarded and the worms were snap frozen in liquid nitrogen. Frozen worms were crushed several times, under liquid nitrogen, using a pre-cooled mortar and pestle until a very fine paste was formed. The worm paste was dissolved in PBS and centrifuged at 20,000 *g* for 1 hour at 4°C. The supernatant was recovered and transferred to a new tube and further centrifuged. The centrifugation was repeated several times until no pellet was visible. The final supernatant was filtered through a 0.45 μm syringe filter and stored in small aliquots at -80°C. Protein quantification was performed as described in Section 2.8.10.

2.2.3 - Preparation of male adult worm excretory-secretory (WES) molecules

Immediately after perfusion, worms were washed several times in washing media (Appendix 1) and transferred to a petri dish. Male worms were carefully sorted and transferred to another petri dish using a plastic pasteur pipette. To avoid mechanical damage to the worms during the sorting, the pipette tip was enlarged by cutting it with scissors. Throughout the sorting process, the worms were kept in cold washing media (Appendix 1). Under these conditions, male and female tend to separate naturally. Whenever necessary, cold washing media was added to the worms to speed up the separation. Male worms were examined using a microscope and any damaged, stunted or dead worms were discarded. Male worms were transferred to a tube (200 worms per aliquot) and washed 3 times with 10 mL of washing media at room temperature. Then washed 5 times with 10 mL of incubation media (Appendix 1) at 37°C under sterile conditions. Two hundred male worms in 15 mL of incubation media were transferred to a cellulose membrane dialysis tubing with a 10 kDa molecular weight cut off (MWCO). The tubing was sealed tying 3 knots on each side and placed in a T-75 cell culture plate containing 30 mL of nutrient media (Appendix 1). Worms were incubated at 37°C for seventy-two hours. The nutrient media was changed after 24 and 48 hours of incubation. The incubation media containing worm excretory secretory (WES) molecules within the dialysis tubing was harvested and processed. For processing, harvested media was concentrated at least 10 fold using a stirred cell concentrator at 50 psi with a 10 kDa MWCO membrane. The concentrated supernatant was then dialyzed with 4 L of PBS over night at 4°C using a 10 kDa MWCO dialysis cassette. WES preparation was then centrifuged at 20,000 *g* and 4°C for 30 minutes, filtered through a 0.22 µm filter and stored at -80°C.

2.2.4 - Male adult worm excretory-secretory (WES) molecules quality control

All WES batches were subjected to a quality control analysis. WES proteins were resolved in a 12% sodium dodecyl sulfate polyacrylamide gel (Section 2.8.1) and visualized by silver staining (Section 2.8.6). Rabbit anti-WES serum (Section 2.3.1) was used in comparative Western blot analysis (Section 2.8.7). Protein and endotoxin levels were assessed as described in Sections 2.8.10 and 2.8.11, respectively.

2.3 - Generation of polyclonal antibody

2.3.1 - Generation of rabbit anti-WES polyclonal antibody

Rabbit anti-WES polyclonal antibody was generated in a New Zealand White rabbit by a commercial company (Harlan Laboratories - http://www.harlan.com). A total of 850 μg of WES antigen was subcutaneously injected into a rabbit according to the protocol below (Table 2.1). Titermax was used as adjuvant and mixed with the antigen at a ratio of 1:1. The serum was screened for specificity by Western blot (Section 2.8.7).

Rabbit anti-WES polyclonal antibody production	
Day number	**Procedure**
0	Pre-Bleed + Immunization - 250 μg
14	Boost 1 - 150 μg
28	Boost 2 - 150 μg
42	Boost 3 - 150 μg
56	Boost 4 - 150 μg
63	Terminal Bleed

Table 2.1: **Immunization protocol for production of rabbit anti-WES polyclonal antibody.**

2.3.2 - Generation of rabbit anti-rSmPrx1 polyclonal antibody

Rabbit anti-SmPrx1 polyclonal antibody was generated in New Zealand White rabbit by a commercial company (Harlan Laboratories - http://www.harlan.com). A total of 500 μg of *E. coli* expressed recombinant *S. mansoni* Peroxiredoxin 1 (rSmPrx1) was subcutaneously injected into a rabbit according to the protocol below (Table 2.2). Titermax was used as adjuvant and mixed to the antigen at a ratio of 1:1. The serum was screened for specificity by Western blot (Section 2.8.7).

Rabbit anti-rSmPrx1 polyclonal antibody production	
Day number	**Procedure**
0	Pre-Bleed + Immunization - 200 μg
14	Boost 1 - 100 μg
28	Boost 2 - 100 μg
42	Boost 3 - 100 μg
56	Terminal Bleed

Table 2.2: **Immunization protocol for production of rabbit anti-rSmPrx1 polyclonal antibody.**

2.3.3 - Generation of rabbit anti-rSmTrx1 polyclonal antibody

Rabbit anti-rSmTrx1 polyclonal antibody was generated in New Zealand White rabbit. Immunization with *E. coli* expressed recombinant *S. mansoni* Thioredoxin (rSmTrx1) was performed following the same protocol described for generation of anti-rSmPrx1 polyclonal antibody (Section 2.3.2).

2.3.4 - Generation of mouse anti-r-his-SmCyp1 polyclonal antibody

Mouse anti-r-his-SmCyp1 polyclonal antibody was generated in 7-8 week old Balb/c mice. A total of 75 μg *E. coli* expressed recombinant polyhistidine-tagged *S. mansoni* Cyclophilin (r-his-SmCyp1) was subcutaneously injected into a mouse according to the protocol below (Table 2.3). Titermax was used as adjuvant and mixed with the antigen at a ratio of 1:1. Mice were anesthetized and the blood was collected from auxiliary vessels. To isolate serum from the blood, the samples were incubated at room temperature for 1 hour followed by incubation at 4°C overnight. After incubation, samples were centrifuged at 20,000g, 4°C for 30 minutes, the serum was collected and screened for specificity by Western blot (Section 2.8.7).

Mouse anti-r-his-SmCyp1 polyclonal antibody production	
Day number	**Procedure**
0	Pre-Bleed + Immunization - 50 μg
14	Boost 1 - 25 μg
28	Terminal Bleed

Table 2.3: **Immunization protocol for production of mouse anti-r-his-SmCyp1 polyclonal antibody.**

2.4 - Generation of recombinant plasmids

2.4.1 - Isolation of total ribonucleic acid (RNA) from *Schistosoma mansoni* male adult worms

Approximately 50 male worms were homogeneized in 0.5 mL Tri-Reagent using a sterile disposable plastic pestle. After homogenization, the sample was centrifuged at

20,000 *g* and 4°C for 10 minutes. The supernatant was transferred to a new tube followed by addition of 40 µL chloroform. The sample was vortexed for 15 seconds, incubated at room temperature for 10 minutes and centrifuged at 20,000 *g* and 4°C for 15 minutes. After centrifugation, the clear phase (upper layer) was carefully collected and transferred to a new tube. Two hundred and seventy µL isopropanol were added and the sample was incubated at room temperature for 5 minutes. After incubation, the sample was centrifuged at 20,000 *g* and 4°C for 10 minutes. The supernantant was discarded and the pellet was washed with 800 µL 75% Ethanol (ETOH). For washing, 75% ETOH was added and the pellet was displaced from the bottom of the tube by pipetting up and down. After washing, the sample was centrifuged at 20,000 *g* and 4°C for 5 minutes. The supernatant was discarded and the pellet was allowed to dry for 30 seconds. The pellet was dissolved in 20 µL sterile ribonuclease (RNAse) free water.

2.4.2 - Synthesis of complementary deoxyribonucleic acid (cDNA) by reverse transcription

SuperScript® II Reverse Transcriptase (Invitrogen) was used for cDNA synthesis according to manufacturer's recommendations. The following reagents were added to a microcentrifuge tube: 1 µL of 500 µg/ml Oligo(dT), 1 µg of *S. mansoni* adult worm total RNA, 1 µL of 10 mM dNTP mix and sterile distilled water up to 12 µL. The mixture was heated to 65°C for 5 minutes and quickly chilled on ice. 4 µL of 5X First-strand Buffer, 2 µL of 0.1 M DTT and 1 µL of 40 units/µL RNaseOUT were added. The contents were gently mixed and the mixture was incubated at 42°C for 2 minutes. 1 µL of SuperScript® II Reverse Transcriptase was added and the sample was incubated at 42°C for 50 minutes. The reaction was inactivated by heating at 70°C for 15 minutes. For the subsequent experiments, the cDNA was diluted at a ratio of 1:100 in sterile water.

2.4.3 - Amplification of target sequences by polymerase chain reaction (PCR)

Amplification of target sequences was performed using Taq DNA Polymerase (Invitrogen) according to manufacturer's recommendations. The following reagents were added to a microcentrifuge tube: 5 µL of 10X Taq Reaction Buffer, 1.5 µL of 50 mM MgCl2, 1.0 µL of 10 mM dNTP mix, 0.5 µL of 100 µM forward primer, 0.5 µL of 100 µM reverse primer, 1.0-3.0 µL of DNA template, 0.2 µL of *Taq* DNA Polymerase and sterile water up to 50 µL.

The PCR cycle was performed using the following conditions: initial denaturation at 94°C for 3 minutes, second denaturation at 94°C for 1 minute, primer annealing at 50-70°C according to the primers set used (Chapter 4, Figures 4.4 and 4.15) for 30 seconds, extension at 72°C for 1 minute and 30 seconds, return to second denaturation step for 35 cycles and final extension at 72°C for 10 minutes. Size and quality of PCR products was verified by 0.8-1.0% agarose gel electrophoresis (Section 2.4.13).

2.4.4 - Extraction and purification of deoxyribonucleic acid DNA molecules from agarose gels

PCR products and vectors were loaded onto a 1% agarose gel for purification. The bands were visualized with ultraviolet (UV) light and excised using a blade. The gel slice was weighed and collected into a microcentrifuge tube. Extraction and purification of the target cDNA sequences were performed using the QIAquick Gel Extraction Kit (QIAGEN) according to manufacturer's recommendations.

2.4.5 - Cloning with restriction enzymes

2.4.5.1 - Ligation of inserts to the pGEM®-T Easy vector

For cloning with restriction enzymes, the gel purified insert (Section 2.4.4) was firstly ligated to the pGEM®-T Easy vector (Novagen) using T4 DNA ligase (Novagen) (Section 2.4.5.3). Two μL of the ligation reaction were transformed into JM109 High Efficiency competent cells (Novagen) (Section 2.4.9) and cells were plated in selective Luria Broth (LB) agar plates supplemented with 100 μg/ml ampicillin, 0.5 mM Isopropyl β-D-1-thiogalactopyranoside (IPTG) and 80 μg/ml bromo-chloro-indolyl-galactopyranoside (X-Gal). White colonies were analyzed for the presence of insert (Section 2.4.10) and the vector was purified from a positive colony (Section 2.4.11).

2.4.5.2 - Enzymatic cleavage of inserts and vectors

Inserts and vectors were digested using restriction endonucleases (New England Biolabs). The following reagents were added to a microcentrifuge tube: 5 μL of 10X NEBuffer, 0.2 μL of BSA 100 μg/mL, 1.0 μL of 20,000 units/mL restriction endonuclease, 1 μg of DNA and sterile water up to 50 μL. The reaction was incubated over night at 37°C. Digested inserts and vector were purified from agarose gel (Section 2.4.4).

2.4.5.3 - Ligation of inserts to vectors

Ligation of inserts to vectors was performed using T4 DNA ligase (Novagen) according to manufacturer's recommendations. The following reagents were added to a microcentrifuge tube: 5 μL of 2X Rapid Ligation Buffer, 1 μL of 50 ng/μL vector, X μL of

insert (Section 2.4.7) and 1 µL of 3 Weiss units/µL T4 DNA ligase and nuclease-free water to a final volume of 10 µL. The reaction was mixed by pippeting up and down and incubated at room temperature for 1 hour or at 4°C overnight. Five µL of the ligation reaction were transformed into One Shot® TOP10 or Library Efficiency® DH5α™ chemically competent *E. coli* (Invitrogen) (Section 2.4.9).

2.4.6 - Cloning by recombination sites - Gateway® system

2.4.6.1 - TOPO® cloning reaction

Inserts were cloned into the entry vector pENTR™/D-TOPO® (Invitrogen) according to manufacturer's recommendations. The following reagents were added to a microcentrifuge: 0.5-4 µL of insert (Section 2.4.7), 1 µL salt solution, 1 µL 20 ng/uL pENTR™/D-TOPO® vector and sterile water to a final volume of 5 µL. The reaction was mixed gently and incubated for 30 minutes at room temperature. After incubation, the reaction was placed in ice. One Shot® TOP10 Competent *E. coli* was transformed with 2 µL of TOPO® Cloning reaction and plated on prewarmed selective LB agar plates containing 50 µg/ml of kanamycin (LB/kan) (Section 2.4.9).

2.4.6.2 - LR recombination reaction between the entry and expression vectors

The insert was transferred from the entry vector into the pDEST™17 expression vector (Invitrogen) using the Gateway® LR Clonase™ II enzyme mix (Invitrogen). The following reagents were added to a microcentrifuge tube: 150 ng of entry vector, 1 µL of 150 ng/mL Gateway® pDEST™17 expression vector, 2 µL of LR Clonase™ II enzyme and TE buffer (Appendix 1) up to 8 µL. The reaction was mixed briefly and incubated at

25°C for 1 hour. After incubation, 1 µL of proteinase k was added to the reaction followed by incubation at 37°C for 10 minutes. To select a positive clone, Library Efficiency® DH5α™ (Invitrogen) were transformed with 1 µL of LR recombination reaction and plated on prewarmed selective LB agar plates containing 100 µg/ml of ampicillin (LB/amp) (Section 2.4.9).

2.4.7 - Optimization of insert:vector molar ratios

For each insert, 3 cloning reactions were set up using the molar ratios of insert:vector of 0.5:1, 1:1 and 2:1. To calculate the amount of insert and vector to use in the reaction, the following formula was used:

$$\frac{\text{ng of vector} \times \text{kb size of insert} \times \text{insert:vector molar ratio}}{\text{kb (size of vector)}} = \text{ng of insert}$$

2.4.8 - Optimization of coding sequences

Optimized sequences were chemically synthesized and cloned by a commercial company (Geneart - http://www.geneart.com/). The codon usage was adapted to the codon bias of *Trichoplusia ni* genes. To prolong mRNA half life, regions of very high (> 80 %) or very low (< 30 %) Guanine Cytosine (GC) content were avoided where possible. A KOZAK sequence and the Honey Bee Mellitin (HBM) secretion signal were added upstream of the coding sequences. Cleavage sites and tags were added downstream of the coding sequences. The optimized sequences were cloned into pFastBac™1 vector (Invitrogen) using restriction enzymes.

2.4.9 - Transformation of vectors into competent *Escherichia coli*

Chemically competent *E. coli* cells were transformed by heat-shock. One to ten µL of vector was added into a 50 µL aliquot of competent cells and mixed gently. The sample was incubated for 30 minutes on ice. Cells were heat-shocked for 30 seconds at 42°C and immediately transferred to ice. 250 µL of Super Optimal Catobolite (SOC) repression medium were added followed by incubation in a rotatory shaker at 150 rpm, 37°C for 1 hour. After incubation, 50 µL and 150 µL from each transformation were plated on prewarmed selective LB agar plates and the plates were incubated over night at 37°C. As a positive control, another aliquot of competent cells was transformed with 1 µL of 10 pg/µL pUC19 (Invitrogen) to verify transformation efficiency. The same procedures were used and transformed cells were plated on LB/amp agar plates.

2.4.10 - Analysis of transformants

The transformants were analysed by PCR (Section 2.4.3). Five to ten well-spaced colonies were picked up and mixed individually in 10 µL sterile water. Three µL of the colony suspensions were used as a template for the PCR. The original colonies were treaked out on new selective LB agar plates and incubated over night at 37°C.

2.4.11 - Purification of vectors from positive colonies

Positive colonies were inoculated into 5 mL of LB medium containing 50 µg/ml Kanamycin or 100 µg/ml Ampicillin and incubated in a rotatory shaker at 150 rpm, 37°C overnight. The vector was purified from overnight-grown colonies using the QIAprep Spin

Miniprep Kit (QIAGEN) according to manufacturer's recommendations. For elution, the spin column was incubated with 25 µL of sterile water.

2.4.12 - Quantification of nucleotides

Adult worm RNA, amplified target sequences and vectors were quantified using the NanoDrop 1000 Spetrophotometer (Thermo Scientific) according to manufacturer's recommendations.

2.4.13 - Agarose gel electrophoresis and gel imaging

PCR products and vectors were visualized in a 1-0.8% w/v agarose gel prepared in Tris-borate EDTA buffer (TBE; Appendix 1). The mixture was boiled for approximately 3 minutes to dissolve the agarose. After cooling, ethidium bromide (EtBr) was added to a final concentration of 0.5 µg/ml in order to visualize the bands under ultraviolet (UV) light. The gel was poured into the casting cassette with the comb and allowed to set for 30 mins. The gel was then placed into the running module containing 1X TBE buffer. 6X loading dye (Invitrogen) was added to the samples. For visualization 5-10 µL of each sample was loaded in the wells. For extraction and purification of DNA molecules, the whole sample was loaded into the gel (Section 2.4.4). A DNA ladder (5000 bp – 100 bp; Invitrogen) was also loaded. Samples were electrophoresed at 100 volts for approximately 40-60 minutes. DNA bands were visualized under UV light using the GelDoc-It® Imaging System (UVP).

2.5 - Generation of recombinant bacmid DNA

2.5.1 - Transformation of DH10Bac competent cells with transfer vectors for transposition of the insert into the bacmid

For generation of a recombinant bacmid, DH10Bac™ *Escherichia coli* competent cells (Invitrogen) were transformed with transfer vectors (pFastBac1 constructs). Plasmids were diluted in sterile water to a final concentration of 0.2 ng/µl. Ten ng of plasmid was added to one aliquot of DH10Bac™ *E. coli*. The vector was gently mixed into the cells by taping the side of the tube. The mixture was incubated on ice for 30 minutes followed by a heat shock at 42°C for 45 seconds in a dry bath without shaking. Cells were immediately transferred to ice and allowed to chill for 2 minutes. Nine hundred µL of SOC medium (Appendix 1) were added to the cells followed by 6 hours incubation at 37°C in a rotatory shaker at 150 rpm. After incubation, cells were spread on the surface of selective LB agar plates (Appendix 1) supplemented with 50 µg/mL Kanamycin, 7 µg/mL gentamicin, 10 µg/mL tetracycline, 100 µg/mL halogenated indolyl-β-galactoside (Bluo-gal) and 40 µg/mL IPTG. Colonies were allowed to grow for 48 hours at 37°C. Plates were incubated at 4°C for 30 minutes to allow better distinction between white and blue colonies. Ten isolated white colonies were selected and spread over new selective plates. One isolated blue colony was also spread in a new plate for use as negative control. Plates were incubated at 37°C for 24 hours. After that, one isolated colony from each plate was inoculated in 5 mL of selective LB medium (Appendix 1) followed by over night incubation at 37°C in a rotatory shaker at 150 rpm. Isolation of recombinant bacmid DNA was performed as described below.

2.5.2 - Isolation of recombinant bacmid DNA

The over night grown culture was centrifuged at 4000 *g* and 4°C for 5 minutes. The supernatant was discarded and the pellet was slowly resuspended in 0.3 mL of buffer P1 (QIAprep spin miniprep kit, Qiagen). The mixture was transferred to a microcentrifuge tube followed by addition of 0.3 mL of buffer P2 (QIAprep spin miniprep kit, Qiagen). The suspension was mixed gently, 0.3 mL of 3M potassium acetate pH 5.5 was added and the mixture was incubated on ice for 10 minutes. After incubation, the mixture was centrifuged at 20,000 *g* for 10 minutes. The supernatant was carefully transferred to a microcentrifuge tube containing 0.8 mL of absolute isopropanol. The tube was inverted a few times and placed on ice for 10 minutes. After incubation, the mixture was centrifuged at 20,000 *g* for 15 minutes at room temperature and the supernatant was carefully removed. The pellet was allowed to air dry for 5 minutes at room temperature and the recombinant bacmid was dissolved in 40 µL of sterile DNAse-free water. The solution was incubated for 10 minutes at room temperature with occasional gentle tapping. Recombinant bacmid was stored at -20°C.

2.5.3 - Analysis of transformants

Each recombinant bacmid DNA isolated was tested for the presence of the insert by PCR (Section 2.4.3) using the M13 forward and M13 reverse primers and 1 µL of recombinant bacmid DNA as template. PCR was performed using the following conditions: initial denaturation at 94°C for 3 minutes, second denaturation at 94°C for 1 minute, primer annealing at 55°C for 45 seconds, extension at 72°C for 5 minutes, return to second denaturation step for 35 cycles and final extension at 72°C for 10 minutes.

2.6 - Generation of recombinant proteins in *E. coli*

2.6.1 - Production of recombinant proteins

2.6.1.1 - Expression of recombinant proteins in *Escherichia coli*

Recombinant proteins were expressed in BL21-AI™ One Shot® (Invitrogen) and Rosetta™ (DE3) (Novagen) *E. coli* cells. The expression vectors were transformed into chemically competent cells (Section 2.4.9) and well isolated colonies were selected for expression.

One single colony was inoculated into 5 mL of LB medium containing 100 μg/mL of ampicillin and incubated at 37°C in a rotatory shaker at 150 rpm overnight. The overnight-grown culture was used to inoculate fresh medium at approximately 1:20 dilution. The culture was grown until it reached optical density at 600 nm (OD_{600}) of approximately 0.5 and the protein expression was initiated by adding the inducer at various concentrations. Protein expression was induced by L-Arabinose in BL21-AI™ and IPTG in Rosetta™ (DE3). The cultures were incubated at 37°C in a rotatory shaker at 150 rpm for 5 hours.

For pilot expression, the culture was split into two. L-arabinose or IPTG was added to one of the cultures (induced culture) to a final concentration of 0.2% or 1M, respectively. The other culture was kept as a negative control (non-induced culture). For analysis of protein expression at different time points, a 0.5 mL aliquot of induced and non-induced culture was harvested at time 0, 1, 2, 3, 4 and 5 hours. The samples were centrifuged at 20,000 g, 4°C for 5 minutes, the pellets were resuspended in 100 μL of 1X reducing sample buffer (Appendix 1) and analyzed in a 15% sodium dodecyl sulfate polyacrylamide gel electrophoresis (SDS-PAGE, Section 2.8.1). For optimization of protein expression in BL21-AI™, the induction of protein expression was performed in 4

different conditions: 0.2 or 0.02% w/v L-arabinose with or without 0.1% w/v glucose.

2.6.1.2 - Cell lysis and analysis of *E. coli* expressed recombinant protein solubility

Cells were lysed by sonication using the Soniprep 150 (Sanyo). For lysis of large scale expression (100 mL culture), the pellet was resuspended in 10 mL of binding buffer (Appendix 1) and sonicated in 2 cycles of 5 minutes at 10 μm of amplitude with 5 minutes interval. The sample was kept in ice to avoid heating and foaming throughout the sonication. After lysis, the sample was centrifuged at 20,000 g, 4°C for 30 minutes and the supernatant was collected for further processing.

For analysis of protein solubility, 1 mL aliquot of induced culture was centrifuged at 20,000 g, 4°C for 5 minutes. The pellet was resuspended in 0.5 mL of PBS and sonicated in 2 cycles of 1 minute at 10 μm of amplitude with 1 minute interval. After lysis, the sample was centrifuged at 20,000 g, 4°C for 30 minutes. The supernatant was harvested and diluted in 0.5 mL of 2X reducing sample buffer (Appendix 1). The pellet was ressuspended in 1 mL of 1X reducing sample buffer (Appendix 1). The samples were analyzed in a 15% SDS-PAGE (Section 2.8.1).

2.6.2 - Production of recombinant proteins in insect cells

Recombinant baculovirus and recombinant proteins were generated in adherent insect cells. Recombinant baculovirus propagation was performed in High Five™ Cells (Invitrogen) adapted to TC100 insect medium (Invitrogen) (HI5-TC100) supplemented with 10% v/v fetal calf serum (Sigma) and 1% v/v non essential amino acid solution (Sigma). Recombinant protein expression was performed in High Five™ Cells adapted to

Express Five® Serum Free Medium (Invitrogen) (HI5-SFM) supplemented with 18 mM L-glutamine. High Five™ Cells are derived from the parental *Trichopulsia ni* cell line.

2.6.2.1 - Growth and maintenance of insect cell lines

High Five™ Cells were kept in 75 cm^2 cell culture flasks with 12 mL of medium at 27°C without antibiotics. Cells were subcultured at confluency and log phase growth was maintained by splitting the cells at a 1:5 dilution. For splitting the cells, the medium was removed, 10 mL of fresh medium was added, cells were dislodged by sloughing and 2 mL of the suspended cells were transferred to a new 75 cm^2 cell culture flask with 10 mL of fresh medium. Cell viability was measured once a month by trypan blue exclusion.

2.6.2.2 - Transfection of insect cells with recombinant bacmid DNA for generation of recombinant baculovirus

HI5-TC100 cells were transfected with recombinant bacmid using PolyFect transfection reagent (Quiagen). 4 x 10^5 cells/well were plated in a 6 well plate in 3 mL of medium and allowed to grow for 24 hours at 27°C. Ten μg of recombinant bacmid was diluted in TC100 insect medium with no FCS or antibiotics (incomplete medium) to a final volume of 100 μL. Ten μL of PolyFect transfection reagent was added and mixed by pipetting up and down 5 times. The mixture was incubated at room temperature to allow complex formation. The medium was gently aspirated from the well, the cells were washed once with 3 mL of Dulbeco's PBS (DPBS; Sigma) and 1.5 mL of complete TC100 insect medium was added per well. 0.4 mL of TC100 complete media was added to the mixture and mixed by pipetting up and down twice and the solution was immediately added to the cells. The solution was released slowly in small drops to avoid disturbing the complexes.

Cells were incubated for 72 hours at 27°C. After that, the media containing recombinant baculovirus passage 0 (P0) stock was harvested and centrifuged at 1500 *g* at room temperature for 5 minutes. The supernatant was collected and stored at 4°C protected from light. Baculovirus is light sensitive therefore, whenever handling the virus stocks, direct light was avoided.

2.6.2.3 - Amplification of the recombinant baculovirus stock

Recombinant baculovirus passage 0 (P0) stock was amplified 3 times generating the P3 stock that was used for protein expression. Firstly, recombinant baculovirus passage 1 (P1) stock was generated by infecting 90-95% confluent HI5-TC100 cells with 300 µL of P0. For that purpose, cells were allowed to grow on T-75 cm^2 tissue culture flasks until they reached 90-95% confluency. Medium was completely removed and 6 mL of TC100 insect cell medium supplemented with 1% v/v non essential aminoacids and 1% v/v FCS was added. 300 µL of recombinant baculovirus P0 stock was added. After 1 hour incubation at 27 °C, the media was replaced by complete TC100 insect cell medium. Cells were incubated at 27°C for 72 hours. The medium containing P1 recombinant baculovirus stock was harvested and centrifuged at 1500 *g* for 5 minutes at room temperature. Supernatant was collected and stored at 4-8°C protected from light. For generation of P2 stock, the same procedures were performed except that, instead of 300 µL, 250 µL of P1 stock was used to infect the HI5-TC100 cells.

Generation of P3 stock was performed in 90-95% confluent HI5-TC100 cells in T-175 cm^2 tissue culture flasks. Medium was completely removed and 13 mL of TC100 insect cell medium supplemented with 1% v/v non-essential amino acids and 1% v/v FCS was added. 750 µL of recombinant baculovirus P2 stock was added. Cells were incubated for 1 hour at 27 °C and the media was replaced by 30 mL of complete TC100 insect cell

medium. P3 stock was harvested as described above and stored at 4°C protected from light.

2.6.2.4 - Expression of recombinant proteins in insect cells

Expression was performed in 90-95% confluent HI5-SFM cells in T-175 cm^2 tissue culture flasks. Medium was completely removed and 7 mL of Express Five® Serum Free Medium plus 5 mL of P3 stock were added. Cells were incubated for 5 hours at 27°C for baculovirus absorption. The media was replaced by complete 30 mL of fresh Express Five® Serum Free Medium. Cells were incubated at 27°C for 72 hours. The medium containing the recombinant protein was harvested and centrifuged at 10,000 *g* at 4°C for 30 minutes. Supernatant was collected and stored at -20°C.

2.6.2.5 – Insect cell culture supernatant processing

Insect cell culture supernatant was concentrated using the Stirred Cell 8400 (Millipore) and a regenerated cellulose Ultrafiltration Disc Membrane (Millipore) of 10 kDa MWCO. The concentration was performed at 4°C. The concentrate was subjected to dialysis with nickel-affinity chromatography binding buffer (Appendix 1, Section 2.7.3).

2.7 - Purification of recombinant proteins

2.7.1 - Purification by affinity chromatography

2.7.1.1 - Nickel-affinity chromatography using gravity-flow

Nickel-nitrilotriacetic acid (Ni-NTA) metal-affinity agarose resin (QIAGEN) was used for purification of proteins by gravity-flow affinity chromatography. The sample, 1-10 mL, was incubated with 1-5 mL NI-NTA agarose at 4°C with shaking for 1 hour. The sample-Ni-NTA mixture was loaded into a disposable polypropylene column and the resin was allowed to set down at the bottom of the column. Once the resin had settled down, the flow through was collected. The column was washed with 5-10 mL of ice-cold washing buffer (Appendix 1), 4 times. Recombinant protein was eluted with 7-16 mL of ice-cold elution buffer (Appendix 1). Elution fractions of 1-2 mL were collected and analysed in a 15% SDS-PAGE (Section 2.8.1). Elution fractions were stored at -20°C.

For optimization of protein elution point, 7 elution buffers (Appendix 1) with increasing concentrations of imidazole (50, 75, 100, 150, 200, 300 and 500 mM) were used. One mL of each elution buffer was added to the column. One elution fraction of 1.0 mL was collected per elution buffer and the samples were analysed in a 15% SDS-PAGE (Section 2.8.1). Elution fractions were stored at -20°C.

2.7.1.2 - Nickel-affinity chromatography using automated systems

Recombinant proteins were also purified using the automated systems ÄKTAFPLC™ (GE Life Sciences) or BioLogic LP low-pressure chromatography system (Bio-Rad) and 5 mL HisTrap™ HP columns (GE Life Sciences). Buffers were prepared

with high quality chemicals and passed through 0.45 μm filters. The sample was centrifuged at 20,000 g, 4°C for 30 minutes and passed through 0.45 μm filters. The column was equilibrated at a 2 mL/min flow rate with 5 column volumes (CV) of binding buffer (Appendix 1) or until UV absorbance baseline was stable. The sample was injected into the column at a 1 ml/min. After sample injection, unbound proteins were washed out with 5 CV of washing buffer (Appendix 1) at a 2 mL/min flow rate. Bound proteins were eluted with 5 CV of elution buffer (Appendix 1) at a 1 ml/min flow rate. Aliquots of 1 mL were collected and analysed in 15% SDS-PAGE (Section 2.8.1).

Samples of 10 mL or less were purified using the ÄKTAFPLC™ system. The Biologic Lp system was used for purification with bigger sample volumes. In this case, the sample was injected into the column in a closed cycle allowing it to pass through the column at least 2-3 times.

2.7.2 - Purification by anion exchange

Anion exchange was performed using 1 mL HiTrap Q HP columns (GE Life Sciences) in the automated systems ÄKTAFPLC™ (GE Life Sciences). Buffers were prepared with high quality chemicals and passed through 0.45 μm filters. The sample was centrifuged at 20,000 g, 4°C for 30 minutes and passed through 0.45 μm filters. The column was equilibrated at a 1 mL/min flow rate with 5 column volumes (CV) of binding buffer (Appendix 1) or until UV absorbance baseline was stable. The sample was injected into the column at a 0.5 ml/min. After sample injection, unbound proteins were washed out with 5 CV of washing buffer (Appendix 1) at a 1 mL/min flow rate. Bound proteins were eluted at a 0.5 ml/min flow rate in 3 steps: a gradient of 0-33.3% 10 CV of elution buffer A, 100% 5 CV of elution buffer A and 100% 5 CV of elution buffer B. Aliquots of 1 mL were collected and analysed in 15% SDS-PAGE (Section 2.8.1).

2.7.3 - Dialysis

Buffer exchange was performed using dialysis cassette Slide-A-Lyzer 3.5 or 10 kDa MWCO (Thermo Scientific Pierce). The sample was loaded into the cassette according to manufacturer's recommendations. The cassette was placed in a beaker with buffer and incubated at 4°C with agitation for 16-24 hours. The buffer was changed 2-3 times and the total volume of buffer used was at least 100 times more than the sample volume. After dialysis, samples were centrifuged at 20,000 *g* and 4°C for 30 minutes to check for precipitation.

2.7.4 - Refolding of recombinant proteins

Insoluble proteins were refolded by dialysis (Section 2.7.3) with PBS solutions containing gradually decreasing concentrations of Urea: 8, 7, 6, 5, 4, 3, 2, 1.5, 1, 0.75, 0.5, 0.25, 0.1 M and PBS (Appendix 1). The sample was incubated at least 1 hour in each solution. After dialysis, samples were centrifuged at 20,000 *g* and 4°C for 30 minutes, the supernantant was harvested and analyzed in a 15% SDS-PAGE (Section 2.8.1).

2.7.5 – Protein sample concentration

Purified recombinant proteins were concentrated using the Vivaspin 20 (Sartorius Stedim Biotech) according to manufacturer's recommendations. Samples were concentrated to at least 1 mL

2.8 - Proteomics analysis

2.8.1 - One dimension sodium dodecyl sulfate polyacrylamide gel electrophoresis (SDS-PAGE)

Protein samples were resolved by sodium dodecyl sulfate polyacrylamide gel electrophoresis (SDS-PAGE) (*142*). Protein samples were loaded into a 8 cm (W) x 7.3 cm (H) 12% or 15% SDS-PAGE and electrophoresed using the BIO-RAD Mini-PROTEAN® 3 Cell electrophoresis system (Bio-Rad). Firstly, glass plates were placed on the casting stand assembly. The resolving gel monomer solution (Appendix 1) was poured in between the plates, immediately covered with a thin layer of isopropanol and allowed to set for 30 minutes at room temperature. After that, the isopropanol was washed out with distilled water and the stacking gel monomer solution (Appendix 1) poured on top of the running gel. A comb with a 2D-well, 10 or 15 wells was inserted and the gel was allowed to set for 30 minutes at room temperature. After that, the comb was removed and the gel sandwich was placed on the electrode assembly. The electrode assembly was placed into the clamping frame and lowered into the mini tank. Running buffer (Appendix 1) was added to the mini tank up to the top of the gel plates. Before loading, samples were diluted in reducing or non-reducing sample buffer (Appendix 1) and heated at 95°C or incubated at room temperature, respectively, for 5 minutes. Samples were loaded into the wells and allowed to settle evenly into the bottom of the well. The lid was placed on top of the mini tank and the gel was run at 30 mA. Running time was approximately 1 hour and 15 minutes. The run was stopped when the sample buffer dye line reached the bottom of the gel. The gel was removed from the glass plates and stained as described (Sections 2.8.4 to 2.8.6).

2.8.2 - Two dimension sodium dodecyl sulfate polyacrylamide gel electrophoresis (2D SDS-PAGE)

WES proteins were resolved by two-dimension sodium dodecyl sulfate polyacrylamide gel electrophoresis (2D SDS-PAGE) (*143, 144*).

2.8.2.1 - Sample precipitation

Three hundred μg of WES proteins were incubated with 10% w/v trichloroacetic acid (TCA; $C_2HCl_3O_2$) at 4°C over night. After incubation, the sample was centrifuged at 20,000 g, 4°C for 10 minutes. The supernatant was discarded and the pellet was washed 3 times with 1 mL of ice-cold acetone. For washing, the acetone was added, the pellet was resuspended and the sample was centrifuged at 20,000 g, 4°C for 1 minute. The remaining pellet was allowed to dry for 1 minute and then solubilized in 250 μL of rehydration buffer (Appendix 1)

2.8.2.2 - First-dimension isoelectric focusing (IEF)

The first-dimension isoelectric focusing (IEF) was performed in a 13 cm immobilized pH gradient (IPG) strip with non-linear pH range from 3 to 11 (GE Life Sciences). The sample was loaded into a strip holder and the strip was placed on top of it. The strip was overlaid with Immobiline DryStrip Cover Fluid (GE Life Sciences). The run was performed in the Etthan IPGphor II unit (GE Life Sciences) at 20°C, 60 volts for 14 hours, 500 volts for 1 hour, 1000 volts for 1 hour and 8000 volts for 2 hours.

2.8.2.3 – Equilibration

After first dimension, proteins were reduced with dithiothreitol (DTT, 1% w/v) and alkylated with iodoacetamide (IAM, 2.5% w/v). For that, the strip was incubated in 1% w/v DTT in equilibration buffer (Appendix 1) for 15 minutes with gentle mixing and then incubated in 2.5% w/v IAM in equilibration buffer for 15 minutes with gentle mixing.

2.8.2.4 - Second dimension

The second dimension separation was performed in a 138 (W) x 130 (H) mm 12% SDS-PAGE using the ATTO Corporation electrophoresis system AE-6220 (ATTO Bioscience and Biotechnology - http://www.atto.co.jp/eng/index.html). Glass plates were placed on the casting unit, the resolving gel monomer solution (Appendix 1) was poured in between the plates, immediately covered with a thin layer of isopropanol and allowed to set for 30 minutes at room temperature. After that, the isopropanol was washed out with distilled water and the gel sandwich was placed on the electrophoresis chamber. The IPG strip was carefully placed on top of the gel ensuring that no air bubbles got trapped between the strip and the gel surface. To seal the IPG strip in place, the strip was covered with pre-heated agarose sealing solution (Appendix 1) and the agarose was allowed to solidify for 5 minutes. Running buffer (Appendix 1) was added to the buffer chamber and the gel was run at 25 mA. Running time was approximately 2 hours and 30 minutes. The run was stopped when the sample buffer dye line reached the bottom of the gel. The gel was removed from the glass plates and stained by colloidal coomassie staining (Section 2.8.5). After staining was completed, gels were imaged (Section 2.8.8) and all visible spots were manually collected using pipette tips. The pipette tip was enlarged to the approximate

size of the spot by cutting it with scissors. Spots were identified by mass spectrometry (Section 2.8.3).

2.8.3 - Mass Spectrometry

Mass spectrometry was performed by the BSRC Mass Spectrometry and Proteomics facility at St. Andrews University (http://www.st-andrews.ac.uk/ ~bmsmspf/). The samples were analyzed by a quadrupole-time-of-flight mass spectrometer, the Q-STAR Pulsar XL (Applied Biosystems). Briefly, samples were digested with trypsin and loaded onto a capillary liquid chromatography system (nanoLC system). The peptides were separated by reverse phase chromatography and directly eluted into the mass spectrometer. The peptides were then subjected to electrospray ionization and tandem mass spectrometry (ESI-MS/MS) generating a mass (m) -to-charge (z) ratios (m/z) spectrum. The mass spectrometry data was analyzed using the Mascot software (http:/www.matrixscience.com/) searching the *S. mansoni* GeneDB sequence database (http://www.genedb.org/Homepage) for protein hits. Protein hits were identified through peptide mass fingerprint. Protein hits that showed at least 2 matched peptides with expectation values lower than 0.05 were considered positive hits. The expectation value is the number of times a peptide score could happen by chance. A completely random match has an expectation value of 1 or more.

2.8.4 - Coomassie Brilliant Blue staining

Before starting any of the staining procedures, gels were rinsed in distilled water (dH_2O). Unless stated, all steps were performed in a rotary shaker at room temperature with gentle shaking. Firstly, gels were incubated over night in coomassie solution

(Appendix 1). After that, gels were washed several times with distilled water and incubated in destain solution (Appendix 1) for several hours until bands were clearly visible. The destain solution was replaced whenever it became bluish. Once bands were clearly visible, the gel was rinsed in distilled water and incubated in SDS-PAGE storage solution (Appendix 1) for at least 20 minutes.

2.8.5 - Colloidal Coomassie Brilliant Blue staining

For colloidal staining, gels were firstly incubated in fixing solution (Appendix 1) for 1 hour followed by over night incubation in final staining solution (Appendix 1). After that, gels were transferred into neutralizing solution (Appendix 1), incubated for 3 minutes and washed in washing solution (Appendix 1) for 45 seconds. Gels were then transferred into stabilizing solution and incubated over night (Appendix 1). Gels were kept in stabilizing solution for storage.

2.8.6 - Silver staining

For silver staining, all solutions were prepared in ultrapure water. Gels were placed in disposable plastic containers and incubated in fixative solution (Appendix 1) for 20 minutes followed by 10 minutes in wash solution (Appendix 1). Afterwards, gels were manually rinsed at least 3 times with ultrapure water and then for a further 10 minutes in the rotatory shaker. Gels were incubated in sensitizer solution (Appendix 1) for 3 minutes followed by 2 washes with ultra-pure water for 30 seconds. After washing, gels were incubated in silver nitrate solution (Appendix 1) for 20 minutes and washed twice with ultrapure water for 1 minute. To develop the reaction, gels were incubated in developer solution (Appendix 1) for 1 minute. The solution was replaced and the gels incubated until

the bands were clearly visible. To stop the reaction, stop solution (Appendix 1) was added and gels were incubated for 2 minutes. After that, gels were washed in ultrapure water for 5 minutes and incubated in storage solution (Appendix 1) for at least 20 minutes.

2.8.7 - Western blot

Sample proteins were detected by Western blot (*145*). Firstly, for each Western blot, concentrations of antibodies or sera dilutions were optimized. The highest dilution that did not show any loss of binding to the target band as compared to the lowest dilution was selected for the final Western blot. Probing was carried out using the BioRad™ mini gel transfer system (Bio-Rad). Prior to use, a polyvinylidene fluoride (PVDF) membrane was activated in methanol for 5 minutes at room temperature with gentle shaking. The gel, activated membrane, filter paper and fibre pads were equilibrated in transfer buffer (Appendix 1) for 10 minutes. A gel/membrane sandwich was assembled in the following order: cassette (anode, gray side), fibre pad, filter paper, gel, membrane, filter paper, fibre pad and cassette (cathode, black side). Air bubbles were gently rolled out during gel/membrane sandwich assembly using a glass tube. The gel/membrane sandwich was placed into the blotting module and transferred to the mini tank containing a cooling unit and transfer buffer (Appendix 1). To keep buffer temperature and ion distribution even, a stirring bar was added to the mini tank. Transfer was carried out at 100 V for 1 hour. After transfer, membrane was incubated in blocking solution A (Appendix 1) at 4°C over night. This step and all subsequent incubations were carried out with gentle shaking. Except for the blocking, all other steps were carried out at room temperature. Membrane was washed 3 times in washing solution (Appendix 1) for 5 minutes each.

For probing with the mouse monoclonal anti-V5 antibody (mouse IgG1 isotype; Sigma), an extra blocking step was carried out in blocking solution B (Appendix 1) for 30

minutes. The monoclonal anti-V5 antibody was used in different dilutions ranging from 1:1000 to 1:100000 depending on the experiment. The membrane was incubated with anti-V5 diluted in incubation solution for 2 hours followed by 3 washes in washing solution for 5 minutes each. After washing, the membrane was incubated in horseradish peroxidase (HRP)-labeled goat anti-mouse IgG1 (Zymed) diluted 1:2000 in incubation solution for 1 hour followed by 3 washes in washing solution for 5 minutes each. The reaction was detected with Immobilon Western Chemiluminescent HRP Substrate (Millipore) according to manufacturer's recommendations. The blot was exposed to an X-ray film for 10 seconds to 30 minutes according to the experiment.

For detection of polyhistidine-tagged protein, the membrane was incubated with HRP-labeled monoclonal anti-6X polyhistidine antibody (R&D), diluted 1:1000 in blocking solution A (Appendix 1), for 1 hour followed by 3 washes in washing solution for 5 minutes each. The reaction was developed with 3,3′-Diaminobenzidine tetrahydrochloride (DAB; $(NH_2)_2C_6H_3C_6H_3(NH_2)_2 \cdot 4HCl$; Sigma). DAB was diluted according to manufacturer's recommendations and the membrane was incubated until bands were clearly visible. Membrane was washed with dH_2O for 5 minutes to stop the reaction.

For detection of proteins using rabbit anti-WES, rabbit anti-SmPrx1, rabbit anti-SmTrx1 or mouse anti-SmCYP1 polyclonal antibodies, membrane was incubated in the sera diluted 1:400 (rabbit sera) or 1:100 (mouse sera) in blocking solution B (Appendix 1) over night at 4°C. Then washed 3 times in washing solution (Appendix 1) for 5 minutes each. After washing, the membrane was incubated in HRP-labeled goat anti-rabbit IgG or HRP-labeled goat anti-mouse IgG (Dako) diluted 1:2000 in incubation solution for 1 hour followed by 3 washes in washing solution for 5 minutes each. The reaction was developed with DAB as described above.

2.8.8 - SDS-PAGE gels and Western blots imaging

Gels and Western blots were imaged using the HP Scanjet G4050 Photo Scanner (Hewlett-Packard - www.hp.com/)

2.8.9 – Densitometry analysis

The density of bands in Western blots was analyzed using the Image Processing and Analysis in Java software (ImageJ, http://rsb.info.nih.gov/ij/) .

2.8.10 - Protein quantification

Protein content was quantified using the Bicinchoninic acid (BCA) Protein Assay Reagent (Thermo Scientific Pierce) according to manufacturer's recommendations.

2.8.11 - Detection of endotoxin

Protein solutions were tested for endotoxin content using the QCL-1000® Endpoint Chromogenic LAL Assay (Lonza) according to manufacturer's recommendations.

2.9 - Bioinformatic analysis

2.9.1 – Identification of homologues

The search for protein homologues was performed using the Protein-Protein Basic Local Alignment Search Tool (BLASTp) accessed at the National Center for Biotechnology Information (NCBI) website (http://blast.ncbi.nlm.nih.gov/Blast.cgi) (*146*). Sequences alignments that showed a bit score higher than 30 and an expected value (E value) lower than 1e-16 were considered homologues.

2.9.2 – Analysis of Gene Ontology

Analysis of Gene Ontology (GO) was performed using the QuickGo web-based browser provided by the European Bioinformatics Institute (EBI, http://www.ebi.ac.uk/) (*147*). GO terms associated with biological process and molecular function were addressed to each protein sequence by searching the UniProtKB-GOA database (*148*).

2.9.3 – Prediction of secretion

Protein sequences were subjected to analysis by the web-based browser SignalP 4.0 Server (http://www.cbs.dtu.dk/services/SignalP/) for predictions of a secretory signal peptide (*149*). Protein sequences that did not contain a signal peptide were subjected to analysis by the web-based browser SecretomeP 2.0 Server for prediction of non-classical secretion *i.e.* not signal peptide triggered protein secretion (*150*). SecretomeP analysis was performed using predictions for mammalian sequences and proteins that showed a SecP score higher than 0.5 where considered non-classically secreted proteins.

2.9.4 – Prediction of transmembrane helices

The TMHMM Server v. 2.0 (http://www.cbs.dtu.dk/services/TMHMM/) was used for the predictions of transmembrane helices in the protein sequences (*151*).

2.9.5 – Protein signatures search

The InterProScan (http://www.ebi.ac.uk/Tools/pfa/iprscan/) sequence search was used for assignment of protein signatures (*152*). This tool combines different protein signature recognition methods that search against specific databases. The protein signatures that describe the same protein family or domain are grouped into unique InterPro entries, with a unique accession number. The protein sequence applications use by InterproScan are listed in the table below (Table 2.4).

Program Name	Description
BlastProDom	Scans the families in the ProDom database. ProDom is a comprehensive set of protein domain families automatically generated from the UniProtKB/Swiss-Prot and UniProtKB/TrEMBL sequence databases using psi-blast. In InterProScan the blastpgb program is used to scan the database. BLASTPGP performs gapped blastp searches and can be used to perform iterative searches in PSI-BLAST and PHI-BLAST mode.
FPrintScan	Scans against the fingerprints in the PRINTS database. These fingerprints are groups of motifs that together are more potent than single motifs by making use of the biological context inherent in a multiple motif method.
HMMPIR	Scans the hidden markov models (HMMs) that are present in the PIR Protein Sequence Database (PSD) of functionally annotated protein sequences, PIR-PSD.
HMMPfam	Scans the hidden markov models (HMMs) that are present in the PFAM Protein families database.
HMMSmart	Scans the hidden markov models (HMMs) that are present in the SMART domain/domain families database.
HMMTigr	Scans the hidden markov models (HMMs) that are present in the TIGRFAMs protein families database.
ProfileScan	Scans against PROSITE profiles. These profiles are based on weight matrices and are more sensitive for the detection of divergent protein families.
HAMAP	Scans against HAMAP profiles. These profiles are based on weight matrices and are more sensitive for the detection of divergent bacterial, archaeal and plastid-encoded protein families.
PatternScan	PatternScan is a new version of the PROSITE pattern search software, which uses new code developed by the PROSITE team.
SuperFamily	SUPERFAMILY is a library of profile hidden Markov models that represent all proteins of known structure.

Table 2.4 - **InterProScan member programs description**. (Source: European Bioinformatics Institute – Retrieved October 28, 2011 from http://www.ebi.ac.uk/Tools/pfa/iprscan/)

2.9.6 – Multiple Sequence Alignment

Alignment of multiple sequences was performed using the ClustalW2 programme provided by the EBI (http://www.ebi.ac.uk/Tools/msa/clustalw2/) (*153*).

Proteomic analysis of *Schistosoma mansoni* male adult worm excretory-secretory molecules

3.1 - Introduction

In the past few years, several studies on the proteomes of helminths and other parasites have been performed. Proteomics studies are a resourceful approach to elucidate the protein composition of helminths that may influence the biology and development of the organisms under investigation. Moreover, in the case of parasites, proteomics studies indisputably contribute to the identification of novel vaccine candidates, drug targets and immunomodulatory candidates. A limitation, however, is the need of a large cDNA transcriptome database for the subsequent successful identification of protein hits.

Several proteomics studies have been carried out on various stages of the schistosome life cycle, using the three major species that infect man. One of the pioneer studies was a comparison of the soluble proteome across 4 life cycle stages of *S. mansoni* (cercaria, lung-schistosomula, adult worm and egg) (*154*). Remarkably, a similar protein composition was detected across the all four stages with no stage-specific marker identified. Subsequent studies have concentrated on the analysis of the worm tegument. Firstly, a comparison between the tegumental proteome with the "stripped worm" proteome identified proteins specific to the tegument (*155*). In another approach, tegument detached membranes were subjected to a sequential protein extraction with reagents of increasing solubilising power (*46*). This study demonstrated morphological and functional compartmentalization of the parasite surface. Another technique, the biotinylation of intact worms, permitted the identification of schistosome proteins exposed at the surface of the parasite which are presumed to be the molecules that are mostly exposed to the host immune system (*156, 157*).

Further development of the proteomics field has focused on the identification of stage- and/or gender-specific helminth secretions. Molecules released by the parasite into the host's tissue and blood circulation are the most likely to interact with the immune cells and mediate the modulation of host immune response. Therefore, the study of helminth secretomes has major implications in the elucidation of this complex parasite-host interface. In the past few years, the numbers of publications with respect to the proteomic analysis of excretory-secretory helminth proteins have dramatically increased (*51, 52, 158, 159*). The excretory-secretory products of *S. bovis* (*160*) and *S. japonicum* (*161*) adult worms have been studied, however, there is no record of proteomic analysis of the *S. mansoni* adult worm excretome-secretome to date.

3.2 – Objective

Isolation of *S. mansoni* adult male worm excretory-secretory (WES) molecules, followed by proteomic analysis of WES molecules and selection of putative immunomodulatory candidates for further characterization.

3.3 - Results

3.3.1 – *In vitro* isolation of *S. mansoni* adult male worm excretory-secretory molecules

For isolation of worm excretory-secretory (WES) molecules, 7-week infected mice were perfused for collection of male adult *S. mansoni* worms followed by incubation of the worms *in vitro*. For that, the male adult worms were transferred to a dialysis bag with incubation media and the dialysis bag was placed in a cell culture plate. Nutrient media, that contains 10% FCS, was added to the plate. Seventy-two hours later, the incubation media was harvested and processed (Figure 3.1).

The quality of each WES batch was evaluated. The protein content of the WES batch was measured, protein degradation and the overall protein profile were assessed and the level of endotoxin was measured. Batches that showed (i) no protein degradation, as shown in the SDS-PAGE, (ii) a similar protein profile, in terms of positive bands visualized in a Western blot using rabbit polyclonal anti-WES and (iii) a maximum of 0.5 Endotoxin unit/mg (EU/mg) were approved (Figure 3.2). It was estimated that each worm produced approximately 0.11 μg of total protein during 72 hrs of *in vitro* incubation. In an attempt to improve the WES protein yield, a longer incubation time of 96 hrs was tested. However, there were no major differences in the protein yield in relation to 72 hr incubation. No longer incubation times were tested as after 96 hours worms become gradually motionless and start dying. The protein profile as seen by Western blot with anti-WES showed slight variations between batches. Therefore, the batches were pooled for use in the experiments.

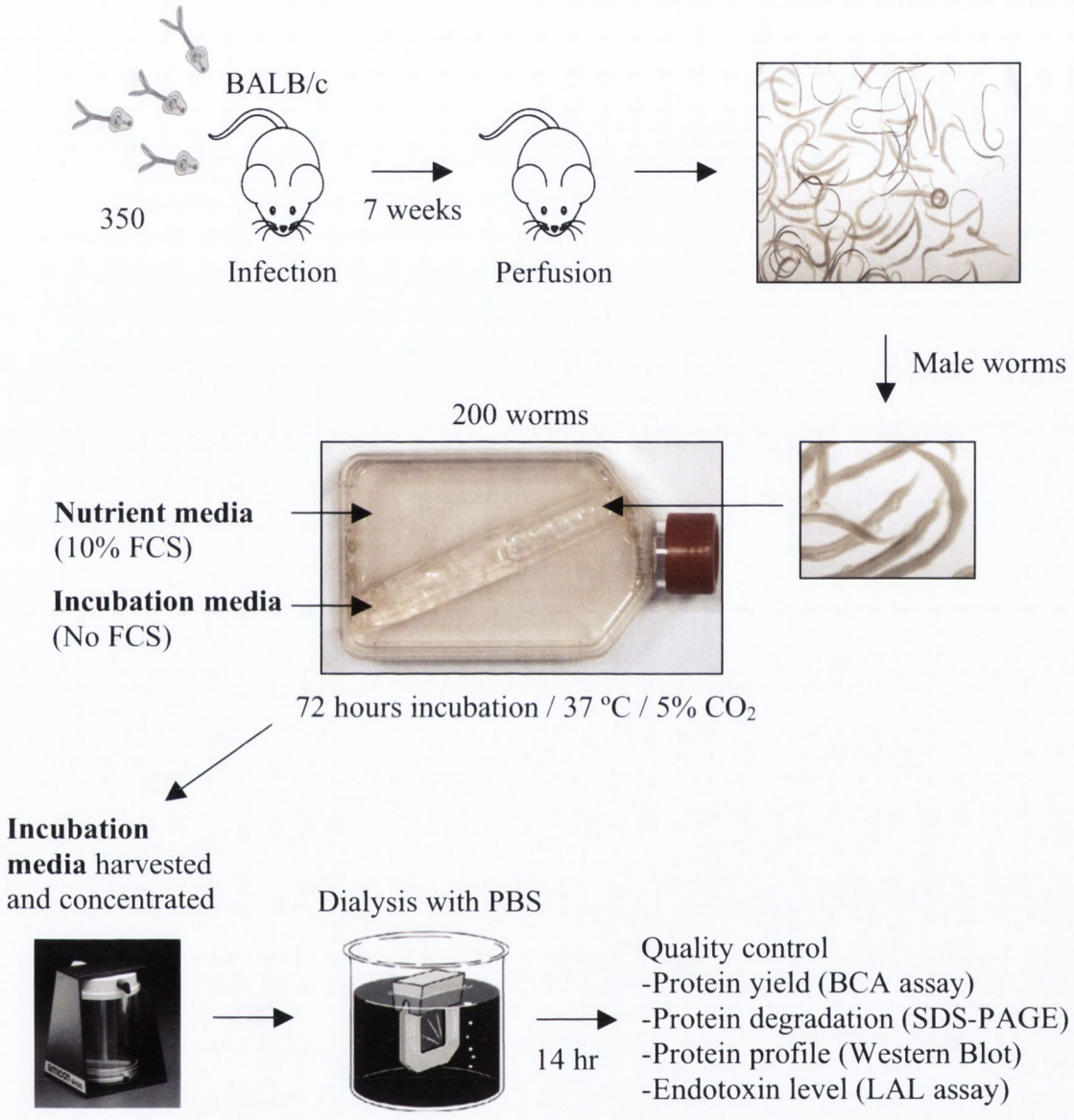

Figure 3.1: **Isolation of *S. mansoni* adult male worm excretory-secretory (WES) molecules.** Mice were infected with *S. mansoni* cercariae and perfused 7 weeks later for collection of adult worms. Males were carefully separated from females and transferred to a dialysis bag with incubation media. Worms were incubated for 72 hours. The incubation media was harvested, concentrated to ~ 1 mL and dialyzed with PBS over night. Each WES batch was tested for quality.

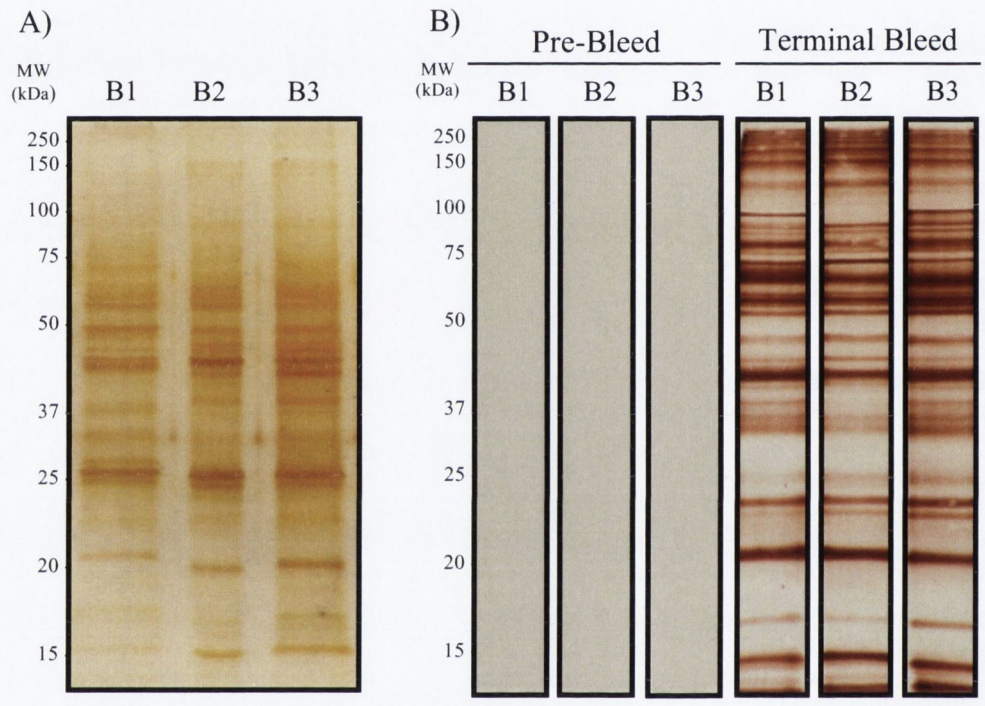

Figure 3.2: **Quality control of *S. mansoni* male worm WES molecules batches**. A) 12% SDS-PAGE and silver staining of 3 independent WES batches (B1, B2 and B3). B) Western blot of WES preparation with rabbit polyclonal anti-WES rabbit serum (1:400 dilution) from terminal bleed and HRP-conjugated anti-rabbit IgG (1:2000 dilution). Serum collected previously to rabbit immunization with WES molecules (pre-bleed) was used as negative control.

3.3.2 – Proteomic analysis of *S. mansoni* adult male worm excretory-secretory proteins

3.3.2.1 – Comparative proteomic analysis of *S. mansoni* male worm excretory-secretory molecules versus adult worm soluble somatic molecules

Initial WES proteomic analysis was a comparison between whole adult worm (AW) somatic soluble proteins and WES proteins. For that, AW and WES preparations, 200 μg of each, were resolved by two-dimensional (2D) electrophoresis in parallel. The overall distribution and intensity of the spots revealed a differing protein composition between the two preparations. To confirm this visual demarcation, one spot unique to the AW preparation (spot 1), two spots common to both preparations, with similar isoelectric point (pI) and molecular weight (spots 2 and 3) and two spots unique to the WES preparation (spots 4 and 5) were selected for identification by mass spectrometry (Figure 3.3).

Spot 1, which is unique to AW preparation, was identified as *S. mansoni* Paramyosin (Smp_021920.1), a major structural protein of schistosomes and other invertebrates. Spots 2 and 3, which are common to WES and AW preparations, were identified as *S. mansoni* Fatty acid-binding protein (Smp_095360.1). *S. mansoni* fatty acid protein, also know as Sm14, was previously identified in the worm tegument and the *S. japonicum* homologue has been detected in the adult worm excretory-secretory proteome (*46, 161*). Spots 4 and 5, that are unique to the WES preparation, were identified as *S. mansoni* Cyclophilin (Smp_040130), also known as Smp17.7. To-date, *S. mansoni* Cyclophilin has not been characterized but the *S. japonicum* homologue was identified in the worm excretory-secretory proteome (*161*). These results demonstrate that WES and

AW preparations have common and unique molecules therefore confirming a demarcation of the protein profile between these preparations.

***S. mansoni* male worm somatic molecules**

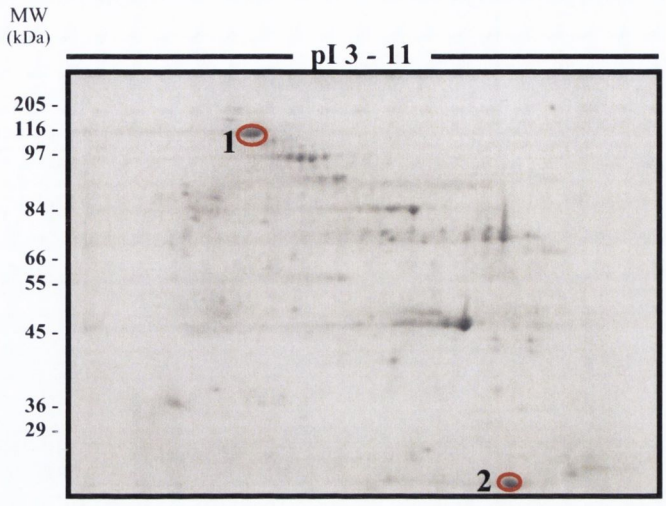

***S. mansoni* male worm excretory-secretory molecules**

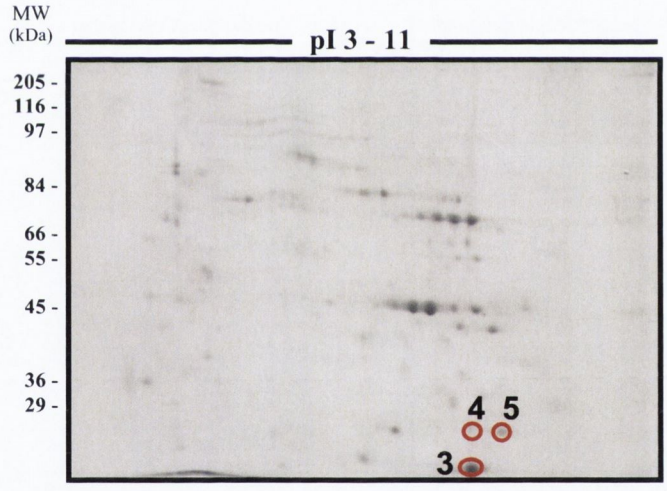

Protein hits:
1: *S. mansoni* Paramyosin (Smp_021920.1)
2-3: *S. mansoni* Fatty acid-binding protein (Smp_095360.1)
4-5: *S. mansoni* Cyclophilin (Smp_040130)

Figure 3.3: **2D proteomic analysis of *S. mansoni* somatic and excretory-secretory molecules.** AW and WES preparations (200 µg) were first electrofocused in a 3-11 IPG strip and then electrophoresed in a 12% SDS-PAGE. The gels were stained with colloidal coomassie blue. Five spots (circled and numbered 1-5) were selected for identification by mass spectrometry. Protein hits are indicated below the gel images.

3.3.2.2 - Identification of *S. mansoni* adult male worm excretory-secretory proteins

Following confirmation that WES protein composition differed from AW somatic proteins, 300 μg of WES preparation were resolved by 2D electrophoresis for identification of WES proteins. A total of 180 spots were identified and collected (Figure 3.4). The 2D spots were subjected to mass spectrometry as described in Chapter 2, section 2.8.3, in an order of decreasing intensity until no detection was possible.

WES mass spectrometry data was analysed using the *S. mansoni* GeneDB sequence database (http://www.genedb.org/Homepage/Smansoni). A total of 170 spots were subjected to mass spectrometry, of which 136 (80 %) showed positive hits resulting in the identification of 111 proteins (Table 3.1).

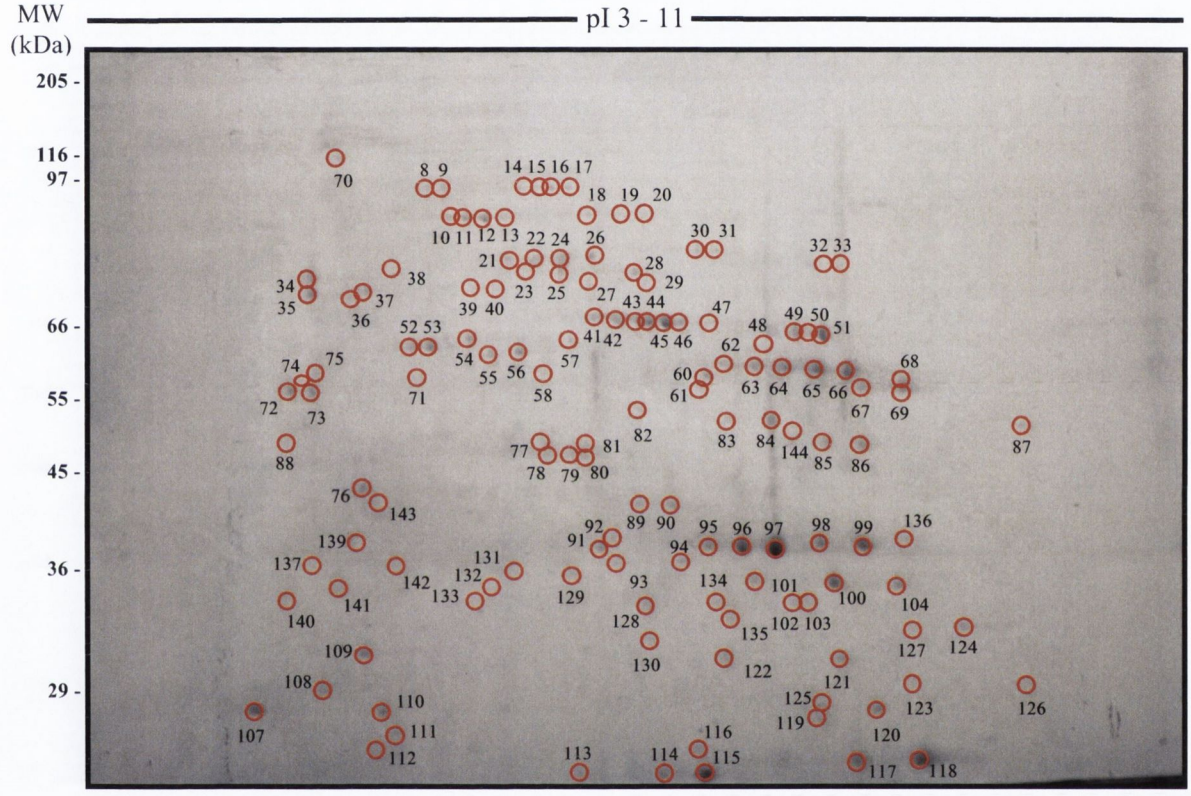

Figure 3.4: **A representative 2D gel of *S. mansoni* WES molecules**. Protein spots are circled in red and numbered according to the order they were collected.

	ID	Protein description	MS	CO	SP	SecP	TM
1	Smp_000100	Filamin	467	5%	-	0.539	-
2	Smp_000660	Ornithine--oxo-acid transaminase	444	25%	-	0.424	-
3	Smp_001360	Thymidylate kinase	596	57%	-	0.747	-
4	Smp_003230	Sh3 domain grb2-like protein B1 (endophilin B1)	218	31%	-	0.801	-
5	Smp_003990	Triosephosphate isomerase, putative	1048	56%	-	0.508	-
6	Smp_004350	Ubiquitin-conjugating enzyme E2 l, putative	74	10%	-	0.681	-
7	Smp_004470.1	Peroxiredoxin, Prx3	136	20%	-	0.672	-
8	Smp_004780.1	Immunophilin, putative	398	24%	-	0.27	-
9	Smp_005350	Calcium-binding protein, putative	512	16%	-	0.834	-
10	Smp_006390	Cystatin B, putative	421	58%	-	0.562	-
11	Smp_007270.1	Alpha-actinin, putative	193	24%	-	0.488	-
12	Smp_008070	Thioredoxin, Trx1	551	79%	-	0.585	-
13	Smp_008110	WD40-repeat containing protein	592	13%	-	0.558	-
14	Smp_008660.1	Gelsolin, putative	1238	62%	-	0.406	-
15	Smp_009760	14-3-3 protein, putative	416	33%	-	0.246	-
16	Smp_009780.2	14-3-3 protein, putative	245	19%	-	0.414	-
17	Smp_011830	Hypothetical protein / C4Q068	118	21%	-	0.845	-
18	Smp_014010	Adenylyl cyclase-associated protein, putative	177	11%	-	0.548	-
19	Smp_017730	200-kDa GPI-anchored surface glycoprotein	134	2%	+	0.667	-
20	Smp_018240.3	Cell division control protein 48 aaa family protein, putative	339	12%	-	0.179	-
21	Smp_018890	Phosphoglycerate kinase	901	78%	-	0.442	-
22	Smp_019050.2	Hypothetical protein / C4Q286	367	32%	-	0.728	-
23	Smp_019640.1	Calcyphosine/tpp, putative	213	26%	-	0.516	-

Table 3.1: ***S. mansoni*** **adult male worm excretory-secretory proteins.** ID – identification number at GeneDB; MS – mowse score; CO - percentage of sequence coverage; SP – signal peptide; SecP – SecretomeP score, values above 0.5 indicate possible secretion; TM - number of transmembrane domains; (+) - signal peptide detected; (-) no signal peptide or transmembrane domain detected.

	ID	Protein description	MS	CO	SP	SecP	TM
24	Smp_020920.1	DNAj homolog subfamily B member 4, putative	608	35%	-	0.661	-
25	Smp_021800	Prefoldin subunit 3-related	358	37%	-	0.49	-
26	Smp_022340	Pdz and lim domain protein, putative	225	14%	-	0.609	-
27	Smp_024110	Phosphopyruvate hydratase	1214	51%	-	0.471	-
28	Smp_028670.1	Carbonic anhydrase II (carbonate dehydratase II), putative	265	22%	-	0.809	-
29	Smp_030000	Leucine aminopeptidase (M17 family)	377	23%	-	0.545	-
30	Smp_030370	Calreticulin autoantigen homolog precursor, putative	1292	53%	+	0.504	-
31	Smp_030730	Tubulin beta chain, putative	1074	47%	-	0.509	-
32	Smp_031770.4	Tropomyosin, putative	2078	90%	-	0.454	-
33	Smp_032580.2	Subfamily T1A non-peptidase homologue (T01 family)	572	43%	-	0.372	-
34	Smp_032950	Calmodulin (CaM), putative	197	44%	-	0.742	-
35	Smp_033540	Carbonyl reductase, putative	131	14%	-	0.387	-
36	Smp_034490	Proteasome catalytic subunit 1 (T01 family)	238	26%	-	0.435	-
37	Smp_034840.2	14-3-3 epsilon	288	25%	-	0.225	-
38	Smp_035270.2	Malate dehydrogenase, putative	404	27%	-	0.343	-
39	Smp_038950	L-lactate dehydrogenase, putative	337	19%	-	0.492	-
40	Smp_040130	Cyclophilin	927	77%	-	0.543	-
41	Smp_040790	Cyclophilin B, putative	113	19%	+	0.884	-
42	Smp_042160.2	Fructose 1,6-bisphosphate aldolase, putative	1775	72%	-	0.317	-
43	Smp_042400	Hypothetical protein / C4Q8L5	161	25%	+	0.739	-
44	Smp_043030	Hexokinase	121	9%	-	0.283	-
45	Smp_043120	Universal stress protein, putative	69	9%	-	0.536	-
46	Smp_044010.2	Tropomyosin, putative	1230	60%	-	0.38	-

Table 3.1 (Continued)

	ID	Protein description	MS	CO	SP	SecP	TM
47	Smp_046600	Actin-1, putative	1188	49%	-	0.5	-
48	Smp_046690	Ubiquitin (ribosomal protein L40), putative	185	16%	-	0.411	-
49	Smp_047370	Malate dehydrogenase, putative	395	19%	-	0.5	-
50	Smp_047650	Ferritin, putative	455	57%	-	0.676	-
51	Smp_049250	Heat shock protein, putative	333	22%	-	0.823	1
52	Smp_049270	Heat shock protein, putative	139	7%	-	0.684	-
53	Smp_049550	Heat shock protein 70 (hsp70), putative	163	6%	+	0.546	-
54	Smp_050390	Aldehyde dehydrogenase, putative	814	36%	-	0.535	-
55	Smp_053220.1	Aldo-keto reductase, putative	759	46%	-	0.393	-
56	Smp_054160	Glutathione S-transferase 28 kDa (GST 28) (GST class-mu), putative	1338	90%	-	0.3	-
57	Smp_054240	Translationally-controlled tumor protein homolog (TCTP) (Histamine-releasing factor), putative	583	59%	-	0.407	-
58	Smp_056440	Superoxide dismutase [mn], putative	88	10%	-	0.689	-
59	Smp_056760	Protein disulfide-isomerase, putative	1340	54%	+	0.805	-
60	Smp_056970.1	Glyceraldehyde-3-phosphate dehydrogenase (phosphorylating)	966	47%	-	0.412	-
61	Smp_059480	Peroxiredoxin, Prx1	450	49%	-	0.597	-
62	Smp_059660	Hypothetical protein / C4QDG6	67	4%	-	0.533	-
63	Smp_059980	Arginase, putative	307	22%	-	0.493	-
64	Smp_063120.1	Inosine triphosphate pyrophosphatase (itpase) (inosine triphosphatase), putative	229	42%	-	0.571	-
65	Smp_063530.1	Apoferritin-2	593	51%	+	0.711	-
66	Smp_064380	Aspartate aminotransferase, putative	231	13%	-	0.544	-
67	Smp_064860	Heat shock protein 70 (hsp70)-interacting protein, putative	517	36%	-	0.448	-
68	Smp_066760.2	Merlin/moesin/ezrin/radixin, putative	102	5%	-	0.328	-

Table 3.1 (Continued)

	ID	Protein description	MS	CO	SP	SecP	TM
69	Smp_067890	Proteasome subunit alpha 2 (T01 family)	588	37%	-	0.443	-
70	Smp_072900.1	Hsp90 co-chaperone (tebp), putative	77	8%	-	0.344	-
71	Smp_078690	Calponin homolog, putative	570	49%	-	0.575	-
72	Smp_079010	Camp-dependent protein kinase type II-alpha regulatory subunit, putative	261	21%	-	0.596	-
73	Smp_079770.1	Protein disulfide-isomerase ER-60 precursor (ERP60), putative	999	41%	+	0.662	-
74	Smp_081430	Short chain dehydrogenase, putative	170	22%	-	0.28	-
75	Smp_082030	Family C56 non-peptidase homologue (C56 family)	386	54%	-	0.498	-
76	Smp_083870	PwLAP aminopeptidase (M17 family)	193	10%	-	0.449	-
77	Smp_086330.2	Calponin-related	260	32%	-	0.732	-
78	Smp_086480	Antigen Sm21.7, putative	222	25%	-	0.658	-
79	Smp_086530	Tegumental protein Sm 20.8, putative	250	29%	-	0.36	-
80	Smp_090080	Serpin, putative	806	36%	-	0.601	-
81	Smp_090120.1	Alpha tubulin, putative	68	3%	-	0.475	-
82	Smp_091010	Glyoxalase II (Hydroxyacylglutathione hydrolase), putative	568	42%	-	0.386	-
83	Smp_092280	Proteasome subunit alpha 3 (T01 family)	724	45%	-	0.384	-
84	Smp_092750	Nucleoside diphosphate kinase	329	63%	-	0.384	-
85	Smp_095360.1	Fatty acid binding protein	325	54%	-	0.798	-
86	Smp_096760	Phosphoglycerate mutase	419	34%	-	0.293	-
87	Smp_102070	GST class-mu, SM26/2 antigen, glutathione S-transferase 26 kDa	878	60%	-	0.445	-
88	Smp_103320	Nuclear movement protein nudc, putative	193	7%	-	0.345	-
89	Smp_105020	Titin, putative	66	4%	-	0.571	-
90	Smp_106930.2	Heat shock protein 70, putative	1324	46%	-	0.273	-
91	Smp_123440.1	Fad oxidoreductase, putative	123	12%	-	0.551	-

Table 3.1 (Continued)

	ID	Protein description	MS	CO	SP	SecP	TM
92	Smp_130110	Proteasome subunit alpha 6 (T01 family)	691	18%	-	0.471	-
93	Smp_132670.1	Myosin regulatory light chain, putative	162	16%	-	0.567	-
94	Smp_135950	Lethal giant larvae homolog 2, cell polarity protein , inorganic pyrophosphatase, putative	316	5%	-	0.476	-
95	Smp_136240.6	Vesicle-associated membrane protein (vamp), putative	161	10%	-	0.556	1
96	Smp_140900.2	Hypothetical protein / C4Q6S1	156	19%	-	0.512	-
97	Smp_143470.2	Spectrin beta chain, brain 3 (Spectrin, non-erythroid beta chain 3) (Beta-IV spectrin), putative	100	1%	-	0.229	-
98	Smp_146950	Hypothetical protein / C4Q9Q0	286	1%	-		-
99	Smp_147470	Leucine-rich transmembrane proteins, putative	116	7%	-	0.064	1
100	Smp_150820	Acyl-CoA thioesterase-related	174	7%	-	0.867	-
101	Smp_151690	Translation initiation inhibitor, putative	205	42%	-	0.649	-
102	Smp_152710.2	Glutathione-s-transferase omega, putative	941	63%	-	0.418	-
103	Smp_155060.2	Set, putative	201	14%	-	0.424	-
104	Smp_157500	Calpain (C02 family)	393	5%	-	0.406	-
105	Smp_158110.2	Peroxiredoxin, Prx2	59	9%	-	0.731	-
106	Smp_161920	Actin, putative	1114	43%	-	0.511	-
107	Smp_163720	Endophilin B1, putative	106	14%	-	0.699	-
108	Smp_176200.2	Superoxide dismutase [Cu-Zn]	372	58%	-	0.569	-
109	Smp_179810	Troponin t, invertebrate, putative	361	20%	-	0.2	-
110	Smp_187370	Phosphoglycerate kinase	805	70%	-	0.352	-
111	Smp_194770	ATP:guanidino kinase (Smc74), putative	834	23%	-	0.402	-

Table 3.1 (Continued)

3.3.3 – Bioinformatic analysis of *S. mansoni* adult male worm excretory-secretory proteins

3.3.3.1 – Identification of *S. mansoni* adult male worm excretory-secretory protein homologues in *S. japonicum* and *S. haematobium*

Homologues of some of the *S. mansoni* WES proteins identified were also present in two other human-infecting species, *S. japonicum* and *S. haematobium* using the Basic Local Alignment Search Tool (BLAST) as described in Chapter 2 (Section 2.9.1). Similarly to *S. mansoni*, above 90% of *S. japonicum* genome was sequenced by July 2009 on a project developed by the Chinese National Human Genome Center at Shangai (*162*). Except for the *S. mansoni* WD40-repeat containing protein Smp_008110 (WES hit 13), *S. japonicum* homologues were detected for all *S. mansoni* WES proteins (Table 3.2). The *S. japonicum* homologues showed similarities to *S. mansoni* WES hits higher than 50%. More than 70% of the homologues (80 proteins) detected showed more than 80% similarity to their respective *S. mansoni* homologues. On the other side, the sequencing of the *S. haematobium* genome is still in progress (*163*) and only 9 homologues were identified (Table 3.2). For details regarding the bit score and expected value (E value) for sequence alignments see Appendix 2.

S. mansoni male adult worm excretory-secretory proteins			*S. japonicum*		*S. haematobium*	
	GeneDB ID	Protein description	GenBank ID	Identity (%)	GenBank ID	Identity (%)
1	Smp_000100	Filamin	AAF13300.1	50.5	-	-
2	Smp_000660	Ornithine--oxo-acid transaminase	CAX70598.1	9252	-	-
3	Smp_001360	Thymidylate kinase	CAX75696.1	84.82	-	-
4	Smp_003230	Sh3 domain grb2-like protein B1 (endophilin B1)	CAX70480.1	68.15	-	-
5	Smp_003990	Triosephosphate isomerase, putative	AAP06170.1	92.86	BAF62292.1	95.24
6	Smp_004350	Ubiquitin-conjugating enzyme E2 l, putative	AAW27854.1	98.08	-	-
7	Smp_004470.1	Peroxiredoxin, Prx3	AAW25436.1	88.18	-	-
8	Smp_004780.1	Immunophilin, putative	AAW27121.1	78.25	-	-
9	Smp_005350	Calcium-binding protein, putative	AAP06154.1	100	-	-
10	Smp_006390	Cystatin B, putative	CAX73577.1	77.23	-	-
11	Smp_007270.1	Alpha-actinin, putative	CAX82586.1	93.75	-	-
12	Smp_008070	Thioredoxin, Trx1	AAD52699.1	65.38	-	-
13	Smp_008110	WD40-repeat containing protein	-	-	-	-
14	Smp_008660.1	Gelsolin, putative	AAW26119.1	83.1	-	-
15	Smp_009760	14-3-3 protein, putative	ACE06842.1	69.05	-	-
16	Smp_009780.2	14-3-3 protein, putative	ACE06842.1	67.23	-	-
17	Smp_011830	Hypothetical protein / C4Q068	AAW26653.1	85.58	-	-
18	Smp_014010	Adenylyl cyclase-associated protein, putative	CAX69899.1	75.83	-	-
19	Smp_017730	200-kDa GPI-anchored surface glycoprotein	AAX26034.2	72.44	-	-
20	Smp_018240.3	Cell division control protein 48 aaa family protein, putative	AAW27581.1	92.28	-	-
21	Smp_018890	Phosphoglycerate kinase	AAP06480.1	94.24	-	-
22	Smp_019050.2	Hypothetical protein / C4Q286	CAX73085.1	80.37	-	-

Table 3.2: ***S. mansoni* adult male worm excretory-secretory protein homologues.** *S. mansoni* WES proteins were subjected to similarity analysis using BLAST. Sequence alignments that showed a bit score higher than 30 and an E value lower than 1e-16 were considered homologs. ID – identification number at GeneDB or GenBank databases; (-) – no homologs found.

S. mansoni male adult worm excretory-secretory proteins			*S. japonicum*		*S. haematobium*	
	GeneDB ID	Protein description	GenBank ID	Identity (%)	GenBank ID	Identity (%)
23	Smp_019640.1	Calcyphosine/tpp, putative	AAW27463.1	83.17	-	-
24	Smp_020920.1	DNAj homolog subfamily B member 4, putative	AAW25539.1	91.94	AAD00565.1	45.45
25	Smp_021800	Prefoldin subunit 3-related	AAW27184.1	90.48	-	-
26	Smp_022340	Pdz and lim domain protein, putative	AAW27396.1	84.26	-	-
27	Smp_024110	Phosphopyruvate hydratase	P33676.1	87.79	-	-
28	Smp_028670.1	Carbonic anhydrase II (carbonate dehydratase II), putative	CAX73485.1	93	-	-
29	Smp_030000	Leucine aminopeptidase (M17 family)	CAX69903.1	88.85	-	-
30	Smp_030370	Calreticulin autoantigen homolog precursor, putative	AAC00515.1	77.27	-	-
31	Smp_030730	Tubulin beta chain, putative	CAX71985.1	99.32	-	-
32	Smp_031770.4	Tropomyosin, putative	CAX76350.1	98.94	Q26503.1	65.02
33	Smp_032580.2	Subfamily T1A non-peptidase homologue (T01 family)	AAP06025.1	97.15	-	-
34	Smp_032950	Calmodulin (CaM), putative	CAX79767.1	76.47	-	-
35	Smp_033540	Carbonyl reductase, putative	CAX77260.1	85.56	-	-
36	Smp_034490	Proteasome catalytic subunit 1 (T01 family)	CAX69953.1	89.78	-	-
37	Smp_034840.2	14-3-3 epsilon	AAW26747.1	81.51	-	-
38	Smp_035270.2	Malate dehydrogenase, putative	CAX72207.1	87.8	-	-
39	Smp_038950	L-lactate dehydrogenase, putative	CAX70888.1	87.65	-	-
40	Smp_040130	Cyclophilin	CAX72371.1	69.18	-	-
41	Smp_040790	Cyclophilin B, putative	AAW27862.1	84.98	-	-
42	Smp_042160.2	Fructose 1,6-bisphosphate aldolase, putative	AAW25258.1	96.14	-	-
43	Smp_042400	Hypothetical protein / C4Q8L5	AAW24701.1	79.01	-	-
44	Smp_043030	Hexokinase	CAX69908.1	88.22	-	-
45	Smp_043120	Universal stress protein, putative	CAX70901.1	80.62	-	-
46	Smp_044010.2	Tropomyosin, putative	ACE06925.1	98.24	-	-

Table 3.2 (continued)

	S. mansoni male adult worm excretory-secretory proteins		*S. japonicum*		*S. haematobium*	
	GeneDB ID	**Protein description**	**GenBank ID**	**Identity (%)**	**GenBank ID**	**Identity (%)**
47	Smp_046600	Actin-1, putative	CAX69775.1	98.14	-	-
48	Smp_046690	Ubiquitin (ribosomal protein L40), putative	CAX72429.1	99.67	-	-
49	Smp_047370	Malate dehydrogenase, putative	CAX74903.1	93.84	-	-
50	Smp_047650	Ferritin, putative	CAX70640.1	87.21	-	-
51	Smp_049250	Heat shock protein, putative	CAX78232.1	62.73	-	-
52	Smp_049270	Heat shock protein, putative	AAW24545.1	90.36	-	-
53	Smp_049550	Heat shock protein 70 (hsp70), putative	ACE06854.1	91.05	-	-
54	Smp_050390	Aldehyde dehydrogenase, putative	CAX73522.1	90.02	-	-
55	Smp_053220.1	Aldo-keto reductase, putative	CAX77280.1	83.87	-	-
56	Smp_054160	Glutathione S-transferase 28 kDa (GST 28) (GST class-mu), putative	CAX72408.1	77.25	P30114.1	91.94
57	Smp_054240	Translationally-controlled tumor protein homolog (TCTP) (Histamine-releasing factor), putative	P91800.1	58.82	Q8I8A2.2	80.29
58	Smp_056440	Superoxide dismutase [mn], putative	AAW26480.1	89.81	-	-
59	Smp_056760	Protein disulfide-isomerase, putative	CAX69780.1	89.83	-	-
60	Smp_056970.1	Glyceraldehyde-3-phosphate dehydrogenase (phosphorylating)	CAX80263.1	90.24	-	-
61	Smp_059480	Peroxiredoxin, Prx1	CAX71944.1	83.7	-	-
62	Smp_059660	Hypothetical protein / C4QDG6	AAP06314.1	77.93	-	-
63	Smp_059980	Arginase, putative	CAX70201.1	80.22	-	-
64	Smp_063120.1	Inosine triphosphate pyrophosphatase (itpase) (inosine triphosphatase), putative	AAX27755.2	84.78	-	-
65	Smp_063530.1	Apoferritin-2	CAX72682.1	84.46	-	-
66	Smp_064380	Aspartate aminotransferase, putative	CAX69569.1	81.29	-	-
67	Smp_064860	Heat shock protein 70 (hsp70)-interacting protein, putative	AAW27834.1	84.64	-	-
68	Smp_066760.2	Merlin/moesin/ezrin/radixin, putative	CAX82442.1	70.44	-	-

Table 3.2 (continued)

S. mansoni male adult worm excretory-secretory proteins			*S. japonicum*		*S. haematobium*	
	GeneDB ID	Protein description	GenBank ID	Identity (%)	GenBank ID	Identity (%)
69	Smp_067890	Proteasome subunit alpha 2 (T01 family)	gAAW25457.1	96.6	-	-
70	Smp_072900.1	Hsp90 co-chaperone (tebp), putative	CAX79556.1	80.43	-	-
71	Smp_078690	Calponin homolog, putative	ACE06952.1	92.8	-	-
72	Smp_079010	Camp-dependent protein kinase type II-alpha regulatory subunit, putative	AAW24538.1	89.92	-	-
73	Smp_079770.1	Protein disulfide-isomerase ER-60 precursor (ERP60), putative	ACE06849.1	76.08	-	-
74	Smp_081430	Short chain dehydrogenase, putative	AAW27200.1	90.08	-	-
75	Smp_082030	Family C56 non-peptidase homologue (C56 family)	CAX70856.1	86.41	-	-
76	Smp_083870	PwLAP aminopeptidase (M17 family)	AAX27247.2	90.56	-	-
77	Smp_086330.2	Calponin-related	AAP06498.1	95.26	-	-
78	Smp_086480	Antigen Sm21.7, putative	CAX72713.1	64.86	AAW49250.1	47.8
79	Smp_086530	Tegumental protein Sm 20.8, putative	AAP06272.1	78.89	BAF62289.1	30.39
80	Smp_090080	Serpin, putative	CAX76359.1	65.1	-	-
81	Smp_090120.1	Alpha tubulin, putative	XP_002580033.1	100	AAW66672.1	40.32
82	Smp_091010	Glyoxalase II (Hydroxyacylglutathione hydrolase), putative	AAP06491.1	88.51	-	-
83	Smp_092280	Proteasome subunit alpha 3 (T01 family)	CAX70764.1	95.67	-	-
84	Smp_092750	Nucleoside diphosphate kinase	AAO59410.1	88.59	-	-
85	Smp_095360.1	Fatty acid binding protein	AAP14675.1	92.42	BAF62288.1	99.24
86	Smp_096760	Phosphoglycerate mutase	CAX76329.1	94	-	-
87	Smp_102070	GST class-mu, SM26/2 antigen, glutathione S-transferase 26 kDa	P08515.3	82.57	-	-
88	Smp_103320	Nuclear movement protein nudc, putative	AAP06040.1	82.98	-	-
89	Smp_105020	Titin, putative	AAW24500.1	91.97	-	-
90	Smp_106930.2	Heat shock protein 70, putative	AAC00519.1	61.99	-	-
91	Smp_123440.1	Fad oxidoreductase, putative	AAW26635.1	83.71	-	-

Table 3.2 (continued)

S. masoni male adult worm excretory-secretory proteins			*S. japonicum*		*S. haematobium*	
	GeneDB ID	Protein description	GenBank ID	Identity (%)	GenBank ID	Identity (%)
92	Smp_130110	Proteasome subunit alpha 6 (T01 family)	AAW25684.1	93.99	-	-
93	Smp_132670.1	Myosin regulatory light chain, putative	AAW26951.1	97.14	-	-
94	Smp_135950	Lethal giant larvae homolog 2, cell polarity protein, inorganic pyrophosphatase, putative	AW25943.1	87.02	-	-
95	Smp_136240.6	Vesicle-associated membrane protein (vamp), putative	AAW26025.1	79.61	-	-
96	Smp_140900.2	Hypothetical protein / C4Q6S1	AAW26313.1	72.65	-	-
97	Smp_143470.2	Spectrin beta chain, brain 3 (Spectrin, non- erythroid beta chain 3) (Beta-IV spectrin), putative	AAX26038.2	93.33	-	-
98	Smp_146950	Hypothetical protein / C4Q9Q0	AAX26800.2	62.64	-	-
99	Smp_147470	Leucine-rich transmembrane proteins, putative	AAW25815.1	86.61	-	-
100	Smp_150820	Acyl-CoA thioesterase-related	AAW27278.1	71.14	-	-
101	Smp_151690	Translation initiation inhibitor, putative	CAX74647.1	78.76	-	-
102	Smp_152710.2	Glutathione-s-transferase omega, putative	CAX74405.1	75.1	-	-
103	Smp_155060.2	Set, putative	CAX72508.1	97.82	-	-
104	Smp_157500	Calpain (C02 family)	BAA74718.1	83.91	-	-
105	Smp_158110.2	Peroxiredoxin, Prx2	BAD90102.1	89.69	-	-
106	Smp_161920	Actin, putative	XP_002578518.1	100	-	-
107	Smp_163720	Endophilin B1, putative	AAP06059.1	64.31	-	-
108	Smp_176200.2	Superoxide dismutase [Cu-Zn]	CAX76410.1	85.62	-	-
109	Smp_179810	Troponin t, invertebrate, putative	AAW25147.1	92.12	-	-
110	Smp_187370	Phosphoglycerate kinase	CAX77845.1	94.77	-	-
111	Smp_194770	ATP:guanidino kinase (Smc74), putative	CAX73626.1	90.08	-	-

Table 3.2 (continued)

3.3.3.2 – Gene ontology: biological process and molecular function

To address the different molecular functions and biological processes in which WES proteins are putatively involved, an analysis of the gene ontology (GO) terms associated with the identified proteins was performed using the QuickGo web-based browser provided by the European Bioinformatics Institute (EBI, http://www.ebi.ac.uk/). Regarding the molecular function gene ontology, the analysis provided 82 GO terms which were assigned to 87 (78.38 % of the total) WES molecules. The major molecular function categories were oxidoreductase activity (GO:0016491) and nucleotide binding (GO:0000166) (Figure 3.5 A). The analysis of the biological process GO terms provided 47 terms that were addressed to 68 (62.16 % of of the total) WES proteins. Most common categories were oxidation-reduction (GO:0055114) and glycolysis (GO:0006096) (Figure 3.5 B). For detailed information with respect to GO terms addressed to individuals WES hits see Appendix 3 (Table A3).

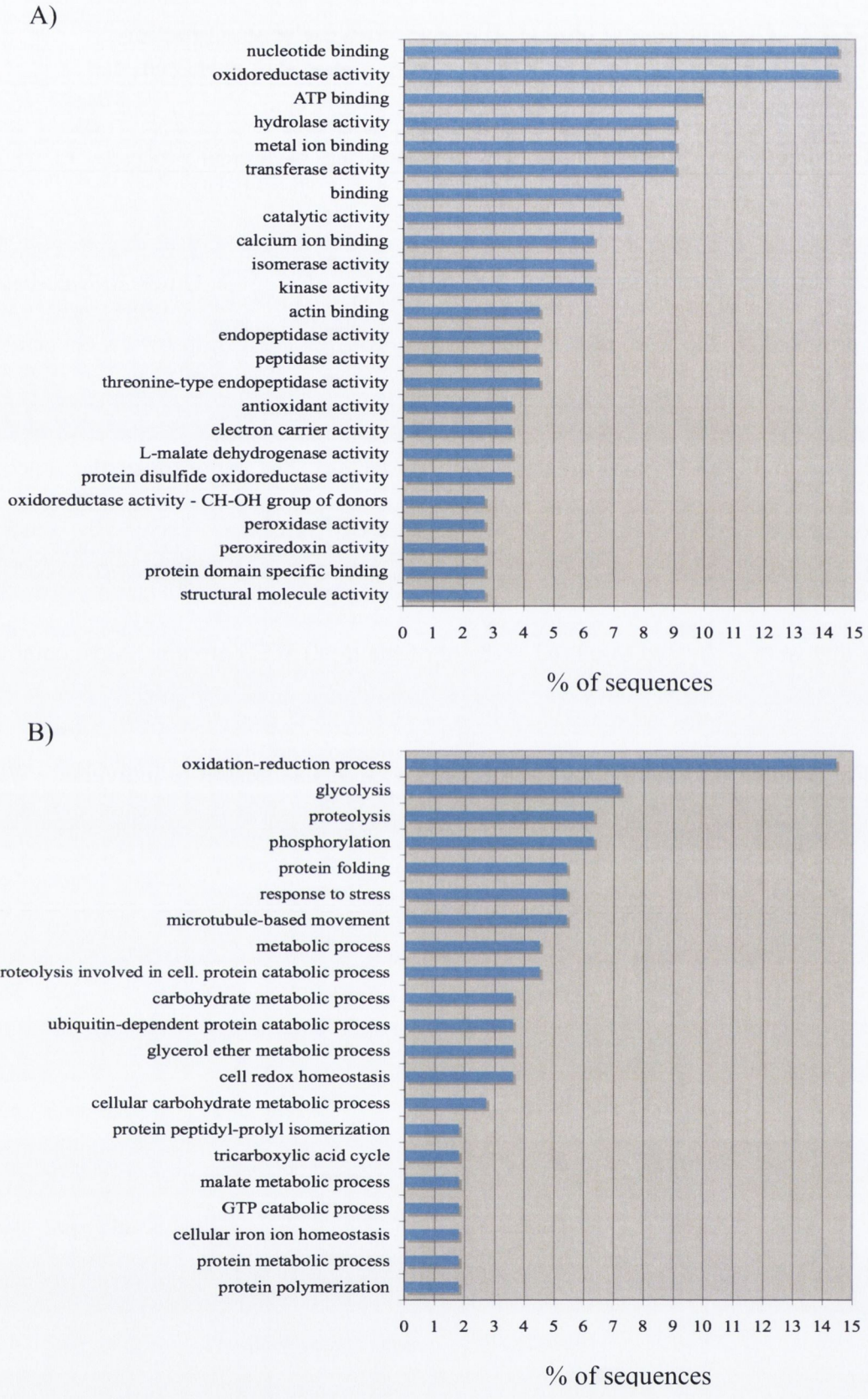

Figure 3.5: **Distribution of gene ontology terms for *S. mansoni* adult male worm excretory-secretory proteins.** A) GO terms associated with molecular functions. B) GO terms associated with biological processes. Lower axis shows the percentage of proteins addressed to each category. Only GO terms with occurrence higher than 2 are shown.

3.3.3.3 – Prediction of secretory, excretory and transmembrane WES proteins

WES proteins were categorised as:

(i) classically secreted proteins – presence of a signal peptide, as detected by the SignalP 4.0 Server (*149*),

(ii) non-classically secreted proteins – predicted to be secreted by a non classical pathway, as detected by the SecretomeP 2.0 Server using predictions for mammalian sequences (*150*),

(iii) transmembrane proteins – predicted to contain one or more than one transmembrane helice by the TMHMM Server v. 2.0 as described in chapter 2 (Sections 2.9.3 and 2.9.4).

(iv) WES proteins that could not be assigned to any of these categories were considered excretory molecules.

Seven point two % (8 molecules) of WES proteins contain a signal peptide for secretion, while 41.4 % (46 proteins) were predicted to be secreted via a non-classical pathway. Therefore, 48.65 % (54 proteins) of WES proteins were classified as secretory proteins. Three WES molecules were predicted to be transmembrane proteins (2.7 % of the total), and the remaining 53 molecules (47.75 % of the total) were classified as excretory proteins. One uncharacterized protein, the hypothetical protein Smp_146950, does not comprise a signal peptide or a transmembrane helice. However, its classification is uncertain since the sequence exceeds the length limit for prediction using the SecretomeP server. Therefore, Smp_146950 was classified as a protein of unknown excretion-secretion status (Figure 3.6).

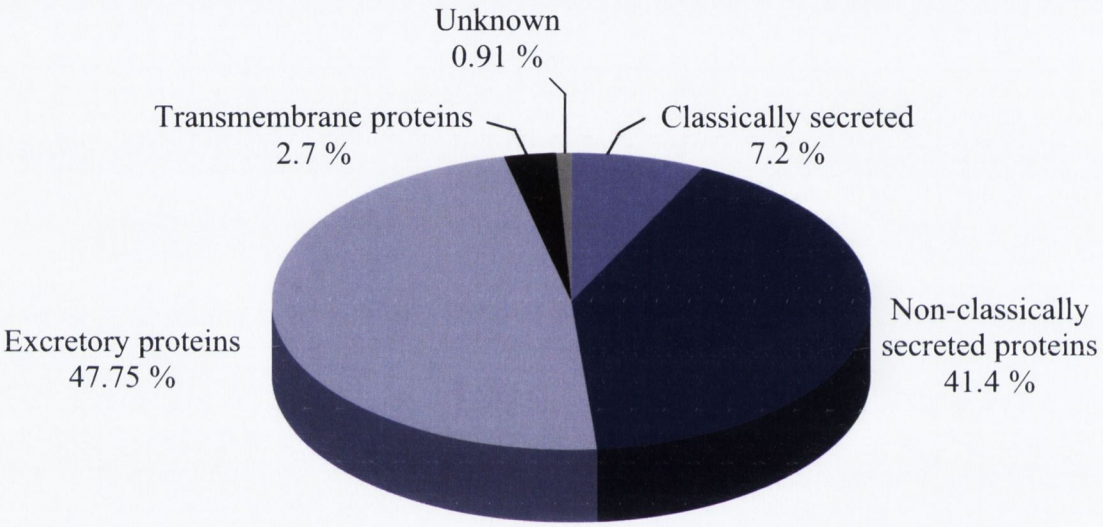

Figure 3.6: **Prediction of secretory, excretory and transmembrane WES proteins**. Prediction of classically secreted, non-classically secreted and transmembrane proteins by bioinformatic analysis. Percentages refer to the relative number of proteins assigned to each category.

3.3.3.4 – Vaccine candidates detected in the *S. mansoni* adult worm WES molecules

As presented in Chapter 1 (Section 1.1.5), several schistosome antigens have been tested as vaccine candidates in different animal models. By reviewing the literature available, *S. mansoni* WES proteins that were tested as vaccine candidates were identified (Table 3.3). With regard to the 6 WHO candidates selected in the 1990s, 3 were detected among the WES proteins, TPI (*164*), Sm28GST (*165*) and Sm14 (*166*). The ECL (200 kDa protein) (*167*), Sm21.7 (*168*), Smp-80 (*169*) and Cu-Zn superoxide dismutase (*170*) were also detected in the WES. Two promising candidates, recently tested, Sm29 (*171*) and Sm-TSP-2 (*36*), were not identified among the WES molecules. Sm29 and Sm-TSP-2 have been characterized as membrane proteins highly expressed in the schistosome tegument and therefore are not expected to be excretory-secretory proteins (*46*).

ID	Protein description	Vaccine name	Vaccine type	Egg reduction	Worm reduction	Ref
Smp_003990	Triosephosphate isomerase, putative	TPI	transfer of anti-TPI monoclonal antibody	ND	30-60%	(*164*)
Smp_017730	200-kDa GPI-anchored surface glycoprotein	ECL (200 kDa protein)	DNA	ND	33-40%	(*167*)
Smp_054160	Glutathione S-transferase 28 kDa (GST 28) (GST class-mu), putative	Sm28GST	DNA	29.6% (liver) 27.5% (intestine)	22.6%	(*165*)
Smp_086480	Antigen Sm21.7, putative	Sm21.7	Recombinant protein	ND	41–70%	(*168*)
Smp_095360.1	Fatty acid binding protein	Sm14	Recombinant protein	ND	67%	(*166*)
Smp_157500	Calpain (C02 family)	Sm-p80	DNA vaccine + recombinant protein boost	75% (liver and intestine)	70%	(*172*)
Smp_176200.2	Cu-Zn superoxide dismutase	Cu-Zn superoxide dismutase	DNA	ND	44-60%	(*170*)

Table 3.3: **Vaccine candidates detected in the *S. mansoni* adult male worm excretory-secretory molecules.** ID – identification number at GeneDB.

3.3.3.5 – Immunomodulatory candidates

Immunomodulatory proteins from helminth parasites were described in Chapter 1 (Section 1.3). *S. mansoni* WES proteins were screened for the presence of immunomodulatory candidates through homology analysis with other helminth proteins with known immunomodulatory activity as described in chapter 2 section 2.9.1. *S. mansoni* WES proteins that showed significant homology, i.e., bit score higher than 30 and an E value lower than 1e-16, to other helminth proteins with known immunomodulatory activities were identified (Table 3.4). Based on this analysis, 3 *S. mansoni* WES proteins were selected as potential immunomodulatory candidates: Calreticulin auto-antigen homologue precursor, Serpin, and Peroxiredoxin 1. Interestingly, these 3 immunomodulatory candidates are predicted to be secreted proteins. *S. mansoni* Calreticulin auto-antigen homologue precursor contains a signal peptide and Serpin and Peroxiredoxin are predicted to be non-classically secreted with a SecP score of 0.601 and 0.597, respectively. *S. mansoni* Peroxiredoxin 1 was further characterized in this thesis and the results are presented in Chapter 4.

Cystatins (cysteine protease inhibitor) from *Nippostrongylus brasiliensis, Brugia malayi, Onchocerca volvulus* and *Acanthocheilonema viteae* function as immunomodulators. They inhibit cysteine proteases involved in the processing and presentation of antigens by APCs and downregulate APC expression of costimulatory molecules by eliciting IL-10 (*173*). A cystatin protein was identified among the *S. mansoni* WES molecules, named Cystatin B (Table 3.1, WES hit no. 10). However, sequence analysis did not indicate a significant degree of homology between *S. mansoni* Cystatin B and the immunomodulatory cystatins described above.

S. mansoni male adult worm excretory-secretory proteins		Immunomodulatory helminth homologs					
ID	**Protein description**	**GenBank ID**	**Description**	**Species**	**Immunomo-dulatory activity**	**Identity (%)**	**Ref**
Smp_030370	Calreticulin autoantigen homolog precursor, putative	AAR99585.1	Calreticulin-like protein	*Haemonchus contortus*	Binds to complement C1q inhibiting the classical complement pathway	59%	(*174*)
		CAL30086.1	Calreticulin precursor	*Heligmosomoides polygyrus*	Th2-skewing property	55%	(*175*)
		CAA07254.1	Calreticulin	*Necator americanus*	Binds to complement C1q inhibiting the classical complement pathway	56%	(*176*)
Smp_090080	Serpin, putative	AAB65744.1	Serpin precursor (Bm-spn-2)	*Brugia malayi*	Specific inhibition of neutrophil proteinases cathepsin G and neutrophil elastase	24%	(*177*)
Smp_059480	Peroxiredoxin Prx1	AAB71727.1	Peroxiredoxin	*Fasciola hepatica*	Induction of alternatively activated macrophages	66%	(*95*)

Table 3.4: ***S. mansoni* adult male worm excretory-secretory proteins with immunomodulatory homologs.** ID – identification number at GeneDB or GenBank databases.

3.4 – Discussion

There is a growing interest in elucidating the molecular basis of helminth immunomodulation. Molecules released by helminths into the host's tissue and blood circulation are the most likely to interact with immune cells thus mediating the induction of the immunomodulatory response. It has been shown that molecules released by the helminth *S. mansoni* induce *in vitro* upregulation of IL-10 producing B regulatory cells (*58*) and modulation of macrophages using live male adult worms in transwells (*178*). It is not completely understood what helminth-derived molecules are involved in the modulation of host's immune system. The identification and characterization of *S. mansoni* worm excretory-secretory molecules may contribute to a better understanding of the helminth-induced immunomodulatory response.

For identification of molecules released by *S. mansoni*, adult male worm molecules were isolated from *in vitro* culture. Although this technique does not completely mimic the *in vivo* environment, it avoids damaging the worm tegument. Damaged or dead worms release structural molecules that could be wrongly interpreted as excretory-secretory molecules. Our results suggest we managed to isolate only excretory-secretory molecules as demonstrated by the absence of paramyosin in WES. Paramyosin is a muscle protein highly expressed by schistosome species that was detected in whole worm antigens but not in the WES (Section 3.3.2.1).

Several studies on helminth excretory-secretory products have been published worldwide. Various helminths such as, *B. malayi*, *Opisthorchis viverrini* and *H. polygyrus*, can be incubated in FCS-free medium and release a significant amount of proteins into the culture medium (*52, 159, 179*). Adult schistosomes, on the other side, do not survive *in vitro* in the absence of FCS. Therefore, alternative approaches should be developed for the isolation of schistosome excretory-secretory products.

Up to date there is no record of a proteomic analysis of the *S. mansoni* adult worm excretory-secretory molecules. However *S. japonicum* and *S. bovis* excretome-secretome have been characterized previously (*160, 161*). To isolate the adult worm excretory-secretory products, these studies have used different approaches. For preparation of the *S. japonicum* excretory-secretory molecules, worms were soaked in PBS during 10 minutes, the PBS containing the worm molecules was centrifuged and the supernatant was harvested (*161*). *S. bovis* excretory-secretory products were extracted from a FCS-free medium after worms were incubated for 6 hour (*160*). The approach I have used allows worm survival for 72 hours using FCS in the incubation medium but at the same time avoids contamination of the worm excretory-secretory products with FCS-derived proteins.

S. mansoni WES molecules were sucessfully isolated and subjected to mass spectrometry. The mass spectrometry data was firstly analysed using the UniProt Knowledgebase (UniProtKB; http://www.uniprot.org/). This database comprises protein sequences derived from the translation of coding sequences that have been submitted to the EMBL-Bank/GenBank/DDBJ nucleotide sequence resources (International Nucleotide Sequence Database Collaboration - INSDC, http://www.insdc.org/). By July 2009, the *S. mansoni* genome was sequenced by a collaborative work between the Sanger Institute in England and the J. Craig Venter Institute in the United States of America. The gene sequences were submitted to GenBank (*180*) The initial proteomic analysis of the WES molecules data was performed during the year of 2010 and generated a list of 52 positive hits.

At a later stage, while reanalysing the mass spectrometry data, it was noticed that new protein hits were assigned to the same set of peptides tested previously. That suggested that the Uniprot *S. mansoni* genome database had been updated. The data was then reanalysed using the GeneDB (http://www.genedb.org/Homepage/Smansoni). This final analysis resulted in the identification of 111 proteins comprising the *S. mansoni*

excretome-secretome. Bioinformatic analysis indicates that 54 WES proteins are putatively secreted (Chapter 3, Section 3.3.3.3). A similar result was found in a recent work on the secretome of *S. japonicum* which detected a total of 101 proteins with 54 putatively secreted (*161*) . Based on homology analysis, WES proteins with homologs of known immunomodulatory activity were selected for further characterization.

By comparison to other proteomics studies, it is possible to identify a common set of proteins that are frequently reported in the excretome-secretome of helminth parasites. Molecules such as, 14 kDa fatty acid-binding protein, enolase, glutathione S-transferase, glyceraldehyde 3-phosphate dehydrogenase and superoxide dismutase are highly conserved in the excretory-secretory proteome from various parasites. That suggests a universal molecular mechanism shaped by the host-parasite interface (*52, 159, 160*).

Some structural proteins such as Alpha-actinin, Gelsolin and Tropomyosin were identified in the *S. mansoni* excretome-secretome. Although these molecules are known as constituents of the cytoskeleton or muscle proteins, a secondary role in the host-parasite interface cannot be discarded. Muscle or cytoskeleton proteins were also identified in the schistosome worm surface and could be part of an immune evasion strategy (*46*).

S. mansoni WES proteins contain homologues to other helminth proteins with known immunomodulatory activity. *S. mansoni* Calreticulin auto-antigen homologue precursor, Serpin, and Peroxiredoxin 1 are potential immunomodulatory candidates, since their homologues *H. contortus* Calreticulin-like protein, *B. malayi* Serpin putative and *F. hepatica* Peroxiredoxin, respectively, are known to modulate the host immune response (*95, 174, 177*).

This homology analysis was used in this study as a strategy to narrow down candidates for further characterization. As shown in chapter 4, *S. mansoni* Peroxiredoxin 1 was produced as a recombinant protein for further use in functional assays. However, other *S. mansoni* WES proteins, that do not present significant homology to helminth proteins

with immunomodulatory activity, may also modulate host immune response. They might present homology to non-helminth immunomodulatory proteins or even present a novel immunomodulatory activity.

The complexity of helminth excretory-secretory proteome suggests that molecular and immunological studies should be associated in order to entirely elucidate the genesis of helminth immunomodulation. The functional characterization of helminth proteins with regulatory activities facilitates the discovery of host receptors and cell types that might play an important role in the immunomodulation. In this chapter, I described the identification of the complete excretome-secretome of the adult male *S. mansoni* worm. Among 111 proteins detected, it was possible to identify potential immunomodulatory molecules. This data was the basis for my subsequent work presented in Chapter 4 and 5 of this thesis.

Cloning, Expression and Purification of *Schistosoma mansoni* Peroxiredoxin 1 and *Schistosoma mansoni* Thioredoxin

4.1 – Introduction

Peroxiredoxins (Prxs) comprise a family of anti-oxidant proteins described in a wide variety of organisms such as, helminths, protozoa, bacteria, fungi, vertebrates and plants. These enzymes are involved in the redox balance and play an important role in the prevention of tissue damage by reactive oxygen species (ROS). Prxs are also involved in several biological processes that involve signal transduction and gene regulation through hydrogen peroxide (H_2O_2), such as apoptosis, cellular differentiation and proliferation (*181-183*).

Prxs contain conserved, redox active cysteines and are classified in 2 groups based on the presence of one (1-Cys) or two (2-Cys) highly conserved reactive cysteine residues. 1-Cys Prxs contain a reactive cysteine in the N-terminal region and 2-Cys Prxs have a second reactive cysteine in the C-terminal. In 1-cys Prxs, the sequence surrounding the N-terminal cysteine is PVCT, whereas in the 2-cys group the sequence is FVCP (*184*).

Prxs are widely distributed amongst helminth parasites and have been identified in the secretome of *S. japonicum*, *Fasciola hepatica*, *Opisthorchis viverrini* and *Brugia malayi* among others helminths (*51, 161, 185-187*). The occurrence of Prxs in the secretomes from various helminth species suggests that these enzymes might have a role in protecting these parasites against ROS generated by the host immune effector cells such as eosinophils, macrophages and neutrophils (*182*).

S. mansoni have three homologues of 2-Cys Prxs, named SmPrx1, 2 and 3. SmPrx1 was the first schistosome prx to be characterized and it is thought to protect *S. mansoni* parasites against oxidative damage by neutralizing H_2O_2 *(188).* Recently, knock down of *S.*

mansoni prx genes using RNA-interference increased the H_2O_2 oxidative damage to parasite proteins and lipids leading to a dramatic reduction of parasite survival (*189*). SmPrx1 requires thioredoxin as an electron donor, hence, it was previously named thioredoxin peroxidase (SmTPx1) (*188*). SmPrx2 and SmPrx3 were subsequently identified and characterized as bifunctional enzymes. In addition to thioredoxin, these proteins also carry out glutathione-dependent reduction of H_2O_2 (*190*).

Recently, helminth Prxs have been suggested to function as immunomodulators. *F. hepatica* and *S. mansoni* Prxs have been shown to induce the alternative activation of macrophages, which downregulates the inflammatory immune responses. The mechanism of action is still unclear but is known to be independent of Prx antioxidant activity (*95, 182, 191*).

In this chapter, the identification and initial characterization of SmPrx1 is described. *S. mansoni* Thioredoxin, an antioxidant protein without known immunomodulatory activity (*192*), was used as a control for technical artifact effects of production of recombinant proteins.

4.2 - Objective

Production of recombinant *S. mansoni* Peroxiredoxin 1 (rSmPrx1) and *S. mansoni* Thioredoxin (rSmTrx1) in *E. coli* and insect cell systems.

4.3 - Results

4.3.1 - Identification of *S. mansoni* Peroxiredoxin 1 (SmPrx1) and *S. mansoni* Thioredoxin (SmTrx1) from the male adult worm excretory-secretory (WES) molecules and sequence analysis

4.3.1.1 – *S. mansoni* Peroxiredoxin 1 (SmPrx1)

Mass spectrometry analysis of the WES 2D spots 94, 133, 176 and 177 were positive for Smp_059480 with a score of 291, 155, 388 and 450, respectively. The highest sequence coverage detected was 55% in spot 176, as reported in chapter 3 (Table 3.1). The nominal mass detected was 21,331 kDa.

Smp_059480 is a 2,449 bp gene located at the supercontig Smp_scaff000166 position 46198 – 48647. The pre-mRNA is edited by splicing. Three exons are joined resulting in a coding sequence of 558 bp, which is translated into a 185 amino acid protein, named Peroxiredoxin (Prx1) (Table 4.1).

S. mansoni Peroxiredoxin 1 (SmPrx1) has a predicted molecular weight of 21,059 kDa and pI of 6.1. It does not contain a N-terminal signal peptide for secretion but is predicted to be secreted through a non-classical pathway with a SecP score of 0.597. Gene ontology analysis indicates that SmPrx1 is involved in the oxidation-reduction biological process (Table 4.1). Scanning of the amino acid sequence by InterPro database addressed 4 protein signatures to SmPrx1: alkyl hydroperoxide reductase and thiol specific antioxidant, thioredoxin-like fold, peroxiredoxin C-terminal and thioredoxin peroxidase (Figure 4.1 A).

Two conserved cysteine residues and the consensus region FVCP places SmPrx1 in the 2-cys family (Figure 4.2 A). The similarity between SmPrx1 and other Prxs detected in helminth secretomes range from 62 to 83 % (Table 4.2).

	Protein name	*S. mansoni* Peroxiredoxin 1	*S. mansoni* Thioredoxin
Gene information	GeneDB ID	Smp_059480	Smp_008070
	GenBank ID	8353172	8350666
	Gene length	2,449 bp	849 bp
	Location	Chr_5 : 5961229-5963671	Chr_7 : 8315123-8315971
	Coding sequence length	558 bp	321 bp
Protein information	GeneDB protein name	Peroxiredoxin, Prx1	Thioredoxin, Trx1
	Alternative names	Thioredoxin peroxidase Thioredoxin peroxidase, putative	Thioredoxin, putative
	UniProtKB/Swiss-Prot accession number	C4QDE3	Q8T9N5
	NCBI RefSeq	XP_002577241.1	XP_002572286.1
	Amino acids	185	106
	Predicted pI	6.1	5.84
	Predicted molecular weight	21,059 kDa	11,924 kDa
	Signal peptide	not detected	not detected
	Non-classical secretion (SecP score)	0.597	0.585
	Biological process GO terms	GO:0055114- oxidation-reduction process	GO:0006662- glycerol ether metabolic process GO:0045454- cell redox homeostasis
	Molecular Function GO terms	GO:0004601- peroxidase activity GO:0016209- antioxidant activity GO:0016491- oxidoreductase activity GO:0051920- peroxiredoxin activity	GO:0009055- electron carrier activity GO:0015035- protein disulfide oxidoreductase activity GO:0046872- metal ion binding
	IUMB - Enzyme nomenclature	EC 1.11.1.15 - Peroxiredoxin	---------
	Reaction catalysed	2 R'-SH + ROOH = R'-S-S-R' + H2O + ROH	---------

Table 4.1: ***S. mansoni* Peroxiredoxin 1 and *S. mansoni* Thioredoxin gene and protein general information.**

A) ***S. mansoni* Peroxiredoxin 1 protein signatures**

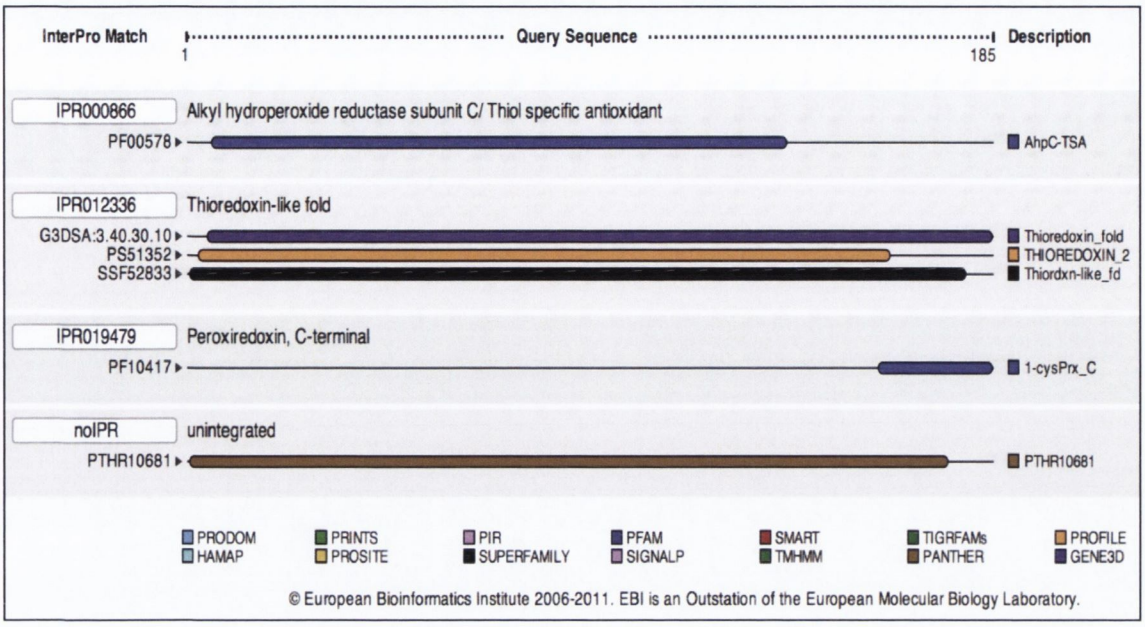

B) ***S. mansoni* Thioredoxin protein signatures**

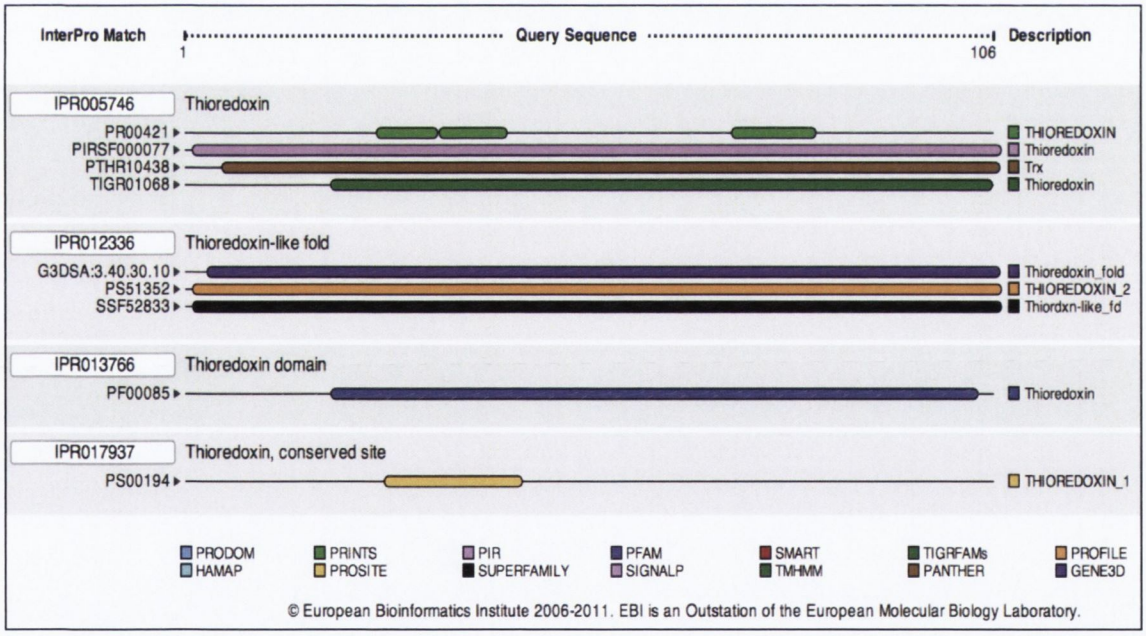

Figure 4.1: **Prediction of *S. mansoni* Peroxiredoxin 1 (SmPrx1) and *S. mansoni* Thioredoxin (SmTrx1) protein signatures by InterProScan integrated database**. SmPrx1 (A) and SmTrx1 (B) amino acid sequences were scanned by InterPro member databases (bottom squares) in search for protein families, domains, regions and sites that are grouped in unique InterPro entries (white boxes). AhpC/TSA: alkyl hydroperoxide reductase (AhpC) and thiol specific antioxidant (TSA). 1-CysPrx_C: C-terminal domain of 1-Cys peroxiredoxin. PTHR10681: Thioredoxin Peroxidase.

Protein	Species	Sequence similarity scores (%)
SjTPx-1	*S. japonicum*	83.0
SjTPx-2	*S. japonicum*	67.0
OvTPx	*O. viverrini*	66.0
Bm-TPx-1	*B. malayi*	65.0
FhPrx	*F. hepatica*	62.0

Table 4.2: **Pairwise sequence similarity between S. mansoni peroxiredoxin 1 (SmPrx1) and other peroxiredoxins detected in helminth secretomes**. Percentage of sequence similarity between *S. mansoni* peroxiredoxin 1 and *S. japonicum* thioredoxin peroxidase-1 (SjTPx-1), *S. japonicum* thioredoxin peroxidase-2 (SjTPx-2, GenBank BAD90102.1), *O. viverrini* thioredoxin peroxidase (OvTPx, GenBank ACB13822.1), *B. malayi* thioredoxin peroxidase 2 (Bm-TPx-1, AAB67873.1) or *F. hepatica* peroxiredoxin (FhPrx, GenBank AAB71727.1) calculated by the ClustalW2 multiple sequence alignment program.

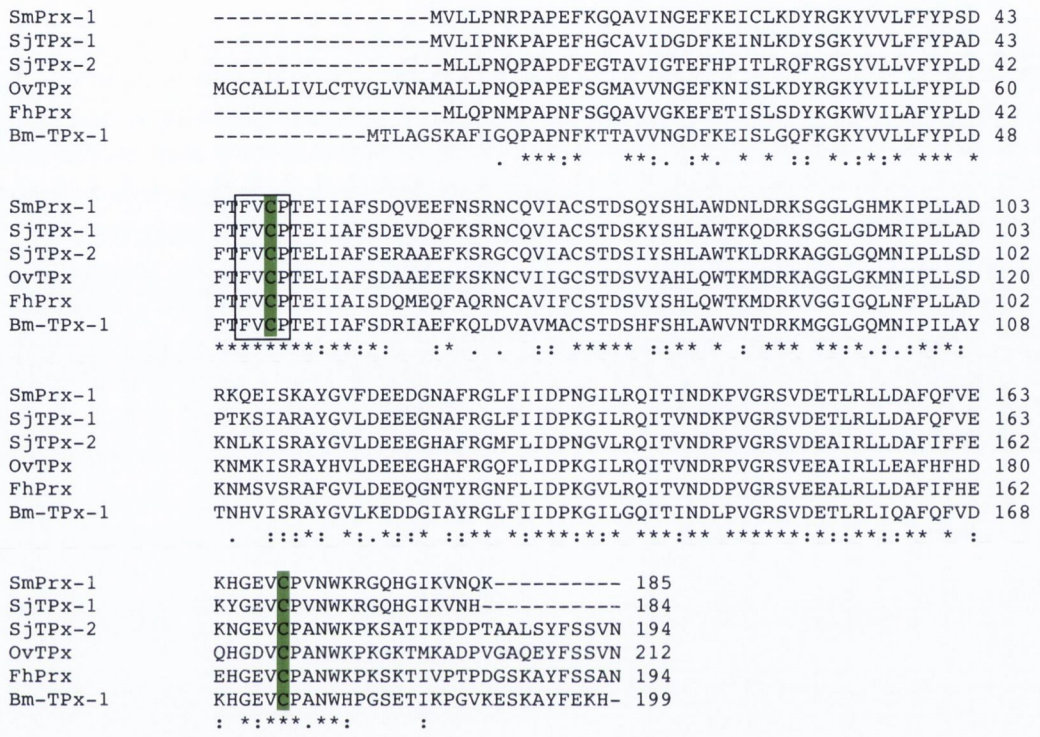

Figure 4.2: **Multiple sequence alignment of peroxiredoxins detected in helminth secretomes.** *S. mansoni* peroxiredoxin 1 sequence was aligned to *S. japonicum* thioredoxin peroxidase-1 (SjTPx-1, GenBank BAD01572.1), *S. japonicum* thioredoxin peroxidase-2 (SjTPx-2, GenBank BAD90102.1), *O. viverrini* thioredoxin peroxidase (OvTPx, GenBank ACB13822.1), *F. hepatica* peroxiredoxin (FhPrx, GenBank AAB71727.1) and *B. malayi* thioredoxin peroxidase 2 (Bm-TPx-1, AAB67873.1) using the ClustalW2 multiple sequence alignment program. The reactive conserved cysteines are indicated in green. White box indicates the 2-Cys group consensus region.

* (asterisk) - positions which have a single, fully conserved residue.

: (colon) - conservation between groups of strongly similar properties.

. (period) - conservation between groups of weakly similar properties.

4.3.1.2 - *S. mansoni* Thioredoxin (SmTrx1)

S. mansoni Thioredoxin (SmTrx1) was used as a control protein for the production of SmPrx1 and subsequent functional experiments. SmTrx1 was detected in WES 2D spot number 158 with a score of 551 and 79% of sequence coverage, as reported in Chapter 3 (Table 3.1). The nominal mass identified was 12,030 kDa. SmTrx1 is encoded by Smp_008070 gene, which consists of 849 bp and is located in the supercontig Smp_scaff000012 position 1411377 – 1412226. The SmTrx1 coding sequence results from the junction of 3 exons by splicing leading to a 321 bp sequence (Table 4.1).

SmTrx1 has 106 amino acids, a predicted molecular weight of 11,924 kDa and pI of 5.84. Similarly to SmPrx1, SmTrx1 does not contain a N-terminal signal peptide for secretion but is predicted to be secreted through a non-classical pathway with an SecP score of 0.585. According to gene ontology analysis, SmTrx1 plays a role in glycerol ether metabolic process and cell redox homeostasis (Table 4.1). Scanning of SmTrx1 amino acid sequence by InterPro database indentified 4 protein signatures: thioredoxin, thioredoxin-like fold, thioredoxin domain and thioredoxin conserved site (Figure 4.1 B).

4.3.2 - Production of recombinants *S. mansoni* Peroxiredoxin 1 (rSmPrx1) and *S. mansoni* Thioredoxin (rSmTrx1) in *E. coli*

The cloning strategy used for production of SmPrx1 and SmTrx1 in *E. coli* is depicted in Figure 4.3.

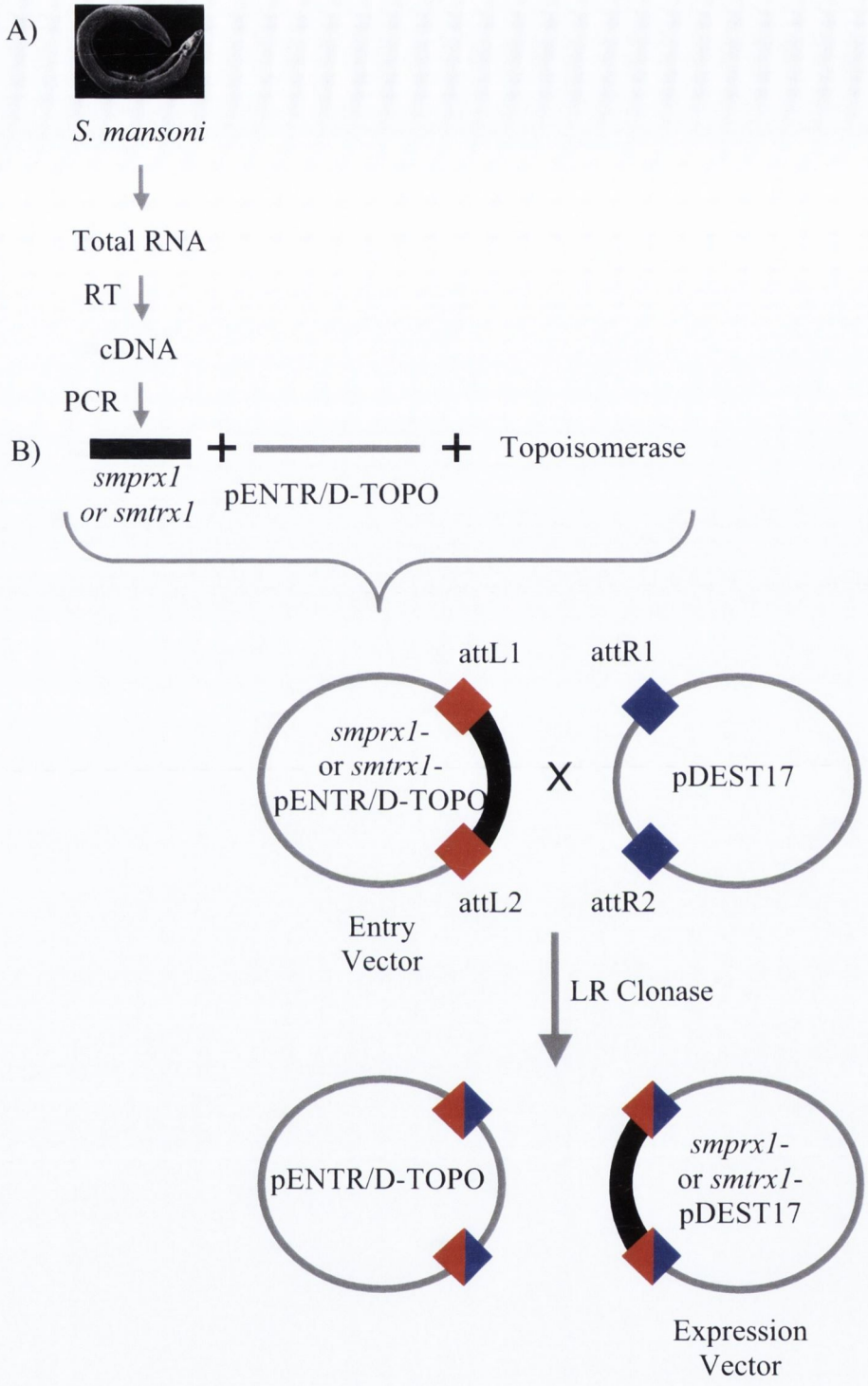

Figure 4.3: **Gateway cloning strategy used for production of recombinant *S. mansoni* Peroxiredoxin 1 (rSmPrx1) and *S. mansoni* Thioredoxin (rSmTrx1) in *E. coli*.** A) Total RNA was extracted from male adult *S. mansoni* worm and cDNA was produced by reverse transcription. *smprx1* and *smtrx1* coding sequences were amplified from the cDNA and cloned into the pENTR™/D-TOPO® vector. B) *smprx1* and *smtrx1* were transferred to the *E. coli* expression vector pDEST17 by recombination of the attL1 and attL2 sites in the entry vector with the attR1 and attR2 sites in the expression vector.

4.3.2.1 - Amplification of SmPrx1 and SmTrx1 coding sequences

Total RNA was extracted from adult male *S. mansoni* worms and cDNA was produced by reverse transcription. The cDNA was then used as a template for amplification of *S. mansoni* Peroxiredoxin 1 (*smprx1*) and *S. mansoni* Thioredoxin (*smtrx1*) coding sequences (Figure 4.3 A). Specific primers were designed based on the cDNA sequences dowloaded from GeneDB. The forward primer included an overhang of 4 nucleotides for cloning into the entry vector (Figure 4.4). The PCR annealing temperature used for amplification of *smprx1* and *smtrx1* was 51°C and 46°C, respectively. The predicted amplicon size is 562 bp for *smprx1* and 325 bp for *smtrx1*. PCR products showed a clear defined band with migration in the agarose gel similar to the expected size (Figure 4.5 A).

A) ***S. mansoni* Peroxiredoxin 1 coding sequence (558 bp)**

ATGGTATTGTTGCCTAATAGACCTGCACCAGAATTCAAAGGACAGGCTGTGATTAATGGT
GAATTCAAAGAGATCTGTTTGAAGGATTATCGAGGAAAATATGTTGTATTATTCTTCTAT
CCATCTGATTTCACATTCGTGTGTCCCACCGAAATCATCGCGTTCAGTGATCAGGTGGAG
GAGTTTAACAGTCGAAATTGTCAAGTGATCGCCTGTTCTACAGATTCTCAATACAGTCAT
CTTGCATGGGACAATTTGGATCGTAAATCGGGTGGATTGGGTCATATGAAAATTCCTCTG
TTGGCTGACCGTAAACAGGAGATTTCCAAAGCATATGGTGTATTCGATGAAGAGGATGGT
AATGCATTCAGAGGTTTATTCATCATTGATCCGAATGGAATTCTACGTCAAATCACGATC
AATGACAAGCCAGTTGGACGATCTGTAGATGAAACATTACGACTACTGGACGCGTTCCAA
TTTGTGGAGAAGCATGGTGAAGTGTGTCCGGTGAACTGGAAACGTGGCCAACATGGGATC
AAGGTTAATCAAAAGTAG

Forward primer: 5' CACCATGGTATTGTTGCCTAATAG 3'

* Length: 20 bp / Melting temperature = 58.37°C

Reverse primer: 5' CTACTTTTGATTAACCTTGATCCC 3'

Length: 24 bp / Melting temperature = 56.12°C

B) ***S. mansoni* Thioredoxin coding sequence (321 bp)**

ATGTCTAAGCTGATTGAACTGAAACAGGATGGTGACTTGGAAAGTTTGCTAGAGCAACAT
AAGAATAAGTTGGTTGTGGTTGATTTCTTTGCCACATGGTGTGGCCCGTGTAAAACCATA
GCTCCTCTGTTCAAAGAATTAAGCGAGAAGTATGATGCAATTTTCGTGAAAGTTGATGTC
GACAAACTTGAAGAGACCGCCAGAAAGTACAATATCTCAGCTATGCCAACGTTTATAGCC
ATTAAAAATGGTGAAAAAGTCGGGGATGTTGTTGGGGCTTCTATTGCTAAAGTTGAGGAC
ATGATCAAGAAATTTATTTAA

Forward primer: 5' CACCATGTCTAAGCTGATTGAACTG 3'

* Length: 21 bp / Melting temperature = 50.66°C

Reverse primer: 5' TTAAATAAATTTCTTGATCATGTCCTC 3'

Length: 27 bp / Melting temperature = 57.03°C

Figure 4.4: ***S. mansoni* Peroxiredoxin 1 (SmPrx1, A) and *S. mansoni* Thioredoxin (SmTrx1, B) coding sequences and primers designed for cloning into the entry vector**. ■ - start codon, ■ - stop codon, ___ - primer binding site, ■ - overhang sequence, *(asterisk) - excluding the nucleotides that do not bind to the cDNA template.

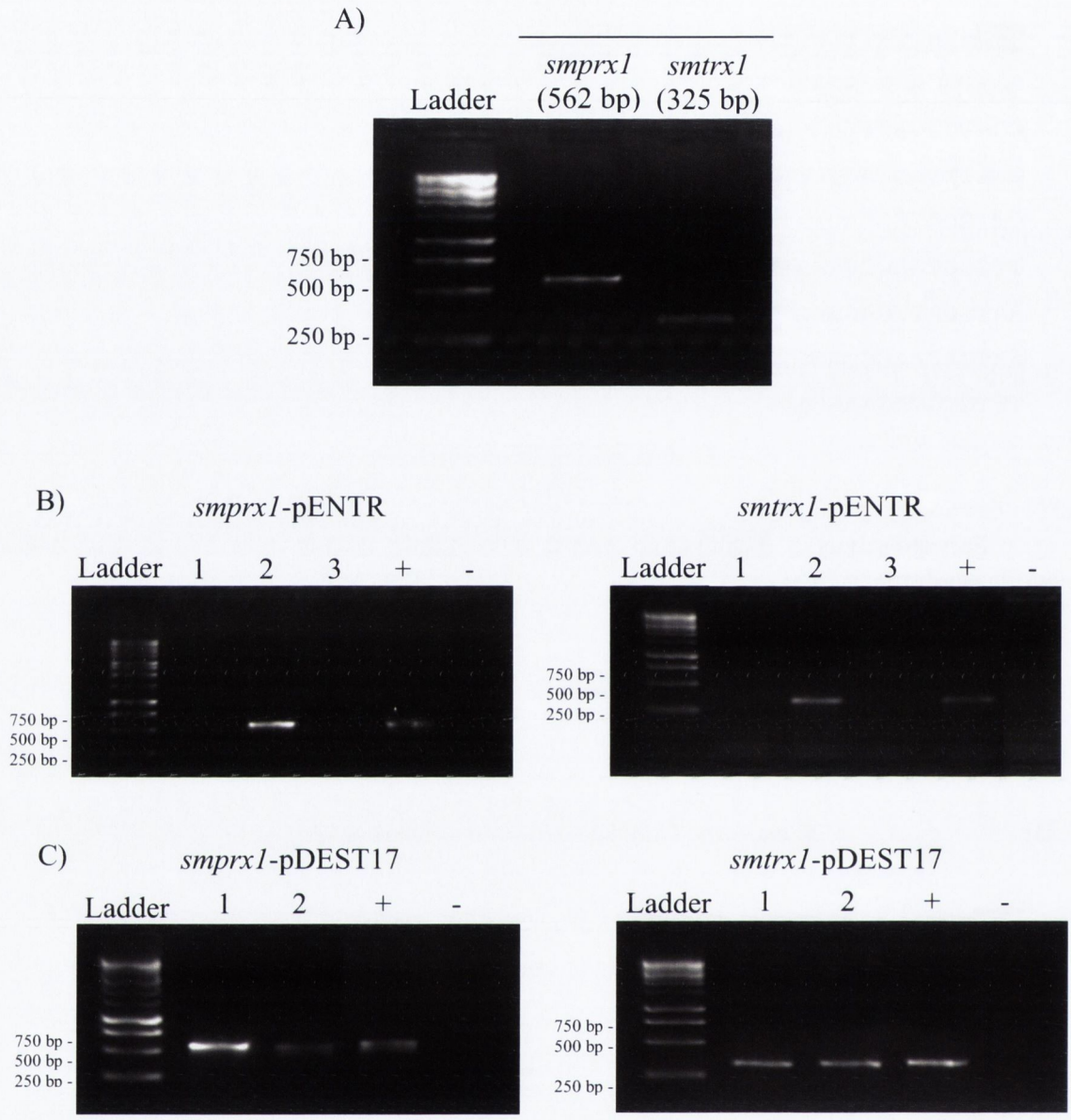

Figure 4.5: **Cloning of *S. mansoni* Peroxiredoxin 1 (SmPrx1) and *S. mansoni* Thioredoxin (SmTrx1) coding sequences into the *E. coli* expression vector pDEST™17**. A) PCR amplification of *smprx1* and *smtrx1* from *S. mansoni* adult worm cDNA. B) PCR amplification of *smprx1* and *smtrx1* from colonies (1-3) of One Shot® TOP10 competent cells transformed with TOPO cloning reaction. C) PCR amplification of smprx1 and smtrx1 from colonies (1 and 2) of Library Efficiency® DH5α™ competent cells transformed with LR recombination reaction. (+) positive control, adult worm cDNA used as template. (–) negative control, no template. Five μL of each PCR reaction was electrophoresed on a 1% agarose gel.

4.3.2.2 - Cloning of *smprx1* and *smtrx1* into *E. coli* expression vector

The Gateway system was the method of choice for cloning of *smprx1* and *smtrx1*. In this method, the gene is first inserted by an overhang into an entry vector and then transferred to the expression vector of choice by recombination (Figure 4.3 B). The coding sequences were firstly cloned into the entry vector pENTR™/D-TOPO® (Appendix 4, Figure A4.1). Positive transformants were selected by PCR using the same set of primers used for coding sequence amplification (Figure 4.5 B). Positive constructs were sequenced for confirmation of in-frame cloning. The insert was then transferred to the expression vector pDEST™17 (Appendix 4, Figure A4.2) and positive transformants were selected by PCR (Figure 4.5 C). The coding sequences were cloned in frame with the DNA enconding a N-terminal polyhistidine tag for detection and purification purposes (Figure 4.6). The molecular mass of the recombinant proteins is approximately 3.1 kDa greater than the native mass due to the presence of 28 amino acid residues arising from the vector pDEST™17. This amino acid residues include the polyhistidine tag (Figure 4.7 and Table 4.3).

A) **Recombinant *S. mansoni* Peroxiredoxin 1 coding sequence (642 bp)**

ATGTCGTACTACCATCACCATCACCATCACCTCGAATCAACAAGTTTGTA
CAAAAAAGCAGGCTCCGCGGCCGCCCCCTTCACCATGGTATTGTTGCCTA
ATAGACCTGCACCAGAATTCAAAGGACAGGCTGTGATTAATGGTGAATTC
AAAGAGATCTGTTTGAAGGATTATCGAGGAAAATATGTTGTATTATTCTT
CTATCCATCTGATTTCACATTCGTGTGTCCCACCGAAATCATCGCGTTCA
GTGATCAGGTGGAGGAGTTTAACAGTCGAAATTGTCAAGTGATCGCCTGT
TCTACAGATTCTCAATACAGTCATCTTGCATGGGACAATTTGGATCGTAA
ATCGGGTGGATTGGGTCATATGAAAATTCCTCTGTTGGCTGACCGTAAAC
AGGAGATTTCCAAAGCATATGGTGTATTCGATGAAGAGGATGGTAATGCA
TTCAGAGGTTTATTCATCATTGATCCGAATGGAATTCTACGCCAAATCAC
GATCAATGACAAGCCAGTTGGACGATCTGTAGATGAAACATTACGACTAC
TGGACGCGTTCCAATTTGTGGAGAAGCATGGTGAAGTGTGTCCGGTGAAC
TGGAAACGTGGCCAACATGGGATCAAGGTTAATCAAAAGTAG

B) **Recombinant *S. mansoni* Thioredoxin 1 coding sequence (405 bp)**

ATGTCGTACTACCATCACCATCACCATCACCTCGAATCAACAAGTTTGTA
CAAAAAAGCAGGCTCCGCGGCCGCCCCCTTCACCATGTCTAAGCTGATTG
AACTGAAACAGGATGGTGACTTGGAAAGTTTGCTAGAGCAACATAAGAAT
AAGTTGGTTGTGGTTGATTTCTTTGCCACATGGTGTGGCCCGTGTAAAAC
CATAGCTCCTCTGTTCAAAGAATTAAGCGAGAAGTATGATGCAATTTTCG
TGAAAGTTGATGTCGACAAACTTGAAGAGACCGCCAGAAAGTACAATATC
TCAGCTATGCCAACGTTTATAGCCATTAAAAATGGTGAAAAAGTCGGGGA
TGTTGTTGGGGCTTCTATTGCTAAAGTTGAGGACATGATCAAGAAATTTA
TTTAA

Figure 4.6: ***E. coli* expressed recombinant *S. mansoni* Peroxiredoxin 1 (SmPrx1, A) and *S. mansoni* Thioredoxin (SmTrx1, B) coding sequences**. ■ - start codon, blue letters - codons derived from pDEST™17, ■ - coding sequence for the polyhistidine tag, ■ - overhang sequence, _____ - nucleotides from *smprx1* or *smtrx1* original coding sequence, ■ - stop codon.

A) **Native and recombinant *S. mansoni* Peroxiredoxin 1 protein sequence alignment**

```
SmPrx1   ----------------------------MVLLPNRPAPEFKGQAVINGEFKEICLKDYRG
rSmPrx1  MSYYHHHHHHLESTSLYKKAGSAAAPFTMVLLPNRPAPEFKGQAVINGEFKEICLKDYRG
                                      ********************************

SmPrx1   KYVVLFFYPSDFTFVCPTEIIAFSDQVEEFNSRNCQVIACSTDSQYSHLAWDNLDRKSGG
rSmPrx1  KYVVLFFYPSDFTFVCPTEIIAFSDQVEEFNSRNCQVIACSTDSQYSHLAWDNLDRKSGG
         ************************************************************

SmPrx1   LGHMKIPLLADRKQEISKAYGVFDEEDGNAFRGLFIIDPNGILRQITINDKPVGRSVDET
rSmPrx1  LGHMKIPLLADRKQEISKAYGVFDEEDGNAFRGLFIIDPNGILRQITINDKPVGRSVDET
         ************************************************************

SmPrx1   LRLLDAFQFVEKHGEVCPVNWKRGQHGIKVNQK
rSmPrx1  LRLLDAFQFVEKHGEVCPVNWKRGQHGIKVNQK
         ********************************
```

B) **Native and recombinant *S. mansoni* Thioredoxin protein sequence alignment**

```
SmTrx1   ----------------------------MSKLIELKQDGDLESLLEQHKNKLVVVDFFAT
rSmTrx1  MSYYHHHHHHLESTSLYKKAGSAAAPFTMSKLIELKQDGDLESLLEQHKNKLVVVDFFAT
                                      ********************************

SmTrx1   WCGPCKTIAPLFKELSEKYDAIFVKVDVDKLEETARKYNISAMPTFIAIKNGEKVGDVVG
rSmTrx1  WCGPCKTIAPLFKELSEKYDAIFVKVDVDKLEETARKYNISAMPTFIAIKNGEKVGDVVG
         ************************************************************

SmTrx1   ASIAKVEDMIKKFI
rSmTrx1  ASIAKVEDMIKKFI
         **************
```

Figure 4.7: **Native and *E. coli* expressed recombinant *S. mansoni* Peroxiredoxin 1 (SmPrx1, rSmPrx1, A) and *S. mansoni* Thioredoxin (SmTrx1, rSmTrx1, B) protein sequence alignment.** - starting methionine, blue letters - amino acids derived from pDEST™17, polyhistidine tag, * (asterisk) - positions which have a single, fully conserved residue.

Protein	Number of amino acids	Predicted pI	Predicted molecular weight (kDa)
Native SmPrx1	185	6.1	21,059
rSmPrx1	213	6.79	24,251
Native SmTrx1	106	5.84	11,924
rSmTrx1	134	7.05	15,116

Table 4.3: **Comparison of native and *E. coli* expressed recombinant *S. mansoni* Peroxiredoxin 1 (SmPrx1, rSmPrx1) and *S. mansoni* Thioredoxin (SmTrx1, rSmTrx1).**

4.3.2.3 – Expression of rSmPrx1 and rSmTrx1 in *E. coli*

rSmPrx1 and rSmTrx1 expression was performed in BL21-AI™ competent cells. In this *E. coli* strain, the expression of the recombinant protein is induced by L-arabinose and its basal expression is repressed by glucose. For pilot analysis, protein expression was induced with 0.2% arabinose. A non-induced culture was kept as control. Samples from both cultures were collected at different time points for evaluation of recombinant protein expression. rSmPrx1 and rSmTrx1 pilot expression resulted in a strong band on a 12% SDS-PAGE that migrated at 24,945 kDa (Rf = 0.726) and at 10,471 kDa (Rf = 0.770), respectively (Figure 4.8 A and B). Expression of rSmPrx1 and rSmTrx1 was confirmed by Western blot with anti-6X polyhistidine antibody (Figure 4.8 C).

4.3.2.4 – Analysis of *E. coli* expressed rSmPrx1 and rSmTrx1 solubility

The solubility of the recombinant proteins was evaluated after lysing of the cells by sonication. rSmPrx1 and rSmTrx1 were present in the insoluble (pellet) and soluble (supernatant) lysate fractions (Figure 4.9 A and B – Condition 1). In order to improve protein solubility, different expression conditions were tested using 2 concentrations of arabinose, 0.2% and 0.02%, with or without 0.1% glucose (Table 4.4). Expression of soluble rSmPrx1 was clearly higher in condition 4 (0,02% arabinose plus 0.1% glucose). Regarding rSmTrx1, the differences in the level of solubility were not as striking as in rSmPrx1. In this case, condition 2 (0.02% arabinose) was used in the subsequent expression experiments (Figure 4.8).

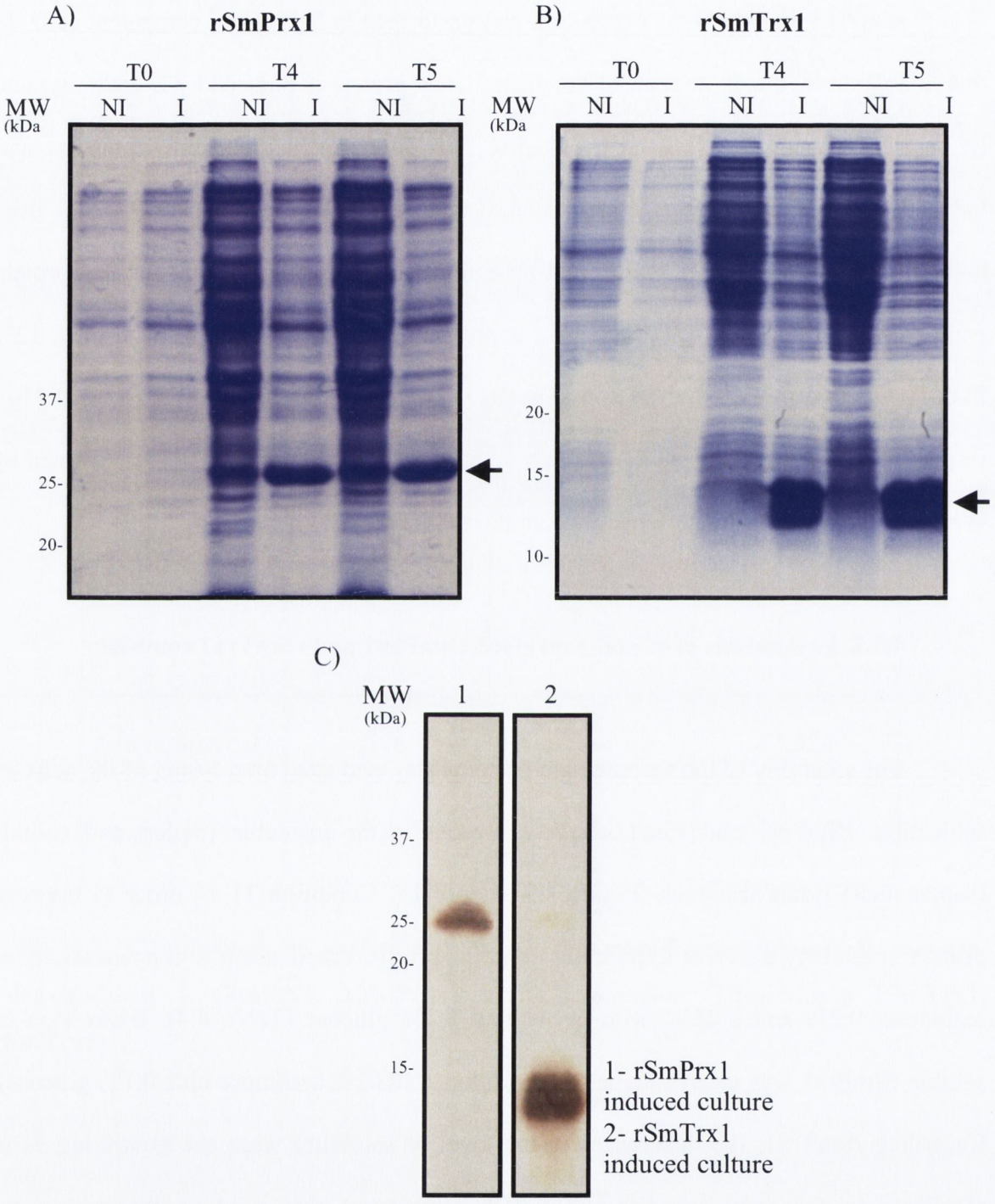

Figure 4.8: **Expression of recombinant *S. mansoni* Peroxiredoxin 1 (rSmPrx1) and *S. mansoni* Thioredoxin (rSmTrx1) in *E. coli*.** Samples from non-induced (NI) and induced (I) cultures were collected at 0 (T0), 4 (T4) and 5 (T5) hours after induction. A and B) 12% SDS-PAGE, coomassie brilliant blue staining. C) rSmPrx1 (1) and rSmTrx1 (2) induced cultures Western blot with anti-6X polyhistidine antibody (1:1000).

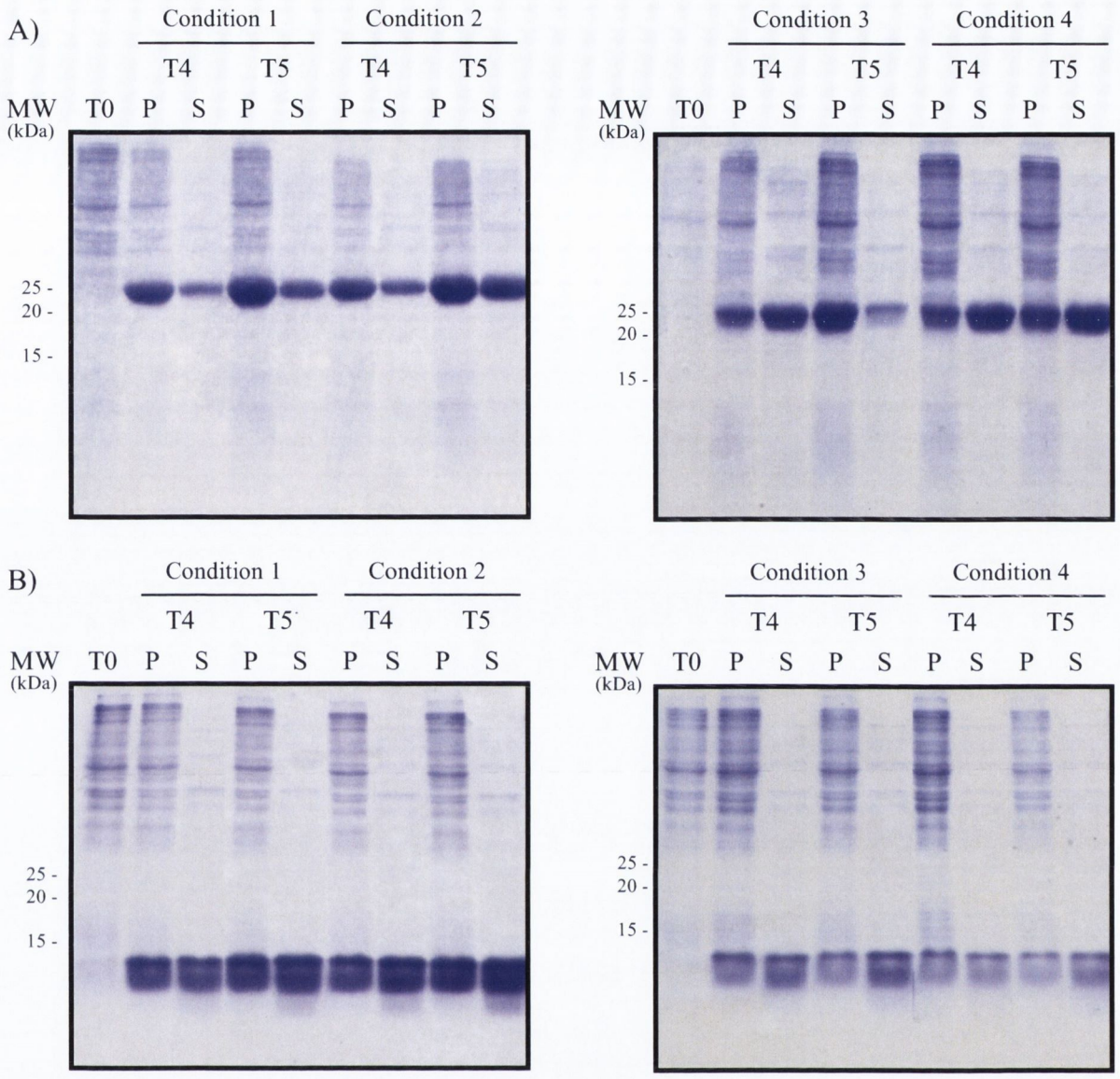

Figure 4.9: **Analysis of *E. coli* expressed recombinant *S. mansoni* Peroxiredoxin 1 (rSmPrx1, A) and *S. mansoni* Thioredoxin (rSmTrx1, B) solubility.** rSmPrx1 and rSmTrx1 were expressed in the presence of different concentrations (Table 4.4) of inducer with or without repressor in order to improve protein solubility. 12% SDS-PAGE, Coomassie Brilliant Blue staining. P- pellet, S – supernatant. T0, T4, T5 - expression time points.

Expression conditions	L-arabinose	Glucose
1	0.2%	----
2	0.02%	----
3	0.2%	0.1%
4	0.02%	0.1%

Table 4.4: **Expression conditions tested in order to increase *E. coli* expressed recombinant *S. mansoni* Peroxiredoxin 1 (rSmPrx1) and *S. mansoni* Thioredoxin (rSmTrx1) solubility.**

4.3.2.5 – Purification of *E. coli* expressed rSmPrx1 and rSmTrx1

For purification of rSmPrx1 and rSmTrx1, expression was performed in a 100 mL culture and the pellet was resuspended and lysed in binding buffer containing 20 mM imidazole. The recombinant proteins were purified by liquid nickel-affinity chromatography using an automated systems as described in chapter 2 (Section 2.7.1.2). After loading the column with the lysate supernatant, unbound proteins were washed with washing buffer, containing 50 mM imidazole and recombinant proteins were eluted with elution buffer containing 300 mM imidazole (Figure 4.10 A). Elution fractions were pooled, dialysed with PBS and checked for purity (Figure 4.10 B). The yield for 100 mL of expression culture was 2.01 mg and 2.60 mg of rSmPrx1 and rSmTrx1, respectively.

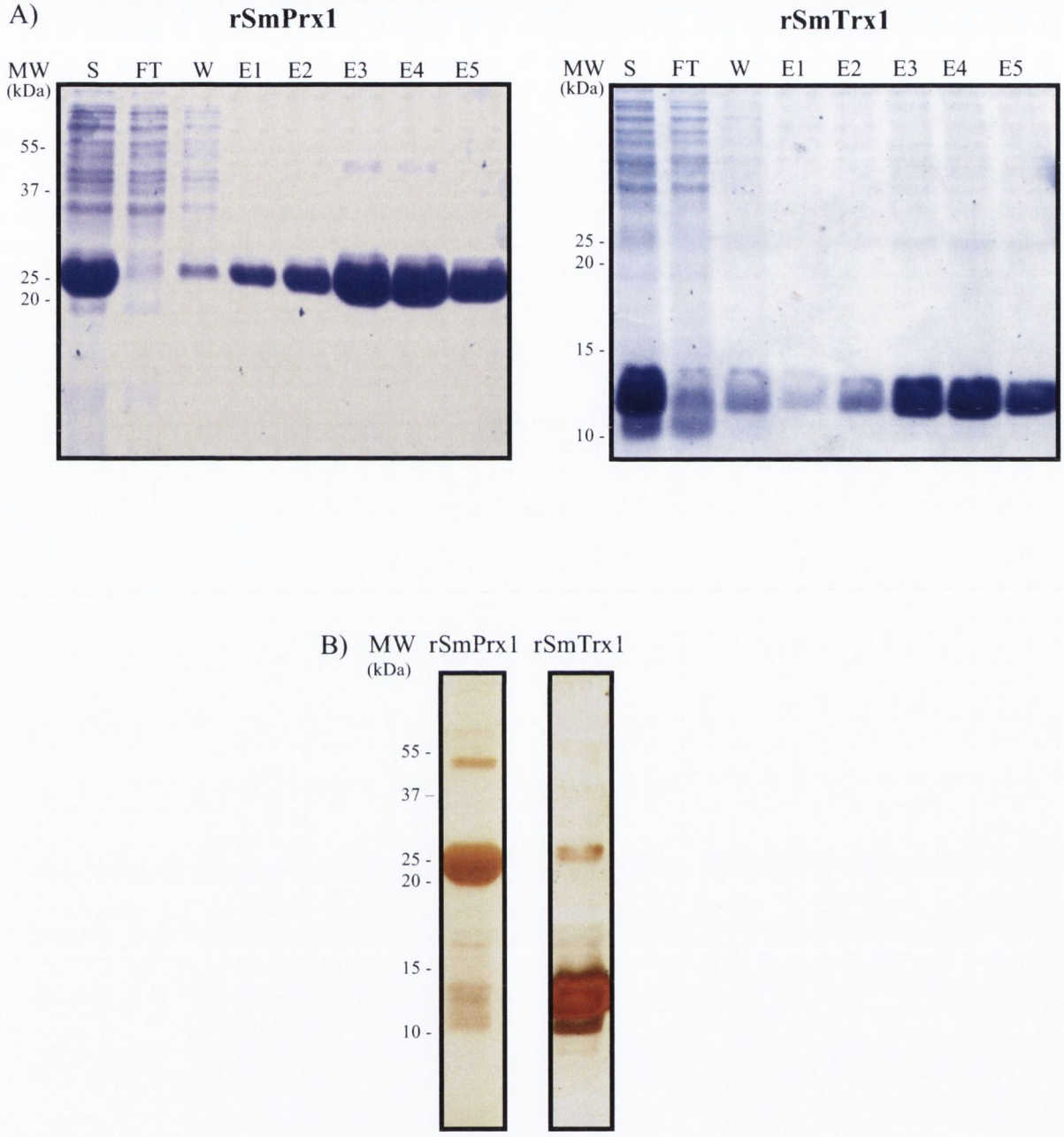

Figure 4.10: **Purification of *E. coli* expressed recombinant *S. mansoni* Peroxiredoxin 1 (SmPrx1) and *S. mansoni* Thioredoxin (SmTrx1).** A) S – supernatant, FT – flow through, W – wash, E1-5- elution fractions 1 to 5, 12% SDS-PAGE, Coomassie Brilliant Blue staining B) Purified rSmPrx1 and rSmTrx1 after reconstitution in PBS. 12% SDS-PAGE, silver staining.

4.3.2.6 – Analysis of *E. coli* expressed rSmPrx1 and rSmTrx1 oligomerization

The oligomerization of rSmPrx1 and rSmTrx1 was analyzed by Western blot. Recombinant proteins were diluted with reducing or non-reducing sample buffer and probed with anti-6X polyhistidine antibody by Western blot. As expected, the anti-6X polyhistidine antibody detected the rSmPrx1 monomer band (~25 kDa). A band that migrated at 53,703 kDa (Rf = 0.21) was detected in rSmPrx1 diluted with non-reducing sample buffer, which corresponds with the formation of a rSmPrx1 dimer (Figure 4.11 A). Densitometry analysis indicated that this band had a lower relative densitity in relation to the monomer band (Figure 4.11 B). Possibly, the dimer conformation reduces the binding efficiency of the anti-6X polyhistidine antibody to the polyhistidine tag. The rSmPrx1 monomer was not detected when the recombinant protein was diluted with non-reducing sample buffer. With respect to rSmTrx1, a monomer band was detected in both conditions tested (Figure 4.11 A). However, densitometry analysis showed that the monomer band detected under non-reducing conditions had a lower relative density as compared to the monomer band detected under reducing conditions (Figure 4.11 C). It is possible that rSmTrx1 forms an oligomer under reducing conditions as seen in the SDS-PAGE (Figure 4.10 B). Probably, the oligomer conformation prevents the binding of the anti-6X polyhistidine antibody to the polyhistidine tag.

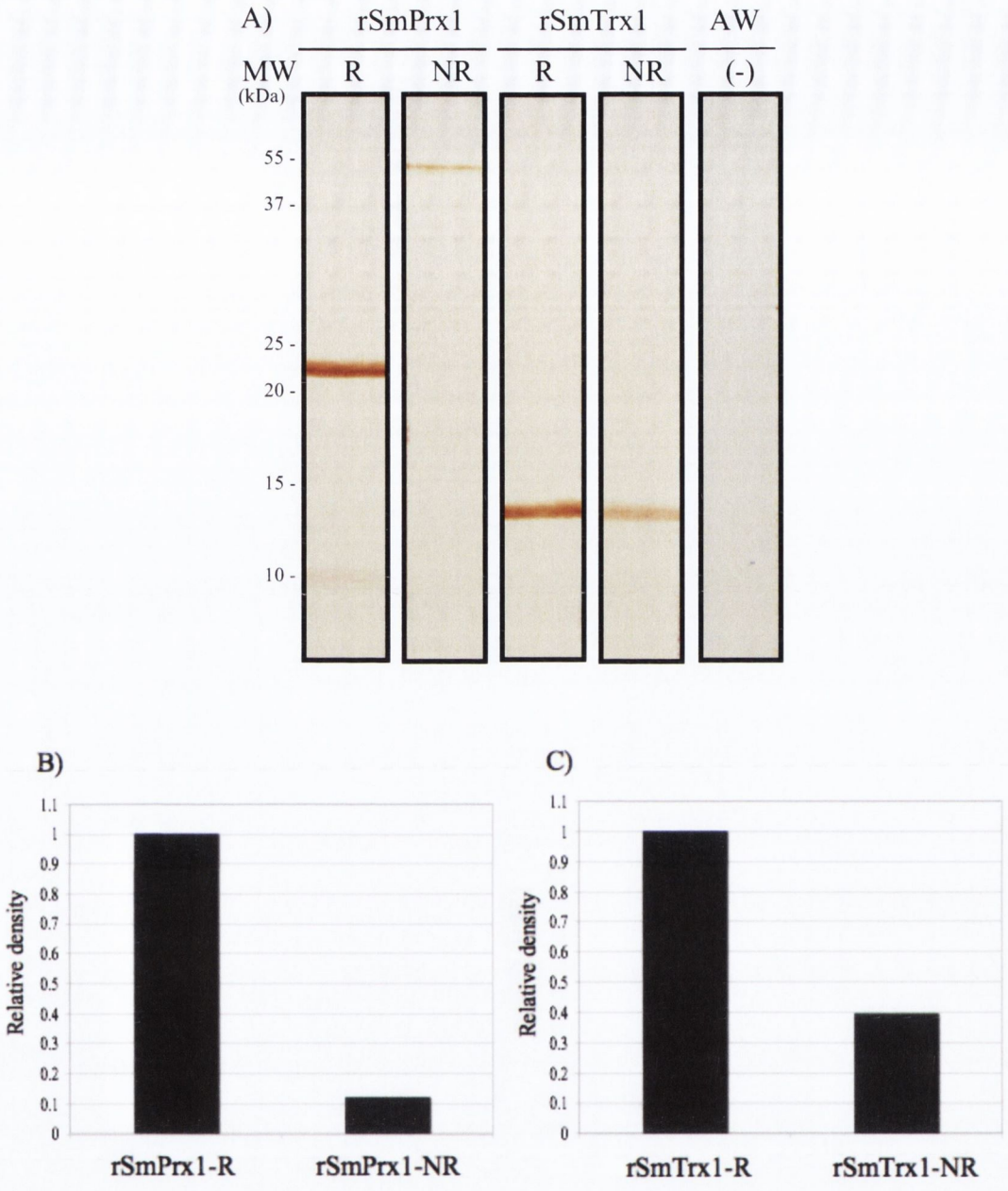

Figure 4.11: **Analysis of *E. coli* expressed recombinant *S. mansoni* Peroxiredoxin 1 (SmPrx1) and *S. mansoni* Thioredoxin (SmTrx1) oligomerization**. A) rSmPrx1 and rSmTrx1 under reducing (R) or non reducing (NR) conditions (1 μg per lane) were incubated with anti-6X polyhistidine antibody (1:1000). Soluble antigens from *S. mansoni* adult worm (AW, 1 μg) were used as negative control (-). The relative density of the bands detected in the Western blot was calculated considering the monomer band detected in the samples under reducing conditions. B) The monomer band of rSmPrx1 under reducing conditions (rSmPrx1-R) was compared to the dimer band detected under non-reducing conditions (rSmPrx1-NR). C) The monomer band of rSmTrx1 under reducing conditions (rSmTrx1-R) was compared to the monomer band detected under non-reducing conditions. There was no oligomer band detected under non-reducing conditions (rSmTrx1-NR).

4.3.2.7 – Detection of *E. coli* expressed rSmPrx1 and rSmTrx1 with specific sera

Anti-rSmPrx1 and anti-rSmTrx1 polyclonal antibody were generated in rabbit as described in Chapter 2, section 2.3. RSmPrx1 and rSmTrx1 were probed with their corresponding polyclonal antibody by Western blot. As expected, rSmPrx1 monomer band (~25 kDa) was detected. Although the protein was pre-treated with reducing sample buffer, the dimer was not completely unfolded and was also detected by the specific serum. rSmPrx1 was also probed with rabbit anti-WES polyclonal antibody by Western blot, however there was no detection under the conditions tested (Figure 4.12).

With respect to rSmTrx1, 2 bands were detected: the monomer band at 10,764 kDa, (Rf = 0.844) and a band at 29,040 kDa (Rf = 0.456) indicative of the rSmTrx1 trimer. Both bands were also detected by the anti-WES polyclonal antibody (Figure 4.12).

4.3.2.8 – Detection of SmPrx1 and SmTrx1 in the *S. mansoni* adult male WES molecules

S. mansoni male adult WES molecules were probed with anti-rSmPrx1 and anti-rSmTrx1 polyclonal antibody by Western blot. Probing of WES with anti-rSmPrx1 detected a band at 19,998 kDa (Rf = 0.617) that could correspond to the native protein. However, the detection of several bands above 50 kDa leads to an inconclusive result. Anti-rSmTrx1 specifically detected a band at 9,268 kDa (Rf = 0.675) which corresponds to the native protein (Figure 4.13).

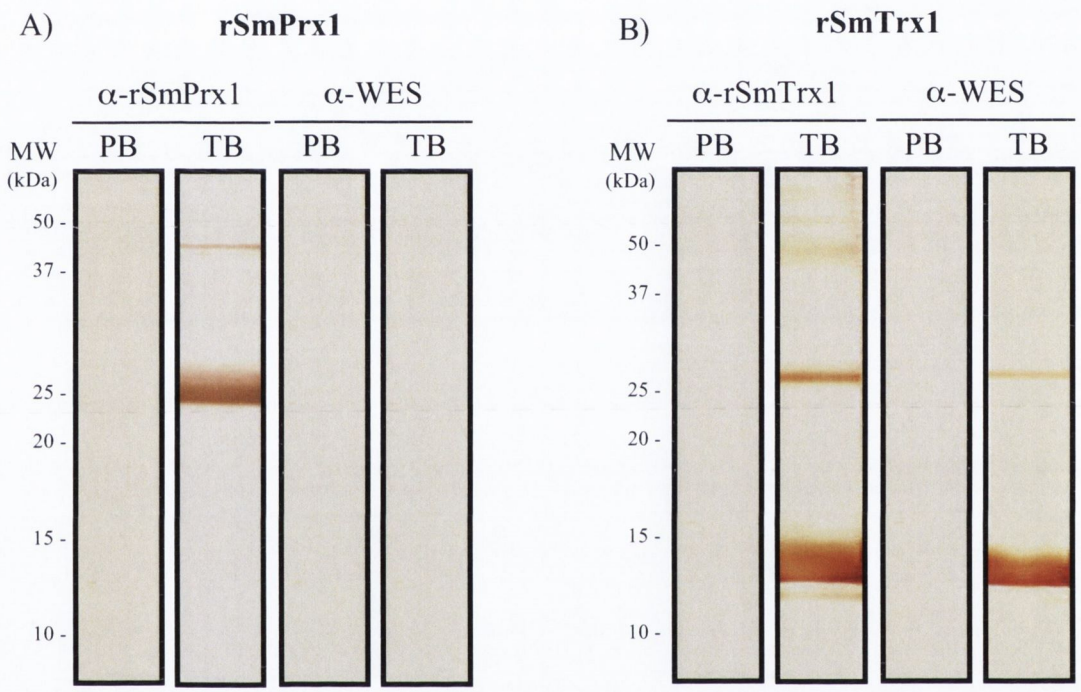

Figure 4.12: **Detection of *E. coli* expressed recombinant *S. mansoni* Peroxiredoxin 1 (SmPrx1, A) and *S. mansoni* Thioredoxin (SmTrx1, B) with specific sera**. rSmPrx1 (1 μg per lane) was probed by Western blot with anti-rSmPrx1 (α-rSmPrx1, 1:5000) and anti-WES (α-WES, 1:100) rabbit sera collected at the end of immunization protocol (terminal bleed, TB). rSmTrx1 (1 μg per lane) was detected with anti-rSmTrx1 (α-rSmTrx1, 1:15000) and anti-WES (α-WES, 1:500) rabbit polyclonal antibody. The pre-bleed (PB), serum harvested before rabbit immunization, was used as control.

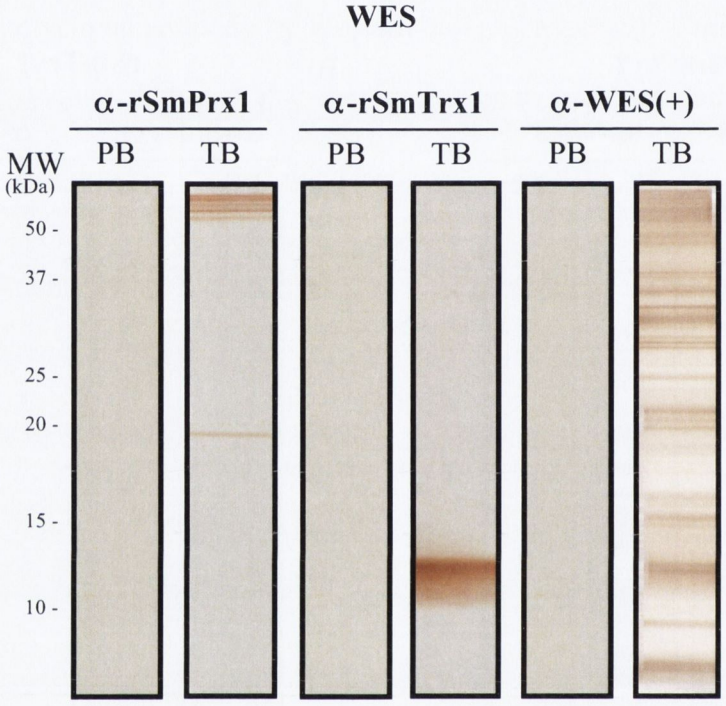

Figure 4.13: **Detection of *S. mansoni* Peroxiredoxin 1 (SmPrx1) and *S. mansoni* Thioredoxin (SmTrx1) in the *S. mansoni* adult male WES molecules**. Male adult WES molecules (1 μg per lane) were probed by Western blot with anti-rSmPrx1 (α-rSmPrx1, 1:5000), (α-rSmTrx1, 1:2000) rabbit sera collected at the end of immunization protocol (terminal bleed, TB). The pre-bleed (PB), serum harvested before rabbit immunization, was used as control and anti-WES (α-WES, 1:500) rabbit serum was used as positive control.

4.3.3 - Production of recombinant *S. mansoni* Peroxiredoxin 1 (rSmPrx1) and *S. mansoni* Thioredoxin (rSmTrx1) in the baculovirus-insect cell system

Recombinant proteins generated in the *E. coli* system contain very high levels of lipopolysaccharide (LPS) which is the major component of the outer membrane of gram-negative bacteria such as *E. coli*. LPS-contaminated recombinant proteins are not reliable for immunological assays because the LPS elicits a strong immune response (*193*) that interferes with protein activity.

In order to generate recombinant proteins with low levels of endotoxin contamination, SmPrx1 and SmTrx1 were produced in the baculovirus-insect cell system. The cloning strategy used for production of baculovirus-insect cell expressed recombinant SmPrx1 and SmTrx1 is summarized in Figure 4.14.

4.3.3.1 - Amplification of SmPrx1 and SmTrx1 coding sequences

For production of recombinant proteins in the baculovirus-insect cell system, SmPrx1 and SmTrx1 coding sequences, *bacsmprx1* and *bacsmtrx1*, were amplified from male adult worm cDNA. Forward and reverse primers contained restriction sites for the enzymes *Bam*HI and *Xba*I, respectively. The reverse primer included 2 extra nucleotides to adjust the insert frame to the vector frame (Figure 4.15). Primer annealing temperature used was 47°C. The predicted amplicon size is 576 bp for *bacsmprx1* and 336 bp for *bacsmtrx1*. PCR products showed a clear defined band with gel migration similar to the expected size (Figure 4.16 A).

4.3.3.2 - Cloning of bacsmprx1 and bacsmtrx1 into the transfer vector

Bacsmprx1 and *bacsmtrx1* coding sequences were cloned into a modified version of the transfer vector pFastBac^{TM}1 (Appendix 4, Figure 4.3). The modified vector, named pFastBac-Mel-V5-His, was kindly donated by Dr. Antonio Alcami – Centro de Biologia Molecular Severo Ochoa/Universidad Autónoma de Madrid. The pFastBac-Mel-V5-His contains a DNA encoding Honey Bee Mellitin (HBM) secretion signal peptide upstream of the multi cloning site (MCS) and a DNA encoding two tags downstream of the MCS, the V5 peptide tag and a polyhistidine tag.

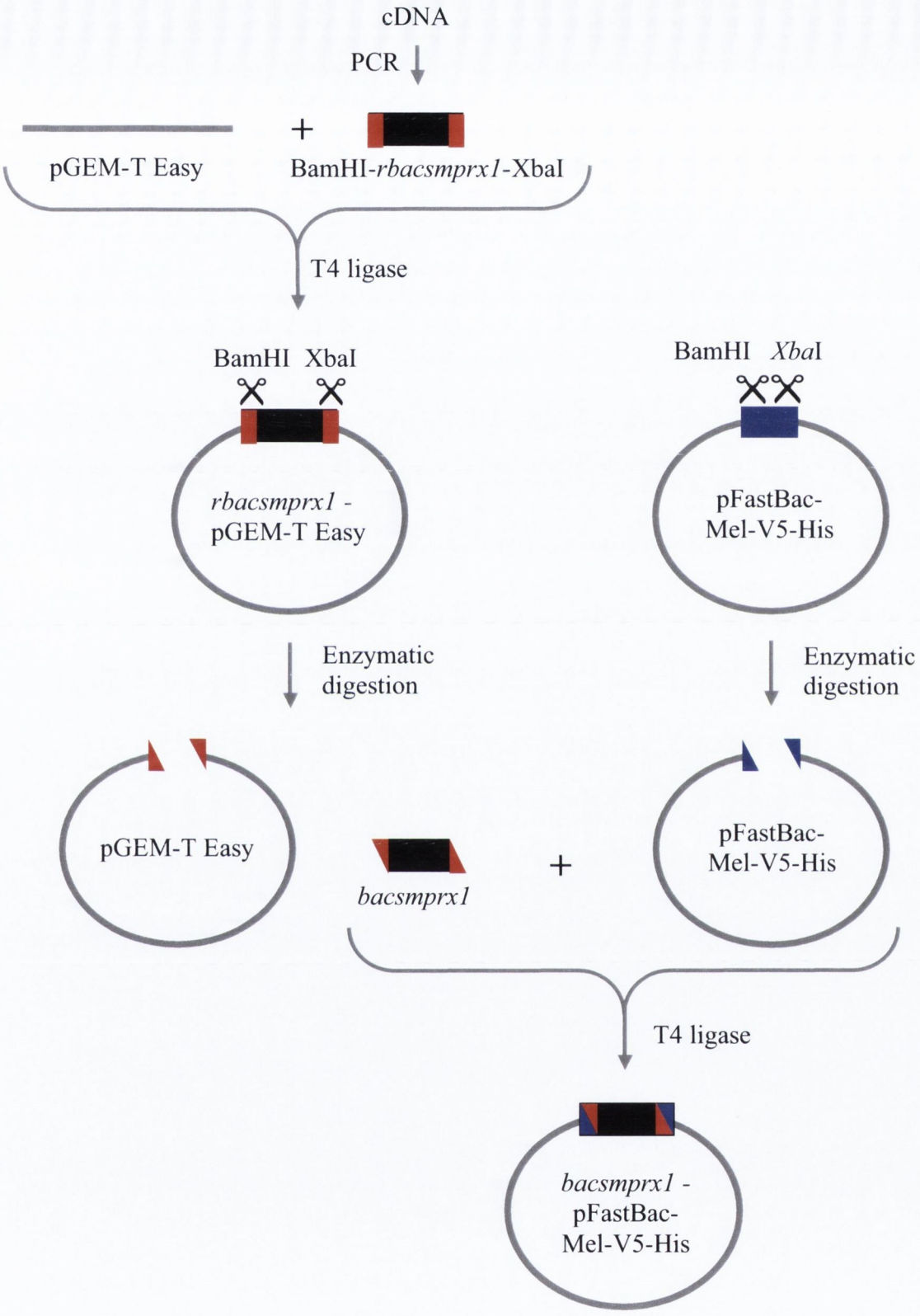

Figure 4.14: **Cloning strategy of *S. mansoni* Peroxiredoxin 1 (SmPrx1) and *S. mansoni* Thioredoxin (SmTrx1) coding sequences for expression of recombinant proteins in the baculovirus-insect cell system.**

A) ***S. mansoni* Peroxiredoxin 1 coding sequence (558 bp)**

ATGGTATTGTTGCCTAATAGACCTGCACCAGAATTCAAAGGACAGGCTGTGATTAATGGT
GAATTCAAAGAGATCTGTTTGAAGGATTATCGAGGAAAATATGTTGTATTATTCTTCTAT
CCATCTGATTTCACATTCGTGTGTCCCACCGAAATCATCGCGTTCAGTGATCAGGTGGAG
GAGTTTAACAGTCGAAATTGTCAAGTGATCGCCTGTTCTACAGATTCTCAATACAGTCAT
CTTGCATGGGACAATTTGGATCGTAAATCGGGTGGATTGGGTCATATGAAAATTCCTCTG
TTGGCTGACCGTAAACAGGAGATTTCCAAAGCATATGGTGTATTCGATGAAGAGGATGGT
AATGCATTCAGAGGTTTATTCATCATTGATCCGAATGGAATTCTACGTCAAATCACGATC
AATGACAAGCCAGTTGGACGATCTGTAGATGAAACATTACGACTACTGGACGCGTTCCAA
TTTGTGGAGAAGCATGGTGAAGTGTGTCCGGTGAACTGGAAACGTGGCCAACATGGGATC
AAGGTTAATCAAAAGTAG

Forward Primer: 5' CGGGATCCATGGTATTGTTGCCTAATAGAC 3'

* Length: 22 bases / Melting temperature: 51.43°C

Reverse Primer: 5' GCTCTAGAGCCTTTTGATTAACCTTGATCCC 3'

* Length: 21 bases / Melting temperature: 53.99°C

B) ***S. mansoni* Thioredoxin coding sequence (321 bp)**

ATGTCTAAGCTGATTGAACTGAAACAGGATGGTGACTTGGAAAGTTTGCTAGAGCAACAT
AAGAATAAGTTGGTTGTGGTTGATTTCTTTGCCACATGGTGTGGCCCGTGTAAAACCATA
GCTCCTCTGTTCAAAGAATTAAGCGAGAAGTATGATGCAATTTTCGTGAAAGTTGATGTC
GACAAACTTGAAGAGACCGCCAGAAAGTACAATATCTCAGCTATGCCAACGTTTATAGCC
ATTAAAAATGGTGAAAAAGTCGGGGATGTTGTTGGGGCTTCTATTGCTAAAGTTGAGGAC
ATGATCAAGAAATTTATTTAA

Forward primer: 5' CGGGATCCATGTCTAAGCTGATTGAACTG 3'

* Length: 21 bp / Melting temperature = 50.66 °C

Reverse primer: 5' GCTCTAGAGCAATAAATTTCTTGATCATGTCC 3'

* Length: 22 bp / Melting temperature = 51.24 °C

Figure 4.15: ***S. mansoni* Peroxiredoxin 1 (SmPrx1, A) and *S. mansoni* Thioredoxin (SmTrx1, B) coding sequences and primers designed for cloning into the entry vector.** - start codon, - stop codon, ___ - primer binding site, - *Bam*HI recognition site, - *Xba*I recognition site, - nucleotides added to adjust the reading frame, * (asterisk) - excluding the nucleotides that do not bind to the template cDNA.

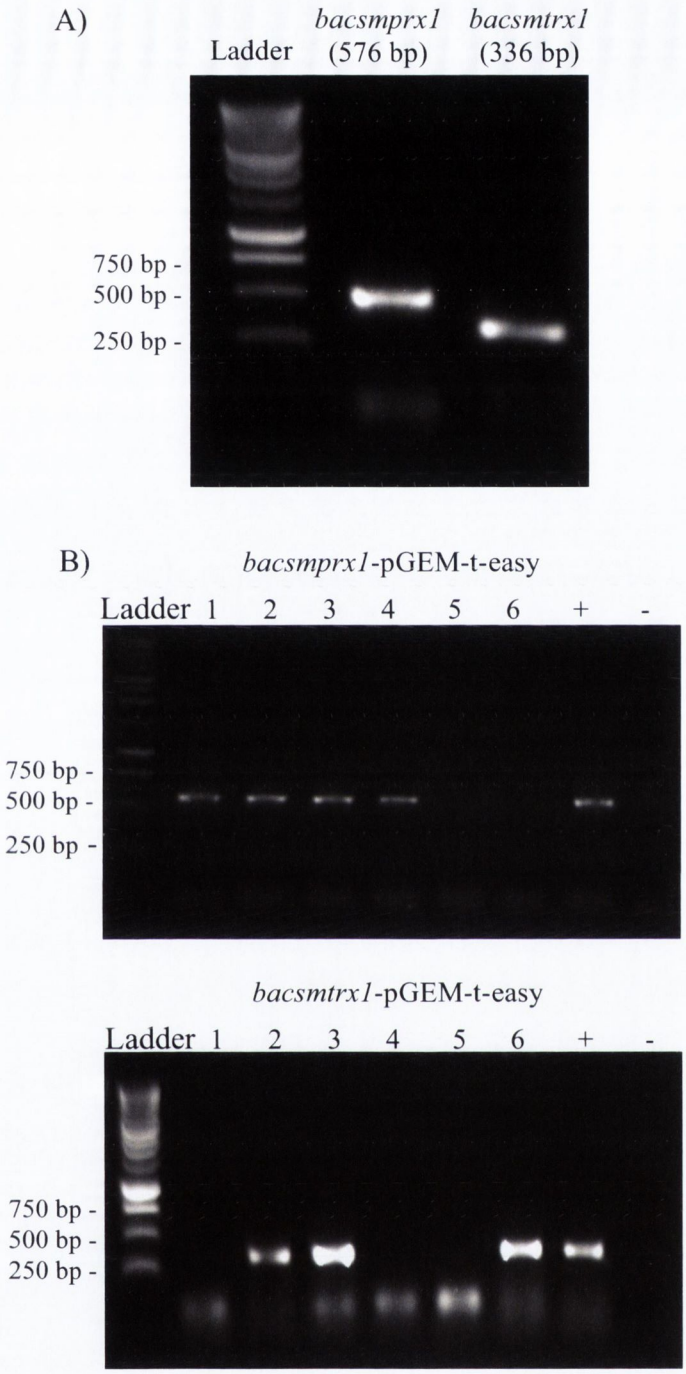

Figure 4.16: **Amplification of *S. mansoni* Peroxiredoxin 1 (SmPrx1) and *S. mansoni* Thioredoxin (SmTrx1) coding sequences and cloning into the pGEM-t-easy vector.** A) PCR amplification of *bacsmprx1* and *bacsmtrx1* from *S. mansoni* adult worm cDNA. B) PCR amplification of *bacsmprx1* and *bacsmtrx1* from colonies (1-6) of JM109 competent cells transformed with *bacsmprx1*-pGEM-T-easy *or* *bacsmtrx1*-pGEM-T-easy ligation reaction. (+) positive control, *smprx1*-pDEST17 or *smtrx1*-pDEST17 used as template. (–) negative control, no template. Five μL of each PCR reaction was electrophoresed on a 1% agarose gel.

For cloning into the pFastBac-Mel-V5-His transfer vector, *bacsmprx1* and *bacsmtrx1* were firstly ligated to the pGEM-T-easy vector (Appendix 4, Figure A4.4). The ligation reaction was transformed into JM109 competent cells for selection and further amplification (Figure 4.16 B). The insert was then released from the pGEM-T-easy by double digestion with *Bam*HI and *Xba*I and ligated to the pFastBac-Mel-V5-His previously digested with the same enzymes (Figure 4.17 A). Positive constructs were selected from DH5α competent cells transformed with the ligation reaction (Figure 4.17 B).

After cloning in the pFastBac-Mel-V5-His, the final open reading frame of *bacsmprx1* and *bacsmtrx1* were 729 bp and 492 bp, respectively (Figure 4.18). The expressed recombinant protein is processed by cleavage of the HBM peptide. The final product has 57 additional amino acids in relation to the native proteins and the predicted molecular weight is increased by 6.376 kDa (Figure 4.19, Table 4.5).

4.3.3.3 – Generation of SmPrx1 and SmTrx1 recombinant bacmids

For generation of the recombinant bacmids, rbacmid-smprx1 and rbacmid-smtrx1, the transfer vectors, *bacsmprx1*-pFastBac-Mel-V5-His and *bacsmtrx1*-pFastBac-Mel-V5-His, were transformed into DH10Bac™ competent cells and recombinant bacmids were isolated from white colonies. Transposition of inserts into the bacmid was verified by PCR using the M13/pUC forward and reverse primers that bind to flanking regions of the recombination site in the bacmid (Appendix 5, Figure A5). The size of the amplified product generated by these primers is 2,300 bp plus the size of the insert. Therefore, expected size for *rbacsmprx1* and *rbacsmtrx1* is 2,876 bp and 2,636 bp, respectively. If transposition does not occur, PCR with M13/pUC primers generates a DNA band of 273 bp. Except for one negative colony, all other colonies tested were positive for their respective bacmids (Figure 4.20).

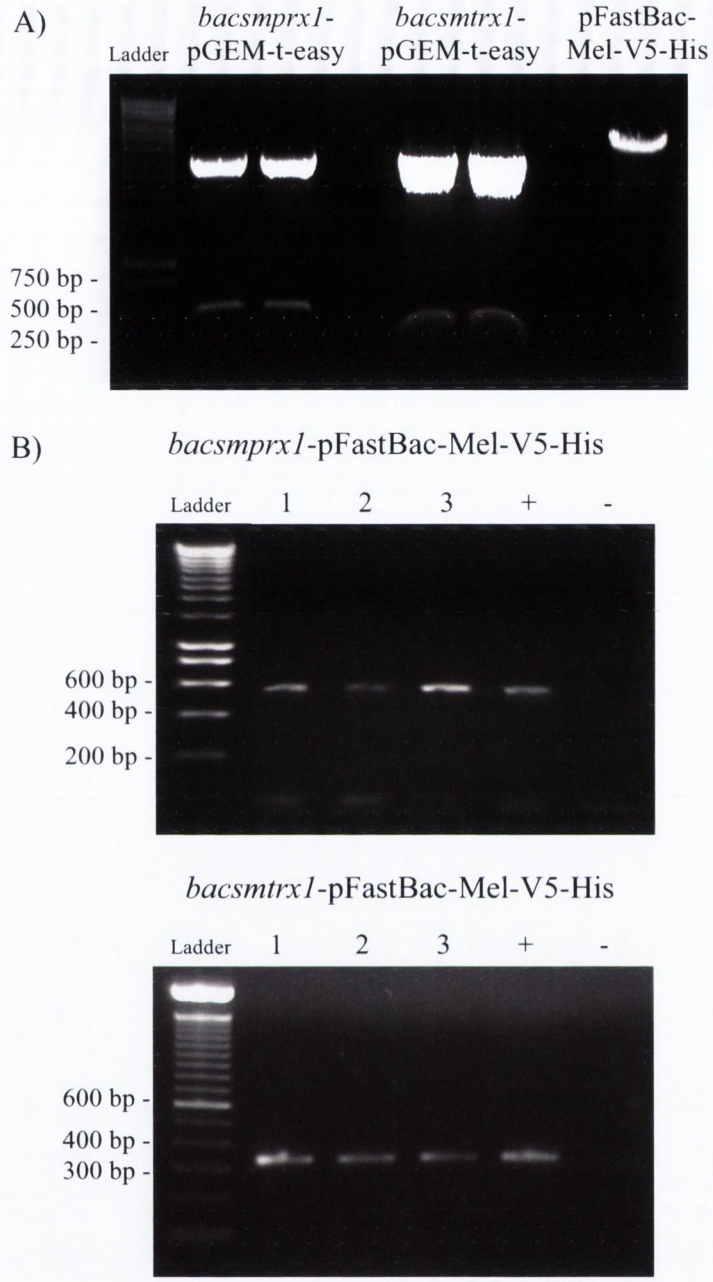

Figure 4.17: **Cloning of *S. mansoni* Peroxiredoxin 1 (SmPrx1) and *S. mansoni* Thioredoxin (SmTrx1) coding sequences into the pFastBac-Mel-V5-His transfer vector.** A) Double enzymatic digestion of the inserts, *bacsmprx1* and *bacsmtrx1*, and the pFastBac-Mel-V5-His transfer vector with *Bam*HI and *Xba*I. B) PCR amplification of *bacsmprx1* and *bacsmtrx1* from colonies (1-3) of DH5α competent cells transformed with *bacsmprx1*-pFastBac-Mel-V5-His *or* *bacsmtrx1*-pFastBac-Mel-V5-His ligation reaction. (+) positive control, *bacsmprx1*-pGEM-t-easy or *bacsmtrx1*-pGEM-t-easy used as template. (–) negative control, no template. Five μL of each PCR reaction was electrophoresed on a 1% agarose gel.

A) **Recombinant baculovirus *S. mansoni* Peroxiredoxin 1 coding sequence (729 bp)**

ATGAAATTCTTAGTCAACGTTGCCCTTGTTTTTATGGTCGTATACATTT
CTTACATCTATGCCGGCCATATGGGATCCATGGTATTGTTGCCTAATAG
ACCTGCACCAGAATTCAAAGGACAGGCTGTGATTAATGGTGAATTCAAA
GAGATCTGTTTGAAGGATTATCGAGGAAAATATGTTGTATTATTCTTCT
ATCCATCTGATTTCACATTCGTGTGTCCCACCGAAATCATCGCGTTCAG
TGATCAGGTGGAGGAGTTTAACAGTCGAAATTGTCAAGTGATCGCCTGT
TCTACAGATTCTCAATACAGTCATCTTGCATGGGACAATTTGGATCGTA
AATCGGGTGGATTGGGTCATATGAAAATTCCTCTGTTGGCTGACCGTAA
ACAGGAGATTTCCAAAGCATATGGTGTATTCGATGAAGAGGATGGTAAT
GCATTCAGAGGTTTATTCATCATTGATCCGAATGGAATTCTACGCCAAA
TCACGATCAATGACAAGCCAGTTGGACGATCTGTAGATGAAACATTACG
ACTACTGGACGCGTTCCAATTTGTGGAGAAGCATGGTGAAGTGTGTCCG
GTGAACTGGAAACGTGGCCAACATGGGATCAAGGTTAATCAAAAGGCTC
TAGAGGGCCCGCGGTTCGAAGGTAAGCCTATCCCTAACCCTCTCCTCGG
TCTCGATTCTACGCGTACCGGTCATCATCACCATCACCATTGA

B) **Recombinant baculovirus *S. mansoni* Thioredoxin coding sequence (492 bp)**

ATGAAATTCTTAGTCAACGTTGCCCTTGTTTTTATGGTCGTATACATTT
CTTACATCTATGCCGGCCATATGGGATCCATGTCTAAGCTGATTGAACT
GAAACAGGATGGTGACTTGGAAAGTTTGCTAGAGCAACATAAGAATAAG
TTGGTTGTGGTTGATTTTTTTGCCACATGGTGTGGCCCGTGTAAAACCA
TAGCTCCTCTGTTCAAAGAATTAAGCGAGAAGTATGATGCAATTTTCGT
GAAAGTTGATGTCGACAAACTTGAAGAGACCGCCAGAAAGTACAATATC
TCAGCTATGCCAACGTTTATAGCCATTAAAAATGGTGAAAAAGTCGGGG
ATGTTGTTGGGGCTTCTATTGCTAAAGTTGAGGACATGATCAAGAAATT
TATTGCTCTAGAGGGCCCGCGGTTCGAAGGTAAGCCTATCCCTAACCCT
CTCCTCGGTCTCGATTCTACGCGTACCGGTCATCATCACCATCACCATTGA

Figure 4.18: **Recombinant baculovirus *S. mansoni* Peroxiredoxin 1 (A) and *S. mansoni* Thioredoxin (B) coding sequences**. ■ - start codon, ■ - coding sequence for HBM secretion signal peptide, blue letters - nucleotides derived from pFastBac-Mel-V5-His, __ - nucleotides from *smprx1* or *smtrx1* original coding sequence, ■ - nucleotides added to adjust the reading frame, ⬚ - coding sequence for the V5 peptide, ⬚ - coding sequence for the polyhistidine tag, ■ - stop codon.

A) **Native and recombinant baculovirus *S. mansoni* Peroxiredoxin 1 protein sequence alignment**

```
SmPrx1      -------------------------MVLLPNRPAPEFKGQAVINGEFKEICLKDYRGKY
rbacSmPrx1 MKFLVNVALVFMVVYISYIYAGHMGSMVLLPNRPAPEFKGQAVINGEFKEICLKDYRGKY
                                     **********************************

SmPrx1      VVLFFYPSDFTFVCPTEIIAFSDQVEEFNSRNCQVIACSTDSQYSHLAWDNLDRKSGGLG
rbacSmPrx1 VVLFFYPSDFTFVCPTEIIAFSDQVEEFNSRNCQVIACSTDSQYSHLAWDNLDRKSGGLG
           ************************************************************

SmPrx1      HMKIPLLADRKQEISKAYGVFDEEDGNAFRGLFIIDPNGILRQITINDKPVGRSVDETLR
rbacSmPrx1 HMKIPLLADRKQEISKAYGVFDEEDGNAFRGLFIIDPNGILRQITINDKPVGRSVDETLR
           ************************************************************

SmPrx1      LLDAFQFVEKHGEVCPVNWKRGQHGIKVNQK----------------------------
rbacSmPrx1 LLDAFQFVEKHGEVCPVNWKRGQHGIKVNQKALEGPRFEGKPIPNPLLGLDSTRTGHHHH
           *******************************

SmPrx1      --
rbacSmPrx1 HH
           **
```

B) **Native and recombinant baculovirus *S. mansoni* Peroxiredoxin 1 protein sequence alignment**

```
SmTrx1      -------------------------MSKLIELKQDGDLESLLEQHKNKLVVVDFFATWC
rbacSmTrx1 MKFLVNVALVFMVVYISYIYAGHMGSMSKLIELKQDGDLESLLEQHKNKLVVVDFFATWC
                                     **********************************

SmTrx1      GPCKTIAPLFKELSEKYDAIFVKVDVDKLEETARKYNISAMPTFIAIKNGEKVGDVVGAS
rbacSmTrx1 GPCKTIAPLFKELSEKYDAIFVKVDVDKLEETARKYNISAMPTFIAIKNGEKVGDVVGAS
           ************************************************************

SmTrx1      IAKVEDMIKKFI-----------------------------
rbacSmTrx1 IAKVEDMIKKFIALEGPRFEGKPIPNPLLGLDSTRTGHHHHHH
           ************
```

Figure 4.19: **Native and recombinant baculovirus SmPrx1 and SmTrx1 protein sequence alignment.** ■ - starting methionine, ■ - HBM secretion signal peptide, ▲ - cleavage site, blue letters - amino acids derived from pFastBac1-Mel-V5-His, ⬚ - V5 peptide, ⬚ polyhistidine tag, * (asterisk) - positions which have a single, fully conserved residue.

Protein	Number of amino acids	Predicted pI	Predicted molecular weight (kDa)
Native SmPrx1	185	6.10	21,059
rbacSmPrx1	242	6.83	27,435
Native SmTrx1	106	5.84	11,924
rbacSmTrx1	163	7.09	18,300

Table 4.5: **Comparison of native and insect cell expressed recombinant proteins baculovirus *S. mansoni* Peroxiredoxin 1 (SmPrx1) and *S. mansoni* Thioredoxin (SmTrx1) after cleavage of HBM secretion signal peptide.**

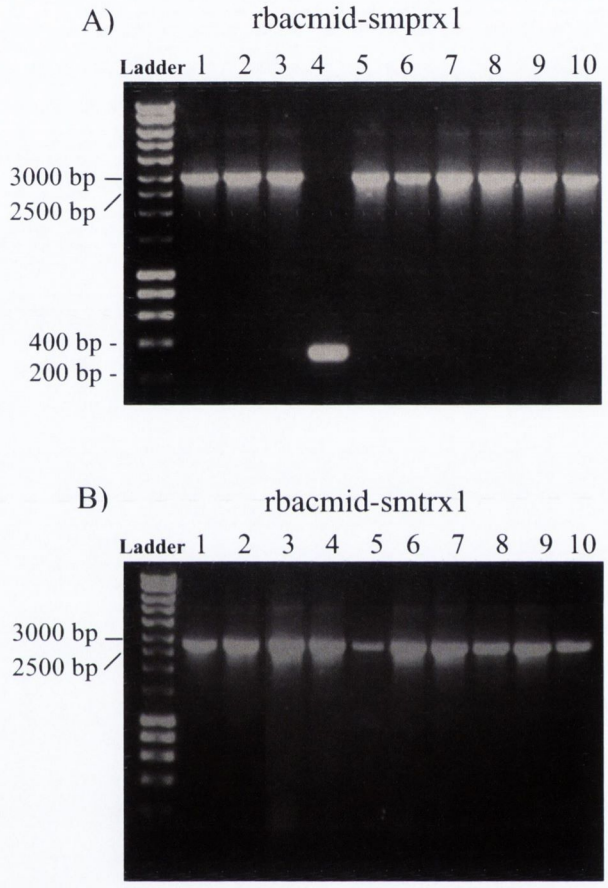

Figure 4.20: **Generation of *S. mansoni* Peroxiredoxin (SmPrx1, A) 1 and *S. mansoni* Thioredoxin (SmTrx1, B) recombinant bacmids**. PCR amplification with M13/pUC forward and reverse primers of DH10Bac^{TM} competent cells colonies (1-10) transformed with *bacsmprx1*-pFastBac-Mel-V5-His *or* *bacsmtrx1*-pFastBac-Mel-V5-His. Five μL of each PCR reaction was electrophoresed on a 0.8% agarose gel.

4.3.3.4 - Generation of recombinant baculovirus stocks and expression of recombinant proteins

For generation of recombinant baculovirus passage 0 (P0), Hi5 cells were transfected with the recombinant bacmids. As SmPrx1 and SmTrx1 coding sequences were cloned in frame with the HBM secretion signal peptide, baculovirus expressed recombinant proteins are expected to be secreted by the infected cells. Therefore, the cell culture supernatant was screened by Western blot with the anti-V5 antibody for detection of the baculovirus-insect cell expressed recombinant proteins, rbacSmPrx1 and rbacSmTrx1 (Figure 4.21). With respect to rbacSmPrx1, the anti-V5 antibody detected a monomer band that migrated at 26,181 kDa (Rf = 0.556). Regarding rbacSmTrx1, 2 bands migrating at 13,092 kDa (Rf = 0.815) and 10,740 kDa (Rf = 0.889) were detected. Presumably, both bands correspond to rbacSmTrx1, which was expressed in slightly different sizes.

S. mansoni Peroxiredoxin 1 recombinant baculovirus P0 was amplified 3 times generating the P3 baculovirus stock used for protein expression. All stages of baculovirus stock production were tested for the presence of the recombinant proteins in the cell culture supernatant. RbacSmPrx1 was successfully detected (Figure 4.22 A). rbacSmPrx1 was expressed by infecting serum free Hi5 cells with P3 baculovirus stock.

4.3.3.5 - Purification of rbacSmPrx1 and rbacSmTrx1

In order to optimize purification of rbacSmPrx1, the recombinant protein was purified by liquid nickel-affinity chromatography using gravity-flow from approximately 50 mL of insect cell culture supernatant. Firstly, purification was performed using the following imidazole concentrations in the buffers: binding buffer with 5 mM imidazole, washing buffer with 20 mM imidazole and elution buffer with 100, 150, 200, 300 and 500

mM imidazole. RbacSmPrx1 was eluted at 100 mM imidazole (Figure 4.22 B).

From a large scale expression of rbacSmPrx1, 320 mL of cell culture supernatant were recovered and processed for purification of the recombinant protein. Based on the results from the first purification, the binding and washing buffer used contained 50 mM imidazole and the elution buffer contained 500 mM. Elution fractions were pooled, concentrated to ~1.5 mL and dialysed with PBS. RbacSmPrx1 purity was evaluated by silver staining. The final protein yield was 150 ug, however the sample was highly contaminated by insect cell secreted proteins (Figure 4.22 C). Immunization of mice with *E. coli* expressed SmPrx1 generated a anti-rSmPrx1 polyclonal antibody that specifically binds to the baculovirus-insect cell expressed protein (Figure 4.22 D).

By comparing the SDS-PAGE of the purified rbacSmPrx1 (Figure 4.22 C) and the Western blot with the anti-rSmPrx1 polyclonal antibody (Figure 4.22 C), it is possible to identify that rbacSmPrx1 was expressed as a doublet. That could result from different glycosilation states of the same molecule which occurs often in the baculovirus-insect cell system.

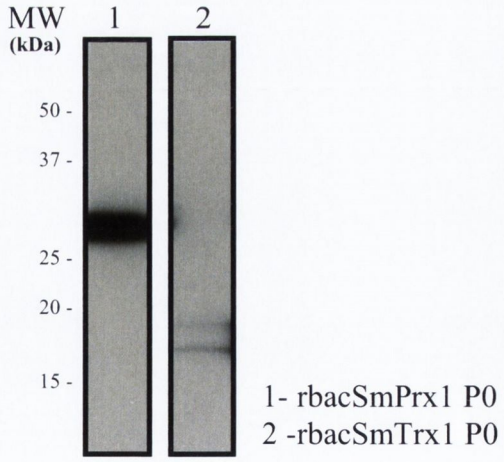

Figure 4.21: **Generation of *S. mansoni* Peroxiredoxin 1 and *S. mansoni* Thioredoxin recombinant baculovirus**. Recombinant baculovirus passage 0 (P0) was generated by transfecting insect cells with rbacmid-smprx1 or rbacmid-smtrx1. The insect cell culture supernatant was screened by Western blot with anti-V5 antibody (1:100000).

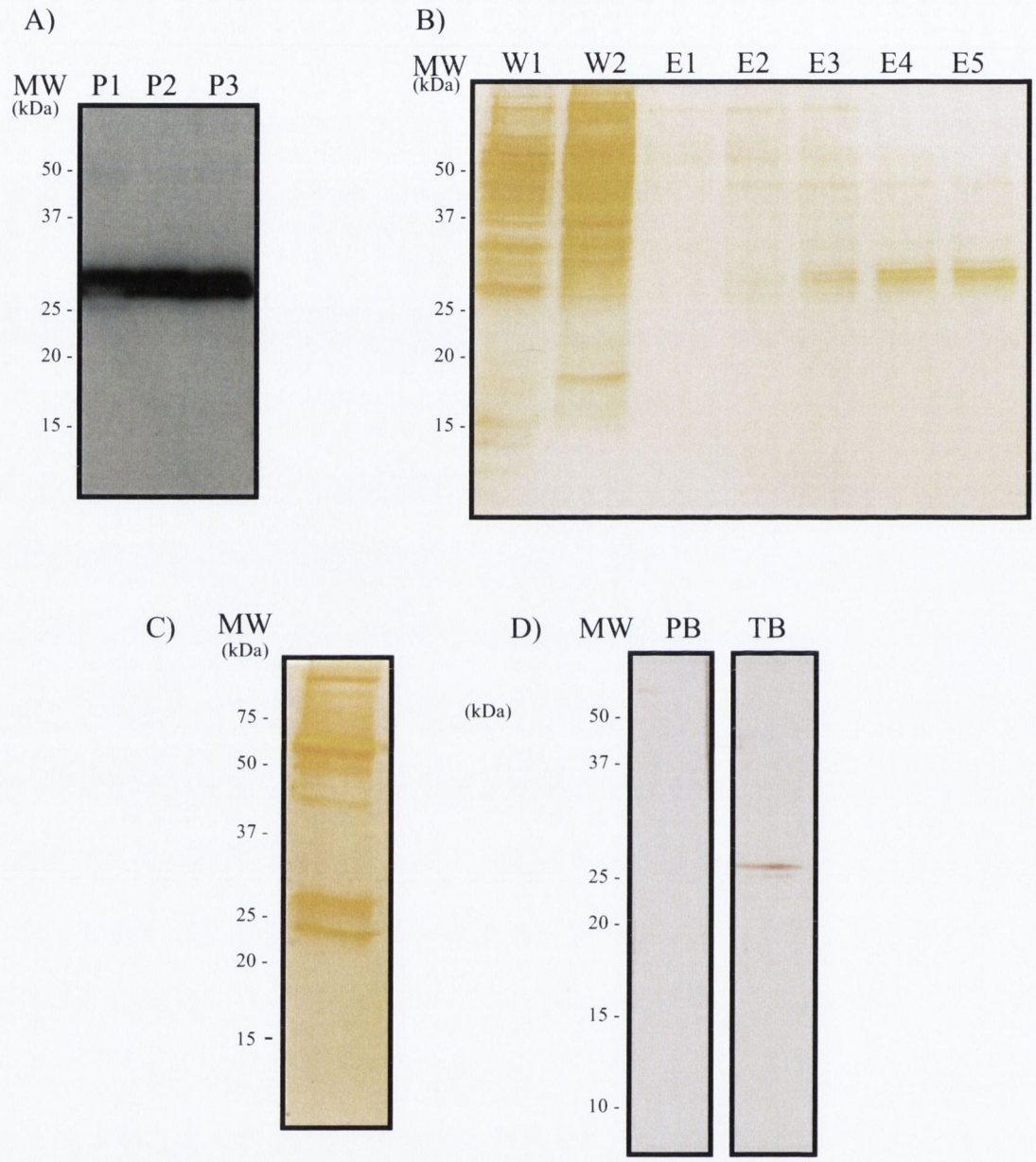

Figure 4.22: **Generation of *S. mansoni* Peroxiredoxin 1 recombinant protein in the baculovirus-insect cell system**. A) Western blot analysis of recombinant baculovirus passage 1 (P1), 2 (P2) and 3 (P3) with anti-V5 antibody (1:100000). B) Initial purification of rbacSmPrx1. W1 and W2 – wash aliquots 1 and 2, E1-5 - elution fractions 1 to 5. 15% SDS-PAGE, silver staining. C) Purified rbacSmPrx1 after concentration and dialysis. 15% SDS-PAGE, silver staining. D) RbacSmPrx1 (0.5 ug per lane) was probed by Western blot with anti-rSmPrx1, 1:100) rabbit sera collected at the end of immunization protocol (Terminal bleed, TB). The pre-bleed (PB), serum harvested before rabbit immunization, was used in the same dilution as control.

4.3.3.6 –rSmPrx1 and rbacSmPrx1 endotoxin levels

The levels of endotoxin contamination were measured in the recombinant SmPrx1 expressed in *E. coli*, rSmPrx1, and insect cell, rbacSmPrx1. rSmPrx1 and rbacSmPrx1 showed 23.551 EU/mg and 0.365 EU/mg, respectively.

4.4 – Discussion

In this chapter, the production of the immunomodulatory protein *S. mansoni* Peroxiredoxin 1 in *E. coli* and baculovirus-insect cell systems was described. SmPrx1 immunomodulatory properties have been elucidated previously (*95*). Recombinant SmPrx1, as well as, the *F. hepatica* homolog, have been shown to drive the alternative activation of macrophages *in vitro* and *in vivo* therefore modulating the host's immune response. SmPrx1 is a potential candidate for the development of novel immunotherapeutics for inflammatory diseases.

For production of the recombinant protein in the *E. coli* expression system, the cloning strategy of choice was the Gateway technology. In this strategy, the gene coding sequence is first ligated to an entry vector and then transferred to a Gateway-adapted destination vector. The destination vector can be selected from a range of options according to the expression system of choice (*E. coli*, yeast, insect cell or mammalian cell). The expression vector of choice may add a N-terminal or C-terminal tag to the recombinant proteins. For generation of soluble *E. coli* expressed recombinant SmPrx1, different expression conditions with various concentrations and combinations of inducer (L-arabinose) and inhibitor (glucose) were tested. The conditions tested induce different synthesis rates. A lower synthesis rate usually increases protein solubility.

Recombinant proteins expressed in *E. coli* show very high levels of lipopolysaccharide (LPS) which is the major component of the outer membrane of gram-negative bacteria (*193*). As LPS elicits an inflammatory response, immunological tests performed with recombinant proteins containing endotoxin contamination are not reliable. For instance, a schistosome recombinant protein, *S. mansoni* chemokine binding protein, smCKBP, expressed in *E. coli* was shown to induce human basophil degranulation (*105*). On the other hand, the recombinant protein expressed in the baculovirus-insect cell system,

a LPS-free expression system, failed to induce similar activity unless exogenous LPS was added (*53*). With that in mind, a LPS-free expression system, the baculovirus-insect cell system, was established in the laboratory for generation of recombinant SmPrx1 (rbacSmPrx1).

For production of recombinant protein in the baculovirus-insect cell system, the initial intention was to transfer the coding sequences from the entry vector to a destination vector adapted for expression in insect cell. This option would be less time consuming than performing the traditional cloning using restriction enzymes. However, the destination vectors available for insect cell expression had a limited choice of tags, only one tag per vector, and did not include a secretion signal peptide. By expressing the recombinant protein with the secretion signal peptide, the downstream processing is facilitated as the recombinant protein is purified directly from the cell culture supernatant without the need of performing laborious cell lysis methods. Thus, SmPrx1 coding sequence was cloned into an insect cell expression vector in frame with a secretion peptide by using the traditional cloning method with restriction enzymes.

One of the main drawbacks of the traditional cloning method is the need to generate large amounts of PCR product for the enzymatic digestion. Additionally, enzymatic digestions of DNA molecules ends, as in the PCR products, tend not to be very efficient with only part of the sample being digested. To overcome this inconvenience, the blunt-end PCR product of the SmPrx1 coding sequence, was initially cloned into a high copy number vector, the pGEM-T-easy, for further amplification followed by digestion.

SmPrx1 was expressed in *E. coli* with the aim to generate an anti-rSmPrx1 specific antibody. This antibody could be further used to purify native SmPrx1 from adult male WES molecules or soluble AW antigens. However, the anti-rSmPrx1 rabbit polyclonal antibody generated did not bind to SmPrx1 in the WES and showed non-specific binding

to high molecular proteins in the WES. Therefore, it can not be used for antibody affinity-purification of the native protein.

Purification of rbacSmPrx1 generated a recombinant protein with low levels of LPS contamination: 0.365 EU/mg or 18.1 pg/mg of LPS. This is a 64,5 fold decrease in the level of endotoxin contamination in relation to the *E. coli* expressed rSmPrx1. The level of purification, however, was less satisfactory. Insect cells in culture release proteins into the supernatant that are usually co-purified with the recombinant polyhistidine-tagged proteins since they bind to the nickel column. For better purification of a baculovirus-insect cell expressed recombinant protein, a second step chromatography method such as, size exclusion or anion exchange, should be performed.

In this chapter, I have described the production and characterization of *S. mansoni* Peroxiredoxin 1. SmPrx1 is a strong immunomodulatory candidate which was identified in the adult male worm excretory-secretory molecules as described in Chapter 3. For further characterization, I have generated recombinant SmPrx1 in 2 different expression systems: *E. coli* and baculovirus-insect cell. Baculovirus-insect cell expressed recombinant SmPrx1 contains very low levels of LPS contamination. Therefore, it is reliable for functional analysis and for the evaluation of its therapeutic potential in mouse models of inflammatory diseases.

Cloning, Expression and Purification of *Schistosoma mansoni* Cyclophilin and *Schistosoma mansoni* Cyclophilin B

5.1 – Introduction

In chapter 3, the proteomic analysis of *S. mansoni* adult male worm excretory-secretory molecules was reported. Among the proteins detected, 2 cyclophilins were identified: *S. mansoni* Cyclophilin and *S. mansoni* Cyclophilin B. In this chapter, the identification and characterization of these two schistosoma cyclophilins are described.

Cyclophilins (Cyps, enzyme commission number 5.1.2.8) are present in all organisms studied up to date, prokaryotes and eukaryotes, and are structurally conserved throughout evolution (*194*). Cyps are enzymes that catalyze the cis-trans transition in peptide bonds preceding proline residues, an activity also known as peptidyl-prolyl cis-trans isomerization. During mRNA translation into an amino acid chain, the ribosome synthetizes peptide bonds in the trans-conformation, which is the lower energetic state. However, peptide bonds preceding proline residues can ocur in the higher energetic state, the cis-conformation. Important cellular processes like protein folding and assembly of multidomains complexes requires the cis-trans transition catalyzed by cyclophilins. Other protein classes, such as parvulins and FK-506-binding proteins (FKBPs), although not sequence correlated to cyclophilins, also present the peptidyl-prolyl cis-trans isomerization activity. Cyclophilins, Parvulins and FKBPs are often considered together and constitute the immunophilin protein family (*195*).

Cyclophilins have been shown to bind to the immunosuppressive drug cyclosporin A (CsA), at varying degrees of affinity. The Cyp-CsA complex, interacts with and inhibits calcineurin, a calcium-calmodulin-activated serine/threonine specific protein phosphatase.

Inhibition of calcineurin blocks translocation of nuclear factor of activated T cells preventing the transcription of cytokines and other genes (*196*).

Parasite cyclophilins have been a subject of study because of the anti-parasitic effects of Cyclosporin A. Cyclosporin A susceptible parasites include *S. mansoni, Echinococus granulosus, Plasmodium falciparum*, *Leishmania donovani* and *Trypanosoma cruzi* among others (*197-201*). However, the Cyclosporin A anti-parasitic effect might result from interactions with different molecules rather than cyclophilins such as, P-glycoproteins, or from some other consequence of binding to cyclophilin unrelated to calcineurin (*195, 202, 203*).

An unexpected role has been described for *Toxoplasma gondii* 18-kDa cyclophilin, TgCyp18. Secreted TgCyp18 interacts directly with cysteine chemokine receptor CCR5 in dendritic cells and macrophages. This interaction triggers IL-12-dependent production of Interferon (IFN)-γ which is critical to host survival of acute toxoplasmosis in mouse models (*204, 205*). Site-direct mutagenesis of putatively surface exposed residues of TgCYP18 have identified regions that are critical for binding to the CCR5 (*206*).

In chapter 3, section 3.3.2.1, two 2D spots detected in the WES preparation but absent in the worm somatic molecules were identified as Cyclophilin. *S. mansoni* Cyclophilin is therefore unique to the worm excretome-secretome. Since this protein has not been previously characterized, it represents a novel molecule in the schistosome field. Cyclophilin B is a novel non characterized schistosome protein as well and it was also detected in the worm excretome-secretome.

5.2 – Objective

Production of recombinant *S. mansoni* Cyclophilin and *S. mansoni* Cyclophilin B in *E. coli* and baculovirus-insect cell systems.

5.3 – Results

5.3.1 – Identification of *S. mansoni* Cyclophilin (SmCyp1) and *S. mansoni* Cyclophilin B (SmCyp2) in the male adult worm excretory-secretory (WES) molecules and sequence analysis

5.3.1.1 – *S. mansoni* Cyclophilin (SmCyp1)

In the comparative mass spectrometry analysis of the *S. mansoni* male worm excretory-secretory molecules and the adult worm somatic molecules, described in chapter 3, section 3.3.2.1, two 2D spots unique to the WES preparation (spot 4 and 5) were identified as Smp_040130. Further mass spectrometry analysis of WES molecules, described in chapter 3, section 3.3.2.2, identified the spots 117, 118, 150 and 152 as Smp_040130. The highest score and sequence coverage detected were 927 and 77%, respectively (Chapter 3, Table 3.1 – ID 40). The nominal mass detected for Smp_040130 was 17,945 kDa.

Smp_040130 is a 650 bp gene located at the chromosome 5 position 7964642-7965291. The pre-mRNA is edited by splicing. One intron is removed and 2 exons are joined. The resulting mRNA has a coding sequence of 486 bp which is translated into 161 amino acids. The resulting protein is named Cyclophilin. In the present study, *S. mansoni* Cyclophilin is abbreviated as SmCyp1 (Table 5.1).

SmCyp1 has a predicted molecular weight of 17,671 kDa and a predicted pI of 8.26. It does not contain a signal peptide for secretion but it is predicted to be secreted through a non-classical pathway with a SecP score of 0.543. Based on gene ontology analysis, SmCyp1 is thought to be involved in protein peptidyl-prolyl isomerization and protein folding. By scanning the protein sequence with the InterPro database the following

protein signatures were addressed to SmCyp1: (1) peptidyl-prolyl cis-trans isomerase, cyclophilin-type; (2) cyclophilin-like and (3) peptidyl-prolyl cis-trans isomerase, cyclophilin-type, conserved site (Figure 5.1 A).

SmCyp1 and TgCYP18 alignment reveals 56% similarity in between these 2 proteins (Table 5.2). The cyclophilin-type peptidyl-prolyl cis-trans isomerase domain shared by SmCyp1 and TgCYP18 is shown in Figure 5.2.

	Protein name	*S. mansoni* Cyclophilin SmCyp1	*S. mansoni* Cyclophilin B SmCyp2
Gene information	GeneDB ID	Smp_040130	Smp_040790
	GenBank ID	8347523	8347588
	Gene length	650 bp	941 bp
	Location	Chr_5 : 7964642-7965291	Chr_3 : 20565686-20566626
	Coding sequence length	486 bp	642 bp
Protein information	GeneDB protein name	Cyclophilin	Cyclophilin B, putative
	Alternative names	Peptidyl-prolyl cis-trans isomerase Cyclophilin Cyclosporin A-binding protein Rotamase Smp17.7 p17.7	Peptidyl-prolyl cis-trans isomerase B Cyclophilin B Rotamase B S-cyclophilin
	UniProtKB/Swiss-Prot accession number	Q26565	Q26551
	NCBI RefSeq	XP_002575376.1	XP_002575437.1
	Amino acids	161	190*
	Predicted pI	8.26	8.10*
	Predicted molecular weight	17,671 kDa	20.798* kDa
	Signal peptide	not detected	detected
	Non-classical secretion (SecP score)	0.543	--
	Biological process GO terms	GO:0000413 protein peptidyl-prolyl isomerization GO:0006457 protein folding	GO:0000413 protein peptidyl-prolyl isomerization GO:0006457 protein folding
	Molecular Function GO terms	GO:0003755 peptidyl-prolyl cis-trans isomerase activity GO:0016853 isomerase activity GO:0042277 peptide binding	GO:0003755 peptidyl-prolyl cis-trans isomerase activity GO:0016853 isomerase activity GO:0042277 peptide binding
	IUMB - Enzyme nomenclature	EC 5.2.1.8 - peptidylprolyl isomerase	EC 5.2.1.8 - peptidylprolyl isomerase
	Reaction catalysed	peptidylproline (ω=180) = peptidylproline (ω=0)	peptidylproline (ω=180) = peptidylproline (ω=0)

Table 5.1: ***S. mansoni* Cyclophilin (SmCyp1) and *S. mansoni* Cyclophilin B (SmCyp2) gene and protein information.** Chr: chromosome. * without signal peptide.

A) ***S. mansoni* Cyclophilin protein signatures**

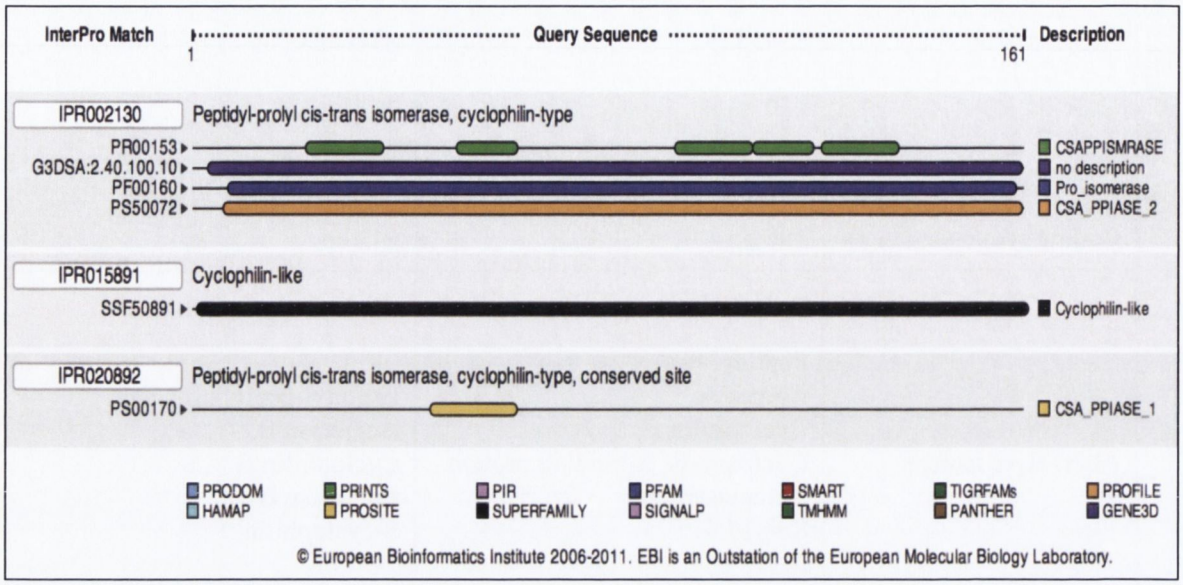

B) ***S. mansoni* Cyclophilin B protein signatures**

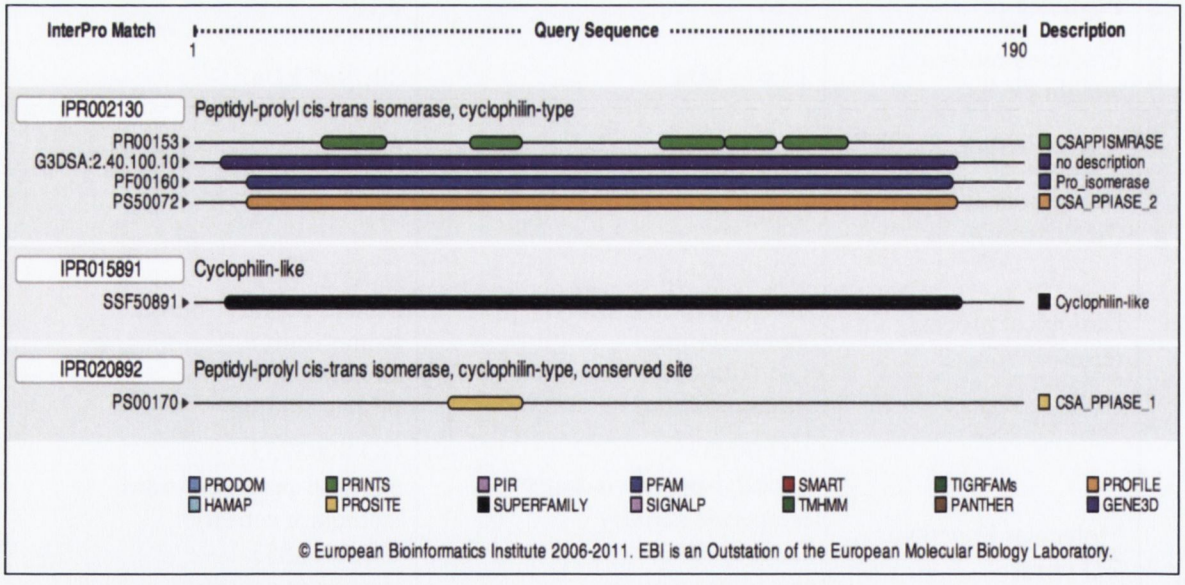

Figure 5.1: **Prediction of *S. mansoni* Cyclophilin (SmCyp1, A) and *S. mansoni* Cyclophilin B (SmCyp2, B) signatures by InterProScan integrated database**. SmCyp1 (A) and SmCyp2 (B) amino acid sequences were scanned by InterPro member databases (bottom squares) in search for protein families, domains, regions and/or sites that are grouped in unique InterPro entries (white boxes). G3DSA: 2.40.100.10: Gene3D Superfamily Cyclophilin.

S. mansoni protein	Sequence similarity scores (%) in relation to TgCYP18
SmCyp1	56.0
SmCyp2	49.0

Table 5.2: **Pairwise sequence similarity between *S. mansoni* Cyclophilin (SmCyp1) or *S. mansoni* Cyclophilin B (SmCyp2) and *T. gondii* Cyclophilin C-18 (TgCYP18).** Percentage of sequence similarity between *S. mansoni* Cyclophilin or *S. mansoni* Cyclophilin B and *T. gondii* Cyclophilin C-18 (TgCYP18, GenBank AAA17997.1) calculated by the ClustalW2 multiple sequence alignment program.

```
SmCyp1   ------------------------------MAAKAFFDIKAGDERLGRIIFELFN-DVPDT
SmCyp2   MAVLKPLCPLLLLSIICFGLIRSEANGPKVTDKVFFDIEVDGKPLARIIIGLFGKTVPKT
TgCYP18  -----MKLVLFFLALAVSGAVAENAG----VRKAYMDIDIDGEHAGRIILELREDIAPKT
                                        . *.::**. ..:  .***: *    .*.*

SmCyp1   TRNFRELCT-----HKNNFGYKGSVFHRIIPGFMCQGGDFTNGDGTGGKSIYGNKFKDEN
SmCyp2   VENFKQLSIGTQLKDGRTASYKGSTFHRVIKSFMIQGGDFTNHDGTGGFSIYGDRFPDEN
TgCYP18  VKNFIGLFD----------KYKGSVFHRIIPDFMIQGGDFENHNGTGGHSIYGRRFDDEN
         ..**  *             ****.***:* .** ***** * :**** **** :* ***

SmCyp1   FNHKHEAFS-LSMANAGPNTNGSQFFITTVPCSWLDGKHVVFGKVVSG-IDVVKKMESLG
SmCyp2   FKLRHVGAGWLSMANAGPDTNGSQFFITTVKTSWLDGKHVVFGKVVEG-MNIVRQIESET
TgCYP18  FDLKHERGV-ISMANAGPNTNGSQFFITTVKTEWLDARHVVFGKITTESWPTVQAIEALG
         *. :*     :*******:***********  .***.:******:.      *: :*:

SmCyp1   STS-GKPSKKIIIEDCGEC---------------
SmCyp2   TDSRDRPVKSIKIASCGHIPVEIPFSVTNSDAVE
TgCYP18  GSG-GRPSKVAKITDIGLLE--------------
              . .:* *   * . *
```

Figure 5.2: **Multiple sequence alignment of *S. mansoni* Cyclophilin (SmCyp1), *S. mansoni* Cyclophilin B (SmCyp2) and *T. gondii* Cyclophilin C-18 (TgCYP18).** *S. mansoni* Cyclophilin and *S. mansoni* Cyclophilin B protein sequence were aligned to *T. gondii* Cyclophilin C-18 (TgCYP18, GenBank AAA17997.1) using the ClustalW2 multiple sequence alignment program. The Cyclophilin-type peptidyl-prolyl cis-trans isomerase domain is highlighted in yellow.

* (asterisk) – positions which have a single, fully conserved residue.

: (colon) – conservation between groups of strongly similar properties.

. (period) – conservation between groups of weakly similar properties.

5.3.1.2 - *S. mansoni* Cyclophilin B (SmCyp2)

Mass spectrometry analysis of WES 2D identified the spot number 123 as Smp_040790 with a score of 113 and sequence coverage of 19% (Chapter 3, Table 3.1 – ID 41). The nominal mass detected was 23,452 kDa.

Smp_040790 is a 941 bp gene located at the chromosome 3 position 20565686-20566626. The pre-mRNA is edited by splicing. Six exons are joined resulting in a coding sequence of 642 bp that generates a protein of 213 amino acids. The translated product is named Cyclophilin B, putative. In the present study, *S. mansoni* cyclophilin B is abbreviated as SmCyp2. SmCyp2 contains a secretion signal peptide. After cleavage, the protein contains 190 amino acids with a predicted molecular weight of 20,798 kDa and a predicted pI of 8.10 (Table 5.1). Based on gene ontology analysis, SmCyp2 is predicted to be involved in the same biological processes as SmCyp1: protein peptidyl-prolyl isomerization and protein folding. SmCyp1 and SmCyp2 also share the same InterPro protein signatures (Figure 5.1).

SmCyp2 and TgCYP18 alignment reveals 49% similarity in between these 2 proteins (Table 5.2). The cyclophilin-type peptidyl-prolyl cis-trans isomerase domain shared by SmCyp1 and TgCYP18 is shown in Figure 5.2.

5.3.2 - Production of recombinant *S. mansoni* Cyclophilin (SmCyp1) and *S. mansoni* Cyclophilin B (SmCyp2) in *E. coli*

The cloning strategy used for production of recombinants SmCyp1 and SmCyp2 in *E. coli* is summarized in Figure 5.3.

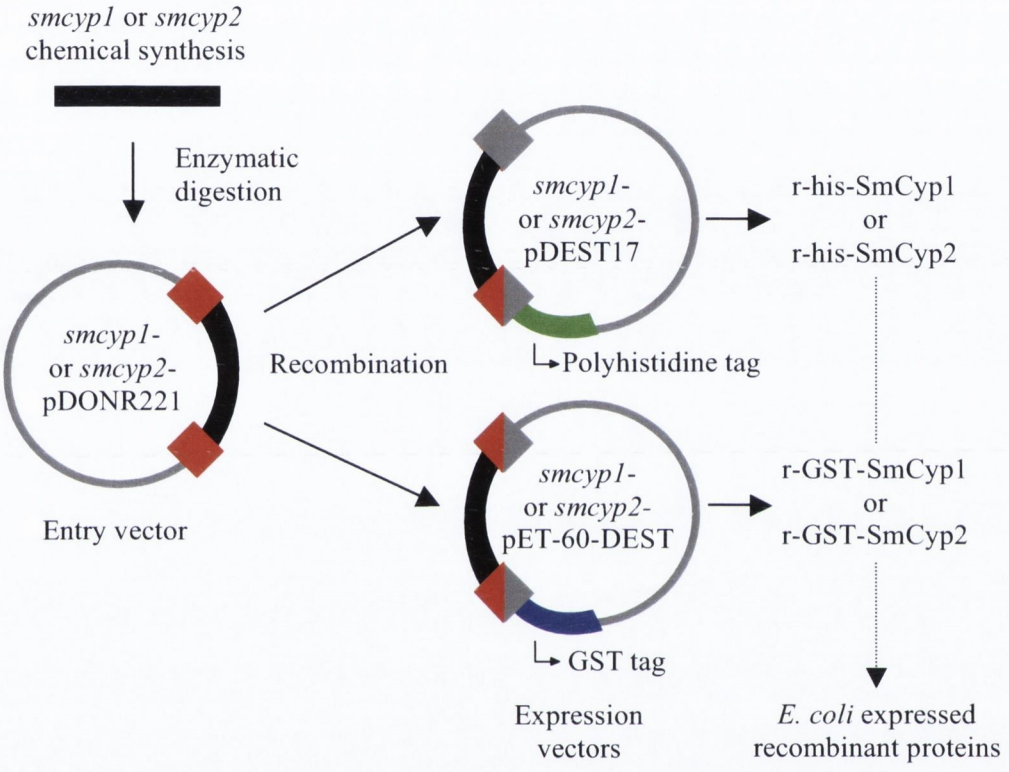

Figure 5.3: **Cloning strategy used for production of recombinant *S. mansoni* Cyclophilin (SmCyp1) and *S. mansoni* Cyclophilin B (SmCyp2) in *E. coli.*** SmCyp1 and SmCyp2 Protein coding sequences were chemically synthesized and cloned into the entry vector pDORNR221 and the expression vector pDEST17 by a commercial company. The cloning into the expression vector pET-60-DEST was carried on in-house.

5.3.2.1 - Cloning, expression and solubility analysis of recombinant polyhistidine-tagged *S. mansoni* Cyclophilin (r-his-SmCyp1) and *S. mansoni* Cyclophilin B (r-his-SmCyp2) in *E. coli.*

5.3.2.1.1 - Synthesis of SmCyp1 and SmCyp2 coding sequences

The coding sequences for SmCyp1 and SmCyp2, named *smcyp1* and *smcyp2,* respectively, were chemically synthesized by a commercial company (Geneart) as described in chapter 2, section 2.4.8. SmCyp1 and SmCyp2 coding sequences were downloaded from *S. mansoni* GeneDB sequence database and used as a template for the chemical synthesis (Figure 5.4). The SmCyp2 coding sequence was synthesized without the signal peptide coding region.

5.3.2.1.2 - Cloning of *smcyp1* and *smcyp2* into pDEST17 *E. coli* expression vector

The coding sequences, *smcyp1* and *smcyp2*, were cloned into the entry vector pDONR221 (Appendix 4) and the *E. coli* expression vector pDEST17 (Appendix 4). The cloning was carried out by a commercial company (Geneart). The coding sequences were cloned in frame with a N-terminal polyhistidine tag for purification and detection purposes (Figure 5.5). The expressed proteins are expected to contain 22 amino acids derived from the pDEST17, with a predicted molecular weight of approximately 2.7 kDa (Figure 5.6). The recombinant proteins, r-his-SmCyp1 and r-his-SmCyp2, have predicted molecular weights of 20,233 kDa and 23,491 kDa, respectively (Table 5.3).

A) ***S. mansoni* Cyclophilin coding sequence (486 bp)**

ATGGCTGCGAAAGCGTTTTTCGATATTAAGGCCGGTGATGAACGATTGGGGAGGATTATA
TTTGAGCTATTCAATGATGTTCCAGATACTACTAGAAACTTTCGCGAGTTATGCACTCAC
AAGAATAATTTTGGTTACAAAGGTTCCGTTTTCCACCGAATAATTCCAGGCTTCATGTGT
CAGGGTGGCGATTTCACCAATGGCGATGGCACGGGTGGAAAAAGTATATACGGAAATAAA
TTCAAAGATGAGAACTTCAATCACAAACACGAAGCGTTCTCACTTTCAATGGCCAATGCG
GGACCTAACACCAATGGTTCGCAATTCTTTATTACTACTGTCCCTTGTTCGTGGCTTGAC
GGCAAACATGTTGTTTTCGGTAAAGTCGTCAGTGGCATAGACGTGGTGAAGAAAATGGAG
AGTTTAGGTTCCACAAGTGGAAAGCCGTCCAAGAAAATTATAATCGAAGATTGTGGAGAA
TGTTAA

B) ***S. mansoni* Cyclophilin B coding sequence (642 bp)**

ATGGCCGTTCTAAAGCTGTTATGCCCGTTATTACTACTGTCTATCATATGTTTCGGCCTT
ATTCGCAGTGAAGCGAATGGACCCAAAGTTACTGACAAAGTGTTTTTCGATATTGAAGTT
GATGGAAAACCACTTGGTCGAATAATTATCGGATTGTTTGGTAAAACAGTGCCTAAGACA
GTGGAAAATTTCAAACAACTTTCAATTGGCACTCAACTGAAGGATGGTCGAACTGCTTCA
TATAAAGGAAGCACTTTTCATCGTGTTATTAAGTCATTCATGATACAAGGTGGAGACTTC
ACAAACCACGATGGAACTGGAGGTTTTAGTATTTATGGCGATAGGTTCCCTGATGAAAAC
TTCAAATTGAGACATGTGGGTGCAGGGTGGCTGTCGATGGCTAATGCTGGTCCTGATACA
AATGGAAGCCAATTCTTTATTACGACCGTGAAGACCTCGTGGTTAGATGGAAAGCATGTT
GTTTTCGGAAAAGTTGTAGAAGGAATGAACATTGTTAGACAGATTGAAAGTGAAACGACG
GATTCAAGAGATAGACCTGTTAAGAGCATCAAGATAGCCAGTTGCGGCCACATTCCCGTG
GAAATACCCTTCTCGGTAACGAACTCTGATGCTGTCGAATGA

Figure 5.4: ***S. mansoni* Cyclophilin (SmCyp1, A) and *S. mansoni* Cyclophilin B (SmCyp2, B) coding sequences.** – start codon, – stop codon, underlined – signal peptide coding region.

A) ***E. coli* expressed recombinant polyhistidine-tagged *S. mansoni* Cyclophilin coding sequence (549 bp)**

ATGTCGTACTACCATCACCATCACCATCACCTCGAATCAACAAGTTTGTACAAAAAAGCA
GGCTTCGCTGCGAAAGCGTTTTTCGATATTAAGGCCGGTGATGAACGATTGGGGAGGATT
ATATTTGAGCTATTCAATGATGTTCCAGATACTACTAGAAACTTTCGCGAGTTATGCACT
CACAAGAATAATTTTGGTTACAAAGGTTCCGTTTTCCACCGAATAATTCCAGGCTTCATG
TGTCAGGGTGGCGATTTCACCAATGGCGATGGCACGGGTGGAAAAAGTATATACGGAAAT
AAATTCAAAGATGAGAACTTCAATCACAAACACGAAGCGTTCTCACTTTCAATGGCCAAT
GCGGGACCTAACACCAATGGTTCGCAATTCTTTATTACTACTGTCCCTTGTTCGTGGCTT
GACGGCAAACATGTTGTTTTCGGTAAAGTCGTCAGTGGCATAGACGTGGTGAAGAAAATG
GAGAGTTTAGGTTCCACAAGTGGAAAGCCGTCCAAGAAAATTATAATCGAAGATTGTGGA
GAATGTTAA

B) ***E. coli* expressed recombinant polyhistidine-tagged *S. mansoni* Cyclophilin B coding sequence (639 bp)**

ATGTCGTACTACCATCACCATCACCATCACCTCGAATCAACAAGTTTGTACAAAAAAGCA
GGCTTCGAAGCGAATGGACCCAAAGTTACTGACAAAGTGTTTTTCGATATTGAAGTTGAT
GGAAAACCACTTGCTCGAATAATTATCGGATTGTTTGGTAAAACAGTGCCTAAGACAGTG
GAAAATTTCAAACAACTTTCAATTGGCACTCAACTGAAGGATGGTCGAACTGCTTCATAT
AAAGGAAGCACTTTTCATCGTGTTATTAAGTCATTCATGATACAAGGTGGAGACTTCACA
AACCACGATGGAACTGGAGGTTTTAGTATTTATGGCGATAGGTTCCCTGATGAAAACTTC
AAATTGAGACATGTGGGTGCAGGGTGGCTGTCGATGGCTAATGCTGGTCCTGATACAAAT
GGAAGCCAATTCTTTATTACGACCGTGAAGACCTCGTGGTTAGATGGAAAGCATGTTGTT
TTCGGAAAAGTTGTAGAAGGAATGAACATTGTTAGACAGATTGAAAGTGAAACGACGGAT
TCAAGAGATAGACCTGTTAAGAGCATCAAGATAGCCAGTTGCGGCCACATTCCCGTGGAA
ATACCCTTCTCGGTAACGAACTCTGATGCTGTCGAATGA

Figure 5.5: ***E. coli* expressed recombinant polyhistidine-tagged *S. mansoni* Cyclophilin (r-his-SmCyp1, A) and *S. mansoni* Cyclophilin B (r-his-SmCyp2, B) coding sequences.** – start codon, – stop codon, – coding sequence for the polyhistidine tag, blue letters – codons derived from pDEST17, underlined – codons from *smcyp1* and *smcyp2* coding sequence.

A) **Native and *E. coli* expressed recombinant polyhistidine-tagged *S. mansoni* Cyclophilin protein sequence alignment**

```
SmCyp1          ----------------------MAAKAFFDIKAGDERLGRIIFELFNDVPDTTRNFRELCT
r-his-SmCyp1    MSYYHHHHHHLESTSLYKKAGFAAKAFFDIKAGDERLGRIIFELFNDVPDTTRNFRELCT
                                      ************************************

SmCyp1          HKNNFGYKGSVFHRIIPGFMCQGGDFTNGDGTGGKSIYGNKFKDENFNHKHEAFSLSMAN
r-his-SmCyp1    HKNNFGYKGSVFHRIIPGFMCQGGDFTNGDGTGGKSIYGNKFKDENFNHKHEAFSLSMAN
                ************************************************************

SmCyp1          AGPNTNGSQFFITTVPCSWLDGKHVVFGKVVSGIDVVKKMESLGSTSGKPSKKIIIEDCG
r-his-SmCyp1    AGPNTNGSQFFITTVPCSWLDGKHVVFGKVVSGIDVVKKMESLGSTSGKPSKKIIIEDCG
                ************************************************************

SmCyp1          EC
r-his-SmCyp1    EC
                **
```

B) **Native and *E. coli* expressed recombinant polyhistidine-tagged *S. mansoni* Cyclophilin B protein sequence alignment**

```
SmCyp2          ----------------------EANGPKVTDKVFFDIEVDGKPLARIIIGLFGKTVPKTV
r-his-SmCyp2    MSYYHHHHHHLESTSLYKKAGFEANGPKVTDKVFFDIEVDGKPLARIIIGLFGKTVPKTV
                                      ************************************

SmCyp2          ENFKQLSIGTQLKDGRTASYKGSTFHRVIKSFMIQGGDFTNHDGTGGFSIYGDRFPDENF
r-his-SmCyp2    ENFKQLSIGTQLKDGRTASYKGSTFHRVIKSFMIQGGDFTNHDGTGGFSIYGDRFPDENF
                ************************************************************

SmCyp2          KLRHVGAGWLSMANAGPDTNGSQFFITTVKTSWLDGKHVVFGKVVEGMNIVRQIESETTD
r-his-SmCyp2    KLRHVGAGWLSMANAGPDTNGSQFFITTVKTSWLDGKHVVFGKVVEGMNIVRQIESETTD
                ************************************************************

SmCyp2          SRDRPVKSIKIASCGHIPVEIPFSVTNSDAVE
r-his-SmCyp2    SRDRPVKSIKIASCGHIPVEIPFSVTNSDAVE
                ********************************
```

Figure 5.6: **Native and *E. coli* expressed recombinant polyhistidine-tagged *S. mansoni* Cyclophilin (SmCyp1, r-his-SmCyp1, A) and *S. mansoni* Cyclophilin B (SmCyp2, r-his-SmCyp2, B) protein sequence alignment**. – starting methionine, blue letters – amino acids derived from pDEST17, – polyhistidine tag, * (asterisk) – positions which have a single, fully conserved residue. Sequence of native SmCyp2 is shown without signal peptide.

Protein	Number of amino acids	Predicted pI	Predicted molecular weight (kDa)
SmCyp1	161	8.26	17,671
r-his-SmCyp1	182	8.55	20,233
SmCyp2*	190	8.10	20,798
r-his-SmCyp2	212	8.57	23,491

Table 5.3: **Comparison of native and *E. coli* expressed recombinant polyhistidine-tagged *S. mansoni* Cyclophilin (SmCyp1, r-his-SmCyp1) and *S. mansoni* Cyclophilin B (SmCyp2, r-his-SmCyp2).** * without signal peptide.

5.3.2.1.3 - Expression of r-his-SmCyp1 and r-his-SmCyp2 in *E. coli*

r-his-SmCyp1 and r-his-SmCyp2 expression was firstly performed in BL21-AI *E. coli* competent cells. For initial analysis, protein expression was initiated with the inducer L-arabinose at the standard concentration of 0.2% suggested by the manufacturer. Samples of the induced cultures were collected every hour until 5 hours after induction. A non-induced culture was kept as control. Induction of r-his-SmCyp1 expression produced an abundant protein band that migrated at 18,155 kDa (Rf = 0.732) on a 15% SDS-PAGE (Figure 5.7 A). Induction of r-his-SmCyp2 expression showed a predominant protein band that migrated at 23,388 kDa (Rf = 0.626) on a 15% SDS-PAGE (Figure 5.7 B).

5.3.2.1.4 - Analysis of r-his-SmCyp1 and r-his-SmCyp2 solubility

The solubility of the recombinant proteins was evaluated after lysing the cells by sonication as described in chapter 2, section 2.6.1.2. The insoluble (pellet) and soluble (supernatant) lysate fractions were screened by Western blot with an anti-6X polyhistidine antibody for the presence of the recombinant proteins. r-his-SmCyp1 was fully expressed as an insoluble form since it was detected in the pellet only. With respect to r-his-SmCyp2, the recombinant protein was expressed mostly in an insoluble form, however a weaker band was also detected in the supernatant. Apart from the main r-his-SmCyp2 band that migrated at 24,717 kDa (Rf = 0.593), 2 other bands were also visible in the pellet fraction: a band migrating at 55,335 kDa (Rf = 0.278) indicating the formation of a protein dimer and a band migrating at 28,774 kDa (Rf = 0.537) that could result from a readthrough of the stop codon during translation (Figure 5.8).

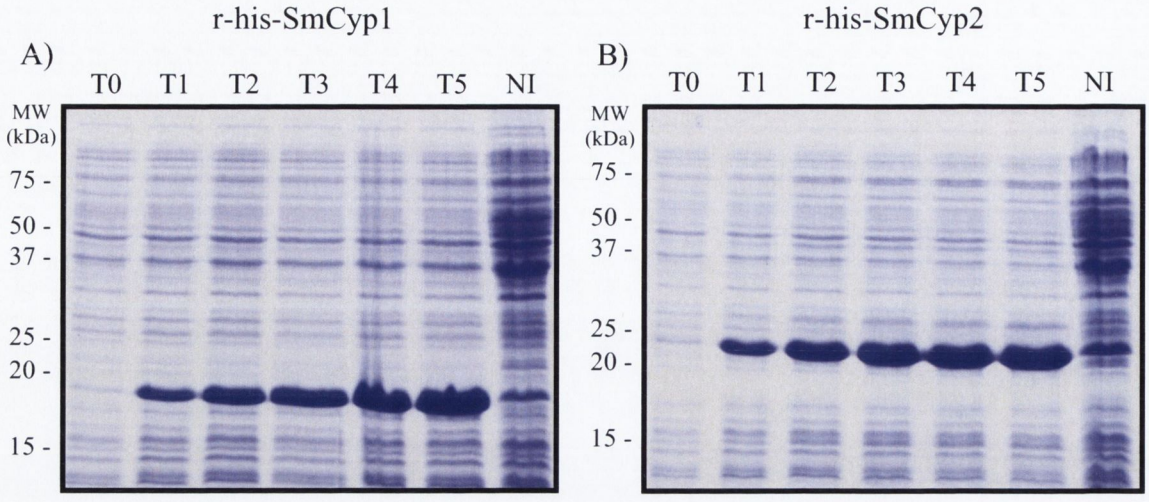

Figure 5.7: **Expression of recombinant polyhistidine-tagged *S. mansoni* Cyclophilin (r-his-SmCyp1, A) and *S. mansoni* Cyclophilin B (r-his-SmCyp2, B) in *E. coli*.** Samples from an induced (I) culture were collected at different time points: 0 (T0), 1 (T1), 2 (T2), 3 (T3), 4 (T4) and 5 (T5) hours after induction. A non-induced (NI) culture was used as control and kept for 5 hours. 15% SDS-PAGE, Coomassie Brilliant Blue staining. MW- molecular weight.

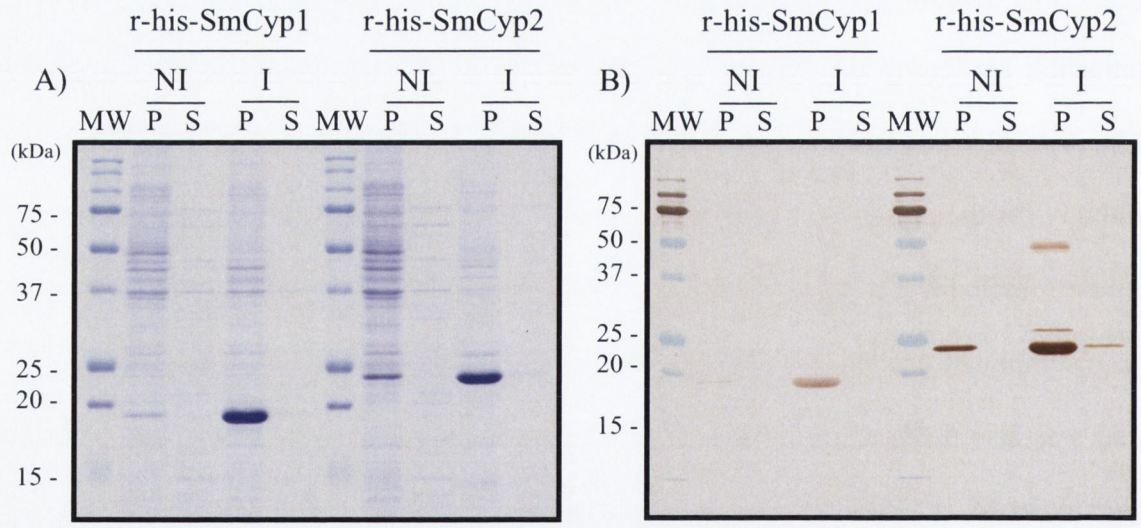

Figure 5.8: **Analysis of *E. coli* expressed recombinant polyhistidine-tagged *S. mansoni* Cyclophilin (r-his-SmCyp1) and *S. mansoni* Cyclophilin B (r-his-SmCyp2) solubility.** r-his-SmCyp1 and r-his-SmCyp2 induced (I) and non-induced (NI) cultures were collected and lysed. The pellet (P) and supernatant (S) were analyzed in a 15% SDS-PAGE (A) stained with Coomassie Brilliant Blue and by a Western blot (B) with anti-6X polyhistidine antibody (1:1000). MW- molecular weight.

In an attempt to improve recombinant protein solubility, production of r-his-SmCyp1 and r-his-SmCyp2 was carried out using different expression conditions: 2 concentrations of the inducer L-arabinose, 0.2% and 0.02%, with or without 0.1% glucose, the expression inhibitor (Table 5.4). None of the conditions tested succeeded to improve r-his-SmCyp1 and r-his-SmCyp2 solubility (Figure 5.9).

To test whether r-his-SmCyp1 and r-his-SmCyp2 could be expressed as soluble proteins using an alternative *E. coli* strain, the expression of the recombinant proteins was induced in the Rossetta (DE3) strain. R-his-SmCyp1 and r-his-SmCyp2 were expressed in 3 different concentrations of the inducer IPTG: 0.1, 0.5 and 1 mM (Table 5.5). However, none of the conditions tested resulted in the expression of soluble protein (Figure 5.10).

Expression conditions	L-Arabinose	Glucose
C1	0.2%	----
C2	0.02%	----
C3	0.2%	0.1%
C4	0.02%	0.1%

Table 5.4: **Expression conditions tested in order to increase solubility of polyhistidine-tagged recombinant *S. mansoni* Cyclophilin (r-his-SmCyp1) and *S. mansoni* Cyclophilin B (r-his-SmCyp2) expressed in BL21-AI *E. coli* strain.**

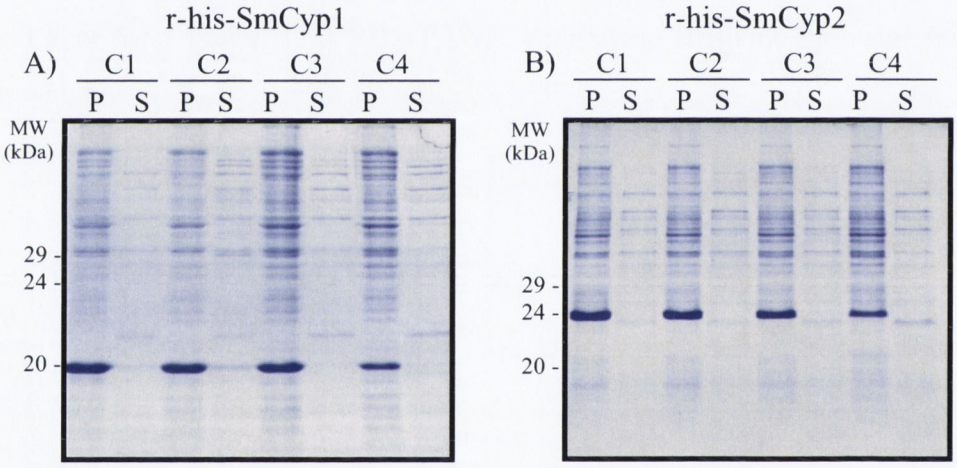

Figure 5.9: **Solubility analysis of polyhistidine-tagged recombinant *S. mansoni* Cyclophilin (r-his-SmCyp1, A) and *S. mansoni* Cyclophilin B (r-his-SmCyp2, B) expressed in BL21-AI *E. coli* under different conditions.** R-his-SmCyp1 and r-his-SmCyp2 were expressed in 4 different concentrations of inducer with or without repressor (C1 to C4, Table 5.4) in order to improve protein solubility. Five hours after induction, cultures were collected and lysed. 15% SDS-PAGE, Coomassie Brilliant Blue staining. P- pellet, S- supernatant, MW- molecular weight.

Expression conditions	IPTG
C1	0.1 mM
C2	0.5 mM
C3	1 mM

Table 5.5: **Expression conditions tested in order to increase solubility of polyhistidine-tagged recombinant *S. mansoni* Cyclophilin (r-his-SmCyp1) and *S. mansoni* Cyclophilin B (r-his-SmCyp2) expressed in Rosetta (DE3) *E. coli strain*.**

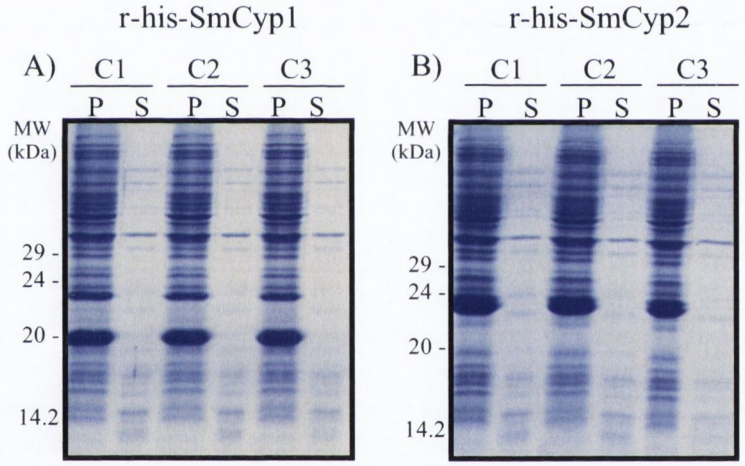

Figure 5.10: **Solubility analysis of recombinant *S. mansoni* Cyclophilin (r-his-SmCyp1, A) and *S. mansoni* Cyclophilin B (r-his-SmCyp2, B) expressed in Rosetta (DE3) *E. coli* under different conditions.** R-his-SmCyp1 and r-his-SmCyp2 were expressed in 3 different concentrations of inducer (C1 to C3, Table 5.5) in order to improve protein solubility. Five hours after induction, cultures were collected and lysed. 15% SDS-PAGE, Coomassie Brilliant Blue staining. P- pellet, S- supernatant, MW- molecular weight.

5.3.2.2 - Cloning, expression and solubility analysis of recombinant Glutathione-S-transferase-tagged *S. mansoni* Cyclophilin (r-GST-SmCyp1) and *S. mansoni* Cyclophilin B (r-GST-SmCyp2) in *E. coli*

To improve expression of soluble recombinant proteins in *E. coli*, SmCyp1 and SmCyp2 were expressed with a N-terminal Glutathione-S-transferase (GST) tag.

5.3.2.2.1 - Cloning of *smcyp1* and *smcyp2* into pET-60-DEST *E. coli* expression vector

The coding sequences, *smcyp1 and smcyp2,* were chemically synthesized and cloned into the entry vector pDONR221 as described in sections 5.3.2.1.1 and 5.3.2.1.2, respectively. *Smcyp1* and *smcyp2* were transferred from the entry vector pDONR221 into the expression vector pET-60-DEST by recombination as described in chapter 2, section 2.4.6 (Figure 5.3). The coding sequences were cloned in-frame with a N-terminal GST tag and a thrombin cleavage site (Figures 5.11 and 5.12). The final recombinant proteins are expected to contain 238 amino acids derived from the pET-60-DEST vector (Figures 5.13 and 5.14), with a predicted molecular weight of approximately 27,546 kDa. The recombinant proteins, r-GST-SmCyp1 and r-GST-SmCyp2, have predicted molecular weights of 45,086 kDa and 48,344 kDa, respectively (Table 5.6).

After recombination, transformants were screened by PCR analysis using specific primers (Figure 5.11 and 5.12). *Smcyp1* and *smcyp2* pET-60-DEST recombinant coding sequences, *smcyp1*-pET-60-DEST and *smcyp2*-pET-60-DEST, have expected amplicon sizes of 491 bp and 581 bp, respectively. All transformants tested were positive for its respective coding sequence (Figure 5.15). Positive constructs were sequenced for confirmation of in-frame cloning.

***E. coli* expressed recombinant GST-tagged**

***S. mansoni* Cyclophilin coding sequence (1322 bp)**

ATGTCCCCTATACTAGGTTATTGGAAAATTAAGGGCCTTGTGCAACCCACTCGACTTCTT
TTGGAATATCTTGAAGAAAAATATGAA...513nt...TGGCCTTTGCAGGGCTGGCAAG
CCACGTTTGGTGGTGGCGACCATCCTCCAAAATCGGATGCAAGCCTTGTTCCACGTGGTT
CTGTCACAAGTTTGTACAAAAAAGCAGGCTTCGCTGCGAAAGCGTTTTTCGATATTAAGG
CCGGTGATGAACGATTGGGGAGGATTATATTTGAGCTATTCAATGATGTTCCAGATACTA
CTAGAAACTTTCGCGAGTTATGCACTCACAAGAATAATTTTGGTTACAAAGGTTCCGTTT
TCCACCGAATAATTCCAGGCTTCATGTGTCAGGGTGGCGATTTCACCAATGGCGATGGCA
CGGGTGGAAAAAGTATATACGGAAATAAATTCAAAGATGAGAACTTCAATCACAAACACG
AAGCGTTCTCACTTTCAATGGCCAATGCGGGACCTAACACCAATGGTTCGCAATTCTTTA
TTACTACTGTCCCTTGTTCGTGGCTTGACGGCAAACATGTTGTTTTCGGTAAAGTCGTCA
GTGGCATAGACGTGGTGAAGAAAATGGAGAGTTTAGGTTCCACAAGTGGAAAGCCGTCCA
AGAAAATTATAATCGAAGATTGTGGAGAATGTTAAGACCCAGCTTTCTTGTACAAAGTGG
T

Forward primer: 5' GCTGCGAAAGCGTTTTTCG 3'

Length: 19 bp / Melting temperature = 62.74°C

Reverse primer: 5' GCTGGGTCTTAACATTCTCCAC 3'

Length: 22 bp / Melting temperature = 58.57°C

Figure 5.11: ***E. coli* expressed recombinant GST-tagged *S. mansoni* Cyclophilin coding sequences (r-GST-SmCyp1).** – start codon, – stop codon, – coding sequence for the GST tag, – coding sequence for the Thrombin cleavage site, – recombination sites, – nucleotides added to adjust the reading frame, □ - primer binding site, blue letters – codons derived from pET-60-DEST, underlined – codons from *smcyp1* and *smcyp2* coding sequence.

***E. coli* expressed recombinant GST-tagged**

***S. mansoni* Cyclophilin B coding sequence (1411 bp)**

ATGTCCCCTATACTAGGTTATTGGAAAATTAAGGGCCTTGTGCAACCCACTCGACTTCTT
TTGGAATATCTTGAAGAAAAATATGAA...513nt...TGGCCTTTGCAGGGCTGGCAAG
CCACGTTTGGTGGTGGCGACCATCCTCCAAAATCGGATGCAAGCCTTGTTCCACGTGGTT
CTGTCACAAGTTTGTACAAAAAAGCAGGCTTCGAAGCGAATGGACCCAAAGTTACTGACA
AAGTGTTTTTCGATATTGAAGTTGATGGAAAACCACTTGCTCGAATAATTATCGGATTGT
TTGGTAAAACAGTGCCTAAGACAGTGGAAAATTTCAAACAACTTTCAATTGGCACTCAAC
TGAAGGATGGTCGAACTGCTTCATATAAAGGAAGCACTTTTCATCGTGTTATTAAGTCAT
TCATGATACAAGGTGGAGACTTCACAAACCACGATGGAACTGGAGGTTTTAGTATTTATG
GCGATAGGTTCCCTGATGAAAACTTCAAATTGAGACATGTGGGTGCAGGGTGGCTGTCGA
TGGCTAATGCTGGTCCTGATACAAATGGAAGCCAATTCTTTATTACGACCGTGAAGACCT
CGTGGTTAGATGGAAAGCATGTTGTTTTCGGAAAAGTTGTAGAAGGAATGAACATTGTTA
GACAGATTGAAAGTGAAACGACGGATTCAAGAGATAGACCTGTTAAGAGCATCAAGATAG
CCAGTTGCGGCCACATTCCCGTGGAAATACCCTTCTCGGTAACGAACTCTGATGCTGTCG
AATGAGACCCAGCTTTCTTGTACAAAGTGGT

Forward primer: 5' CTTCGAAGCGAATGGACCC 3'

Length: 19 bp / Melting temperature = 61.47°C

Reverse primer: 5' GGTCTCATTCGACAGCATCAGAG 3'

Length: 23 bp / Melting temperature = 62.02°C

Figure 5.12: ***E. coli* expressed recombinant GST-tagged *S. mansoni* Cyclophilin B coding sequences (r-GST-SmCyp2).** – start codon, – stop codon, – coding sequence for the GST tag, – coding sequence for the Thrombin cleavage site, – recombination sites, – nucleotides added to adjust the reading frame, □ - primer binding site, blue letters – codons derived from pET-60-DEST, underlined – codons from *smcyp1* and *smcyp2* coding sequence.

Native and *E. coli* expressed recombinant GST-tagged *S. mansoni* Cyclophilin protein sequence alignment

```
SmCyp1          ------------------------------------------------------------
r-GST-SmCyp1    MSPILGYWKIKGLVQPTRLLLEYLEEKYEEHLYERDEGDKWRNKKFELGLEFPNLPYYID

SmCyp1          ------------------------------------------------------------
r-GST-SmCyp1    GDVKLTQSMAIIRYIADKHNMLGGCPKERAEISMLEGAVLDIRYGVSRIAYSKDFETLKV

SmCyp1          ------------------------------------------------------------
r-GST-SmCyp1    DFLSKLPEMLKMFEDRLCHKTYLNGDHVTHPDFMLYDALDVVLYMDPMCLDAFPKLVCFK

SmCyp1          ------------------------------------------------------------MAA
r-GST-SmCyp1    KRIEAIPQIDKYLKSSKYIAWPLQGWQATFGGGDHPPKSDASLVPRGSVTSLYKKAGFAA
                                                                            **

SmCyp1          KAFFDIKAGDERLGRIIFELFNDVPDTTRNFRELCTHKNNFGYKGSVFHRIIPGFMCQGG
r-GST-SmCyp1    KAFFDIKAGDERLGRIIFELFNDVPDTTRNFRELCTHKNNFGYKGSVFHRIIPGFMCQGG
                ************************************************************

SmCyp1          DFTNGDGTGGKSIYGNKFKDENFNHKHEAFSLSMANAGPNTNGSQFFITTVPCSWLDGKH
r-GST-SmCyp1    DFTNGDGTGGKSIYGNKFKDENFNHKHEAFSLSMANAGPNTNGSQFFITTVPCSWLDGKH
                ************************************************************

SmCyp1          VVFGKVVSGIDVVKKMESLGSTSGKPSKKIIIEDCGEC
r-GST-SmCyp1    VVFGKVVSGIDVVKKMESLGSTSGKPSKKIIIEDCGEC
                ***************************************
```

Figure 5.13: **Native and *E. coli* expressed recombinant GST-tagged *S. mansoni* Cyclophilin (SmCyp1, r-GST-SmCyp1) protein sequence alignment**. – starting methionine, blue letters – amino acids derived from pET-60-DEST, – GST tag, – Thrombin cleavage site, * (asterisk) – positions which have a single, fully conserved residue.

Native and *E. coli* expressed recombinant GST-tagged *S. mansoni* Cyclophilin B protein sequence alignment

```
SmCyp2          ------------------------------------------------------------
r-GST-SmCyp2    MSPILGYWKIKGLVQPTRLLLEYLEEKYEEHLYERDEGDKWRNKKFELGLEFPNLPYYID

SmCyp2          ------------------------------------------------------------
r-GST-SmCyp2    GDVKLTQSMAIIRYIADKHNMLGGCPKERAEISMLEGAVLDIRYGVSRIAYSKDFETLKV

SmCyp2          ------------------------------------------------------------
r-GST-SmCyp2    DFLSKLPEMLKMFEDRLCHKTYLNGDHVTHPDFMLYDALDVVLYMDPMCLDAFPKLVCFK

SmCyp2          ------------------------------------------------------------EA
r-GST-SmCyp2    KRIEAIPQIDKYLKSSKYIAWPLQGWQATFGGGDHPPKSDASLVPRGSVTSLYKKAGFEA
                                                                            **

SmCyp2          NGPKVTDKVFFDIEVDGKPLARIIIGLFGKTVPKTVENFKQLSIGTQLKDGRTASYKGST
r-GST-SmCyp2    NGPKVTDKVFFDIEVDGKPLARIIIGLFGKTVPKTVENFKQLSIGTQLKDGRTASYKGST
                ************************************************************

SmCyp2          FHRVIKSFMIQGGDFTNHDGTGGFSIYGDRFPDENFKLRHVGAGWLSMANAGPDTNGSQF
r-GST-SmCyp2    FHRVIKSFMIQGGDFTNHDGTGGFSIYGDRFPDENFKLRHVGAGWLSMANAGPDTNGSQF
                ************************************************************

SmCyp2          FITTVKTSWLDGKHVVFGKVVEGMNIVRQIESETTDSRDRPVKSIKIASCGHIPVEIPFS
r-GST-SmCyp2    FITTVKTSWLDGKHVVFGKVVEGMNIVRQIESETTDSRDRPVKSIKIASCGHIPVEIPFS
                ************************************************************

SmCyp2          VTNSDAVE
r-GST-SmCyp2    VTNSDAVE
                ********
```

Figure 5.14: **Native and *E. coli* expressed recombinant GST-tagged *S. mansoni* Cyclophilin B (SmCyp2, r-GST-SmCyp2) protein sequence alignment**. – starting methionine, blue letters – amino acids derived from pET-60-DEST, – GST tag, – thrombin cleavage site, * (asterisk) – positions which have a single, fully conserved residue.

Protein	Number of amino acids	Predicted pI	Predicted molecular weight (kDa)
SmCyp1	161	8.26	17,671
r-GST-SmCyp1	398	7.56	45,086
SmCyp2*	190	8.10	20,798
r-GST-SmCyp2	428	7.16	48,344

Table 5.6: **Comparison of native and *E. coli* expressed recombinant GST-tagged *S. mansoni* Cyclophilin (SmCyp1, r-GST-SmCyp1) and *S. mansoni* Cyclophilin B (SmCyp2, r-GST-SmCyp2).** * without signal peptide.

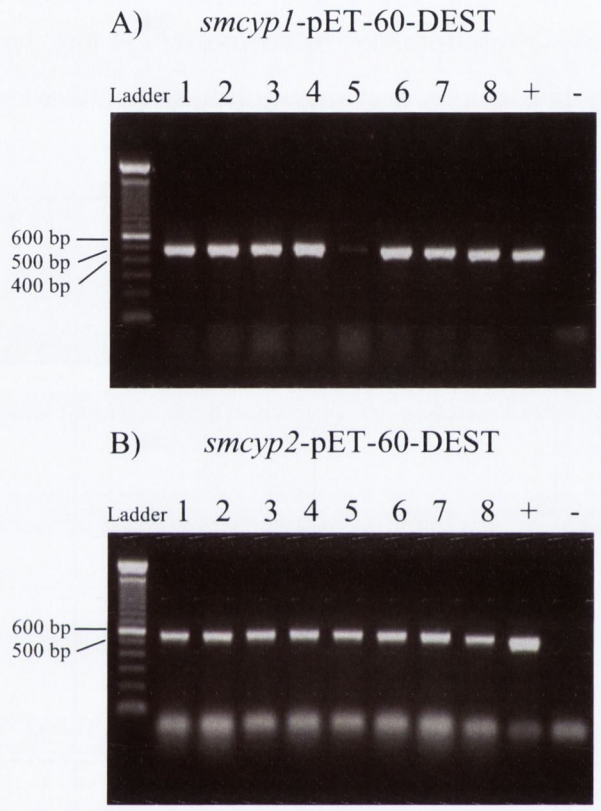

Figure 5.15: **Cloning of *S. mansoni* Cyclophilin (*smcyp1*-pET-60-DEST, A) and *S. mansoni* Cyclophilin B (*smcyp2*-pET-60-DEST, B) coding sequences into the pET-60-DEST expression vector.** PCR amplification of colonies (1-8) of TOP10 competent cells transformed with *smcyp1*-pET-60-DEST or *smcyp2*-pET-60-DEST. (+) positive control, *smcyp1*-pDEST17 or *smcyp2*-pDEST17 used as template. (-) negative control, no template. Five µL of each PCR reaction was electrophoresed on a 1.5% agarose gel.

5.3.2.2.2 - Expression and solubility analysis of r-GST-SmCyp1 and r-GST-SmCyp2 in *E. coli*

R-GST-SmCyp1 and r-GST-SmCyp2 were expressed in *E. coli* BL21-AI using 2 different expression conditions: 37 °C for 5 hours or 22 °C over night (Figure 5.16). After expression, competent cells were lysed as described in chapter 2, section 2.6.1.2. The supernatant and pellet were visualized in a 12% SDS-PAGE. R-GST-SmCyp1 and r-GST-SmCyp2 were detected in the pellet only. The addition of a N-terminal GST tag did not enhance solubility of the recombinant proteins.

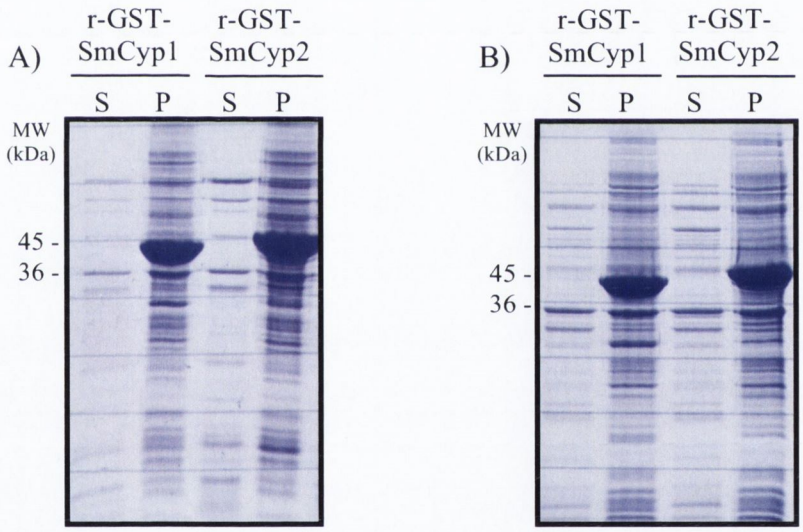

Figure 5.16: **Expression and solubility analysis of recombinant GST-tagged *S. mansoni* Cyclophilin (r-GST-SmCyp1) and *S. mansoni* Cyclophilin B (r-GST-SmCyp2) produced in *E. coli* BL21-AI.** R-GST-SmCyp1 and r-GST-SmCyp2 were expressed in 2 different conditions: 37 °C for 5 hours (A) or 22 °C over night (B). Cultures were collected and lysed. 12% SDS-PAGE, Coomassie Brilliant Blue staining. S- supernatant, P- pellet, MW- molecular weight.

5.3.2.3 – Production of *E. coli* expressed polyhistidine-tagged *S. mansoni* Cyclophilin (r-his-SmCyp1)

As described in the sections 5.3.2.1 and 5.3.2.2 of this chapter, recombinant SmCyp1 and SmCyp2 were not expressed as soluble proteins, either by expression with a N-terminal polyhistidine tag or a GST tag or by testing different expression conditions. Therefore, in order to generate soluble protein another approach was performed: the refolding of the polyhistidine-tagged recombinant proteins. R-his-SmCyp2, however, was was not expressed as a single band, but two bands of slightly different sizes. Therefore, the refolding was performed with r-his-SmCyp1 only.

5.3.2.3.1 - Purification of r-his-SmCyp1

All purification procedures were performed under denaturing conditions, i.e., adding 8M Urea to the buffers used. R-his-SmCyp1 was expressed in BL21-A1 strain as described in section 5.3.2.1.3. The competent cells were lysed with lysing buffer containing 8M Urea and following centrifugation the lysis supernatant was used for purification. Firstly, the r-his-SmCyp1 elution point in nickel-affinity chromatography was evaluated using elution buffers with increasing concentrations of imidazole (Table 5.7). The chromatography was performed using nickel agarose resin in a gravity-flow system (chapter 2, section 2.7.1.1). R-his-SmCyp1 elution started at 20 mM imidazole (Figure 5.17). For the final purification steps, the binding of loading sample was performed at 5 mM imidazole and the column washing step at 10 mM imidazole. The elution was performed with 500 mM imidazole (Figure 5.18 A and B). In order to increase r-his-SmCyp1 purity, protein was repurified using the same conditions (Figure 5.18 C and D). However, there were no improvements in the protein purity.

Buffers	Imidazole concentration
Binding	5 mM
Washing	5 mM
Elution 1	20 mM
Elution 2	50 mM
Elution 3	75 mM
Elution 4	100 mM
Elution 5	150 mM
Elution 6	200 mM
Elution 7	300 mM
Elution 8	500 mM
Elution 9	500 mM

Table 5.7: **Imidazole concentrations used to optimize the purification of *E. coli* expressed recombinant polyhistidine-tagged (r-his-SmCyp1) or baculovirus-insect cell expressed recombinant *S. mansoni* Cyclophilin (rbacSmCyp1).**

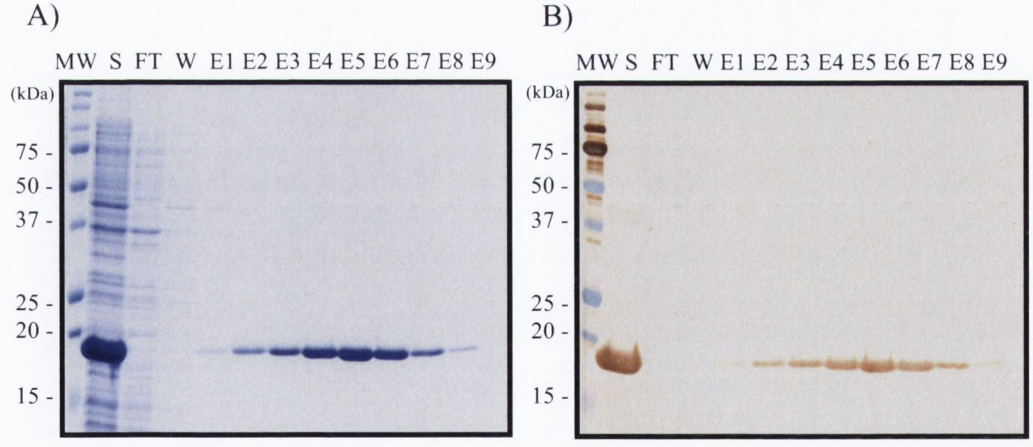

Figure 5.17: **Optimization of the purification of recombinant *S. mansoni* Cyclophilin expressed in BL21-AI *E. coli* (r-his-SmCyp1).** R-his-SmCyp1 was purified under denaturing conditions (8M urea). Samples from supernatant (S), flow-through (FT), wash (W) and elution fractions 1 to 9 (E1-9) were analysed in a 15% SDS-PAGE (A) stained with Coomassie Brilliant Blue and by a Western blot (B) with anti-6X polyhistidine antibody (1:1000). For imidazole concentrations see Table 5.7. MW - molecular weight

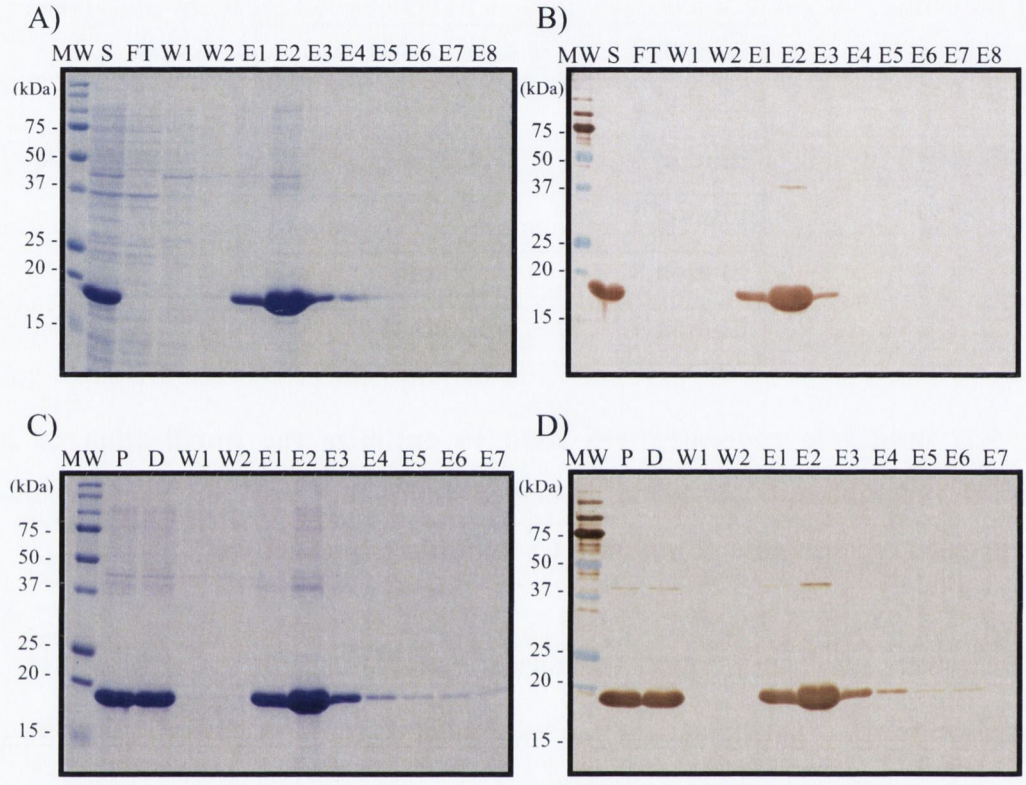

Figure 5.18: **Purification of recombinant *S. mansoni* Cyclophilin expressed in *E. coli* BL21-AI (r-his-SmCyp1).** R-his-SmCyp1 was purified under denaturing conditions (8M Urea) using binding, washing and elution buffers with 5 mM, 10 mM and 500 mM imidazole, respectively. Samples were analyzed in a 15% SDS-PAGE (A) stained with Coomassie Brilliant Blue and probed by Western blot (B) with anti-6X polyhistidine antibody (1:1000). After first purification, rSmCyp1 elution fractions 1, 2 and 3 were pooled (P), dialyzed (D) with binding buffer and re-purified using the same conditions from previous purification (C and D). MW- molecular weight.

5.3.2.3.1 - Refolding of r-his-SmCyp1

Elution fractions from final purification described in the previous section were pooled and refolding was performed as described in chapter 2, section 2.7.3. Thirteen PBS solutions containing decreasing concentrations of Urea were used for refolding. During dialysis with the 1.5 M Urea buffer, there was formation of a precipitate. Nonetheless, the refolding process was carried on until incubation with the final solution of PBS only. The supernatant was loaded on a 15% SDS-PAGE and screened for the presence of r-his-SmCyp1 by Western blot with an anti-6X polyhistidine antibody (Figure 5.19). The final yield was approximately 400 ug of soluble r-his-SmCyp1 from 100 mL of *E. coli* expression culture.

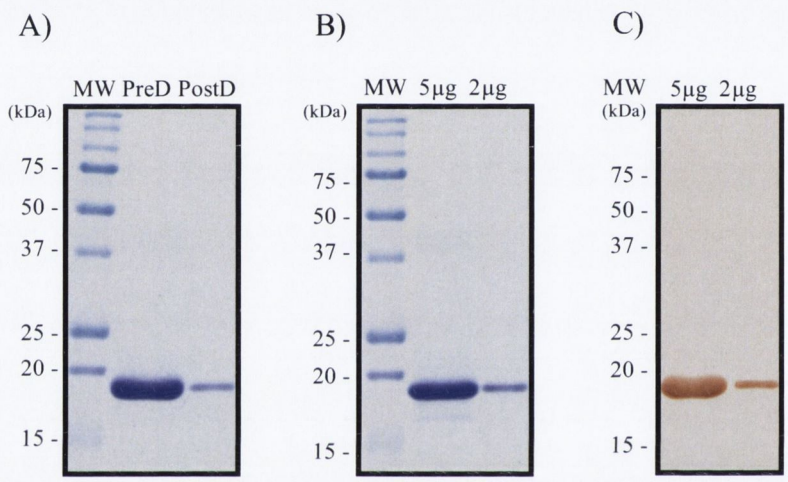

Figure 5.19: **BL21-AI *E. coli* expressed recombinant *S. mansoni* Cyclophilin (r-his-SmCyp1) reconstitution in PBS.** R-his-SmCyp1 was dialyzed with several buffers containing decreasing concentrations of Urea and at last PBS. A pre-dialysis (PreD) and a post-dialysis (PostD) sample was collected and analyzed in a 15% SDS-PAGE (A) stained with Coomassie Brilliant Blue. 5µg and 2µg of PBS soluble r-his-SmCyp1 were visualized in a 15% SDS-PAGE (B) stained with Coomassie Brilliant Blue and analyzed by Western blot (C) with anti-6X polyhistidine (1:1000) antibody. MW- molecular weight.

5.3.2.3.2 – Detection of r-his-SmCyp1 with anti-r-his-SmCyp1 and anti-WES polyclonal antibodies

Anti-WES and anti-r-his-SmCyp1 polyclonal antibodies were generated in rabbit and mouse as described in chapter 2, sections 2.3.1 and 2.3.4, respectively. Purified R-his-SmCyp1 was probed by Western blot with anti-WES and anti-r-his-SmCyp1 sera. Probing with both sera detected the r-his-SmCyp1 monomer band migrating at 18,450 kDa (Rf = 0.485) (Figure 5.20). A band migrating at 35,892 kDa (Rf = 0.224) was also detected by probing with anti-r-his-SmCyp1, indicating the formation of r-his-SmCyp1 dimer (Figure 5.20).

5.3.2.3.3 – Detection of *S. mansoni* Cyclophilin in the adult male worm excretory-secretory proteins with anti-r-his-SmCyp1 polyclonal antibody

S. mansoni male adult WES molecules were probed with anti-r-his-SmCyp1 polyclonal antibody by Western blot. *S. mansoni* Cyclophilin has a predicted molecular weight of 17,671 kDa and a nominal mass detected by mass spectrometry of 17,945 kDa. A specific band migrating at 17,060 kDa (Rf = 0.533) was detected. This band corresponds with rSmCyp1 size (Figure 5.21).

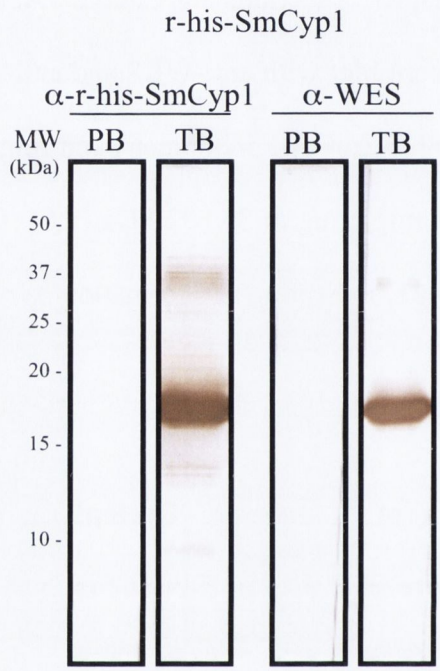

Figure 5.20: **Detection of *E. coli* expressed recombinant polyhistidine tagged *S. mansoni* Cyclophilin (r-his-SmCyp1) with anti-r-his-SmCyp1 polyclonal antibody.** r-his-SmCyp1 (2 ug per lane) was probed by Western blot with anti-r-his-SmCyp1 (α-r-his-SmCyp1, 1:1000) mouse sera and anti-WES (α-WES, 1:1000) rabbit sera collected at the end of immunization protocol (terminal bleed, TB). The pre-bleed (PB), serum harvested before rabbit immunization, was used as negative control. MW – molecular weight.

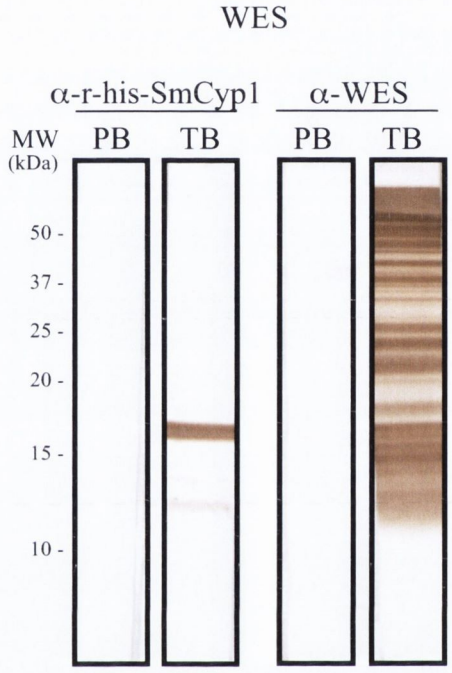

Figure 5.21: **Detection of *S. mansoni* Cyclophilin in the adult male worm excretory-secretory proteins with anti-r-his-SmCyp1 polyclonal antibody.** WES (1 ug per lane) was probed by Western blot with anti-r-his-SmCyp1 (α-r-his-SmCyp1, 1:1000) mouse sera and anti-WES (α-WES, 1:500, positive control) rabbit sera collected at the end of immunization protocol (terminal bleed, TB). The pre-bleed (PB), serum harvested before rabbit immunization, was used as negative control. MW- molecular weight.

5.3.3 - Production of recombinant *S. mansoni* Cyclophilin and *S. mansoni* Cyclophilin B in the baculovirus-insect cell system

The cloning strategy used for production of recombinant baculovirus-insect cell expressed *S. mansoni* Cyclophilin (rbacSmCyp1) and *S. mansoni* Cyclophilin B (rbacSmCyp2) is summarized in Figure 5.22.

5.3.3.1 - Cloning of rbacSmCyp1 and rbacSmCyp2 coding sequences into the transfer vector

For production of recombinant proteins in the baculovirus-insect cell system, SmCyp1 and SmCyp2 coding sequences were chemically synthesized and cloned into the insect cell expression vector pFastBac1 (Appendix 4) by a commercial company (Geneart). RbacSmCyp1 and rbacSmCyp2 coding sequences, *rbacsmcyp1* and *rbacsmcyp2*, respectively, included coding regions for a N-terminal HBM secretion signal peptide and C-terminal thrombin cleavage site, V5 peptide, TEV cleavage site and polyhistidine tag (Figure 5.23). *Rbacsmcyp1* and *rbacsmcyp2* were codon optimized for expression in Hi5 insect cells, which are derived from the parental *Trichopulsia ni* cell line. Cloning of *rbacsmcyp1* and *rbacsmcyp2* into the transfer vector generated the constructs *rbacsmcyp1*-pFastBac1 and *rbacsmcyp2*-pFastBac1.

After cleavage of the HBM secretion signal peptide, recombinant molecules have an increase in the predicted molecular weight in relation to the native processed molecules of 3,688 kDa due to the addition of 33 amino acids as part of the N-terminal tags and cleavage sites. RbacSmCyp1 and rbacSmCyp2 predicted molecular weights are 21,359 and 24,486 kDa, respectively (Figure 5.24, Table 5.8).

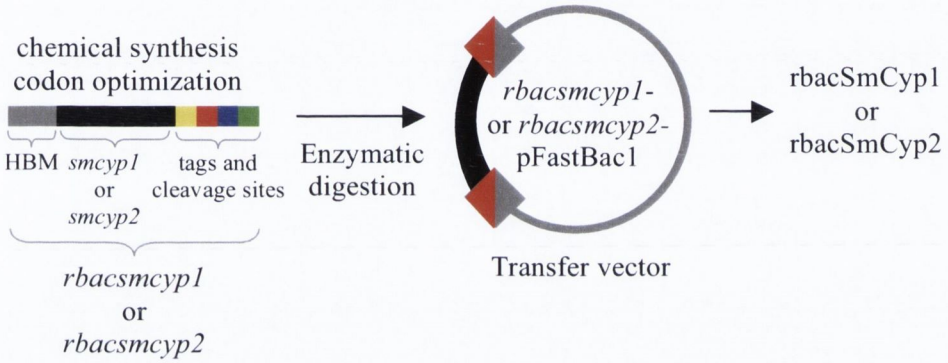

Figure 5.22: **Cloning strategy used for production of recombinant *S. mansoni* Cyclophilin (rbacSmCyp1) and *S. mansoni* Cyclophilin B (rbacSmCyp2) in the baculovirus-insect cell expression system**. For production of rbacSmCyp1 and rbacSmCyp2, SmCyp1 and SmCyp2 coding sequences were codon optimized and chemically synthesized including the HBM secretion signal peptide, tags and cleavage sites. rbacSmCyp1 and rbacSmCyp2 coding sequences, *rbacsmcyp1* and *rbacsmcyp2*, were cloned into the transfer vector pFastBac1 generating the constructs *rbacsmcyp1*-pFastBac1 and *rbacsmcyp2*-pFastBac1. These procedures were performed by a commercial company.

A) **Recombinant baculovirus-insect cell expressed *S. mansoni* Cyclophilin coding sequence (648 bp)**

ATGAAGTTCCTCGTCAACGTCGCCCTGGTGTTCATGGTCGTCTACATCTCTTACATCTAC
GCCATGGCCGCCAAGGCTTTCTTCGACATCAAGGCCGGCGACGAAAGGCTGGGAAGGATC
ATCTTCGAACTGTTCAACGACGTCCCCGACACCACCCGCAACTTCAGGGAACTGTGCACC
CACAAGAACAACTTCGGATACAAGGGAAGCGTGTTCCACAGGATCATCCCCGGATTCATG
TGCCAGGGCGGAGACTTCACCAACGGCGACGGAACCGGTGGAAAGTCTATCTACGGCAAC
AAGTTCAAGGACGAGAACTTCAACCACAAGCACGAAGCCTTCTCCCTGTCTATGGCCAAC
GCCGGACCCAACACCAACGGATCTCAGTTCTTCATCACCACCGTCCCTTGCTCTTGGCTG
GACGGAAAGCACGTCGTGTTCGGAAAGGTCGTCAGCGGAATCGACGTCGTCAAGAAGATG
GAATCTCTGGGATCTACCTCCGGAAAGCCCTCCAAGAAGATCATCATCGAGGACTGCGGA
GAATGCCTGGTCCCCAGGGGATCTGGAAAGCCCATCCCCAACCCCCTGCTGGGACTGGAC
TCTACCGAAAACCTGTACTTCCAAGGACACCACCACCACCACCACTAA

B) **Recombinant baculovirus-insect cell expressed *S. mansoni* Cyclophilin B coding sequence (735 bp)**

ATGAAGTTCCTCGTCAACGTCGCCCTGGTGTTCATGGTCGTCTACATCTCTTACATCTAC
GCCGAAGCCAACGGACCCAAGGTCACCGACAAGGTGTTCTTCGACATCGAAGTCGACGGA
AAGCCCCTGGCCAGGATCATCATCGGACTGTTCGGAAAGACCGTCCCCAAGACCGTCGAA
AACTTCAAGCAGCTGTCTATCGGAACCCAGCTGAAGGACGGAAGGACCGCCTCTTACAAG
GGATCTACCTTCCACCGCGTCATCAAGAGCTTCATGATCCAGGGCGGAGACTTCACCAAC
CACGACGGAACCGGTGGATTCTCTATCTACGGCGACAGGTTCCCCGACGAGAACTTCAAG
CTGAGGCACGTCGGAGCCGGATGGCTGTCTATGGCCAACGCCGGACCCGACACCAACGGA
TCTCAGTTCTTCATCACCACCGTCAAGACCTCTTGGCTGGACGGAAAGCACGTCGTGTTC
GGCAAGGTCGTCGAGGGAATGAACATCGTCCGCCAGATCGAATCTGAAACCACCGACTCT
AGGGACAGGCCCGTCAAGTCTATCAAGATCGCCTCTTGCGGACACATCCCCGTCGAAATC
CCTTTCTCTGTCACCAACTCTGACGCCGTCGAACTGGTCCCCAGGGGATCTGGAAAGCCC
ATCCCCAACCCCCTGCTGGGACTGGACTCTACCGAAAACCTGTACTTCCAAGGACACCAC
CACCACCACCACTAA

Figure 5.23: **Recombinant baculovirus-insect cell expressed *S. mansoni* Cyclophilin (rbacSmCyp1, A) and *S. mansoni* Cyclophilin B (rbacSmCyp2, B) coding sequences.** – start codon, – coding sequence for HBM secretion signal peptide, underlined - nucleotides from *smcyp1* or *smcyp2* coding sequence, yellow letters – coding sequence for the thrombin cleavage site, red letters – coding sequence for the V5 peptide, blue letters – coding sequence for the TEV cleavage site, green letters – coding sequence for the polyhistidine tag, – stop codon.

A) **Native and recombinant baculovirus-insect cell expressed *S. mansoni* Cyclophilin protein sequence alignment**

```
SmCyp1       ---------------------  MAAKAFFDIKAGDERLGRIIFELFNDVPDTTRNFRELCT
rbacSmCyp1   MKFLVNVALVFMVVYISYIYA|MAAKAFFDIKAGDERLGRIIFELFNDVPDTTRNFRELCT
                                    ************************************

SmCyp1       HKNNFGYKGSVFHRIIPGFMCQGGDFTNGDGTGGKSIYGNKFKDENFNHKHEAFSLSMAN
rbacSmCyp1   HKNNFGYKGSVFHRIIPGFMCQGGDFTNGDGTGGKSIYGNKFKDENFNHKHEAFSLSMAN
             ************************************************************

SmCyp1       AGPNTNGSQFFITTVPCSWLDGKHVVFGKVVSGIDVVKKMESLGSTSGKPSKKIIIEDCG
rbacSmCyp1   AGPNTNGSQFFITTVPCSWLDGKHVVFGKVVSGIDVVKKMESLGSTSGKPSKKIIIEDCG
             ************************************************************

SmCyp1       EC--------------------------------
rbacSmCyp1   ECLVPRGSGKPIPNPLLGLDSTENLYFQGHHHHHH
```

B) **Native and recombinant baculovirus-insect cell expressed *S. mansoni* Cyclophilin B protein sequence alignment**

```
SmCyp2       ---------------------  EANGPKVTDKVFFDIEVDGKPLARIIIGLFGKTVPKTVE
rbacSmCyp2   MKFLVNVALVFMVVYISYIYA|EANGPKVTDKVFFDIEVDGKPLARIIIGLFGKTVPKTVE
                                    ************************************

SmCyp2       NFKQLSIGTQLKDGRTASYKGSTFHRVIKSFMIQGGDFTNHDGTGGFSIYGDRFPDENFK
rbacSmCyp2   NFKQLSIGTQLKDGRTASYKGSTFHRVIKSFMIQGGDFTNHDGTGGFSIYGDRFPDENFK
             ************************************************************

SmCyp2       LRHVGAGWLSMANAGPDTNGSQFFITTVKTSWLDGKHVVFGKVVEGMNIVRQIESETTDS
rbacSmCyp2   LRHVGAGWLSMANAGPDTNGSQFFITTVKTSWLDGKHVVFGKVVEGMNIVRQIESETTDS
             ************************************************************

SmCyp2       RDRPVKSIKIASCGHIPVEIPFSVTNSDAVE----------------------------
rbacSmCyp2   RDRPVKSIKIASCGHIPVEIPFSVTNSDAVELVPRGSGKPIPNPLLGLDSTENLYFQGHH
             ********************************

SmCyp2       ----
rbacSmCyp2   HHHH
```

Figure 5.24: **Native and recombinant baculovirus-insect cell expressed *S. mansoni* Cyclophilin (SmCyp1, rbacSmCyp1, A) and *S. mansoni* Cyclophilin B (SmCyp2, rbacSmCyp2, B) protein sequence alignment.** – start methionine, – HBM secretion signal peptide, | – HBM cleavage site, yellow letters – thrombin cleavage site, red letters – V5 peptide, blue letters – TEV cleavage site, green letters – polyhistidine tag, * (asterisk) – positions which have a single, fully conserved residue.

Protein	Number of amino acids	Predicted pI	Predicted molecular weight (kDa)
SmCyp1	161	8.26	17,671
rbacSmCyp1	194	8.26	21,359
SmCyp2*	190	8.10	20,798
rbacSmCyp2	223	8.12	24,486

Table 5.8: **Comparison of native and recombinant baculovirus-insect cell expressed *S. mansoni* Cyclophilin (SmCyp1, rbacSmCyp1) and *S. mansoni* Cyclophilin B (SmCyp2, rbacSmCyp2).** The number of amino acids, predicted pI and predicted molecular weight were calculated for rbacSmCyp1 and rbacSmCyp2 deducting the HBM secretion signal peptide. * without native signal peptide.

5.3.3.2 - Generation of rbacSmCyp1 and rbacSmCyp2 bacmids

For generation of rbacSmCyp1 and rbacSmCyp2 bacmids, the transfer vectors, *rbacsmcyp1*-pFastBac1 or *rbacsmcyp2*-pFastBac1, were transformed into DH10Bac competent cells and the recombinant bacmids were isolated from white colonies as described in Chapter 2, section 2.5. Transposition of inserts into the bacmid was verified by PCR using the M13/pUC forward and reverse primers that bind to either side of the recombination site in the bacmid (Appendix 5). Expected size for *rbacsmcyp1* and *rbacsmcyp2* are 2,948 bp and 3,035 bp, respectively. All colonies tested were positive for their respective recombinant bacmids (Figure 5.25).

5.3.3.3 - Generation of rbacSmCyp1 and rbacSmCyp2 baculovirus stocks

For generation of the recombinant baculovirus stock passage 0 (P0), Hi5 cells were firstly transfected with the recombinant bacmids, rbacmid-smcyp1 or rbacmid-smcyp2, as described in chapter 2, section 2.6.2.2. The recombinant baculovirus stock P0 was amplified 3 times generating the stocks P1, P2 and P3. The 4 stages of baculovirus stock production were screened for the presence of the recombinant proteins, rbacSmCyp1 and rbacSmCyp2, by Western blot with the anti-V5 antibody. RbacSmCyp1 and rbacSmCyp2 were successfully detected in all stages of stock production (Figure 5.26).

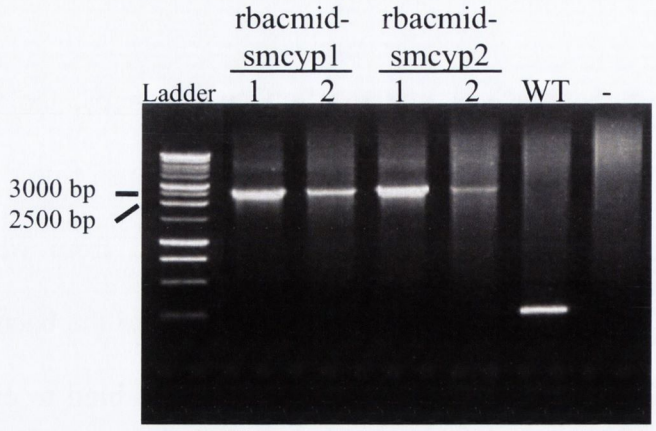

Figure 5.25: **Generation of recombinant *S. mansoni* Cyclophilin (rbacmid-smcyp1) and *S. mansoni* Cyclophilin B (rbacmid-smcyp2) bacmids.** PCR amplification with M13/pUC forward and reverse primers of DH10Bac competent cell colonies (1 and 2) transformed with r*bacsmcyp1*-pFastBac1 or r*bacsmcyp2*-pFastBac1. Five µL of each PCR reaction was electrophoresed on a 0.8% agarose gel. WT - wild type bacmid (without the insert). (-) - negative control, no template.

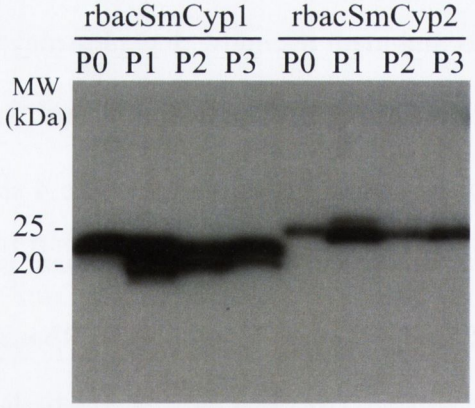

Figure 5.26: **Generation of recombinant *S. mansoni* Cyclophilin (rbacSmCyp1) and *S. mansoni* Cyclophilin B (rbacSmCyp2) baculovirus.** Recombinant baculovirus passage 0 (P0) was generated by transfecting insect cells with rbacmid-smcyp1 or rbacmid-smcyp2. Recombinant baculovirus passage 1 (P1), passage 2 (P2) and passage 3 (P3) were generated from amplifications of P0. Insect cell culture supernatant was screened by Western blot with anti-V5 antibody (1:100000).

5.3.3.4 - Expression of rbacSmCyp1 and rbacSmCyp2

The recombinant baculovirus stock P3 was used for expression of recombinant protein. Firstly the amount of P3 stock to be used per expression plate and the incubation time that produced the highest level of recombinant protein expression was determined. Insect cells were infected with 1, 5 or 10 mL of rbacSmCyp1 or rbacSmCyp2 baculovirus stock P3. A non-infected culture was used as control. Samples of the supernatants were harvested at different time points (24, 48, 72 and 96 hours after infection) and screened for the presence of the recombinant proteins by Western blot with anti-V5 antibody.

Regarding rbacSmCyp1, the expression conditions that showed higher level of recombinant protein expression was infection of cells with 5 mL of stock P3 and incubation for 72 hours (Figure 5.27 A). The same conditions were optimal for expression of rbacsmCyp2 (Figure 5.27 B). However, expression levels of rbacSmCyp2 were lower than rbacSmCyp1 since a two times more concentrated antibody was needed to detect the recombinant protein.

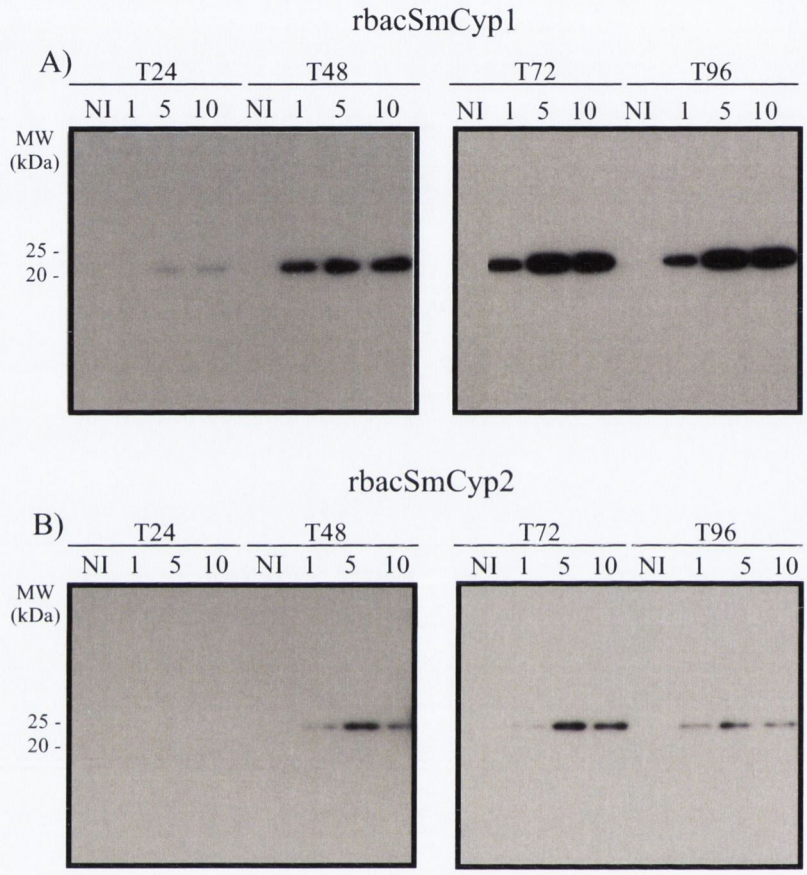

Figure 5.27: **Optimization of recombinant *S. mansoni* Cyclophilin (rbacSmCyp1, A) and *S. mansoni* Cyclophilin B (rbacSmCyp2, B) expression in the baculovirus-insect cell system.** Insect cells were infected with 1, 5 or 10 mL of rbacSmCyp1 (A) or rbacSmCyp2 (B) baculovirus stock passage 3 (P3). A non-infected (NI) culture was used as control. Samples of the supernatants were harvested at different time points: 24 (T24), 48 (T48), 72 (T72) and 96 (T96) hours after infection. Insect cell culture supernatant was screened by Western blot with anti-V5 antibody (rbacSmCyp1- 1:60000, rbacSmCyp2 - 1:30000).

5.3.3.5 - Small-scale purification of rbacSmCyp1

For the small-scale purification, approximately 800 mL of rbacSmCyp1 insect cell culture supernatant were concentrated to 20 mL and processed as described in section 2.6.2.5. Purification of rbacSmCyp1 was firstly optimized by determining the elution peak of the recombinant protein using a nickel agarose resin and a gravity-flow system as described in chapter 2, section 2.7.1.2. Two mL of the processed sample was used for the optimization. Binding to the column and washing steps were performed using 5 mM imidazole in the buffers. Elution was carried out with 8 buffers with increasing concentrations of imidazole (Table 5.7). It was not possible to visualize a major protein band in a 15% SDS-PAGE (Figure 5.28 A) but rbacSmCyp1 was detected in the elution fractions by Western blot with anti-V5 antibody (Figure 5.28 B). rbacSmCyp1 was eluted at 100 mM imidazole.

Purification of rbacSmCyp1 was performed using the remaining 18 mL of the processed supernatant. Column binding and washing steps were performed using 75 mM imidazole concentration. Elution was performed with 500 mM imidazole. rbacSmCyp1 was detected in the elution fractions 1 to 4 (Figure 5.29). Positive elution fractions were pooled, concentrated to less than 1 mL and dialyzed against DPBS. Samples from the elution fractions pool and the concentrated sample before and after dialysis with DPBS were analysed in a 15% SDS-PAGE and rbacSmCyp1 was detected by Western blot (Figure 5.30). The final protein yield was 98.7 ug.

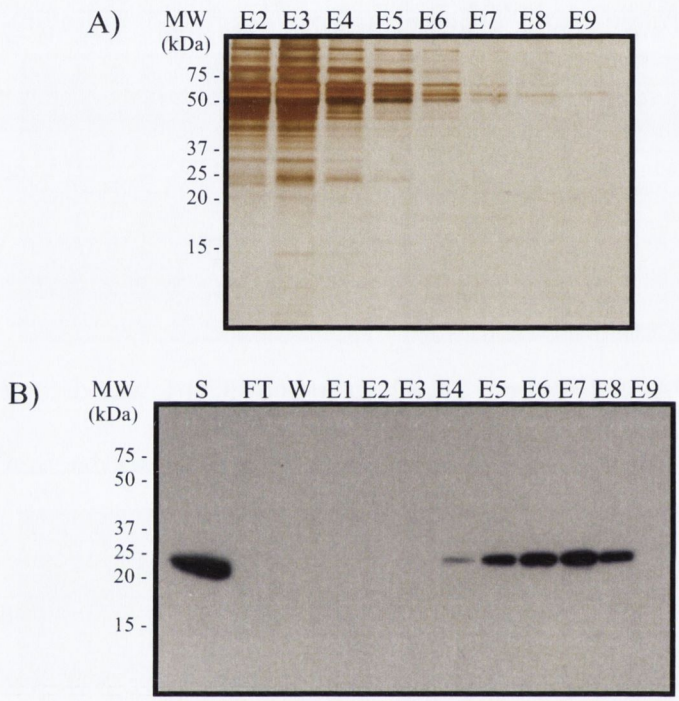

Figure 5.28: **Optimization of the purification of recombinant baculovirus-insect cell expressed *S. mansoni* Cyclophilin (rbacSmCyp1).** Samples from cell culture supernatant ready for purification (S), flow-through (FT), wash (W) and elution fractions 1 to 9 (E1-9) were analyzed in a 15% SDS-PAGE (A) silver stained and by Western blot (B) with anti-V5 antibody (1:100000). For imidazole concentrations in the purification buffers see Table 5.7. MW- molecular weight.

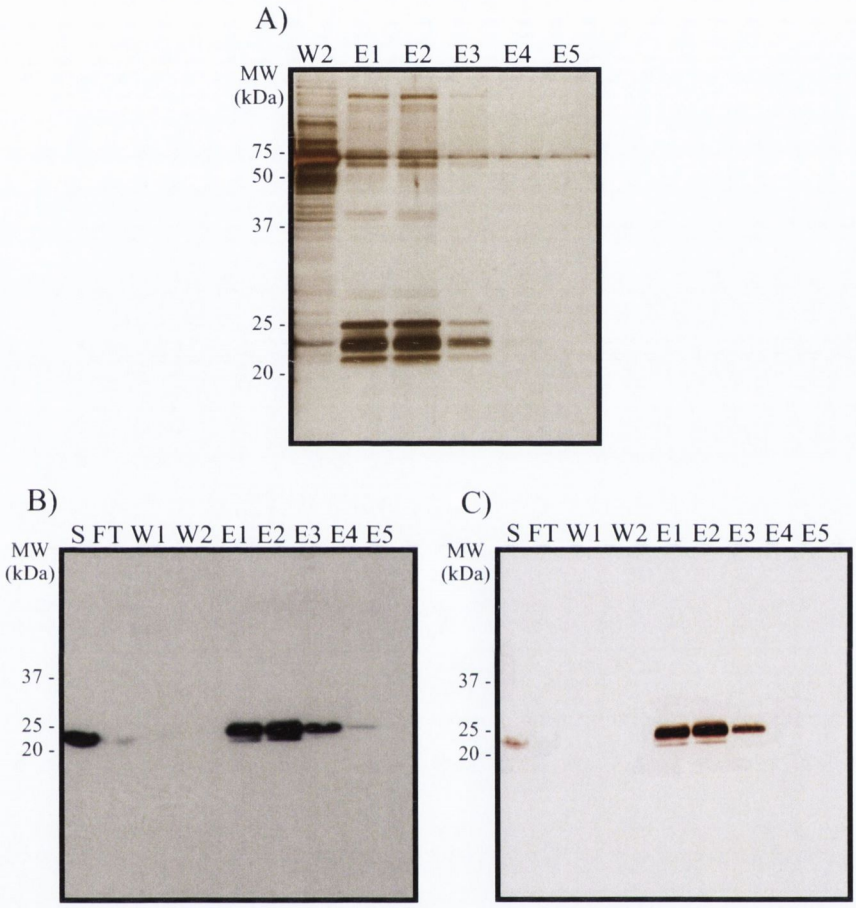

Figure 5.29: **Small-scale purification of recombinant *S. mansoni* Cyclophilin (rbacSmCyp1) expressed in the baculovirus-insect cell system.** rbacSmCyp1 was purified using binding and washing buffer with 75 mM imidazole and elution buffer with 500 mM imidazole. Samples from elution fractions 1 to 5 (E1-5) were visualised in a silver stained 15% SDS-PAGE (A). Samples from cell culture supernatant ready for purification (S), flow-through (FT), wash 1 (W1), wash 2 (W2) and elution fractions were analyzed by Western blot with anti-V5 (B, 1:100000) or anti-6X polyhistidine (C, 1:1000) antibody. MW- molecular weight.

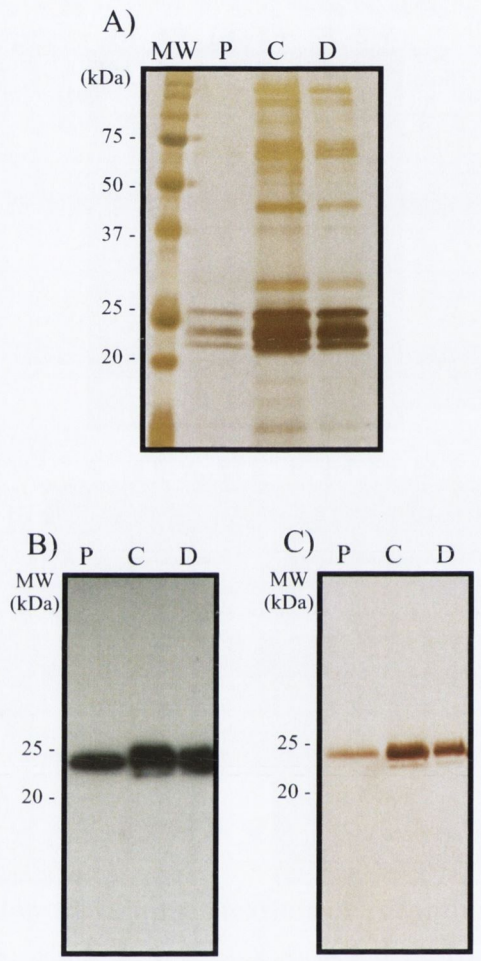

Figure 5.30: **Post purification processing of recombinant baculovirus-insect expressed *S. mansoni* Cyclophilin (rbacSmCyp1).** rbacSmCyp1 elution fractions 1 to 4 were pooled (P), concentrated to less than 1 mL (C) and dialyzed with DPBS (D). Samples were visualised in a silver stained 15% SDS-PAGE (A) and analyzed by Western blot with anti-V5 (B, 1:100000) or anti-6X polyhistidine (C, 1:1000) antibody. MW- molecular weight.

5.3.3.6 - Large-scale purification of rbacSmCyp1

Approximately 5L of rbacSmCyp1 insect cell culture supernatant were concentrated to 125 mL and processed as described in section 2.6.2.5. For large-scale purification, a nickel sepharose prepacked column was used in a low-pressure chromatography automated system as described in chapter 2, section 2.7.1.2. Purification conditions used were the same as optimized for small-scale purification: binding and washing were performed with 75 mM imidazole and elution was carried out with 500 mM imidazole. Elution fractions showed several contaminant bands (Figure 5.31 A). In spite of this, rbacSmcyp1 was detected in elution fractions 5 to 15 (Figure 5.31 B). In an attempt to reduce contaminant proteins, the positive elution fractions were pooled and dialyzed with binding buffer for repurification of rbacSmCyp1. The recombinant protein was detected in elution fractions 6 to 14 but elution fractions showed no major improvement in the purity level (Figure 5.32).

In order to repeat the same purification level achieved through the small-scale purification, positive elution fractions were pooled and dialyzed with binding buffer and rbacSmCyp1 was purified using the nickel agarose resin and gravity-flow system. Contaminant bands were still present in the elution fractions but to a much lower extent as compared to the previous purifications (Figure 5.33). The positive elution fractions were pooled and used for further purification steps.

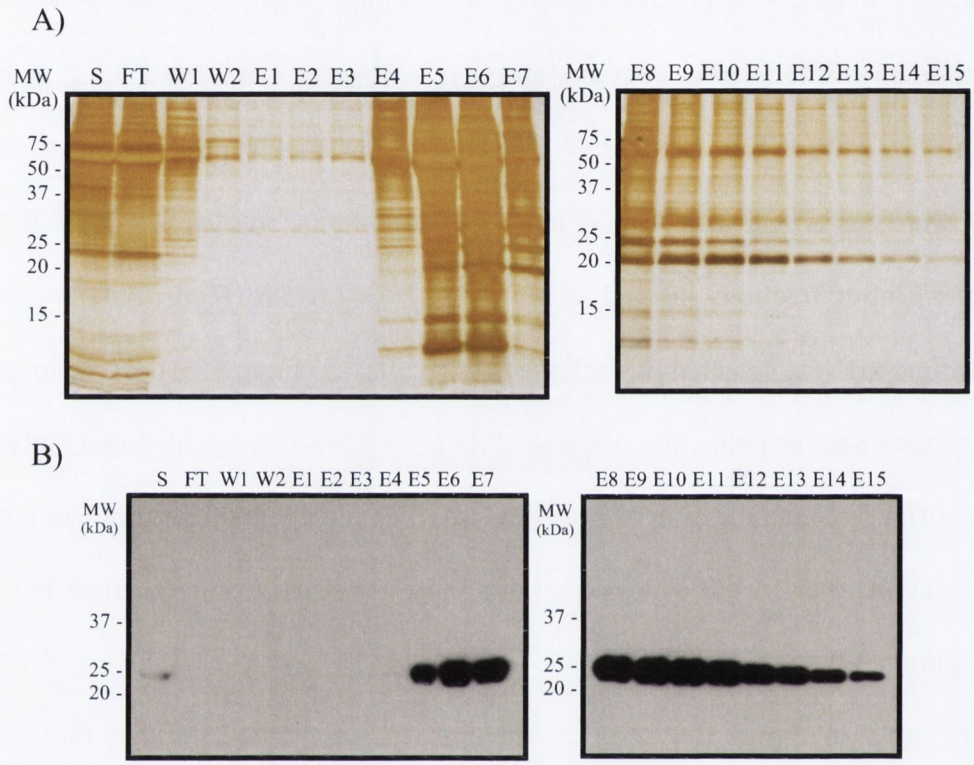

Figure 5.31: **Large-scale purification of recombinant baculovirus-insect cell expressed *S. mansoni* Cyclophilin (rbacSmCyp1).** rbacSmCyp1 was purified using binding and washing buffer with 75 mM imidazole and elution buffer with 500 mM imidazole. Samples from cell culture supernatant ready for purification (S), flow-through (FT), wash 1 (W1), wash 2 (W2) and elution fractions 1 to 15 (E1-15) were visualised in a silver stained 15% SDS-PAGE (A) and screened for the presence of rbacSmCyp1 by Western blot (B) with anti-V5 (1:100000). MW- molecular weight.

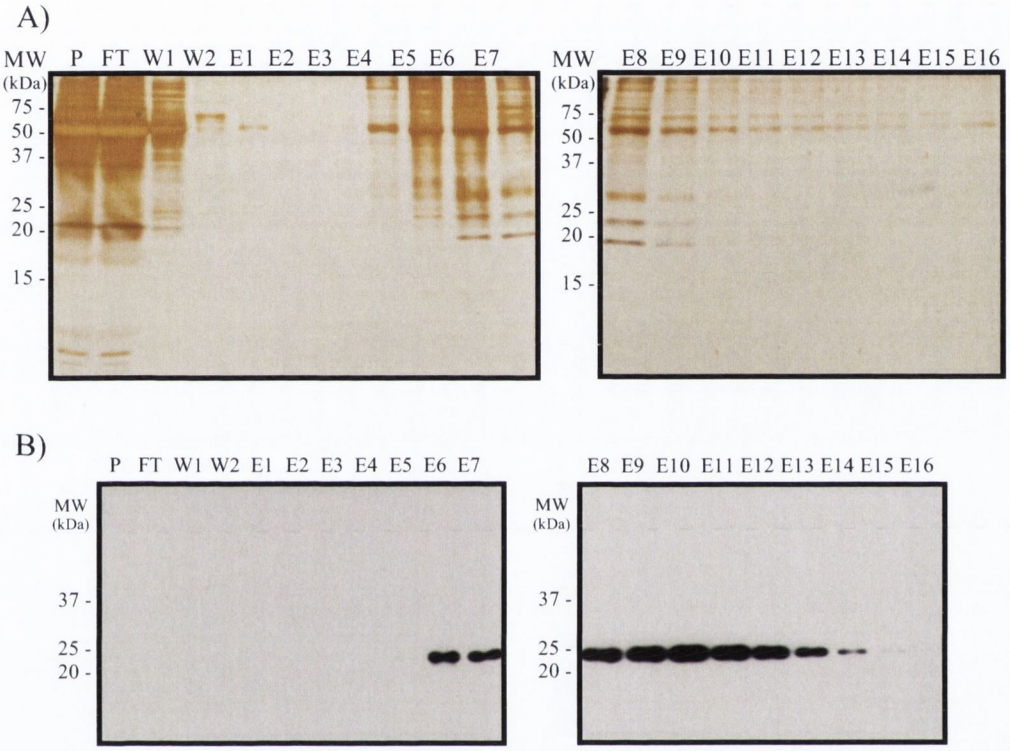

Figure 5.32: **Repurification of recombinant baculovirus-insect cell expressed *S. mansoni* Cyclophilin (rbacSmCyp1).** rbacSmCyp1 was purified using binding and washing buffer with 75 mM imidazole and elution buffer with 500 mM imidazole. Elution fractions 4 to 15 from previous purification (Figure 5.28) were pooled and dialyzed with binding buffer. Elution fractions pool (P), flow-through (FT), wash 1 (W1), wash 2 (W2) and elution fractions 1 to 15 (E1-15) were visualised in a silver stained 15% SDS-PAGE (A) and screened for the presence of rbacSmCyp1 by Western blot (B) with anti-V5 (1:100000). MW- molecular weight.

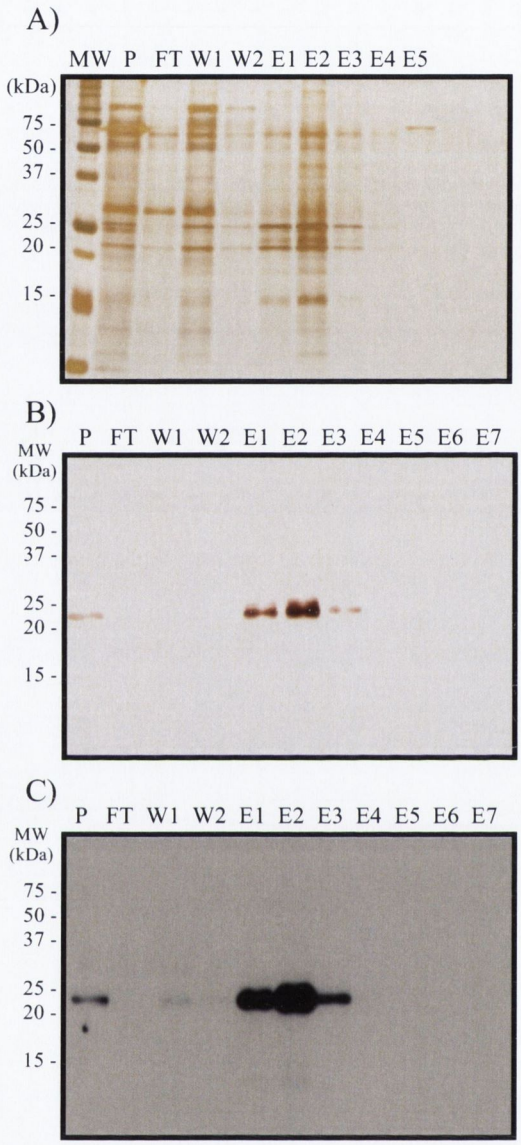

Figure 5.33: **Large-scale purification of recombinant baculovirus-insect cell expressed *S. mansoni* Cyclophilin (rbacSmCyp1).** rbacSmCyp1 was purified using binding and washing buffer with 75 mM imidazole and elution buffer with 500 mM imidazole. Elution fractions 6 to 15 from previous purification (Figure 5.32) were pooled and dialyzed with binding buffer. Elution fractions pool (P), flow-through (FT), wash 1 (W1), wash 2 (W2) and elution fractions 1 to 7 (E1-7) were visualised in a silver stained 15% SDS-PAGE (A) and screened for the presence of rbacSmCyp1 by Western blot (B) with anti-V5 (1:100000). MW- molecular weight.

5.3.3.7 – r-his-SmCyp1 and rbacSmCyp1 endotoxin levels

The levels of endotoxin contamination were measured in the recombinant SmCyp1 expressed in *E. coli*, r-his-SmCyp1, and in the baculovirus-insect cell system, rbacSmCyp1. R-his-SmCyp1 and rbacSmCyp1 showed 11.40 EU/mg and 0.277 EU/mg, respectively.

5.3.3.8 - Detection of rbacSmCyp1 with anti-r-his-SmCyp1 polyclonal antibody

RbacSmCyp1 was probed with anti-r-his-SmCyp1 mouse sera by Western blot. A band migrating at 24,322 kDa (Rf = 0.407) was detected (Figure 5.34). This result shows that immunization of mice with *E. coli* expressed r-his-SmCyp1 generated an anti-r-his-SmCyp1 polyclonal antibody that specifically binds to the baculovirus-insect cell expressed protein.

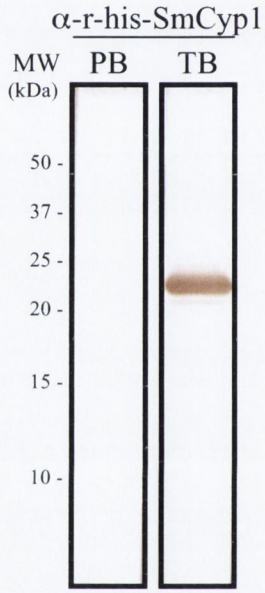

Figure 5.34: **Detection of recombinant baculovirus-insect cell expressed recombinant *S. mansoni* Cyclophilin with anti-r-his-SmCyp1 polyclonal antibody.** rbacSmCyp1 (1 ug per lane) was probed by Western blot with anti-r-his-SmCyp1 (α-r-his-SmCyp1, 1:1000) polyclonal antibody collected at the end of immunization protocol (terminal bleed, TB). The pre-bleed (PB), serum harvested before rabbit immunization, was used as negative control. MW – molecular weight.

5.3.3.9 - Purification of rbacSmCyp1 by anion exchange

In order to achieve a higher purity level, an alternative approach for purification of rbacSmCyp1 was designed. This approach comprised a three-step purification: anion exchange, cation exchange and nickel-affinity chromatography (Appendix 6). RbacSmCyp1 has a pI of 8.26, deducting the HBM secretion signal peptide (Table 5.8). At a pI lower than 8.26, i.e. pH 6.0, rbacSmCyp1 would be expected to bind to a negatively charged medium or cation exchanger. Therefore, by passing the loading sample into an anion exchange column, rbacSmCyp1 would be collected with the column flow through while some of the contaminant proteins would remain bound to the column. The column flow through would then be loaded into a cation exchange column. rbacSmCyp1 would be expected to bind to the column and would be collected at the elution phase of the purification. The elution fractions containing rbacSmCyp1 would then be subjected to nickel-affinity chromatography for further clearance of contaminants.

Firstly, a small sample of a pool of the elution fractions from the large-scale purification (section 5.3.2.6) was used for testing the three-step purification approach. The anion exchange chromatography was performed and samples from the loading, flow-through, wash and elution were screened for the presence of rbacSmCyp1. Unexpectedly, rbacSmCyp1 was not detected in the flow-through but in the elution fractions (Figure 5.35 A).

To check protein stability after anion exchange chromatography, the elution fractions, which were positive for rbacSmCyp1, were pooled, concentrated to less than 1 mL and dialyzed with PBS. After dialysis, there was a visible precipitation in the sample. However, rbacSmCyp1 was still detected as a soluble protein in the supernatant (Figure 5.35 B).

Subsequently, the remaining sample of the pool of the elution fractions from large-scale purification (section section 5.3.2.6) was subjected to anion exchange purification using the same conditions of the test sample. However, rbacSmCyp1 showed a different behaviour. The recombinant protein was not eluted out of the column while using the standard elution buffer. To unbind rbacSmCyp1 from the column, it was necessary to use a denaturing elution buffer containing 8M Urea. The loading sample, flow through, wash and elution fractions were screened for the presence of rbacSmCyp1 (Figure 5.35 C).

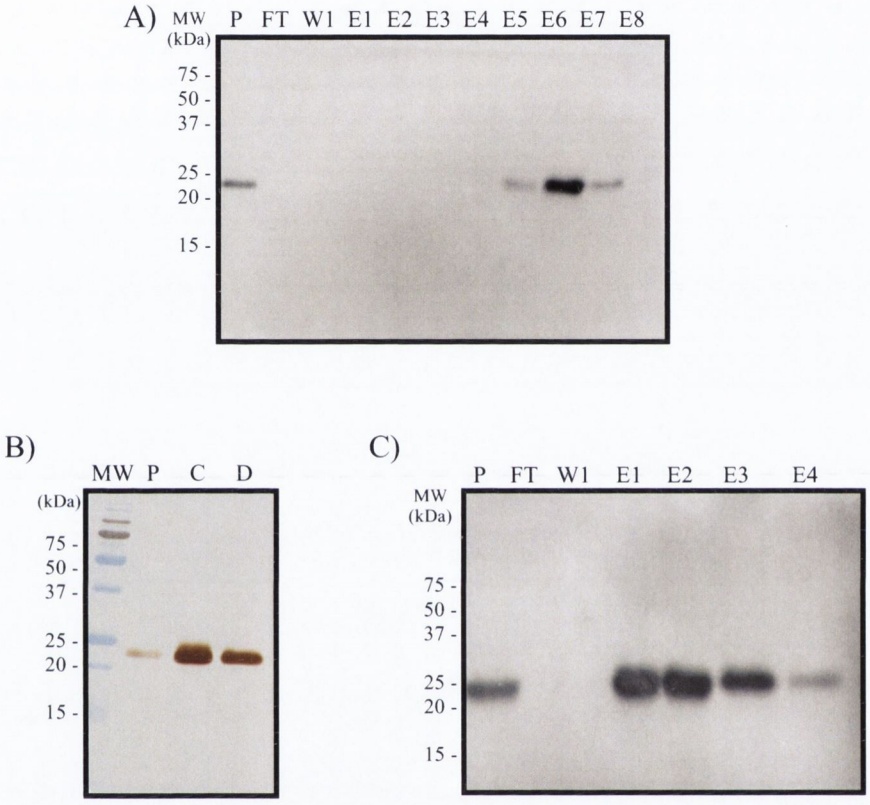

Figure 5.35: **Anion exchange purification of recombinant baculovirus-insect cell expressed *S. mansoni* Cyclophilin (rbacSmCyp1).** rbacSmCyp1 was purified by anion exchange chromatography. A) Elution fractions pool from previous experiment (Figure 5.33) were pooled and dialyzed with binding buffer. The pool (P), flow-through (FT), wash (W) and elution fractions 1 to 8 (E1-8) were screened for the presence of rbacSmCyp1 by Western blot with anti-V5 antibody (1:100000). B) The positive fractions were pooled (P), concentrated to less than 1 mL (C) and dialyzed with DPBS (D). Samples were screened for the presence of rbacSmCyp1 by Western blot with anti-polyhistidine antibody (1:1000). C) MW- molecular weight.

5.4 - Discussion

This chapter describes the production of *S. mansoni* Cyclophilin (SmCyp1) and *S. mansoni* Cyclophilin B (SmCyp2) in *E. coli* and baculovirus-insect cell systems. SmCyp1 and SmCyp2 were identified within the adult male worm excretome-secretome reported in Chapter 3 of this thesis. Additionally, SmCyp1 was identified as unique to the *S. mansoni* worm excreted-secreted molecules in the comparative analysis with the adult worm somatic molecules (Chapter 3, section 3.3.2.1). Up to this time an immunomodulatory activity has not been described for SmCyp1, SmCyp2 or other helminth cyclophilins. On the other hand TgCyp18, *T. gondii* 18-kDa cyclophilin, has been characterized as an inducer of IL-12-dependent production of Interferon (IFN)-γ by dendritic cells and macrophages (*204*). On this basis, SmCyp1 and SmCyp2 were selected as potential immunomodulatory candidates. They were cloned and expressed as recombinant proteins in two systems: *E. coli* and baculovirus-insect cell.

For production of the recombinant proteins in *E. coli*, the cloning strategy of choice was the Gateway technology. Firstly, SmCyp1 and SmCyp2 were expressed in frame with a N-terminal polyhistidine tag. Nonetheless, the recombinants were not expressed as soluble proteins. In an attempt to increase solubility, SmCyp1 and SmCyp2 were expressed in frame with a GST tag. But protein solubility was not enhanced. Therefore, another approach was used: the refolding of the polyhistidine-tagged protein. The refolding was performed with polyhistidine-tagged SmCyp1 (r-his-SmCyp2) only since polyhistidine-tagged SmCyp2 (r-his-SmCyp2) was not expressed as a single band, but two bands of slightly different sizes. Although there was a significant loss of the recombinant protein due to precipitation during the refolding procedures, soluble r-his-SmCyp1 was collected from the supernatant after dialysis with PBS. Soluble r-his-SmCyp1 was used for production of anti-r-his-SmCyp1 polyclonal antibody in mice.

As stated previously (Chapter 4, section 4.4), recombinant proteins produced in *E. coli* contain very high levels of contamination with LPS. Since LPS itself elicits an inflammatory response, those proteins are unreliable for use in immunological assays. Therefore, in order to produce recombinant protein with low levels of endotoxin, SmCyp1 and SmCyp2 were also expressed in the baculovirus-insect cell system.

For production in the baculovirus-insect cell system, SmCyp1 and SmCyp2 nucleotide sequences were codon optimized to improve protein expression and recombinant proteins were expressed in frame with the HBM secretion signal peptide for enhancement of protein solubility. Recombinant baculovirus-insect cell expressed *S. mansoni* Cyclophilin B (RbacSmCyp2) was expressed in much lower levels than recombinant baculovirus-insect cell expressed *S. mansoni* Cyclophilin (rbacSmCyp1). Therefore, the large-scale protein expression and downstream experiments were performed with rbacSmCyp1 only.

Two different approaches were used for the purification of rbacSmCyp1: nickel-affinity chromatography and ion exchange. The nickel-affinity chromatography was firstly optimized using a nickel agarose resin in a gravity-flow system. To scale up the purification, the procedure was performed using a nickel sepharose prepacked column in a low-pressure chromatography automated system. Nonetheless, the purification carried out in the prepacked column did not show the same purity level as compared to the small-scale purification. On this basis, the elution fractions from the large-scale purification were subjected to another purification with the same resin and system that was used for the optimization.

RbacSmCyp1 showed very low levels of endotoxin contamination, 0.277 EU/mg which corresponds to 13.85 pg/mg of LPS. In relation to the *E. coli* expressed protein, r-his-SmCyp1, rbacSmCyp1 showed a 41,2 fold decrease in the level of LPS contamination.

In order to increase rbacSmCyp1 purity level, another purification approach was carried out: ion exchange. At a pH lower than its predicted pI, rbacSmCyp1 would be expected to bind to a cation exchange column. Conversely, it bound to an anion exchange column. The anion exchange chromatography was initially carried out with the aim to eliminate some of the contaminant proteins prior to the cation exchange chromatography. When carrying out the anion exchange in a larger amount of sample, rbacSmCyp1 precipitated in the column. It was not possible to collect it until the column was loaded with a denaturing reducing buffer. Thus, under the conditions used for the anion exchange chromatography, rbacSmCyp1 was insoluble.

In summary, in this chapter, I described the production of *S. mansoni* Cyclophilin (SmCyp1) and *S. mansoni* Cyclophilin B (SmCyp2) in two different expression systems: *E. coli* and baculovirus-insect cell. As expected, baculovirus-insect cell expressed recombinant SmCyp1 showed very low levels of endotoxin contamination and therefore can be used for future work regarding its functional analysis and modulation of the immune response.

6.1 - Discussion

Helminth infections induce a strong modulation of the host's immune system. This effect does not only favour parasite and host survival, but also interferes with non-related diseases that the host might develop during infection, such as allergies and inflammatory diseases. Depending on several factors e.g. parasite species, infection intensity, host age and nutritional status, among others, the helminth-derived immunomodulation may suppress or exacerbate non-related disorders (*40*).

The therapeutic potential of helminth infections has been tested in human clinical trials in the treatment of patients with allergy or inflammatory bowel disease. Two candidates currently in trial are the human hookworm *Necator americanus* and the porcine whipworm *Trichuris suis*. These species were chosen based on the premise that they have a relatively benign association with humans (*207*). However, the use of helminths in a clinical setting has inevitable risks of side effects since parasites have an inherent potential to cause damage to the host. On this basis, the use of helminth-derived molecules that mimic the immunodulatory effects of an infection would be a safer approach.

During my Ph.D, I have carried out the isolation, identification and recombinant molecule production of helminth-derived molecules with immunomodulatory potential. I have used *S. mansoni* as a model of a parasitic helminth that is a potent modulator of the immune system. The molecules released by the blood fluke into the host's blood circulation are the mostly likely to interact with the host's immune cells and, therefore, generate an immunomodulatory response. On this basis, I have focused my work on the search of immunomodulatory molecules excreted and secreted by *S. mansoni*.

Firstly, I have optimized the *ex vivo* isolation of *S. mansoni* male adult worm excretory-secretory (WES) molecules. Previous to my work, it has been shown that conventional *S. mansoni* egg-laying male and female worm infection of mice exacerbates airway hyperresponsiveness and do not render mice resistant to colitis induced by DSS. On the contrary, infection with male schistosome worms protects mice from OVA-induced airway hyperresponsiveness and DSS-induced colitis (*77, 208*). Therefore, I have used only male adult worms for the characterization of the schistosome immunomodulatory excretome-secretome.

I have focused my work on the search of immunomodulatory proteins excreted-secreted by *S. mansoni*. However, other molecules secreted by schistosomes such as, glycans and lipids, may also induce modulation of host's immune system. For instance, the Lewis-X motifs from schistosome glycoproteins have been shown to trigger Th2 response mediated by TLR4 in vivo (*123*) and the lipid schistosome phosphatidylserine (PS) have been shown to induce DCs that polarize IL-4/IL-10-producing T cells (*92*). In order to elucidate the complete set of schistosome molecules that function as immunomodulators, proteomics studies should be associated to the identification of the excreted-secreted schistosome glycome and lipidome.

In contrast with other helminths, such as *B. malayi* and *H. polygyrus*, isolation of schistosome WES molecules from adult worms is hampered by the fact that adult worms survive only for a few hours outside the host body. *In vitro* lifespan can be increased to approximately a week by adding FCS to the incubation medium. However, FCS has a rich variety and high concentration of proteins that masks the identification of the schistosome-derived molecules. The approach I have used for the *in vitro* incubation of the worms, described in Chapter 2 (section 2.2.3), allows the survival of the parasites by adding FCS into the nutrient media and, concomitantly, keeps the FCS proteins of molecular weight higher than 10 kDa apart from the parasite excreted-secreted molecules. All the

downstream procedures were performed using devices with 10 kDa molecular weight cut off. Therefore, the final WES preparation does not contain any FCS-derived protein. On the other hand, schistosome-derived proteins of 10 kDa or less are also excluded from the preparation. The use of a dialysis membrane with a lower molecular weight cut off, i.e., 2 kDa, to incubate the worms could result in the isolation of schistosome-derived proteins of smaller size. But worm survival under this condition should be evaluated since it could be affected by the reduction in the availability of FCS-derived proteins.

Another factor to consider regarding the *in vitro* isolation of a worm's excretome-secretome is the contamination of the preparation by worm somatic molecules released from damaged and/or dead worms. To confirm that the WES preparation did not contain somatic molecules, I performed a 2D comparative analysis of the WES and somatic adult worm (AW) molecules (Chapter 3, Section 3.3.2.1). The identification of a major structural protein, *S. mansoni* paramyosin, in the AW but not in the WES, confirmed a demarcation of the protein composition between the two preparations.

In order to characterize the *S. mansoni* WES immunomodulatory candidates, I have generated recombinant molecules using 2 different expression systems: *E. coli* and baculovirus-insect cell systems. The *E. coli* expression system provides a high yield of recombinant protein and has relativelly cheap and simple culture techniques. However, *E. coli* does not present post-translational modifications such as, formation of disulfide bonds, glycosylation, and phosphorylation and the recombinant proteins expressed in this system have high levels of LPS contamination (*209*). The eukaryotic expression systems such as, yeast, baculovirus-insect cell and mammalian cell are alternatives to the *E. coli* system. Although these eukaryotic systems provide lower protein yield and require more expensive and complicated culture techniques, they are free of LPS and contain post-translational modifications at different levels. Yeast and baculovirus-insect cell have a more limited

post-translational machinery with glycosilation patterns different from mammalian cells (*210-212*).

S. mansoni Peroxiredoxin (SmPrx1), Thioredoxin (SmTrx1), Cyclophilin (SmCyp1) and Cyclophilin B (putative (SmCyp2) coding sequences were cloned into *E. coli* expression vectors (Table 6.1). The protein coding sequences were generated by amplification from the worm cDNA or by chemical synthesis and cloned into the expression vectors using the Gateway system.

SmPrx1 is a immunosupressive molecule that acts through induction of alternatively activated macrophages (*95*). SmPrx1 identification and characterization was described in Chapter 4. SmTrx1 was used as a control for technical artifact effects of production of recombinant proteins.

S. mansoni Cyclophilin, (SmCyp1) was identified in the 2D comparative analysis between AW and WES. It was detected in a strong spot unique to the WES 2D (Chapter 3, Section 3.3.2.1). Further mass spectrometry analysis revealed that WES contains another cyclophilin, the Cyclophilin B, putative (SmCyp2). *S. mansoni* Cyclophilin may induce exacerbation, as opposed to immunosupression, of non related diseases since a *Toxoplasma gondii* homolog, *T. gondii* Cyclophilin (TgCyP18), has a inflammatory effect. TgCyP18 binds to the cysteine-cysteine chemokine receptor 5 (CCR5) on the surface of dendritic cells (DCs) and macrophages inducing expression of NO, interleukin-12 (IL-12) and TNF-α (*213*).

The main purpose of generating these recombinant proteins using *E. coli* was to produce specific antibodies for further use in the functional characterization of the immunomodulatory molecules. *E. coli* expressed recombinant proteins are highly contaminated with bacteria-derived lipopolysaccharide (LPS) and are not suitable for functional studies since they may show an activity that do not result from the protein itself but from the LPS contamination. For instance, a schistosome recombinant protein, *S.*

mansoni chemokine binding protein, smCKBP, expressed in *E. coli* was shown to induce human basophil degranulation (*105*). On the other hand, the recombinant protein expressed in the baculovirus-insect cell system, an LPS-free expression system, failed to induce similar activity unless exogenous LPS was added (*53*). This highlights the need to generate recombinant molecules with low endotoxin levels in order to accurately dissect their functional activity. As described in Chapter 4 (section 4.3.3.6) and Chapter 5 (section 5.3.2.7), the recombinant molecules I generated in the baculovirus-insect cell system showed less than 0.5 EU/mg, i.e., less than 50 pg/mg of LPS (Table 6.2).

Recombinant proteins with low endotoxin contamination, were generated using the baculovirus-insect cell system which I have reestablished in the laboratory. In order to set up the expression system, I trained with Dr. Alcami's group at the Centro de Biologia Molecular Severo Ochoa - Universidad Autonoma de Madrid – Spain.

E. coli expression system		*S. mansoni* recombinant proteins			
		SmPrx1	**SmTrx1**	**SmCyp1**	**SmCyp2**
Coding sequence generated by amplification from *S. mansoni* worm cDNA		√	√	-	-
Coding sequence generated by chemical synthesis		-	-	√	√
Entry vector	pENTR/D-TOPO	√	√		
	pDONR221			√	√
Destination vector	pDEST17	√	√	√	√
	pET-60-DEST	-	-	√	√
Expression		√	√	√	√
Generation of specific sera	Rabbit	√	√	-	-
	Mouse	-	-	√	-

Table 6.1: **Generation of *S. mansoni* recombinant molecules in the *E. coli* expression system.** For vector maps see Appendix 4.

S. mansoni recombinant proteins	Expression systems	
	E. coli	Baculovirus-insect cell
SmPrx1	23.551 EU/mg	0.365 EU/mg
SmCyp1	11.40 EU/mg	0.277 EU/mg

Table 6.2: **Endotoxin levels of recombinant molecules expressed in the *E. coli* and baculovirus-insect cell systems.** EU – endotoxin unit. For vector maps see Appendix 4.

For generating insect cell expressed proteins, I have used the traditional cloning method with restriction endonucleases or the chemical synthesis of the coding sequences followed by cloning using the Gateway system (Table 6.3). Baculovirus-insect cell expressed recombinants SmPrx1, SmTrx1, SmCyp1 and SmCyp2 were generated and rbacSmPrx1 and rbacSmCyp1 were purified. I have also worked with the *H. polygyrus* Calreticulin (HpCrt), a molecule with known immunomodulatory effect, and with its *S. mansoni* homolog, *S. mansoni* Calreticulin (SmCrt). SmCrt was detected in the WES as described in Chapter 3 (Section 3.3.3.5).

In summary, I have described the complete *S. mansoni* male adult worm excretome-secretome. These molecules may play an important role in the immunomodulation of host response to infection since they mediate the interaction of the parasite with the host's immune system. On this basis, I have identified proteins with potential immunomodulatory activity. In order to further characterize these immunomodulators, I have generated recombinant proteins. Furthermore, I have optimized methods to generate recombinant molecules with low endotoxin contamination. These molecules are currently being screened for immunomodulation and will be further tested as novel immunotherapeutics in mouse models of inflammatory diseases.

Baculovirus-insect cell expression system		Recombinant proteins					
		rbacSmPrx1	**rbacSmTrx1**	**rbacSmCyp1**	**rbacSmCyp2**	**rbacSmCrt**	**rbacHpCrt**
Coding sequence amplification generated from *S. mansoni* worm cDNA		√	√	-	-	-	-
Cloning of the PCR product into the p-GEM-T-easy vector		√	√	-	-	-	-
Coding sequence generated by chemical synthesis		-	-	√	√	√	√
Codin sequence optimization		-	-	√	√	√	√
Expression vector	pFastBac-Mel-V5-His	√	√				
	pFast-Bac1			√	√	√	√
Generation of recombinant bacmid		√	√	√	√	√	√
Generation of baculovirus stocks		√	√	√	√	-	-
Expression		√	√	√	-	-	-

Table 6.3: **Generation of *S. mansoni* and *H. polygyrus* recombinant molecules in the baculovirus-insect cell system**. For vector maps see Appendix 4.

6.2 - Future work

Since there were problems encountered with the purification of recombinant proteins expressed in the baculovirus-insect cell system, a diferrent purification approach should be tested in order to achieve a higher level of purity. RbacSmPrx1 and rbacSmCyp1 were both expressed with a polyhistidine tag for purification by nickel-affinity chromatography. Although several purification conditions were tested in order to determine the optimal concentration of imidazol, nickel-affinity purified rbacSmPrx1 and rbacSmCyp1 showed several contaminant bands.

With regard to rbacSmPrx1, a second step purification, such as ion exchange or size exclusion, can be applied after the nickel-affinity chromatography. In the case of RbacSmCyp1, which was expressed with a thrombin and a TEV cleavage sites upstream of the polyhistidine tag (Figure 5.22), removal of the polyhistidine tag after the nickel-affinity chromatography can be performed by treating the elution fractions with the TEV or thrombin protease. After proteolytic removal of the polyhistidine tag, the recombinant protein is loaded into the nickel column again. The target recombinant protein is expected to be collected in the column flow through while the contaminant proteins remain bound to the column.

Regarding functional analysis of the recombinants, SmPrx1 and SmCyp1 immunomodulatory activity should be characterized using *in vitro* assays and transgenic mouse models. With respect to SmPrx1, intraperitoneal administration of rbacSmPrx1 in mice can be performed for confirmation of induction of alternatively activated macrophages *in vivo*. After administration of rbacSmPrx1, the intraperitoneal macrophages are isolated and checked for the expression of the transcription factors FIZZ/RELM-α and Ym1 using real-time polymerase chain reaction (RT-PCR). Induction of alternatively activated macrophages can also be tested *in vitro*. For that, macrophages are differentiated

from bone marrow cells, incubated with rbacSmPrx1 and the markers FIZZ/RELM-α and Ym1 are analysed by RT-PCR. The immunomodulation of the Th2 response induced by SmPrx1 can be tested in a mouse model of experimental asthma. For that, rbacSmPrx1 is administrated to mice concurrent with ovalbumin (OVA) sensitization and OVA aerosol priming. The airway responsiveness of mice is assessed by barometric whole body plethysmography in response to a methacholine challenge. Cellular phenotypes in the spleen, lung and bronchoalveolar lavage (BAL) are assessed by flow cytometry. Cytokine responses and cell proliferation are measured in the spleen and mediastinal lymph node cultures. The lung inflammation can be evaluated by histology. Mice with dual deficiency in IL-4 and IL-13, that fail to develop alternatively activated macrophages, can be used to address the induction of inflammatory cells.

With respect to functional characterization of SmCyp1, induction of IL-12 production should be assessed *in vitro* in murine DCs incubated with WES preparation, rbacSmCyp1, or cyclophilin-depleted WES. Dendritic cell-chemotatic response to intravenous injection of rbacSmCyp1 should be evaluated in mice using the air pouch model. Furthemore, SmCyp1 binding to human CCR5 could be evaluated in transfected cells using radio labelled recombinant protein.

In my thesis, I described the complete identification of the *S. mansoni* male worm excretome-secretome and the selection of potential immunomodulatory proteins that are homologs to other helminth proteins with known modulatory activities. However, other *S. mansoni* excretory-secretory proteins, although they do not present a high homology with know helmith immunomodulators, could also be potential immunomodulatory candidates.

A *S. mansoni* cystatin, Cystatin B (Smp_006390) was detected in the *S. mansoni* WES molecules. Cystatins from *A. viteae*, *B. malayi*, *O. volvulus* and *N. brasiliensis* act as immunomodulators. They inhibit cysteine proteases required for host APC antigen processing and presentation leading to reduced T cell priming and also elicit the

immunosuppressive cytokine IL-10 reducing T cell proliferation (*109*).

The 14-3-3 proteins regulate a diverse range of signaling pathways in eukaryotic cells. Three proteins of the 14-3-3 family were detected in the *S. mansoni* WES molecules: 14-3-3 protein -Smp_009760, 14-3-3 protein - Smp_009780.2 and 14-3-3 epsilon - Smp_034840.2. An *E. multilocularis* 14-3-3 protein, the E14t recombinant 14-3-3 protein (E14ζ), has been shown to hamper the *in vitro* nitric oxide (NO) production from activated macrophages. Macrophages *in vitro* pre-stimulated with lipopolysaccharide (LPS) and further incubated with the E14ζ protein results in a strong, dose-dependent reduction of NO and iNOS mRNA production of the cells when compared with macrophages incubated with LPS alone (*214*).

Heat shock proteins are powerful immunomodulatory molecules with dual activity: immunoestimulatory or immunosuppressive, depending on the context wich they are encountered (*215*). Three heat shock proteins were detected in the *S. mansoni* WES molecules: heat shock protein - Smp_049250, Heat shock protein - Smp_049270 and Heat shock protein 70 - Smp_049550. A heat shock protein from a pathogenic bacterium, the 71-kD heat shock protein from *Mycobacterium tuberculosis*, has been shown to induce a modulatory effects on experimental rat arthritis (*216*).

All of the proteins described above are of interest to further investigation of the immunomodulatory effect of *S. mansoni* adult male worm. The elucidation of their activities can contribute to the development of new immunotherapeutics for the treatment of inflammatory diseases.

References

1. B. Gryseels, K. Polman, J. Clerinx, L. Kestens, Human schistosomiasis. *Lancet* **368**, 1106 (Sep 23, 2006).
2. C. H. King, Parasites and poverty: the case of schistosomiasis. *Acta Trop* **113**, 95 (Feb, 2010).
3. World Health Organization, 2010, vol. 2011.
4. P. Steinmann, J. Keiser, R. Bos, M. Tanner, J. Utzinger, Schistosomiasis and water resources development: systematic review, meta-analysis, and estimates of people at risk. *Lancet Infect Dis* **6**, 411 (Jul, 2006).
5. M. L. Burke *et al.*, Immunopathogenesis of human schistosomiasis. *Parasite Immunol* **31**, 163 (Apr, 2009).
6. E. Hansell *et al.*, Proteomic analysis of skin invasion by blood fluke larvae. *PLoS Negl Trop Dis* **2**, e262 (2008).
7. J. Dvorak *et al.*, Differential use of protease families for invasion by schistosome cercariae. *Biochimie* **90**, 345 (Feb, 2008).
8. B. H. Al-Adhami *et al.*, The role of acidic organelles in the development of schistosomula of Schistosoma mansoni and their response to signalling molecules. *Parasitology* **130**, 309 (Mar, 2005).
9. Y. X. He, B. Salafsky, K. Ramaswamy, Comparison of skin invasion among three major species of Schistosoma. *Trends Parasitol* **21**, 201 (May, 2005).
10. G. N. Gobert, M. Chai, D. P. McManus, Biology of the schistosome lung-stage schistosomulum. *Parasitology* **134**, 453 (Apr, 2007).
11. E. J. Pearce, A. S. MacDonald, The immunobiology of schistosomiasis. *Nat Rev Immunol* **2**, 499 (Jul, 2002).

12. D. M. Karanja, D. G. Colley, B. L. Nahlen, J. H. Ouma, W. E. Secor, Studies on schistosomiasis in western Kenya: I. Evidence for immune-facilitated excretion of schistosome eggs from patients with Schistosoma mansoni and human immunodeficiency virus coinfections. *Am J Trop Med Hyg* **56**, 515 (May, 1997).

13. A. G. Ross, D. Vickers, G. R. Olds, S. M. Shah, D. P. McManus, Katayama syndrome. *Lancet Infect Dis* **7**, 218 (Mar, 2007).

14. S. Jaureguiberry, L. Paris, E. Caumes, Acute schistosomiasis, a diagnostic and therapeutic challenge. *Clin Microbiol Infect* **16**, 225 (Mar, 2010).

15. J. Clerinx, A. Van Gompel, Schistosomiasis in travellers and migrants. *Travel Med Infect Dis* **9**, 6 (Jan, 2011).

16. C. L. King *et al.*, B cell sensitization to helminthic infection develops in utero in humans. *J Immunol* **160**, 3578 (Apr 1, 1998).

17. I. Malhotra *et al.*, In utero exposure to helminth and mycobacterial antigens generates cytokine responses similar to that observed in adults. *J Clin Invest* **99**, 1759 (Apr 1, 1997).

18. D. P. McManus *et al.*, Schistosomiasis in the People's Republic of China: the era of the Three Gorges Dam. *Clin Microbiol Rev* **23**, 442 (Apr, 2010).

19. K. S. Warren, E. O. Domingo, R. B. Cowan, Granuloma formation around schistosome eggs as a manifestation of delayed hypersensitivity. *Am J Pathol* **51**, 735 (Nov, 1967).

20. H. Jorulf, E. Lindstedt, Urogenital schistosomiasis: CT evaluation. *Radiology* **157**, 745 (Dec, 1985).

21. M. C. Botelho, J. C. Machado, J. M. da Costa, Schistosoma haematobium and bladder cancer: what lies beneath? *Virulence* **1**, 84 (Mar-Apr, 2010).

22. R. Bedwani *et al.*, Schistosomiasis and the risk of bladder cancer in Alexandria, Egypt. *Br J Cancer* **77**, 1186 (Apr, 1998).

23. M. H. Mostafa, S. A. Sheweita, P. J. O'Connor, Relationship between schistosomiasis and bladder cancer. *Clin Microbiol Rev* **12**, 97 (Jan, 1999).

24. M. O. Rocha *et al.*, Gastro-intestinal manifestations of the initial phase of schistosomiasis mansoni. *Ann Trop Med Parasitol* **89**, 271 (Jun, 1995).

25. A. W. Cheever, Z. A. Andrade, Pathological lesions associated with Schistosoma mansoni infection in man. *Trans R Soc Trop Med Hyg* **61**, 626 (1967).

26. Z. A. Andrade, Schistosomiasis and liver fibrosis. *Parasite Immunol* **31**, 656 (Nov, 2009).

27. E. Kolosionek, B. B. Graham, R. M. Tuder, G. Butrous, Pulmonary vascular disease associated with parasitic infection--the role of schistosomiasis. *Clin Microbiol Infect* **17**, 15 (Jan, 2011).

28. T. C. Ferrari, P. R. Moreira, Neuroschistosomiasis: clinical symptoms and pathogenesis. *Lancet Neurol* **10**, 853 (Sep, 2011).

29. D. J. Gray, A. G. Ross, Y. S. Li, D. P. McManus, Diagnosis and management of schistosomiasis. *BMJ* **342**, d2651 (2011).

30. P. Minard, D. A. Dean, R. H. Jacobson, W. E. Vannier, K. D. Murrell, Immunization of mice with cobalt-60 irradiated Schistosoma mansoni cercariae. *Am J Trop Med Hyg* **27**, 76 (Jan, 1978).

31. Q. D. Bickle, Radiation-attenuated schistosome vaccination--a brief historical perspective. *Parasitology* **136**, 1621 (Oct, 2009).

32. N. R. Bergquist, D. G. Colley, Schistosomiasis vaccine:research to development. *Parasitol Today* **14**, 99 (Mar, 1998).

33. A. Capron, M. Capron, D. Dombrowicz, G. Riveau, Vaccine strategies against schistosomiasis: from concepts to clinical trials. *Int Arch Allergy Immunol* **124**, 9 (Jan-Mar, 2001).

34. W. Zhang *et al.*, Sm-p80-based DNA vaccine provides baboons with levels of protection against Schistosoma mansoni infection comparable to those achieved by the irradiated cercarial vaccine. *J Infect Dis* **201**, 1105 (Apr 1, 2010).

35. M. Tendler, A. J. Simpson, The biotechnology-value chain: development of Sm14 as a schistosomiasis vaccine. *Acta Trop* **108**, 263 (Nov-Dec, 2008).

36. M. H. Tran *et al.*, Tetraspanins on the surface of Schistosoma mansoni are protective antigens against schistosomiasis. *Nat Med* **12**, 835 (Jul, 2006).

37. C. M. Rezende *et al.*, Immunization with rP22 induces protective immunity against Schistosoma mansoni: effects on granuloma down-modulation and cytokine production. *Immunol Lett* **141**, 123 (Dec 30, 2011).

38. E. Moreau, A. Chauvin, Immunity against helminths: interactions with the host and the intercurrent infections. *J Biomed Biotechnol* **2010**, 428593 (2010).

39. R. M. Maizels *et al.*, Helminth parasites--masters of regulation. *Immunol Rev* **201**, 89 (Oct, 2004).

40. P. G. Fallon, N. E. Mangan, Suppression of TH2-type allergic reactions by helminth infection. *Nat Rev Immunol* **7**, 220 (Mar, 2007).

41. M. Capron, A. Capron, Effector functions of eosinophils in schistosomiasis. *Mem Inst Oswaldo Cruz* **87 Suppl 4**, 167 (1992).

42. R. T. Gazzinelli, I. P. Oswald, S. L. James, A. Sher, IL-10 inhibits parasite killing and nitrogen oxide production by IFN-gamma-activated macrophages. *J Immunol* **148**, 1792 (Mar 15, 1992).

43. D. L. Boros, R. P. Pelley, K. S. Warren, Spontaneous modulation of granulomatous hypersensitivity in schistosomiasis mansoni. *J Immunol* **114**, 1437 (May, 1975).

44. A. Chauvin, C. Boulard, Local immune response to experimental Fasciola hepatica infection in sheep. *Parasite* **3**, 209 (Sep, 1996).

45. W. M. Kemp, P. R. Brown, S. C. Merritt, R. E. Miller, Tegument-associated antigen modulation by adult male Schistosoma mansoni. *J Immunol* **124**, 806 (Feb, 1980).

46. S. Braschi, R. S. Curwen, P. D. Ashton, S. Verjovski-Almeida, A. Wilson, The tegument surface membranes of the human blood parasite Schistosoma mansoni: a proteomic analysis after differential extraction. *Proteomics* **6**, 1471 (Mar, 2006).

47. P. J. Skelly, Intravascular schistosomes and complement. *Trends Parasitol* **20**, 370 (Aug, 2004).

48. A. M. Smith, A. J. Dowd, M. Heffernan, C. D. Robertson, J. P. Dalton, Fasciola hepatica: a secreted cathepsin L-like proteinase cleaves host immunoglobulin. *Int J Parasitol* **23**, 977 (Dec, 1993).

49. A. K. Dixit, P. Dixit, R. L. Sharma, Immunodiagnostic/protective role of cathepsin L cysteine proteinases secreted by Fasciola species. *Vet Parasitol* **154**, 177 (Jul 4, 2008).

50. F. J. Culley *et al.*, Eotaxin is specifically cleaved by hookworm metalloproteases preventing its action in vitro and in vivo. *J Immunol* **165**, 6447 (Dec 1, 2000).

51. J. P. Hewitson *et al.*, The secretome of the filarial parasite, Brugia malayi: proteomic profile of adult excretory-secretory products. *Mol Biochem Parasitol* **160**, 8 (Jul, 2008).

52. J. Mulvenna *et al.*, The secreted and surface proteomes of the adult stage of the carcinogenic human liver fluke Opisthorchis viverrini. *Proteomics* **10**, 1063 (Mar, 2010).

53. P. Smith *et al.*, Schistosoma mansoni secretes a chemokine binding protein with antiinflammatory activity. *J Exp Med* **202**, 1319 (Nov 21, 2005).

54. J. E. Allen, R. M. Maizels, Diversity and dialogue in immunity to helminths. *Nat Rev Immunol* **11**, 375 (Jun, 2011).

55. D. R. Neill *et al.*, Nuocytes represent a new innate effector leukocyte that mediates type-2 immunity. *Nature* **464**, 1367 (Apr 29, 2010).

56. R. M. Maizels, M. Yazdanbakhsh, Immune regulation by helminth parasites: cellular and molecular mechanisms. *Nat Rev Immunol* **3**, 733 (Sep, 2003).

57. C. L. King *et al.*, Cytokine control of parasite-specific anergy in human urinary schistosomiasis. IL-10 modulates lymphocyte reactivity. *J Immunol* **156**, 4715 (Jun 15, 1996).

58. S. Amu *et al.*, Regulatory B cells prevent and reverse allergic airway inflammation via FoxP3-positive T regulatory cells in a murine model. *J Allergy Clin Immunol* **125**, 1114 (May, 2010).

59. M. D. Taylor, A. Harris, M. G. Nair, R. M. Maizels, J. E. Allen, F4/80+ alternatively activated macrophages control CD4+ T cell hyporesponsiveness at sites peripheral to filarial infection. *J Immunol* **176**, 6918 (Jun 1, 2006).

60. T. Kreider, R. M. Anthony, J. F. Urban, Jr., W. C. Gause, Alternatively activated macrophages in helminth infections. *Curr Opin Immunol* **19**, 448 (Aug, 2007).

61. M. I. Araujo *et al.*, Inverse association between skin response to aeroallergens and Schistosoma mansoni infection. *Int Arch Allergy Immunol* **123**, 145 (Oct, 2000).

62. M. Medeiros, Jr. *et al.*, Schistosoma mansoni infection is associated with a reduced course of asthma. *J Allergy Clin Immunol* **111**, 947 (May, 2003).

63. D. Dagoye *et al.*, Wheezing, allergy, and parasite infection in children in urban and rural Ethiopia. *Am J Respir Crit Care Med* **167**, 1369 (May 15, 2003).

64. J. Feary, J. Britton, J. Leonardi-Bee, Atopy and current intestinal parasite infection: a systematic review and meta-analysis. *Allergy* **66**, 569 (Apr, 2011).

65. G. Davey, A. Venn, H. Belete, Y. Berhane, J. Britton, Wheeze, allergic sensitization and geohelminth infection in Butajira, Ethiopia. *Clin Exp Allergy* **35**, 301 (Mar, 2005).

66. N. E. Mangan *et al.*, Helminth infection protects mice from anaphylaxis via IL-10-producing B cells. *J Immunol* **173**, 6346 (Nov 15, 2004).

67. M. S. Wilson *et al.*, Suppression of allergic airway inflammation by helminth-induced regulatory T cells. *J Exp Med* **202**, 1199 (Nov 7, 2005).

68. M. E. Bashir, P. Andersen, I. J. Fuss, H. N. Shi, C. Nagler-Anderson, An enteric helminth infection protects against an allergic response to dietary antigen. *J Immunol* **169**, 3284 (Sep 15, 2002).

69. C. C. Wang, T. J. Nolan, G. A. Schad, D. Abraham, Infection of mice with the helminth Strongyloides stercoralis suppresses pulmonary allergic responses to ovalbumin. *Clin Exp Allergy* **31**, 495 (Mar, 2001).

70. A. M. Dittrich *et al.*, Helminth infection with Litomosoides sigmodontis induces regulatory T cells and inhibits allergic sensitization, airway inflammation, and hyperreactivity in a murine asthma model. *J Immunol* **180**, 1792 (Feb 1, 2008).

71. G. Wohlleben *et al.*, Helminth infection modulates the development of allergen-induced airway inflammation. *Int Immunol* **16**, 585 (Apr, 2004).

72. R. T. Strait, S. C. Morris, K. Smiley, J. F. Urban, Jr., F. D. Finkelman, IL-4 exacerbates anaphylaxis. *J Immunol* **170**, 3835 (Apr 1, 2003).

73. I. M. Richards *et al.*, Ascaris-induced bronchoconstriction in primates experimentally infected with Ascaris suum ova. *Clin Exp Immunol* **54**, 461 (Nov, 1983).

74. J. V. Weinstock *et al.*, The possible link between de-worming and the emergence of immunological disease. *J Lab Clin Med* **139**, 334 (Jun, 2002).

75. M. El-Malky, N. Nabih, M. Heder, N. Saudy, M. El-Mahdy, Helminth infections: therapeutic potential in autoimmune disorders. *Parasite Immunol* **33**, 589 (Nov, 2011).

76. A. Cooke *et al.*, Infection with Schistosoma mansoni prevents insulin dependent diabetes mellitus in non-obese diabetic mice. *Parasite Immunol* **21**, 169 (Apr, 1999).

77. P. Smith *et al.*, Infection with a helminth parasite prevents experimental colitis via a macrophage-mediated mechanism. *J Immunol* **178**, 4557 (Apr 1, 2007).

78. D. Sewell *et al.*, Immunomodulation of experimental autoimmune encephalomyelitis by helminth ova immunization. *Int Immunol* **15**, 59 (Jan, 2003).

79. Y. Osada, S. Shimizu, T. Kumagai, S. Yamada, T. Kanazawa, Schistosoma mansoni infection reduces severity of collagen-induced arthritis via down-regulation of pro-inflammatory mediators. *Int J Parasitol* **39**, 457 (Mar, 2009).

80. M. C. Salinas-Carmona *et al.*, Spontaneous arthritis in MRL/lpr mice is aggravated by Staphylococcus aureus and ameliorated by Nippostrongylus brasiliensis infections. *Autoimmunity* **42**, 25 (Jan, 2009).

81. R. W. Summers *et al.*, Trichuris suis seems to be safe and possibly effective in the treatment of inflammatory bowel disease. *Am J Gastroenterol* **98**, 2034 (Sep, 2003).

82. J. Croese *et al.*, A proof of concept study establishing Necator americanus in Crohn's patients and reservoir donors. *Gut* **55**, 136 (Jan, 2006).

83. R. W. Summers, D. E. Elliott, J. F. Urban, Jr., R. Thompson, J. V. Weinstock, Trichuris suis therapy in Crohn's disease. *Gut* **54**, 87 (Jan, 2005).

84. P. G. Fallon, A. Alcami, Pathogen-derived immunomodulatory molecules: future immunotherapeutics? *Trends Immunol* **27**, 470 (Oct, 2006).

85. M. J. Johnston, J. A. MacDonald, D. M. McKay, Parasitic helminths: a pharmacopeia of anti-inflammatory molecules. *Parasitology* **136**, 125 (Feb, 2009).

86. A. Doetze *et al.*, Antigen-specific cellular hyporesponsiveness in a chronic human helminth infection is mediated by T(h)3/T(r)1-type cytokines IL-10 and

transforming growth factor-beta but not by a T(h)1 to T(h)2 shift. *Int Immunol* **12**, 623 (May, 2000).

87. C. Schnoeller *et al.*, A helminth immunomodulator reduces allergic and inflammatory responses by induction of IL-10-producing macrophages. *J Immunol* **180**, 4265 (Mar 15, 2008).

88. I. B. McInnes *et al.*, A novel therapeutic approach targeting articular inflammation using the filarial nematode-derived phosphorylcholine-containing glycoprotein ES-62. *J Immunol* **171**, 2127 (Aug 15, 2003).

89. A. J. Melendez *et al.*, Inhibition of Fc epsilon RI-mediated mast cell responses by ES-62, a product of parasitic filarial nematodes. *Nat Med* **13**, 1375 (Nov, 2007).

90. M. Okano, A. R. Satoskar, K. Nishizaki, D. A. Harn, Jr., Lacto-N-fucopentaose III found on Schistosoma mansoni egg antigens functions as adjuvant for proteins by inducing Th2-type response. *J Immunol* **167**, 442 (Jul 1, 2001).

91. P. G. Thomas, M. R. Carter, A. A. Da'dara, T. M. DeSimone, D. A. Harn, A helminth glycan induces APC maturation via alternative NF-kappa B activation independent of I kappa B alpha degradation. *J Immunol* **175**, 2082 (Aug 15, 2005).

92. D. van der Kleij *et al.*, A novel host-parasite lipid cross-talk. Schistosomal lyso-phosphatidylserine activates toll-like receptor 2 and affects immune polarization. *J Biol Chem* **277**, 48122 (Dec 13, 2002).

93. S. J. Jenkins, J. P. Hewitson, G. R. Jenkins, A. P. Mountford, Modulation of the host's immune response by schistosome larvae. *Parasite Immunol* **27**, 385 (Oct-Nov, 2005).

94. S. Donnelly, S. M. O'Neill, M. Sekiya, G. Mulcahy, J. P. Dalton, Thioredoxin peroxidase secreted by Fasciola hepatica induces the alternative activation of macrophages. *Infect Immun* **73**, 166 (Jan, 2005).

95. S. Donnelly *et al.*, Helminth 2-Cys peroxiredoxin drives Th2 responses through a mechanism involving alternatively activated macrophages. *FASEB J* **22**, 4022 (Nov, 2008).

96. W. Harnett, I. B. McInnes, M. M. Harnett, ES-62, a filarial nematode-derived immunomodulator with anti-inflammatory potential. *Immunol Lett* **94**, 27 (Jun 15, 2004).

97. K. M. Houston *et al.*, Presence of phosphorylcholine on a filarial nematode protein influences immunoglobulin G subclass response to the molecule by an interleukin-10-dependent mechanism. *Infect Immun* **68**, 5466 (Sep, 2000).

98. H. S. Goodridge *et al.*, Phosphorylcholine mimics the effects of ES-62 on macrophages and dendritic cells. *Parasite Immunol* **29**, 127 (Mar, 2007).

99. H. S. Goodridge *et al.*, Immunomodulation via novel use of TLR4 by the filarial nematode phosphorylcholine-containing secreted product, ES-62. *J Immunol* **174**, 284 (Jan 1, 2005).

100. F. Trottein *et al.*, Schistosoma mansoni activates host microvascular endothelial cells to acquire an anti-inflammatory phenotype. *Infect Immun* **67**, 3403 (Jul, 1999).

101. C. Valle *et al.*, Stage-specific expression of a Schistosoma mansoni polypeptide similar to the vertebrate regulatory protein stathmin. *J Biol Chem* **274**, 33869 (Nov 26, 1999).

102. K. V. Rao, Y. X. He, K. Ramaswamy, Suppression of cutaneous inflammation by intradermal gene delivery. *Gene Ther* **9**, 38 (Jan, 2002).

103. P. Holmfeldt *et al.*, The Schistosoma mansoni protein Sm16/SmSLP/SmSPO-1 is a membrane-binding protein that lacks the proposed microtubule-regulatory activity. *Mol Biochem Parasitol* **156**, 225 (Dec, 2007).

104. A. Alcami, Viral mimicry of cytokines, chemokines and their receptors. *Nat Rev Immunol* **3**, 36 (Jan, 2003).

105. G. Schramm *et al.*, Molecular characterization of an interleukin-4-inducing factor from Schistosoma mansoni eggs. *J Biol Chem* **278**, 18384 (May 16, 2003).

106. K. Kim, I. H. Kim, K. Y. Lee, S. G. Rhee, E. R. Stadtman, The isolation and purification of a specific "protector" protein which inhibits enzyme inactivation by a thiol/Fe(III)/O2 mixed-function oxidation system. *J Biol Chem* **263**, 4704 (Apr 5, 1988).

107. R. Chandrashekar, K. C. Curtis, W. Lu, G. J. Weil, Molecular cloning of an enzymatically active thioredoxin peroxidase from Onchocerca volvulus. *Mol Biochem Parasitol* **93**, 309 (Jun 1, 1998).

108. K. Henkle-Duhrsen, A. Kampkotter, Antioxidant enzyme families in parasitic nematodes. *Mol Biochem Parasitol* **114**, 129 (May, 2001).

109. S. Hartmann, R. Lucius, Modulation of host immune responses by nematode cystatins. *Int J Parasitol* **33**, 1291 (Sep 30, 2003).

110. S. Lustigman, B. Brotman, T. Huima, A. M. Prince, J. H. McKerrow, Molecular cloning and characterization of onchocystatin, a cysteine proteinase inhibitor of Onchocerca volvulus. *J Biol Chem* **267**, 17339 (Aug 25, 1992).

111. A. Schonemeyer *et al.*, Modulation of human T cell responses and macrophage functions by onchocystatin, a secreted protein of the filarial nematode Onchocerca volvulus. *J Immunol* **167**, 3207 (Sep 15, 2001).

112. J. Murray, B. Manoury, A. Balic, C. Watts, R. M. Maizels, Bm-CPI-2, a cystatin from Brugia malayi nematode parasites, differs from Caenorhabditis elegans cystatins in a specific site mediating inhibition of the antigen-processing enzyme AEP. *Mol Biochem Parasitol* **139**, 197 (Feb, 2005).

113. F. C. Morales, D. R. Furtado, F. D. Rumjanek, The N-terminus moiety of the cystatin SmCys from Schistosoma mansoni regulates its inhibitory activity in vitro and in vivo. *Mol Biochem Parasitol* **134**, 65 (Mar, 2004).

114. T. Resende Co, C. S. Hirsch, Z. Toossi, R. Dietze, R. Ribeiro-Rodrigues, Intestinal helminth co-infection has a negative impact on both anti-Mycobacterium tuberculosis immunity and clinical response to tuberculosis therapy. *Clin Exp Immunol* **147**, 45 (Jan, 2007).

115. D. van der Kleij, M. Yazdanbakhsh, Control of inflammatory diseases by pathogens: lipids and the immune system. *Eur J Immunol* **33**, 2953 (Nov, 2003).

116. A. Capron, G. Riveau, M. Capron, F. Trottein, Schistosomes: the road from host-parasite interactions to vaccines in clinical trials. *Trends Parasitol* **21**, 143 (Mar, 2005).

117. P. G. Thomas, D. A. Harn, Jr., Immune biasing by helminth glycans. *Cell Microbiol* **6**, 13 (Jan, 2004).

118. P. Velupillai, W. E. Secor, A. M. Horauf, D. A. Harn, B-1 cell (CD5+B220+) outgrowth in murine schistosomiasis is genetically restricted and is largely due to activation by polylactosamine sugars. *J Immunol* **158**, 338 (Jan 1, 1997).

119. P. Velupillai, D. A. Harn, Oligosaccharide-specific induction of interleukin 10 production by B220+ cells from schistosome-infected mice: a mechanism for regulation of CD4+ T-cell subsets. *Proc Natl Acad Sci U S A* **91**, 18 (Jan 4, 1994).

120. L. I. Terrazas, K. L. Walsh, D. Piskorska, E. McGuire, D. A. Harn, Jr., The schistosome oligosaccharide lacto-N-neotetraose expands Gr1(+) cells that secrete anti-inflammatory cytokines and inhibit proliferation of naive CD4(+) cells: a potential mechanism for immune polarization in helminth infections. *J Immunol* **167**, 5294 (Nov 1, 2001).

121. O. Atochina, T. Daly-Engel, D. Piskorska, E. McGuire, D. A. Harn, A schistosome-expressed immunomodulatory glycoconjugate expands peritoneal Gr1(+) macrophages that suppress naive CD4(+) T cell proliferation via an IFN-gamma and nitric oxide-dependent mechanism. *J Immunol* **167**, 4293 (Oct 15, 2001).

122. O. Atochina, A. A. Da'dara, M. Walker, D. A. Harn, The immunomodulatory glycan LNFPIII initiates alternative activation of murine macrophages in vivo. *Immunology* **125**, 111 (Sep, 2008).

123. P. G. Thomas *et al.*, Maturation of dendritic cell 2 phenotype by a helminth glycan uses a Toll-like receptor 4-dependent mechanism. *J Immunol* **171**, 5837 (Dec 1, 2003).

124. D. Van der Kleij *et al.*, Triggering of innate immune responses by schistosome egg glycolipids and their carbohydrate epitope GalNAc beta 1-4(Fuc alpha 1-2Fuc alpha 1-3)GlcNAc. *J Infect Dis* **185**, 531 (Feb 15, 2002).

125. R. K. Grencis, G. M. Entwistle, Production of an interferon-gamma homologue by an intestinal nematode: functionally significant or interesting artefact? *Parasitology* **115 Suppl**, S101 (1997).

126. M. Gnanasekar, R. Velusamy, Y. X. He, K. Ramaswamy, Cloning and characterization of a high mobility group box 1 (HMGB1) homologue protein from Schistosoma mansoni. *Mol Biochem Parasitol* **145**, 137 (Feb, 2006).

127. X. Zang *et al.*, Homologues of human macrophage migration inhibitory factor from a parasitic nematode. Gene cloning, protein activity, and crystal structure. *J Biol Chem* **277**, 44261 (Nov 15, 2002).

128. M. Gnanasekar, K. Ramaswamy, Translationally controlled tumor protein of Brugia malayi functions as an antioxidant protein. *Parasitol Res* **101**, 1533 (Nov, 2007).

129. N. Gomez-Escobar, E. Lewis, R. M. Maizels, A novel member of the transforming growth factor-beta (TGF-beta) superfamily from the filarial nematodes Brugia malayi and B. pahangi. *Exp Parasitol* **88**, 200 (Mar, 1998).

130. M. E. Bianchi, A. A. Manfredi, High-mobility group box 1 (HMGB1) protein at the crossroads between innate and adaptive immunity. *Immunol Rev* **220**, 35 (Dec, 2007).

131. J. J. Vermeire, Y. Cho, E. Lolis, R. Bucala, M. Cappello, Orthologs of macrophage migration inhibitory factor from parasitic nematodes. *Trends Parasitol* **24**, 355 (Aug, 2008).

132. P. D. Senter *et al.*, Inhibition of macrophage migration inhibitory factor (MIF) tautomerase and biological activities by acetaminophen metabolites. *Proc Natl Acad Sci U S A* **99**, 144 (Jan 8, 2002).

133. M. Rodriguez-Sosa *et al.*, Macrophage migration inhibitory factor plays a critical role in mediating protection against the helminth parasite Taenia crassiceps. *Infect Immun* **71**, 1247 (Mar, 2003).

134. Y. Cho *et al.*, Structural and functional characterization of a secreted hookworm Macrophage Migration Inhibitory Factor (MIF) that interacts with the human MIF receptor CD74. *J Biol Chem* **282**, 23447 (Aug 10, 2007).

135. U. A. Bommer, B. J. Thiele, The translationally controlled tumour protein (TCTP). *Int J Biochem Cell Biol* **36**, 379 (Mar, 2004).

136. M. Gnanasekar *et al.*, Molecular characterization of a calcium binding translationally controlled tumor protein homologue from the filarial parasites Brugia malayi and Wuchereria bancrofti. *Mol Biochem Parasitol* **121**, 107 (Apr 30, 2002).

137. M. J. Beall, S. McGonigle, E. J. Pearce, Functional conservation of Schistosoma mansoni Smads in TGF-beta signaling. *Mol Biochem Parasitol* **111**, 131 (Nov, 2000).

138. A. Osman, E. G. Niles, S. Verjovski-Almeida, P. T. LoVerde, Schistosoma mansoni TGF-beta receptor II: role in host ligand-induced regulation of a schistosome target gene. *PLoS Pathog* **2**, e54 (Jun, 2006).

139. R. Zavala-Gongora, A. Kroner, B. Wittek, P. Knaus, K. Brehm, Identification and characterisation of two distinct Smad proteins from the fox-tapeworm Echinococcus multilocularis. *Int J Parasitol* **33**, 1665 (Dec, 2003).

140. P. Smith, N. E. Mangan, P. G. Fallon, Generation of parasite antigens for use in Toll-like receptor research. *Methods Mol Biol* **517**, 401 (2009).

141. S. R. Smithers, R. J. Terry, The infection of laboratory hosts with cercariae of Schistosoma mansoni and the recovery of the adult worms. *Parasitology* **55**, 695 (Nov, 1965).

142. U. K. Laemmli, Cleavage of structural proteins during the assembly of the head of bacteriophage T4. *Nature* **227**, 680 (Aug 15, 1970).

143. P. H. O'Farrell, High resolution two-dimensional electrophoresis of proteins. *J Biol Chem* **250**, 4007 (May 25, 1975).

144. B. Bjellqvist *et al.*, Isoelectric focusing in immobilized pH gradients: principle, methodology and some applications. *J Biochem Biophys Methods* **6**, 317 (Sep, 1982).

145. H. Towbin, T. Staehelin, J. Gordon, Electrophoretic transfer of proteins from polyacrylamide gels to nitrocellulose sheets: procedure and some applications. *Proc Natl Acad Sci U S A* **76**, 4350 (Sep, 1979).

146. S. F. Altschul *et al.*, Gapped BLAST and PSI-BLAST: a new generation of protein database search programs. *Nucleic Acids Res* **25**, 3389 (Sep 1, 1997).

147. D. Binns *et al.*, QuickGO: a web-based tool for Gene Ontology searching. *Bioinformatics* **25**, 3045 (Nov 15, 2009).

148. D. Barrell *et al.*, The GOA database in 2009--an integrated Gene Ontology Annotation resource. *Nucleic Acids Res* **37**, D396 (Jan, 2009).

149. T. N. Petersen, S. Brunak, G. von Heijne, H. Nielsen, SignalP 4.0: discriminating signal peptides from transmembrane regions. *Nat Methods* **8**, 785 (2011).

150. J. D. Bendtsen, L. J. Jensen, N. Blom, G. Von Heijne, S. Brunak, Feature-based prediction of non-classical and leaderless protein secretion. *Protein Eng Des Sel* **17**, 349 (Apr, 2004).

151. E. L. Sonnhammer, G. von Heijne, A. Krogh, A hidden Markov model for predicting transmembrane helices in protein sequences. *Proc Int Conf Intell Syst Mol Biol* **6**, 175 (1998).

152. S. Hunter *et al.*, InterPro: the integrative protein signature database. *Nucleic Acids Res* **37**, D211 (Jan, 2009).

153. M. Goujon *et al.*, A new bioinformatics analysis tools framework at EMBL-EBI. *Nucleic Acids Res* **38**, W695 (Jul, 2010).

154. R. S. Curwen, P. D. Ashton, D. A. Johnston, R. A. Wilson, The Schistosoma mansoni soluble proteome: a comparison across four life-cycle stages. *Mol Biochem Parasitol* **138**, 57 (Nov, 2004).

155. B. W. van Balkom *et al.*, Mass spectrometric analysis of the Schistosoma mansoni tegumental sub-proteome. *J Proteome Res* **4**, 958 (May-Jun, 2005).

156. S. Braschi, R. A. Wilson, Proteins exposed at the adult schistosome surface revealed by biotinylation. *Mol Cell Proteomics* **5**, 347 (Feb, 2006).

157. J. Mulvenna *et al.*, Exposed proteins of the Schistosoma japonicum tegument. *Int J Parasitol* **40**, 543 (Apr, 2010).

158. S. Bennuru *et al.*, Brugia malayi excreted/secreted proteins at the host/parasite interface: stage- and gender-specific proteomic profiling. *PLoS Negl Trop Dis* **3**, e410 (2009).

159. Y. Moreno, T. G. Geary, Stage- and gender-specific proteomic analysis of Brugia malayi excretory-secretory products. *PLoS Negl Trop Dis* **2**, e326 (2008).

160. R. Perez-Sanchez, A. Ramajo-Hernandez, V. Ramajo-Martin, A. Oleaga, Proteomic analysis of the tegument and excretory-secretory products of adult Schistosoma bovis worms. *Proteomics* **6 Suppl 1**, S226 (Apr, 2006).

161. F. Liu *et al.*, Excretory/secretory proteome of the adult developmental stage of human blood fluke, Schistosoma japonicum. *Mol Cell Proteomics* **8**, 1236 (Jun, 2009).

162. The Schistosoma japonicum genome reveals features of host-parasite interplay. *Nature* **460**, 345 (Jul 16, 2009).

163. P. J. Brindley, M. Mitreva, E. Ghedin, S. Lustigman, Helminth genomics: The implications for human health. *PLoS Negl Trop Dis* **3**, e538 (2009).

164. S. R. Reynolds, C. E. Dahl, D. A. Harn, T and B epitope determination and analysis of multiple antigenic peptides for the Schistosoma mansoni experimental vaccine triose-phosphate isomerase. *J Immunol* **152**, 193 (Jan 1, 1994).

165. L. Dupre *et al.*, Immunostimulatory effect of IL-18-encoding plasmid in DNA vaccination against murine Schistosoma mansoni infection. *Vaccine* **19**, 1373 (Jan 8, 2001).

166. M. Tendler *et al.*, A Schistosoma mansoni fatty acid-binding protein, Sm14, is the potential basis of a dual-purpose anti-helminth vaccine. *Proc Natl Acad Sci U S A* **93**, 269 (Jan 9, 1996).

167. E. J. Nascimento *et al.*, Assessment of a DNA vaccine encoding an anchored-glycosylphosphatidylinositol tegumental antigen complexed to protamine sulphate on immunoprotection against murine schistosomiasis. *Mem Inst Oswaldo Cruz* **102**, 21 (Feb, 2007).

168. P. Francis, Q. Bickle, Cloning of a 21.7-kDa vaccine-dominant antigen gene of Schistosoma mansoni reveals an EF hand-like motif. *Mol Biochem Parasitol* **50**, 215 (Feb, 1992).

169. G. Ahmad *et al.*, Prime-boost and recombinant protein vaccination strategies using Sm-p80 protects against Schistosoma mansoni infection in the mouse model to levels previously attainable only by the irradiated cercarial vaccine. *Parasitol Res* **105**, 1767 (Nov, 2009).

170. K. A. Shalaby *et al.*, Protection against Schistosoma mansoni utilizing DNA vaccination with genes encoding Cu/Zn cytosolic superoxide dismutase, signal peptide-containing superoxide dismutase and glutathione peroxidase enzymes. *Vaccine* **22**, 130 (Dec 8, 2003).

171. F. C. Cardoso *et al.*, Schistosoma mansoni tegument protein Sm29 is able to induce a Th1-type of immune response and protection against parasite infection. *PLoS Negl Trop Dis* **2**, e308 (2008).

172. W. Zhang, G. Ahmad, W. Torben, A. A. Siddiqui, Sm-p80-based DNA vaccine made in a human use approved vector VR1020 protects against challenge infection with Schistosoma mansoni in mouse. *Parasite Immunol* **32**, 252 (Apr, 2010).

173. J. P. Hewitson, J. R. Grainger, R. M. Maizels, Helminth immunoregulation: the role of parasite secreted proteins in modulating host immunity. *Mol Biochem Parasitol* **167**, 1 (Sep, 2009).

174. S. Naresha, A. Suryawanshi, M. Agarwal, B. P. Singh, P. Joshi, Mapping the complement C1q binding site in Haemonchus contortus calreticulin. *Mol Biochem Parasitol* **166**, 42 (Jul, 2009).

175. J. Rzepecka *et al.*, Calreticulin from the intestinal nematode Heligmosomoides polygyrus is a Th2-skewing protein and interacts with murine scavenger receptor-A. *Mol Immunol* **46**, 1109 (Mar, 2009).

176. G. Kasper *et al.*, A calreticulin-like molecule from the human hookworm Necator americanus interacts with C1q and the cytoplasmic signalling domains of some integrins. *Parasite Immunol* **23**, 141 (Mar, 2001).

177. X. Zang, M. Yazdanbakhsh, H. Jiang, M. R. Kanost, R. M. Maizels, A novel serpin expressed by blood-borne microfilariae of the parasitic nematode Brugia malayi inhibits human neutrophil serine proteinases. *Blood* **94**, 1418 (Aug 15, 1999).

178. P. Smith *et al.*, Schistosoma mansoni worms induce anergy of T cells via selective up-regulation of programmed death ligand 1 on macrophages. *J Immunol* **173**, 1240 (Jul 15, 2004).

179. J. P. Hewitson *et al.*, Proteomic analysis of secretory products from the model gastrointestinal nematode Heligmosomoides polygyrus reveals dominance of venom allergen-like (VAL) proteins. *J Proteomics* **74**, 1573 (Aug 24, 2011).

180. M. Berriman *et al.*, The genome of the blood fluke Schistosoma mansoni. *Nature* **460**, 352 (Jul 16, 2009).

181. S. McGonigle, J. P. Dalton, E. R. James, Peroxidoxins: a new antioxidant family. *Parasitol Today* **14**, 139 (Apr, 1998).

182. M. W. Robinson, A. T. Hutchinson, J. P. Dalton, S. Donnelly, Peroxiredoxin: a central player in immune modulation. *Parasite Immunol* **32**, 305 (May, 2010).

183. Z. A. Wood, L. B. Poole, P. A. Karplus, Peroxiredoxin evolution and the regulation of hydrogen peroxide signaling. *Science* **300**, 650 (Apr 25, 2003).

184. Z. A. Wood, E. Schroder, J. Robin Harris, L. B. Poole, Structure, mechanism and regulation of peroxiredoxins. *Trends Biochem Sci* **28**, 32 (Jan, 2003).

185. M. W. Robinson, R. Menon, S. M. Donnelly, J. P. Dalton, S. Ranganathan, An integrated transcriptomics and proteomics analysis of the secretome of the helminth pathogen Fasciola hepatica: proteins associated with invasion and infection of the mammalian host. *Mol Cell Proteomics* **8**, 1891 (Aug, 2009).

186. S. Suttiprapa *et al.*, Characterization of the antioxidant enzyme, thioredoxin peroxidase, from the carcinogenic human liver fluke, Opisthorchis viverrini. *Mol Biochem Parasitol* **160**, 116 (Aug, 2008).

187. R. Chandrashekar *et al.*, Removal of hydrogen peroxide by a 1-cysteine peroxiredoxin enzyme of the filarial parasite Dirofilaria immitis. *Parasitol Res* **86**, 200 (Mar, 2000).

188. M. A. Kwatia, D. J. Botkin, D. L. Williams, Molecular and enzymatic characterization of Schistosoma mansoni thioredoxin peroxidase. *J Parasitol* **86**, 908 (Oct, 2000).

189. A. A. Sayed, S. K. Cook, D. L. Williams, Redox balance mechanisms in Schistosoma mansoni rely on peroxiredoxins and albumin and implicate peroxiredoxins as novel drug targets. *J Biol Chem* **281**, 17001 (Jun 23, 2006).

190. A. A. Sayed, D. L. Williams, Biochemical characterization of 2-Cys peroxiredoxins from Schistosoma mansoni. *J Biol Chem* **279**, 26159 (Jun 18, 2004).

191. M. Sekiya *et al.*, Biochemical characterisation of the recombinant peroxiredoxin (FhePrx) of the liver fluke, Fasciola hepatica. *FEBS Lett* **580**, 5016 (Sep 18, 2006).

192. H. M. Alger, A. A. Sayed, M. J. Stadecker, D. L. Williams, Molecular and enzymatic characterisation of Schistosoma mansoni thioredoxin. *Int J Parasitol* **32**, 1285 (Sep, 2002).

193. B. Beutler, E. T. Rietschel, Innate immune sensing and its roots: the story of endotoxin. *Nat Rev Immunol* **3**, 169 (Feb, 2003).

194. A. R. Marks, Cellular functions of immunophilins. *Physiol Rev* **76**, 631 (Jul, 1996).

195. A. Bell, P. Monaghan, A. P. Page, Peptidyl-prolyl cis-trans isomerases (immunophilins) and their roles in parasite biochemistry, host-parasite interaction and antiparasitic drug action. *Int J Parasitol* **36**, 261 (Mar, 2006).

196. S. L. Schreiber, G. R. Crabtree, The mechanism of action of cyclosporin A and FK506. *Immunol Today* **13**, 136 (Apr, 1992).

197. L. J. Gourlay *et al.*, The three-dimensional structure of two redox states of cyclophilin A from Schistosoma mansoni. Evidence for redox regulation of peptidyl-prolyl cis-trans isomerase activity. *J Biol Chem* **282**, 24851 (Aug 24, 2007).

198. A. L. Colebrook, D. D. Jenkins, M. W. Lightowlers, Anti-parasitic effect of cyclosporin A on Echinococcus granulosus and characterization of the associated cyclophilin protein. *Parasitology* **125**, 485 (Nov, 2002).

199. A. Marin-Menendez, A. Bell, Overexpression, purification and assessment of cyclosporin binding of a family of cyclophilins and cyclophilin-like proteins of the human malarial parasite Plasmodium falciparum. *Protein Expr Purif* **78**, 225 (Aug, 2011).

200. W. L. Yau *et al.*, Cyclosporin A treatment of Leishmania donovani reveals stage-specific functions of cyclophilins in parasite proliferation and viability. *PLoS Negl Trop Dis* **4**, e729 (2010).

201. R. Carraro, J. Bua, A. Ruiz, M. Paulino, Modelling and study of cyclosporin A and related compounds in complexes with a Trypanosoma cruzi cyclophilin. *J Mol Graph Model* **26**, 48 (Jul, 2007).

202. J. Bua *et al.*, Anti-Trypanosoma cruzi effects of cyclosporin A derivatives: possible role of a P-glycoprotein and parasite cyclophilins. *Parasitology* **135**, 217 (Feb, 2008).

203. S. Azouzi, S. Morandat, K. El Kirat, The potent antimalarial peptide cyclosporin A induces the aggregation and permeabilization of sphingomyelin-rich membranes. *Langmuir* **27**, 9465 (Aug 2, 2011).

204. J. Aliberti *et al.*, Molecular mimicry of a CCR5 binding-domain in the microbial activation of dendritic cells. *Nat Immunol* **4**, 485 (May, 2003).

205. G. S. Yap, A. Sher, Cell-mediated immunity to Toxoplasma gondii: initiation, regulation and effector function. *Immunobiology* **201**, 240 (Dec, 1999).

206. F. Yarovinsky *et al.*, Structural determinants of the anti-HIV activity of a CCR5 antagonist derived from Toxoplasma gondii. *J Biol Chem* **279**, 53635 (Dec 17, 2004).

207. D. I. Pritchard, D. G. Blount, P. Schmid-Grendelmeier, S. J. Till, Parasitic worm therapy for allergy: Is this incongruous or avant-garde medicine? *Clin Exp Allergy*, (Dec 14, 2011).

208. N. E. Mangan, N. van Rooijen, A. N. McKenzie, P. G. Fallon, Helminth-modified pulmonary immune response protects mice from allergen-induced airway hyperresponsiveness. *J Immunol* **176**, 138 (Jan 1, 2006).

209. K. Terpe, Overview of bacterial expression systems for heterologous protein production: from molecular and biochemical fundamentals to commercial systems. *Appl Microbiol Biotechnol* **72**, 211 (Sep, 2006).

210. S. Macauley-Patrick, M. L. Fazenda, B. McNeil, L. M. Harvey, Heterologous protein production using the Pichia pastoris expression system. *Yeast* **22**, 249 (Mar, 2005).

211. R. B. Hitchman, R. D. Possee, L. A. King, Baculovirus expression systems for recombinant protein production in insect cells. *Recent Pat Biotechnol* **3**, 46 (2009).

212. L. Baldi, D. L. Hacker, M. Adam, F. M. Wurm, Recombinant protein production by large-scale transient gene expression in mammalian cells: state of the art and future perspectives. *Biotechnol Lett* **29**, 677 (May, 2007).

213. H. M. Ibrahim, H. Bannai, X. Xuan, Y. Nishikawa, Toxoplasma gondii cyclophilin 18-mediated production of nitric oxide induces Bradyzoite conversion in a CCR5-dependent manner. *Infect Immun* **77**, 3686 (Sep, 2009).

214. M. A. Andrade *et al.*, Echinococcus multilocularis laminated-layer components and the E14t 14-3-3 recombinant protein decrease NO production by activated rat macrophages in vitro. *Nitric Oxide* **10**, 150 (May, 2004).

215. A. G. Pockley, M. Muthana, S. K. Calderwood, The dual immunoregulatory roles of stress proteins. *Trends Biochem Sci* **33**, 71 (Feb, 2008).

216. U. Wendling *et al.*, A conserved mycobacterial heat shock protein (hsp) 70 sequence prevents adjuvant arthritis upon nasal administration and induces IL-10-producing T cells that cross-react with the mammalian self-hsp70 homologue. *J Immunol* **164**, 2711 (Mar 1, 2000).

List of Abbreviations

2D	Two-dimensional
AAMΦs	Alternatively activated macrophages
ADCC	Antibody dependent cellular cytotoxicity
APC	Antigen presenting cells
AW	Adult worm
BCA	Bicinchoninc acid
BLAST	Basic Local Alignment Search Tool
Breg	B regulatory cell
CD	Cercarial Dermatitis
cDNA	Complementary deoxyribonucleic acid
CV	Column volume
CyP	Cyclophilin
DNA	Deoxyribonucleic acid
DPBS	Dulbecco's Phosphate-Buffered Saline
DSS	Dextran sodim sulphate
DTT	Dithiothreitol
EAE	Experimental autoimmune encephalomyelitis
EDTA	Ethylenediaminetetraacetic acid
ELISA	Enzyme-linked immunosorbent
ES-62	*Acanthocheilonema viteae* excretory-secretory 62 kDa protein
ETOH	Ethanol
EU/mg	Endotoxin unit/miligram
Fcr	Fc receptor
FCS	Fetal calf serum
GC	Guanine Cytosine
GO	Gene ontology
GST	Glutathione S-transferase
HBM	Honey Bee Mellitin
HMGB1	High-Mobility Group Box 1

HpCrt	*Heligmosomoides polygyrus* Calreticulin
HRP	Horseradish peroxidase
I	Induced *E. coli* expression culture
IAM	Alkylated with iodoacetamide
IBD	Inflammatory bowel disease
IEF	First-dimension isoelectric focusing
IFN-γ	Interferon-gamma
Ig	Immunoglobulin
IL	Interleukin
IL- 4Rα	Interleukin-4 receptor α-chain
IPG	Immobilized pH gradient
IPTG	Isopropyl b-D-1-thiogalactopyranoside
IrV5	Myosin heavy chain
kDa	Kilodalton
LNFPIII	Lacto-N-fucopentaose III
LPS	Lipopolysaccharide
Lyso-PS	Lysophosphatidylserine
MCS	Multiple cloning site
MIF	Macrophage migration inhibition factor
MS	Mass spectrometry
MWCO	Molecular weight cut off
NI	Non-induce *E. coli* culture
Ni-NTA	Nickel-nitrilotriacetic acid
NOD	Non-obese diabetic
OVA	Ovalbumin
P	Pellet
P0	Passage 0
P1	Passage 1
P2	Passage 2
P3	Passage 3
PBS	Phosphate-buffered saline

PC	Phosphorylcholine
PCR	Polymerase chain reaction
PQZ	Praziquantel
Prx	Peroxiredoxin
PVDF	Polyvinylidene fluoride
RA	Radiation-attenuated
rbacHpCrt	Baculovirus-insect cell expressed recombinant *H. polygyrus* Calreticulin
rbacSmCrt	Baculovirus-insect cell expressed recombinant *S. mansoni* Calreticulin
rbacSmCyp1	Baculovirus-insect cell expressed recombinant *S. mansoni* Cyclophilin 1
rbacSmCyp2	Baculovirus-insect cell expressed recombinant *S. mansoni* Cyclophilin B
rbacSmPrx1	Baculovirus-insect cell expressed recombinant *S. mansoni* Peroxiredoxin 1
rbacSmTrx1	Baculovirus-insect cell expressed recombinant *S. mansoni* Thioredoxin
r-GST-SmCyp1	*E. coli* expressed recombinant GST-tagged *S. mansoni* Cyclophilin 1
r-GST-SmCyp2	*E. coli* expressed recombinant GST-tagged *S. mansoni* Cyclophilin B
r-his-SmCyp1	*E. coli* expressed recombinant polyhistidine-tagged *S. mansoni* Cyclophilin 1
r-his-SmCyp2	*E. coli* expressed recombinant polyhistidine-tagged *S. mansoni* Cyclophilin B
RNA	Ribonucleic acid
ROS	Reactive oxygen species
rSmPrx1	*E. coli* expressed recombinant *S. mansoni* Peroxiredoxin 1
rSmTrx1	*E. coli* expressed recombinant *S. mansoni* Thioredoxin
S	Supernatant
SDS-PAGE	Sodium dodecyl sulfate polyacrylamide gel electophoresis
SecP	Secretome P prediction
Sh28-GST	*S. haematobium* 28 kDa Glutathione-S-transferase
Sm14	*S. mansoni* 14 kDa
Sm16	*S. mansoni* 16.8 kDa protein
Sm23	*S. mansoni* 23 kDa
Sm28GST	*S. mansoni* 28 kDa Glutathione-S-transferase
Sm97	*S. mansoni* 97 kDa

smCKBP	*S. mansoni* Chemokine binding protein
SmCrt	*S. mansoni* Calreticulin
SmCyp1	*S. mansoni* Cyclophilin 1
SmCyp2	*S. mansoni* Cyclophilin B
Sm-p80	DNA vaccine encoding the large subunit of *S. mansoni* Calpain
SmPrx1	*S. mansoni* Peroxiredoxin 1
SmTrx1	*S. mansoni* Thioredoxin
Sm-TSP-2	Second extracellular domain of *S. mansoni* Tetraspanin
SOC	Super Optimal Catabolite
Spp.	Species
TCTP	Translationally Controlled Tumor Protein
TGF-β	Transforming growth factor-beta
Th1	T helper 1
Th2	T helper 2
TNF-α	Tumor necrosis factor-alpha
TPI	Triose Phosphate Isomerase
UV	Ultravioleta
WES	Worm excretory-secretory
WHO	World Health Organization

Appendix 1

1 - 10X Lepple water

13.90 g Calcium chloride ($CaCl_2$)

30.70 g Magnesium sulfate ($MgSO_4.7H_2O$)

1.07 g Potassium sulfate (K_2SO_4)

10.50 g Sodium hydrogen carbonate ($NaHCO_3$)

1.2 mL of a solution containing 2.5 g of Ferric chloride ($FeCl_2.6H_2O$)

dH_2O to a final volume of 5L

2 - Double-strength saline

1.8 g NaCl

dH_2O up to 100 mL

3 - Lugol's Iodine

1.0 g Iodine

2.0 g Potassium iodate (KIO_3)

dH_2O to a final volume of 100 mL

4 - Perfusion media

13.65 g of minimum essential medium with Earle's salts

2.2 g of sodium bicarbonate $NaHCO_3$

15 g of tri-sodium citrate

dH_2O to a final volume of 1L

5 - Washing media

13.65 g of minimum essential medium with Earle's salts

2.2 g of sodium bicarbonate $NaHCO_3$

dH_2O to a final volume of 1L

6 - Phosphate buffered saline

8 g NaCl

0.2 g KCl

1.44 g Na2HPO4

0.24 g KH2PO4

dH_2O to a final volume of 1L

Adjust pH to 7.4 using HCl

7 - Incubation media

RPMI-1640 Medium (Sigma)

1% v/v 200 mM L-glutamine

1% v/v Penicilin-Streptomycin - 10,000 units penicillin and 10 mg/mL streptomycin

0.01% v/v 50mg/mL Gentamicin

8 - Nutrient media

RPMI-1640 Medium (Sigma)

10% v/v Fetal Calf Serum (FCS)

1% v/v 200 mM L-glutamine

1% v/v Penicilin-Streptomycin - 10,000 units penicillin and 10 mg/mL streptomycin

0.01% v/v 50mg/mL Gentamicin

9 - TE Buffer

10 mM Tris-HCl, pH 8.0,

1 mM EDTA

10 - 10 X Tris-borate EDTA (TBE) buffer

107.8 g Tris-base

50 g Boric acid

7.44 g EDTA

Adjust to pH 8.3

Dilute in dH_2O 1:10 prior to use.

11 - Super Optimal Catobolite (SOC) repression medium

2% w/v tryptone

0.5% w/v yeast extract

10 mM sodium chloride

2.5 mM potassium chloride

10 mM magnesium chloride

10 mM magnesium sulfate

20 mM glucose

12 - Luria Broth (LB) medium

1% w/v g/L Tryptone

0.5% w/v Yeast extract

1% w/v NaCl

13 - Luria Broth (LB) agar plates

1% w/v g/L Tryptone

0.5% w/v Yeast extract

1% w/v NaCl

1.5 % w/v agar

14 - Nickel-affinity chromatography binding buffers

20 mM Sodium Phosphate

500 mM NaCl

5 mM imidazole

pH 7.2

15 - Nickel-affinity chromatography washing buffers

20 mM Sodium Phosphate

500 mM NaCl

20 mM imidazole

pH 7.2

16 - Nickel-affinity chromatography elution buffers

20 mM Sodium Phosphate

500 mM NaCl

500 mM imidazole

pH 7.2

17 – Anion exchange chromatography binding buffer

50 mM MES (2-(N-Morpholino)ethanesulfonic acid)

pH 6.0

18 – Anion exchange chromatography washing buffer

50 mM MES

50 mM NaCl

pH 6.0

19 - Anion-exchange chromatography elution buffer

50 mM MES

3 M NaCl

pH 6.0

20 - 4% Stacking gel SDS-PAGE monomer solution - 8 cm (W) x 7.3 cm (H)

1.22 mL dH2O

260 µL 30% Degassed Acrylamide/Bis

0.5 mL 0.5 M Tris-HCl, pH 6.8

20 µL 10% w/v Sodium dodecyl sulfate (SDS; $C_{12}H_{25}SO_4Na$)

10 µL 10% w/v Ammonium persulfate (APS; $(NH_4)_2S_2O_8$)

2 µL Tetramethylethylenediamine (TEMED; $(CH_3)_2NCH_2CH_2N(CH_3)_2$)

21 - 12% Resolving gel SDS-PAGE monomer solution - 8 cm (W) x 7.3 cm (H)

1.36 mL dH2O

1.6 mL 30% Degassed Acrylamide/Bis

1.0 mL 1.5 M Tris-HCl, pH 8.8

40 µL 10% w/v Sodium dodecyl sulfate (SDS; $C_{12}H_{25}SO_4Na$)

20 µL 10% w/v Ammonium persulfate (APS; $(NH_4)_2S_2O_8$)

2 µL Tetramethylethylenediamine (TEMED; $(CH_3)_2NCH_2CH_2N(CH_3)_2$)

22 - 15% Resolving gel SDS-PAGE monomer solution - 8 cm (W) x 7.3 cm (H)

0.96 mL dH2O

2.0 mL 30% Degassed Acrylamide/Bis

1.0 mL 1.5 M Tris-HCl, pH 8.8

40 µL 10% w/v Sodium dodecyl sulfate (SDS; $C_{12}H_{25}SO_4Na$)

20 µL 10% w/v Ammonium persulfate (APS; $(NH_4)_2S_2O_8$)

2 µL Tetramethylethylenediamine (TEMED; $(CH_3)_2NCH_2CH_2N(CH_3)_2$)

23 - 2X Reducing sample buffer

3.55 mL dH_2O

1.25 mL 0.5 M Tris-HCl, pH 6.8

2.5 mL Glycerol

2.0 mL 10% w/v Sodium dodecyl sulfate (SDS; $C_{12}H_{25}SO_4Na$)

0.2 mL 0.5% w/v Bromophenol blue $C_{19}H_{10}Br_4O_5S$

500 µL β-Mercaptoethanol (**β-met;** C_2H_6OS)

Store in small aliquots at -20°C protected from light

24 - 2X Non-reducing sample buffer

4.05 mL dH_2O

1.25 mL 0.5 M Tris-HCl, pH 6.8

2.5 mL Glycerol

2.0 mL 10% w/v Sodium dodecyl sulfate (SDS; $C_{12}H_{25}SO_4Na$)

0.2 mL 0.5% w/v Bromophenol blue $C_{19}H_{10}Br_4O_5S$

25 - 10 X Running buffer

30.3 g Tris base

144.0 g Glycine

10.0 g SDS

dH_2O up to 1L

26 - Rehydration buffer

12 g Urea

0.5 g 3-[(3-cholamidopropyl)dimethylammonio]-1 propanesulfonate (CHAPS;

$C_{32}H_{58}N_2O_7S$)

500 µL IPG buffer ph 3-10 NL (GE Healthcare Life Sciences)

100 µL 0.5% w/v Bromophenol blue

dH2O up to 25 mL

Add 0.007 g of DTT prior to use

27 - Equilibration buffer

660 µL 1.5 M Tris-HCl, pH 8.8

7.3 g Urea

6.9 mL 87% v/v Glycerol

0.4 g SDS

80 µL 0.5% Bromophenol Blue

dH2O up to 20 mL

Add 0.2 g of DTT or 0.5 g IAM prior to use

28 - Agarose sealing solution

100 mL 1X running buffer

0.5 g Agarose

400 µL 0.5% Bromophenol Blue

29 - 12% Resolving gel SDS-PAGE monomer solution - 138 (W) x 130 (H) mm

3.4 mL dH2O

4.0 mL 30% Degassed Acrylamide/Bis

2.5 mL 1.5 M Tris-HCl, pH 8.8

0.1 µL 10% w/v Sodium dodecyl sulfate (SDS; $C_{12}H_{25}SO_4Na$)

50 µL 10% w/v Ammonium persulfate (APS; $(NH_4)_2S_2O_8$)

5 µL Tetramethylethylenediamine (TEMED; $(CH_3)_2NCH_2CH_2N(CH_3)_2$)

30 - Coomassie solution

0.1% w/v Coomassie R250

40% v/v Methanol

10% v/v Acetic acid

Solution must be filtered in a paper filter to remove particulates before use.

31 - Destain solution

20% v/v Methanol

10% v/v Acetic acid

32 - Colloidal Coomassie fixing solution

1.3% v/v o-phosphoric acid (85%)

20% v/v methanol

33 - Colloidal Coomassie staining solution A

2% v/v o-phosphoric acid (85%)

10% w/v ammonium sulfate

This solution must be used fresh.

34 - Colloidal Coomassie staining solution B

5% w/v coomassie brilliant blue G-250

This solution must be used fresh.

35 - Colloidal Coomassie final staining solution

400 mL staining solution A

10 mL staining solution B

100 mL methanol

This solution must be used fresh.

36 - Colloidal Coomassie neutralization Solution

1.2 % w/v Tris-base ($(HOCH_2)_3CNH_2$)

Use o-phosphoric acid (85%) to titrate to pH 6.5

37 - Colloidal Coomassie washing solution

25% v/v methanol

38 – Colloidal Coomassie stabilizing solution

20% w/v amonium sulfate ($(NH_4)_2SO_4$)

39 – Silver staining fixative solution

50% v/v methanol, 5% v/v acetic acid

40 - Silver staining wash solution

50% v/v methanol

41 - Silver staining sensitizer solution

0.02% w/v sodium thiosulfate

42 - Silver staining silver nitrate solution

0.1% w/v silver nitrate

0.08% v/v formalin 37%

43 - Silver staining developer solution

2% w/v sodium carbonate

0.04% v/v formalin 37%

44 - Silver staining stop solution

5% v/v acetic acid

45 – SDS-PAGE storage solution

10% v/v glycerol

46 – Western blot transfer buffer

25 mM tris-base

192 mM glycine

20% v/v methanol

pH 8.3

Do not add acid or base to adjust pH.

47 - Western blot blocking solution A

5% w/v non-fat dry milk in PBS

48 - Western blot blocking solution B

1% w/v bovine serum albumin in PBS

49 - Western blot washing solution

0.05% Tween-20 in PBS

50 - Western blot incubation solution

1% w/v bovine serum albumin

0.05% Tween-20 in PBS

Appendix 2 - Similarity analysis of *S. mansoni* adult male worm excretory-secretory proteins and *S. japonicum* and *S. haematobium* proteins

S. mansoni male adult worm excretory-secretory proteins			*S. japonicum*				*S. haematobium*			
	GeneDB ID	Protein description	GenBank ID	Score	E value	Identity (%)	GenBank ID	Score	E value	Identity (%)
1	Smp_000100	Filamin	AAF13300.1	191	2e-55	50.5	-	-	-	-
2	Smp_000660	Ornithine--oxo-acid transaminase	CAX70598.1	835	0	92.52	Q8I8A2.2	23.9	0.36	52.63
3	Smp_001360	Thymidylate kinase	CAX75696.1	399	3e-144	84.82	BAF62290.1	19.2	6.5	23.68
4	Smp_003230	Sh3 domain grb2-like protein B1 (endophilin B1)	CAX70480.1	341	1e-120	68.15	Q26503.1	20	4.3	37.04
5	Smp_003990	Triosephosphate isomerase, putative	AAP06170.1	491	7e-180	92.86	BAF62292.1	499	0	95.24
6	Smp_004350	Ubiquitin-conjugating enzyme E2 l, putative	AAW27854.1	312	4e-112	98.08	YP_626523.1	18.9	5.1	15.38
7	Smp_004470.1	Peroxiredoxin, Prx3	AAW25436.1	407	2e-147	88.18	AAR84358.1	21.9	2.3	40
8	Smp_004780.1	Immunophilin, putative	AAW27121.1	697	0	78.25	-	-	-	-
9	Smp_005350	Calcium-binding protein, putative	AAP06154.1	321	2e-110	100	Q8I8A2.2	22.7	1	32
10	Smp_006390	Cystatin B, putative	CAX73577.1	169	2e-57	77.23	BAF62289.1	18.1	4.4	22.22
11	Smp_007270.1	Alpha-actinin, putative	CAX82586.1	352	4e-127	93.75	-	-	-	-
12	Smp_008070	Thioredoxin, Trx1	AAD52699.1	144	4e-47	65.38	AAW66672.1	24.3	0.05	41.67
13	Smp_008110	WD40-repeat containing protein	AAX26533.2	31.2	0.31	24.58	YP_626527.1	22.3	2.6	47.37

Table A1: **Similarity analysis of *S. mansoni* adult male worm excretory-secretory proteins and *S. japonicum* and *S. haematobium* proteins**. *S. mansoni* WES proteins were subjected to similarity analysis using BLAST. Score – BLAST bit score; E-value - Expect value; ID – identification number at GeneDB or GenBank databases; (-) – No significant similarity detected.

S. mansoni male adult worm excretory-secretory proteins			*S. japonicum*				*S. haematobium*			
	GeneDB ID	Protein description	GenBank ID	Score	E value	Identity (%)	GenBank ID	Score	E value	Identity (%)
14	Smp_008660.1	Gelsolin, putative	AAW26119.1	617	0	83.1	YP_626531.1	21.6	2.2	24.79
15	Smp_009760	14-3-3 protein, putative	ACE06842.1	348	5e-123	69.05	-	-	-	-
16	Smp_009780.2	14-3-3 protein, putative	ACE06842.1	313	8e-109	67.23	-	-	-	-
17	Smp_011830	Hypothetical protein / C4Q068	AAW26653.1	183	4e-61	85.58	ABO52901.1	18.9	3.2	31.91
18	Smp_014010	Adenylyl cyclase-associated protein, putative	CAX69899.1	748	0	75.83	ADE41027.1	24.6	0.28	32.26
19	Smp_017730	200-kDa GPI-anchored surface glycoprotein	AAX26034.2	345	6e-110	72.44	ACZ66263.1	24.6	1.1	24.1
20	Smp_018240.3	Cell division control protein 48 aaa family protein, putative	AAW27581.1	1514	0	92.28	ABO52903.1	25	0.48	26.83
21	Smp_018890	Phosphoglycerate kinase	AAP06480.1	471	2e-169	94.24	-	-	-	-
22	Smp_019050.2	Hypothetical protein / C4Q286	CAX73085.1	155	4e-51	80.37	-	-	-	-
23	Smp_019640.1	Calcyphosine/tpp, putative	AAW27463.1	367	3e-132	83.17	BAF62290.1	30.8	0.001	25.81
24	Smp_020920.1	DNAj homolog subfamily B member 4, putative	AAW25539.1	603	0	91.94	AAD00565.1	26.2	0.053	45.45
25	Smp_021800	Prefoldin subunit 3-related	AAW27184.1	347	4e-125	90.48	BAF62291.1	21.9	0.8	39.39
26	Smp_022340	Pdz and lim domain protein, putative	AAW27396.1	407	8e-146	84.26	AAZ57313.1	21.2	2.6	28.89

Table A1 (continued)

S. mansoni male adult worm excretory-secretory proteins			*S. japonicum*				*S. haematobium*			
	GeneDB ID	Protein description	GenBank ID	Score	E value	Identity (%)	GenBank ID	Score	E value	Identity (%)
27	Smp_024110	Phosphopyruvate hydratase	P33676.1	808	0	87.79	-	-	-	-
28	Smp_028670.1	Carbonic anhydrase II (carbonate dehydratase II), putative	CAX73485.1	508	0	93	AAW66672.1	25	0.11	26.09
29	Smp_030000	Leucine aminopeptidase (M17 family)	CAX69903.1	966	0	88.85	AAO62355.1	21.2	4.1	19.1
30	Smp_030370	Calreticulin autoantigen homolog precursor, putative	AAC00515.1	593	0	77.27	BAF62290.1	20	7.4	53.85
31	Smp_030730	Tubulin beta chain, putative	CAX71985.1	929	0	99.32	AAR84358.1	20	9.9	33.33
32	Smp_031770.4	Tropomyosin, putative	CAX76350.1	526	0	98.94	Q26503.1	320	4e-113	65.02
33	Smp_032580.2	Subfamily T1A non-peptidase homologue (T01 family)	AAP06025.1	500	0	97.15	ADE41018.1	20.4	2.5	25
34	Smp_032950	Calmodulin (CaM), putative	CAX79767.1	107	8e-34	76.47	BAF62289.1	24.3	0.018	27.94
35	Smp_033540	Carbonyl reductase, putative	CAX77260.1	483	1e-175	85.56	Q26503.1	20.4	3.6	25
36	Smp_034490	Proteasome catalytic subunit 1 (T01 family)	CAX69953.1	414	4e-150	89.78	ABO52901.1	20.4	2.9	34.29
37	Smp_034840.2	14-3-3 epsilon	AAW26747.1	400	9e-144	81.51	Q8I8A2.2	20.4	2.2	35
38	Smp_035270.2	Malate dehydrogenase, putative	CAX72207.1	558	0	87.8	YP_626531.1	19.6	8.3	31.82
39	Smp_038950	L-lactate dehydrogenase, putative	CAX70888.1	607	0	87.65	AAW66672.1	21.9	1.5	43.48

Table A1 (continued)

S. mansoni male adult worm excretory-secretory proteins			*S. japonicum*				*S. haematobium*			
	GeneDB ID	Protein description	GenBank ID	Score	E value	Identity (%)	GenBank ID	Score	E value	Identity (%)
40	Smp_040130	Cyclophilin	CAX72371.1	229	7e-79	69.18	ADE41027.1	18.9	5.2	25.86
41	Smp_040790	Cyclophilin B, putative	AAW27862.1	383	2e-138	84.98	-	-	-	-
42	Smp_042160.2	Fructose 1,6-bisphosphate aldolase, putative	AAW25258.1	724	0	96.14	BAF62288.1	20.8	2.5	29.03
43	Smp_042400	Hypothetical protein / C4Q8L5	AAW24701.1	306	5e-109	79.01	AAM43944.1	20	2.4	31.25
44	Smp_043030	Hexokinase	CAX69908.1	842	0	88.22	BAF62288.1	20.4	4.2	28.95
45	Smp_043120	Universal stress protein, putative	CAX70901.1	280	2e-99	80.62	AAR84357.1	20.4	1.8	29.31
46	Smp_044010.2	Tropomyosin, putative	ACE06925.1	531	0	98.24	Q26503.1	534	0	98.59
47	Smp_046600	Actin-1, putative	CAX69775.1	776	0	98.14	AAO62355.1	20.8	4.5	18.18
48	Smp_046690	Ubiquitin (ribosomal protein L40), putative	CAX72429.1	603	0	99.67	-	-	-	-
49	Smp_047370	Malate dehydrogenase, putative	CAX74903.1	662	0	93.84	AAR84357.1	21.6	1.9	26.83
50	Smp_047650	Ferritin, putative	CAX70640.1	315	7e-113	87.21	-	-	-	-
51	Smp_049250	Heat shock protein, putative	CAX78232.1	469	1e-167	62.73	AAX59989.1	20.4	5.3	72.73
52	Smp_049270	Heat shock protein, putative	AAW24545.1	829	0	90.36	ABO52903.1	23.5	0.86	37.5

Table A1 (continued)

S. mansoni male adult worm excretory-secretory proteins			*S. japonicum*				*S. haematobium*			
	GeneDB ID	Protein description	GenBank ID	Score	E value	Identity (%)	GenBank ID	Score	E value	Identity (%)
53	Smp_049550	Heat shock protein 70 (hsp70), putative	ACE06854.1	1192	0	91.05	BAF62292.1	23.5	1	30.3
54	Smp_050390	Aldehyde dehydrogenase, putative	CAX73522.1	937	0	90.02	BAF62288.1	22.3	1	33.33
55	Smp_053220.1	Aldo-keto reductase, putative	CAX77280.1	547	0	83.87	BAF62290.1	23.5	0.5	32.69
56	Smp_054160	Glutathione S-transferase 28 kDa (GST 28) (GST class-mu), putative	CAX72408.1	340	3e-121	77.25	P30114.1	405	4e-149	91.94
57	Smp_054240	Translationally-controlled tumor protein homolog (TCTP) (Histamine-releasing factor), putative	P91800.1	215	2e-73	58.82	Q8I8A2.2	211	1e-74	80.29
58	Smp_056440	Superoxide dismutase [mn], putative	AAW26480.1	416	6e-151	89.81	AAO62355.1	18.9	9.7	44.44
59	Smp_056760	Protein disulfide-isomerase, putative	CAX69780.1	900	0	89.83	AAA29878.1	20.4	6.8	42.11
60	Smp_056970.1	Glyceraldehyde-3-phosphate dehydrogenase (phosphorylating)	CAX80263.1	640	0	90.24	AAO62355.1	20.4	4.4	27.27
61	Smp_059480	Peroxiredoxin, Prx1	CAX71944.1	328	1e-117	83.7	BAF62292.1	21.2	1.1	25.86
62	Smp_059660	Hypothetical protein / C4QDG6	AAP06314.1	379	1e-132	77.93	CAB97520.1	23.5	0.45	32.26
63	Smp_059980	Arginase, putative	CAX70201.1	620	0	80.22	AAO62355.1	20	7.4	25
64	Smp_063120.1	Inosine triphosphate pyrophosphatase (itpase) (inosine triphosphatase), putative	AAX27755.2	330	6e-118	84.78	Q8I8A2.2	25.8	0.028	38.71
65	Smp_063530.1	Apoferritin-2	CAX72682.1	338	5e-121	84.46	ADE40986.1	20	2.8	25.81

Table A1 (continued)

S. mansoni male adult worm excretory-secretory proteins			*S. japonicum*				*S. haematobium*			
	GeneDB ID	Protein description	GenBank ID	Score	E value	Identity (%)	GenBank ID	Score	E value	Identity (%)
66	Smp_064380	Aspartate aminotransferase, putative	CAX69569.1	692	0	81.29	-	-	-	-
67	Smp_064860	Heat shock protein 70 (hsp70)-interacting protein, putative	AAW27834.1	541	0	84.64	2F8F|A	24.3	0.22	36.36
68	Smp_066760.2	Merlin/moesin/ezrin/radixin, putative	CAX82442.1	781	0	70.44	P30114.1	23.5	0.67	26.56
69	Smp_067890	Proteasome subunit alpha 2 (T01 family)	gAAW25457.1	473	2e-173	96.6	ABO52903.1	20.4	2.9	22.5
70	Smp_072900.1	Hsp90 co-chaperone (tebp), putative	CAX79556.1	242	9e-84	80.43	-	-	-	-
71	Smp_078690	Calponin homolog, putative	ACE06952.1	693	0	92.8	BAF62291.1	21.2	2.8	42.86
72	Smp_079010	Camp-dependent protein kinase type II-alpha regulatory subunit, putative	AAW24538.1	683	0	89.92	ACZ66263.1	21.9	1.6	42.86
73	Smp_079770.1	Protein disulfide-isomerase ER-60 precursor (ERP60), putative	ACE06849.1	775	0	76.08	YP_626524.1	23.5	0.4	28.57
74	Smp_081430	Short chain dehydrogenase, putative	AAW27200.1	454	9e-164	90.08	Q26499.1	21.6	1.4	26.32
75	Smp_082030	Family C56 non-peptidase homologue (C56 family)	CAX70856.1	302	3e-107	86.41	AAN78324.1	19.6	2.9	28.79
76	Smp_083870	PwLAP aminopeptidase (M17 family)	AAX27247.2	445	4e-157	90.56	ABO52903.1	20.8	6.7	43.75
77	Smp_086330.2	Calponin-related	AAP06498.1	384	2e-139	95.26	ABO52903.1	19.6	4.1	25
78	Smp_086480	Antigen Sm21.7, putative	CAX72713.1	249	2e-86	64.86	AAW49250.1	176	5e-59	47.8

Table A1 (continued)

S. mansoni male adult worm excretory-secretory proteins			*S. japonicum*				*S. haematobium*			
	GeneDB ID	Protein description	GenBank ID	Score	E value	Identity (%)	GenBank ID	Score	E value	Identity (%)
79	Smp_086530	Tegumental protein Sm 20.8, putative	AAP06272.1	308	7e-110	78.89	BAF62289.1	97.4	2e-28	30.39
80	Smp_090080	Serpin, putative	CAX76359.1	576	0	65.1	AAA19730.3	629	0	76.11
81	Smp_090120.1	Alpha tubulin, putative	XP_002580033.1	944	0	100	AAW66672.1	353	5e-121	40.32
82	Smp_091010	Glyoxalase II (Hydroxyacylglutathione hydrolase), putative	AAP06491.1	487	9e-178	88.51	AAD00565.1	20.8	2.2	21.28
83	Smp_092280	Proteasome subunit alpha 3 (T01 family)	CAX70764.1	509	0	95.67	-	-	-	-
84	Smp_092750	Nucleoside diphosphate kinase	AAO59410.1	288	1e-102	88.59	BAF62289.1	18.9	4.2	42.86
85	Smp_095360.1	Fatty acid binding protein	AAP14675.1	243	1e-85	92.42	BAF62288.1	266	3e-96	99.24
86	Smp_096760	Phosphoglycerate mutase	CAX76329.1	490	2e-179	94	ACB58719.1	20.8	1.6	22.97
87	Smp_102070	GST class-mu, SM26/2 antigen, glutathione S-transferase 26 kDa	P08515.3	359	1e-128	82.57	AAA29892.1	52.8	4e-11	27.36
88	Smp_103320	Nuclear movement protein nudc, putative	AAP06040.1	513	0	82.98	AAR84357.1	20.4	5.3	34.15
89	Smp_105020	Titin, putative	AAW24500.1	1458	0	91.97	ACZ66263.1	23.5	1.1	22.73
90	Smp_106930.2	Heat shock protein 70, putative	AAC00519.1	760	0	61.99	BAF62291.1	25.4	0.3	25
91	Smp_123440.1	Fad oxidoreductase, putative	AAW26635.1	672	0	83.71	YP_626522.1	19.6	4.8	30.77

Table A1 (continued)

S. mansoni male adult worm excretory-secretory proteins			*S. japonicum*				*S. haematobium*			
	GeneDB ID	Protein description	GenBank ID	Score	E value	Identity (%)	GenBank ID	Score	E value	Identity (%)
92	Smp_130110	Proteasome subunit alpha 6 (T01 family)	AAW25684.1	465	1e-162	93.99	-	-	-	-
93	Smp_132670.1	Myosin regulatory light chain, putative	AAW26951.1	344	3e-123	97.14	ABO52901.1	20.4	2.8	31.58
94	Smp_135950	Lethal giant larvae homolog 2, cell polarity protein , inorganic pyrophosphatase, putative	AW25943.1	545	0	87.02	BAF62291.1	23.9	2.7	42.31
95	Smp_136240.6	Vesicle-associated membrane protein (vamp), putative	AAW26025.1	606	0	79.61	AF510342_1	19.6	6.7	18.37
96	Smp_140900.2	Hypothetical protein / C4Q6S1	AAW26313.1	330	2e-117	72.65	AAA19730.3	19.2	5.8	46.67
97	Smp_143470.2	Spectrin beta chain, brain 3 (Spectrin, non-erythroid beta chain 3) (Beta-IV spectrin), putative	AAX26038.2	439	2e-142	93.33	BAF62291.1	32	0.012	22.13
98	Smp_146950	Hypothetical protein / C4Q9Q0	AAX26800.2	427	1e-135	62.64	ACZ66263.1	26.6	1.1	22.29
99	Smp_147470	Leucine-rich transmembrane proteins, putative	AAW25815.1	412	1e-145	86.61	BAF62289.1	20.4	5.2	31.11
100	Smp_150820	Acyl-CoA thioesterase-related	AAW27278.1	227	4e-73	71.14	-	-	-	-
101	Smp_151690	Translation initiation inhibitor, putative	CAX74647.1	195	1e-66	78.76	AAO62355.1	20	1.8	53.33
102	Smp_152710.2	Glutathione-s-transferase omega, putative	CAX74405.1	377	6e-135	75.1	AAZ29530.1	23.5	0.17	33.33
103	Smp_155060.2	Set, putative	CAX72508.1	464	1e-168	97.82	BAF62291.1	20.4	4	21.05
104	Smp_157500	Calpain (C02 family)	BAA74718.1	1339	0	83.91	BAF62290.1	1496	0	94.68

Table A1 (continued)

S. mansoni male adult worm excretory-secretory proteins			*S. japonicum*				*S. haematobium*			
	GeneDB ID	Protein description	GenBank ID	Score	E value	Identity (%)	GenBank ID	Score	E value	Identity (%)
105	Smp_158110.2	Peroxiredoxin, Prx2	BAD90102.1	369	2e-133	89.69	AAR84358.1	18.5	9.1	35.14
106	Smp_161920	Actin, putative	XP_002578518.1	786	0	100	AAS88235.1	19.2	7.9	26.32
107	Smp_163720	Endophilin B1, putative	AAP06059.1	322	4e-113	64.31	AAZ57314.1	30.4	0.002	31.91
108	Smp_176200.2	Superoxide dismutase [Cu-Zn]	CAX76410.1	270	2e-95	85.62	YP_626520.1	23.9	0.093	28.89
109	Smp_179810	Troponin t, invertebrate, putative	AAW25147.1	358	7e-125	92.12	AAZ29530.1	21.6	0.95	27.5
110	Smp_187370	Phosphoglycerate kinase	CAX77845.1	335	1e-119	94.77	-	-	-	-
111	Smp_194770	ATP:guanidino kinase (Smc74), putative	CAX73626.1	1357	0	90.08	ACZ66263.1	26.2	0.22	30.77

Table A1 (continued)

Appendix 3 - Biological process and molecular function gene ontology terms from *S. mansoni* adult male worm excretory-secretory proteins

S. mansoni adult male worm excretory-secretory proteins		Biological Process GO terms		Molecular Function GO terms	
ID	Protein description	Term ID	Term name	Term ID	Term name
1 Smp_000100	Filamin	-	-	GO:0003779	actin binding
2 Smp_000660	Ornithine--oxo-acid transaminase	GO:0008152	metabolic process	GO:0003824	catalytic activity
					transaminase activity
					pyridoxal phosphate binding
3 Smp_001360	Thymidylate kinase	GO:0006233	dTDP biosynthetic process	GO:0004798	thymidylate kinase activity
		GO:0016310	phosphorylation	GO:0005524	ATP binding
				GO:0016301	kinase activity
				GO:0016740	transferase activity
4 Smp_003230	Sh3 domain grb2-like protein B1 (endophilin B1)	-	-	-	-
5 Smp_003990	Triosephosphate isomerase, putative	GO:0008152	metabolic process	GO:0003824	catalytic activity
				GO:0004807	triose-phosphate isomerase activity
				GO:0016853	isomerase activity

Table A3: **Gene ontology terms from *S. mansoni* adult male worm excretory-secretory proteins.** GO terms associated to biological process or molecular function addressed to each protein identified in the *S. mansoni* adult male worm excretome-secretome.

S. mansoni adult male worm excretory-secretory proteins		Biological Process GO terms		Molecular Function GO terms	
ID	Protein description	Term ID	Term name	Term ID	Term name
6 Smp_004350	Ubiquitin-conjugating enzyme E2 l, putative	-	-	GO:0000166 GO:0005524 GO:0016874 GO:0016881	nucleotide binding ATP binding ligase activity acid-amino acid ligase activity
7 Smp_004470.1	Peroxiredoxin, Prx3	GO:0055114	oxidation-reduction process	GO:0004601 GO:0016209 GO:0016491 GO:0051920	peroxidase activity antioxidant activity oxidoreductase activity peroxiredoxin activity
8 Smp_004780.1	Immunophilin, putative	GO:0006457	protein folding	GO:0005488	binding
9 Smp_005350	Calcium-binding protein, putative	GO:0005509	calcium ion binding	-	-
10 Smp_006390	Cystatin B, putative	GO:0006508 GO:0010951	proteolysis negative regulation of endopeptidase activity	GO:0004866 GO:0004869 GO:0008233	endopeptidase inhibitor activity cysteine-type endopeptidase inhibitor activity peptidase activity
11 Smp_007270.1	Alpha-actinin, putative	-	-	-	-

Table A3 (continued)

S. mansoni adult male worm excretory-secretory proteins			Biological Process GO terms		Molecular Function GO terms	
	ID	Protein description	Term ID	Term name	Term ID	Term name
12	Smp_008070	Thioredoxin, Trx1	GO:0006662 GO:0045454	glycerol ether metabolic process cell redox homeostasis	GO:0009055 GO:0015035 GO:0046872	electron carrier activity protein disulfide oxidoreductase activity metal ion binding
13	Smp_008110	WD40-repeat containing protein	-	-	-	-
14	Smp_008660.1	Gelsolin, putative	-	-	GO:0003779	actin binding
15	Smp_009760	14-3-3 protein, putative	-	-	GO:0019904	protein domain specific binding
16	Smp_009780.2	14-3-3 protein, putative	-	-	GO:0019904	protein domain specific binding
17	Smp_011830	Hypothetical protein / C4Q068	-	-	-	-
18	Smp_014010	Adenylyl cyclase-associated protein, putative	GO:0000902 GO:0007010	cell morphogenesis cytoskeleton organization	GO:0003779 GO:0005488	actin binding binding
19	Smp_017730	200-kDa GPI-anchored surface glycoprotein	-	-	-	-

Table A3 (continued)

S. mansoni adult male worm excretory-secretory proteins			Biological Process GO terms		Molecular Function GO terms	
ID		Protein description	Term ID	Term name	Term ID	Term name
20	Smp_018240.3	Cell division control protein 48 aaa family protein, putative	GO:0051301	cell division	GO:0000166 GO:0005488 GO:0005524 GO:0016787 GO:0017111	nucleotide binding binding ATP binding hydrolase activity nucleoside-triphosphatase activity
21	Smp_018890	Phosphoglycerate kinase	GO:0006096 GO:0016310	glycolysis phosphorylation	GO:0004618 GO:0016301 GO:0016740	phosphoglycerate kinase activity kinase activity transferase activity
22	Smp_019050.2	Hypothetical protein / C4Q286	GO:0007021	tubulin complex assembly	GO:0051082	unfolded protein binding
23	Smp_019640.1	Calcyphosine/tpp, putative	-	-	GO:0005509	calcium ion binding
24	Smp_020920.1	DNAj homolog subfamily B member 4, putative	GO:0006457 -	protein folding -	GO:0031072 GO:0051082	heat shock protein binding unfolded protein binding
25	Smp_021800	Prefoldin subunit 3-related	GO:0006457	protein folding	GO:0051082	unfolded protein binding
26	Smp_022340	Pdz and lim domain protein, putative	-	-	GO:0008270 GO:0046872	zinc ion binding metal ion binding

Table A3 (continued)

S. mansoni adult male worm excretory-secretory proteins			Biological Process GO terms		Molecular Function GO terms	
	ID	Protein description	Term ID	Term name	Term ID	Term name
27	Smp_024110	Phosphopyruvate hydratase	GO:0006096	glycolysis	GO:0000287	magnesium ion binding
					GO:0004634	phosphopyruvate hydratase activity
					GO:0016829	lyase activity
					GO:0046872	metal ion binding
28	Smp_028670.1	Carbonic anhydrase II (carbonate dehydratase II), putative	-	-	-	-
29	Smp_030000	Leucine aminopeptidase (M17 family)	GO:0006508	proteolysis	GO:0004177	aminopeptidase activity
			GO:0019538	protein metabolic process	GO:0008235	metalloexopeptidase activity
					GO:0016787	hydrolase activity
					GO:0030145	manganese ion binding
30	Smp_030370	Calreticulin autoantigen homolog precursor, putative	GO:0006457	protein folding	GO:0005509	calcium ion binding
					GO:0051082	unfolded protein binding
					GO:0005529	sugar binding
					GO:0046872	metal ion binding

Table A3 (continued)

S. mansoni adult male worm excretory-secretory proteins		Biological Process GO terms		Molecular Function GO terms	
ID	Protein description	Term ID	Term name	Term ID	Term name
31 Smp_030730	Tubulin beta chain, putative	GO:0006184	GTP catabolic process	GO:0000166	nucleotide binding
		GO:0007017	microtubule-based process	GO:0003924	GTPase activity
		GO:0007018	microtubule-based movement	GO:0005198	structural molecule activity
		GO:0051258	protein polymerization	GO:0005525	GTP binding
32 Smp_031770.4	Tropomyosin, putative	-	-	-	-
33 Smp_032580.2	Subfamily T1A non-peptidase homologue (T01 family)	GO:0006508	proteolysis	GO:0004175	endopeptidase activity
		GO:0006511	ubiquitin-dependent protein catabolic process	GO:0004298	threonine-type endopeptidase activity
		GO:0051603	proteolysis involved in cellular protein catabolic process	GO:0008233	peptidase activity
				GO:0016787	hydrolase activity
34 Smp_032950	Calmodulin (CaM), putative	-	-	GO:0005509	calcium ion binding
35 Smp_033540	Carbonyl reductase, putative	GO:0008152	metabolic process	GO:0000166	nucleotide binding
		GO:0055114	oxidation-reduction process	GO:0016491	oxidoreductase activity

Table A3 (continued)

S. mansoni adult male worm excretory-secretory proteins			Biological Process GO terms		Molecular Function GO terms	
ID		Protein description	Term ID	Term name	Term ID	Term name
36	Smp_034490	Proteasome catalytic subunit 1 (T01 family)	GO:0006508	proteolysis	GO:0004175	endopeptidase activity
			GO:0051603	proteolysis involved in cellular protein catabolic process	GO:0004298	threonine-type endopeptidase activity
					GO:0008233	peptidase activity
					GO:0016787	hydrolase activity
37	Smp_034840.2	14-3-3 epsilon	-	-	GO:0019904	protein domain specific binding
38	Smp_035270.2	Malate dehydrogenase, putative	GO:0005975	carbohydrate metabolic process	GO:0000166	nucleotide binding
			GO:0006099	tricarboxylic acid cycle	GO:0003824	catalytic activity
			GO:0006108	malate metabolic process	GO:0016491	oxidoreductase activity
			GO:0044262	cellular carbohydrate metabolic process	GO:0016615	malate dehydrogenase activity
			GO:0055114	oxidation-reduction process	GO:0016616	oxidoreductase activity, acting on the CH-OH group of donors, NAD or NADP as acceptor
					GO:0030060	L-malate dehydrogenase activity

Table A3 (continued)

S. mansoni adult male worm excretory-secretory proteins			Biological Process GO terms		Molecular Function GO terms	
	ID	Protein description	Term ID	Term name	Term ID	Term name
39	Smp_038950	L-lactate dehydrogenase, putative	GO:0005975	carbohydrate metabolic process	GO:0000166	nucleotide binding
			GO:0006096	glycolysis	GO:0003824	catalytic activity
			GO:0044262	cellular carbohydrate metabolic process	GO:0004459	L-lactate dehydrogenase activity
			GO:0055114	oxidation-reduction process	GO:0016491	oxidoreductase activity
					GO:0016616	oxidoreductase activity, acting on the CH-OH group of donors, NAD or NADP as acceptor
40	Smp_040130	Cyclophilin	GO:0000413	protein peptidyl-prolyl isomerization	GO:0003755	peptidyl-prolyl cis-trans isomerase activity
			GO:0006457	protein folding	GO:0016853	isomerase activity
					GO:0042277	peptide binding
41	Smp_040790	Cyclophilin B, putative	GO:0000413	protein peptidyl-prolyl isomerization	GO:0003755	peptidyl-prolyl cis-trans isomerase activity
			GO:0006457	protein folding	GO:0016853	isomerase activity
					GO:0042277	peptide binding
42	Smp_042160.2	Fructose 1,6-bisphosphate aldolase, putative	GO:0006096	glycolysis	GO:0003824	catalytic activity
			GO:0008152	metabolic process	GO:0004332	fructose-bisphosphate aldolase activity
					GO:0016829	lyase activity
43	Smp_042400	Hypothetical protein / C4Q8L5	-	-	-	-

Table A3 (continued)

S. mansoni adult male worm excretory-secretory proteins		Biological Process GO terms		Molecular Function GO terms	
ID	Protein description	Term ID	Term name	Term ID	Term name
44 Smp_043030	Hexokinase	GO:0005975	carbohydrate metabolic process	GO:0000166	nucleotide binding
		GO:0006096	glycolysis	GO:0004396	hexokinase activity
		GO:0016310	phosphorylation	GO:0005524	ATP binding
				GO:0016301	kinase activity
				GO:0016740	transferase activity
				GO:0016773	phosphotransferase activity, alcohol group as acceptor
45 Smp_043120	Universal stress protein, putative	GO:0006950	response to stress	-	-
46 Smp_044010.2	Tropomyosin, putative	-	-	GO:0000166	nucleotide binding
				GO:0005524	ATP binding
47 Smp_046600	Actin-1, putative	-	-	GO:0000166	nucleotide binding
				GO:0005524	ATP binding
48 Smp_046690	Ubiquitin (ribosomal protein L40), putative	-	-	-	-

Table A3 (continued)

S. mansoni adult male worm excretory-secretory proteins			Biological Process GO terms		Molecular Function GO terms	
ID		Protein description	Term ID	Term name	Term ID	Term name
49	Smp_047370	Malate dehydrogenase, putative	GO:0005975	carbohydrate metabolic process	GO:0000166	nucleotide binding
			GO:0006099	tricarboxylic acid cycle	GO:0003824	catalytic activity
			GO:0044262	cellular carbohydrate metabolic process	GO:0016491	oxidoreductase activity
			GO:0006108	malate metabolic process	GO:0030060	L-malate dehydrogenase activity
			GO:0055114	oxidation-reduction process	GO:0016616	oxidoreductase activity, acting on the CH-OH group of donors, NAD or NADP as
					GO:0030060	L-malate dehydrogenase activity
50	Smp_047650	Ferritin, putative	GO:0006879	cellular iron ion homeostasis	GO:0004322	ferroxidase activity
			GO:0055114	oxidation-reduction process	GO:0008199	ferric iron binding
					GO:0016491	oxidoreductase activity
					GO:0046872	metal ion binding
					GO:0046914	transition metal ion binding
51	Smp_049250	Heat shock protein, putative	GO:0006950	response to stress	-	-
52	Smp_049270	Heat shock protein, putative	GO:0006950	response to stress	-	-
53	Smp_049550	Heat shock protein 70 (hsp70), putative	GO:0006950	response to stress	GO:0000166	nucleotide binding
					GO:0005524	ATP binding

Table A3 (continued)

S. mansoni adult male worm excretory-secretory proteins			Biological Process GO terms		Molecular Function GO terms	
ID		Protein description	Term ID	Term name	Term ID	Term name
54	Smp_050390	Aldehyde dehydrogenase, putative	GO:0008152 GO:0055114	metabolic process oxidation-reduction process	GO:0016491 GO:0016620	oxidoreductase activity oxidoreductase activity, acting on the aldehyde or oxo group of donors, NAD or NADP as acceptor
55	Smp_053220.1	Aldo-keto reductase, putative	GO:0055114	oxidation-reduction process	GO:0016491	oxidoreductase activity
56	Smp_054160	Glutathione S-transferase 28 kDa (GST 28) (GST class-mu), putative	-	-	GO:0004364 GO:0016740	glutathione transferase activity transferase activity
57	Smp_054240	Translationally-controlled tumor protein homolog (TCTP) (Histamine-releasing factor), putative	-	-	-	-
58	Smp_056440	Superoxide dismutase [mn], putative	GO:0006801 GO:0055114	superoxide metabolic proc oxidation-reduction process	GO:0004784 GO:0016491 GO:0046872	superoxide dismutase activity oxidoreductase activity metal ion binding
59	Smp_056760	Protein disulfide-isomerase, putative	GO:0006662 GO:0045454	glycerol ether metabolic process cell redox homeostasis	GO:0009055 GO:0015035 GO:0016853	electron carrier activity protein disulfide oxidoreductase activity isomerase activity

Table A3 (continued)

S. mansoni adult male worm excretory-secretory proteins		Biological Process GO terms		Molecular Function GO terms	
ID	Protein description	Term ID	Term name	Term ID	Term name
60 Smp_056970.1	Glyceraldehyde-3-phosphate dehydrogenase (phosphorylating)	GO:0006006	glucose metabolic process	GO:0000166	nucleotide binding
		GO:0006096	glycolysis	GO:0004365	glyceraldehyde-3-phosphate dehydrogenase (NAD+) (phosphorylating) activity
		GO:0055114	oxidation-reduction process	GO:0016491	oxidoreductase activity
				GO:0016620	oxidoreductase activity, acting on the aldehyde or oxo group of donors, NAD or NADP as acceptor
				GO:0050661	NADP binding
				GO:0051287	NAD binding
61 Smp_059480	Peroxiredoxin, Prx1	GO:0055114	oxidation-reduction process	GO:0004601	peroxidase activity
				GO:0016209	antioxidant activity
				GO:0016491	oxidoreductase activity
				GO:0051920	peroxiredoxin activity
62 Smp_059660	Hypothetical protein / C4QDG6	-	-	GO:0016787	hydrolase activity

Table A3 (continued)

S. mansoni adult male worm excretory-secretory proteins			Biological Process GO terms		Molecular Function GO terms	
ID		Protein description	Term ID	Term name	Term ID	Term name
63	Smp_059980	Arginase, putative	GO:0006525	arginine metabolic process	GO:0004053	arginase activity
					GO:0016787	hydrolase activity
					GO:0016813	hydrolase activity, acting on carbon-nitrogen (but not peptide) bonds, in linear amidines
					GO:0046872	metal ion binding
64	Smp_063120.1	Inosine triphosphate pyrophosphatase (itpase) (inosine triphosphatase), putative	-	-	GO:0016787	hydrolase activity
65	Smp_063530.1	Apoferritin-2	GO:0006826	iron ion transport	GO:0005488	binding
			GO:0006879	cellular iron ion homeostasis	GO:0008199	ferric iron binding
			GO:0055114	oxidation-reduction process	GO:0016491	oxidoreductase activity
					GO:0046914	transition metal ion binding

Table A3 (continued)

S. mansoni adult male worm excretory-secretory proteins		Biological Process GO terms		Molecular Function GO terms	
ID	Protein description	Term ID	Term name	Term ID	Term name
66 Smp_064380	Aspartate aminotransferase, putative	GO:0006520	cellular amino acid metabolic process	GO:0003824	catalytic activity
		GO:0009058	biosynthetic process	GO:0004069	L-aspartate:2-oxoglutarate aminotransferase activity
				GO:0008483	transaminase activity
				GO:0016740	transferase activity
				GO:0016769	transferase activity, transferring nitrogenous groups
				GO:0030170	pyridoxal phosphate binding
				GO:0080130	L-phenylalanine:2-oxoglutarate aminotransferase activity
67 Smp_064860	Heat shock protein 70 (hsp70)-interacting protein,	GO:0006950	response to stress	GO:0005488	binding
68 Smp_066760.2	Merlin/moesin/ezrin/radixin, putative	-	-	GO:0005488	binding
				GO:0008092	cytoskeletal protein binding
69 Smp_067890	Proteasome subunit alpha 2 (T01 family)	GO:0006508	proteolysis	GO:0004175	endopeptidase activity
		GO:0006511	ubiquitin-dependent protein catabolic process	GO:0004298	threonine-type endopeptidase activity
		GO:0051603	proteolysis involved in cellular protein catabolic process	GO:0008233	peptidase activity
				GO:0016787	hydrolase activity
70 Smp_072900.1	Hsp90 co-chaperone (tebp), putative	-	-	-	-

Table A3 (continued)

S. mansoni adult male worm excretory-secretory proteins			Biological Process GO terms		Molecular Function GO terms	
	ID	Protein description	Term ID	Term name	Term ID	Term name
71	Smp_078690	Calponin homolog, putative	GO:0031032	actomyosin structure organization	GO:0003779	actin binding
72	Smp_079010	Camp-dependent protein kinase type II-alpha regulatory subunit, putative	GO:0001932 GO:0007165 GO:0016310	regulation of protein phosphorylation signal transduction phosphorylation	GO:0008603 GO:0016301	cAMP-dependent protein kinase regulator activity kinase activity
73	Smp_079770.1	Protein disulfide-isomerase ER-60 precursor (ERP60), putative	GO:0006662 GO:0045454	glycerol ether metabolic process cell redox homeostasis	GO:0003756 GO:0009055 GO:0015035 GO:0016853	protein disulfide isomerase activity electron carrier activity protein disulfide oxidoreductase activity isomerase activity
74	Smp_081430	Short chain dehydrogenase, putative	GO:0006662 GO:0045454	glycerol ether metabolic process cell redox homeostasis	GO:0003756 GO:0009055 GO:0015035 GO:0016853	protein disulfide isomerase activity electron carrier activity protein disulfide oxidoreductase activity isomerase activity
75	Smp_082030	Family C56 non-peptidase homologue (C56 family)	-	-	-	-

Table A3 (continued)

S. mansoni adult male worm excretory-secretory proteins			Biological Process GO terms		Molecular Function GO terms	
ID		**Protein description**	**Term ID**	**Term name**	**Term ID**	**Term name**
76	Smp_083870	PwLAP aminopeptidase (M17 family)	GO:0006508 GO:0019538	proteolysis protein metabolic process	GO:0004177 GO:0008235 GO:0030145	aminopeptidase activity metalloexopeptidase activity manganese ion binding
77	Smp_086330.2	Calponin-related	GO:0007517	muscle organ development	-	-
78	Smp_086480	Antigen Sm21.7, putative	GO:0007017	microtubule-based process	GO:0005509	calcium ion binding
79	Smp_086530	Tegumental protein Sm 20.8, putative	GO:0007017	microtubule-based process	GO:0005509	calcium ion binding
80	Smp_090080	Serpin, putative	-	-	GO:0004867	serine-type endopeptidase inhibitor activity
81	Smp_090120.1	Alpha tubulin, putative	GO:0006184 GO:0007017 GO:0007018 GO:0051258	GTP catabolic process microtubule-based process microtubule-based movement protein polymerization	GO:0000166 GO:0003924 GO:0005198 GO:0005525	nucleotide binding GTPase activity structural molecule activity GTP binding
82	Smp_091010	Glyoxalase II (Hydroxyacylglutathione hydrolase), putative	-	-	GO:0004416 GO:0008270 GO:0016787 GO:0046872	hydroxyacylglutathione hydrolase activity zinc ion binding hydrolase activity metal ion binding

Table A3 (continued)

S. mansoni adult male worm excretory-secretory proteins		Biological Process GO terms		Molecular Function GO terms	
ID	Protein description	Term ID	Term name	Term ID	Term name
83 Smp_092280	Proteasome subunit alpha 3 (T01 family)	GO:0006511	ubiquitin-dependent protein catabolic process	GO:0004175	endopeptidase activity
		GO:0051603	proteolysis involved in cellular protein catabolic process	GO:0004298	threonine-type endopeptidase activity
84 Smp_092750	Nucleoside diphosphate kinase	GO:0006165	nucleoside diphosphate phosphorylation	GO:0004550	nucleoside diphosphate kinase activity
		GO:0006183	GTP biosynthetic process	GO:0005524	ATP binding
		GO:0006228	UTP biosynthetic process	GO:0016301	kinase activity
		GO:0006241	CTP biosynthetic process	GO:0016740	transferase activity
		GO:0016310	phosphorylation		
85 Smp_095360.1	Fatty acid binding protein	GO:0006810	transport	GO:0005215	transporter activity
				GO:0005488	binding
				GO:0008289	lipid binding
86 Smp_096760	Phosphoglycerate mutase	GO:0006096	glycolysis	GO:0004619	phosphoglycerate mutase activity
				GO:0016853	isomerase activity
				GO:0016868	intramolecular transferase activity, phosphotransferases
87 Smp_102070	GST class-mu, SM26/2 antigen, glutathione S-transferase 26 kDa	-	-	GO:0004364	glutathione transferase activity
				GO:0016740	transferase activity

Table A3 (continued)

S. mansoni adult male worm excretory-secretory proteins			Biological Process GO terms		Molecular Function GO terms	
	ID	Protein description	Term ID	Term name	Term ID	Term name
88	Smp_103320	Nuclear movement protein nudc, putative	-	-	-	-
89	Smp_105020	Titin, putative	-	-	-	-
90	Smp_106930.2	Heat shock protein 70, putative	GO:0006950	response to stress	GO:0000166 GO:0005524	nucleotide binding ATP binding
91	Smp_123440.1	Fad oxidoreductase, putative	GO:0055114	oxidation-reduction process	GO:0016491	oxidoreductase activity
92	Smp_130110	Proteasome subunit alpha 6 (T01 family)	GO:0006511 GO:0007205 GO:0051603	ubiquitin-dependent protein catabolic process activation of protein kinase C activity by G-protein coupled receptor protein signaling pathway proteolysis involved in cellular protein catabolic process	GO:0004143 GO:0004175 GO:0004298	diacylglycerol kinase activity endopeptidase activity threonine-type endopeptidase activity
93	Smp_132670.1	Myosin regulatory light chain, putative	-	-	GO:0005509	calcium ion binding
94	Smp_135950	Lethal giant larvae homolog 2, cell polarity protein , inorganic pyrophosphatase, putative	GO:0006796	phosphate-containing compound metabolic process	GO:0000287 GO:0004427	magnesium ion binding inorganic diphosphatase activity
95	Smp_136240.6	Vesicle-associated membrane protein (vamp), putative	-	-	GO:0005198	structural molecule activity
96	Smp_140900.2	Hypothetical protein / C4Q6S1	-	-	-	-

Table A3 (continued)

S. mansoni adult male worm excretory-secretory proteins			Biological Process GO terms		Molecular Function GO terms	
	ID	Protein description	Term ID	Term name	Term ID	Term name
97	Smp_143470.2	Spectrin beta chain, brain 3 (Spectrin, non- erythroid beta chain 3) (Beta-IV spectrin), putative	-	-	GO:0003779	actin binding
98	Smp_146950	Hypothetical protein / C4Q9Q0	-	-	GO:0005488	binding
99	Smp_147470	Leucine-rich transmembrane proteins, putative	-	-	-	-
100	Smp_150820	Acyl-CoA thioesterase-related	GO:0006637	acyl-CoA metabolic process	GO:0016291	acyl-CoA thioesterase activity
101	Smp_151690	Translation initiation inhibitor, putative	-	-	-	-
102	Smp_152710.2	Glutathione-s-transferase omega, putative	-	-	GO:0016740	transferase activity
103	Smp_155060.2	Set, putative	GO:0006334	nucleosome assembly		
104	Smp_157500	Calpain (C02 family)	GO:0006508	proteolysis	GO:0004197 GO:0004198 GO:0005509 GO:0008233 GO:0008234 GO:0016787	cysteine-type endopeptidase activity calcium-dependent cysteine-type endopeptidase activity calcium ion binding peptidase activity cysteine-type peptidase activity hydrolase activity

Table A3 (continued)

S. mansoni adult male worm excretory-secretory proteins			Biological Process GO terms		Molecular Function GO terms	
	ID	Protein description	Term ID	Term name	Term ID	Term name
105	Smp_158110.2	Peroxiredoxin, Prx2	GO:0055114	oxidation-reduction process	GO:0004601	peroxidase activity
					GO:0016209	antioxidant activity
					GO:0016491	oxidoreductase activity
					GO:0051920	peroxiredoxin activity
106	Smp_161920	Actin, putative	-	-	GO:0000166	nucleotide binding
					GO:0005524	ATP binding
107	Smp_163720	Endophilin B1, putative	-	-	-	-
108	Smp_176200.2	Superoxide dismutase [Cu-Zn]	GO:0006801	superoxide metabolic process	GO:0004784	superoxide dismutase activity
			GO:0055114	oxidation-reduction process	GO:0016209	antioxidant activity
					GO:0016491	oxidoreductase activity
					GO:0046872	metal ion binding
109	Smp_179810	Troponin t, invertebrate, putative	-	-	-	-
110	Smp_187370	Phosphoglycerate kinase	GO:0006096	glycolysis	GO:0004618	phosphoglycerate kinase activity
			GO:0016310	phosphorylation	GO:0016301	kinase activity
					GO:0016740	transferase activity

Table A3 (continued)

S. mansoni adult male worm excretory-secretory proteins		Biological Process GO terms		Molecular Function GO terms	
ID	Protein description	Term ID	Term name	Term ID	Term name
111 Smp_194770	ATP:guanidino kinase (Smc74), putative	GO:0016310	phosphorylation	GO:0000166	nucleotide binding
		GO:0055114	oxidation-reduction process	GO:0003824	catalytic activity
				GO:0005524	ATP binding
				GO:0016301	kinase activity
				GO:0016491	oxidoreductase activity
				GO:0016740	transferase activity
				GO:0016772	transferase activity, transferring phosphorus-containing groups
				GO:0046872	metal ion binding
				GO:0050324	taurocyamine kinase activity

Table A3 (continued)

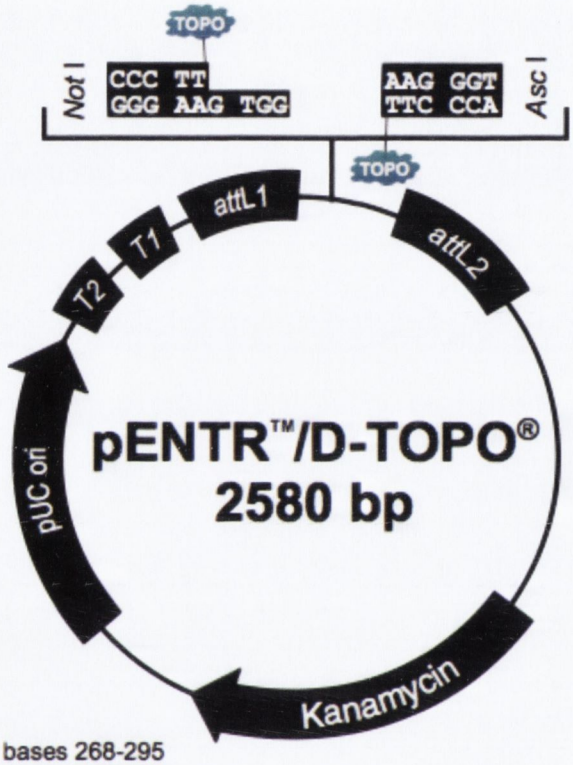

Comments for pENTR™/D-TOPO®
2580 nucleotides

*rrn*B T2 transcription termination sequence: bases 268-295
*rrn*B T1 transcription termination sequence: bases 427-470
M13 forward (-20) priming site: bases 537-552
*attL*1: bases 569-668 (c)
TOPO® recognition site 1: bases 680-684
Overhang: bases 685-688
TOPO® recognition site 2: bases 689-693
*attL*2: bases 705-804
T7 Promoter/priming site: bases 821-840 (c)
M13 reverse priming site: bases 845-861
Kanamycin resistance gene: bases 974-1783
pUC origin: bases 1904-2577

(c) = complementary sequence

Figure A4.1 - **pENTR™/D-TOPO® vector map** (Source: Invitrogen life technologies. Retrieved September 30, 2011 from www.invitrogen.com).

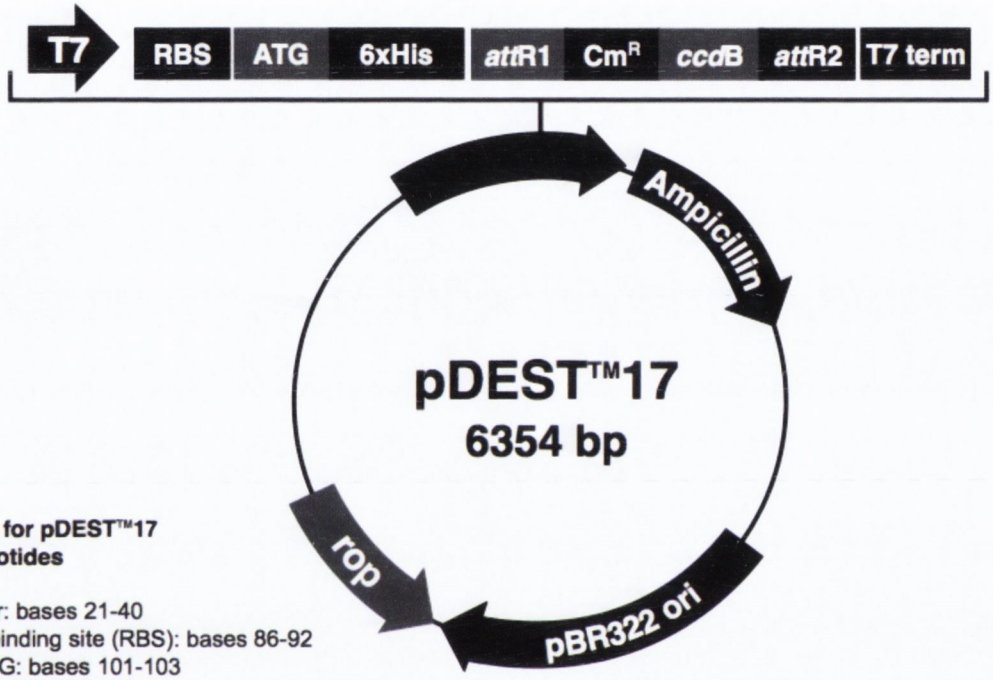

Comments for pDEST™17
6354 nucleotides

T7 promoter: bases 21-40
Ribosome binding site (RBS): bases 86-92
Initiation ATG: bases 101-103
6xHis tag: bases 113-130
*att*R1: bases 140-264
Chloramphenicol resistance gene (Cm^R): bases 373-1032
*ccd*B gene: bases 1374-1679
*att*R2: bases 1720-1844
T7 transcription termination region: bases 1855-1983
bla promoter: bases 2471-2569
Ampicillin (*bla*) resistance gene: bases 2570-3430
pBR322 origin: bases 3575-4248
ROP ORF: bases 4619-4810 (C)
C=complementary strand

Figure A4.2 - **pDEST™17 vector map** (Source: Invitrogen life technologies. Retrieved September 30, 2011 from www.invitrogen.com).

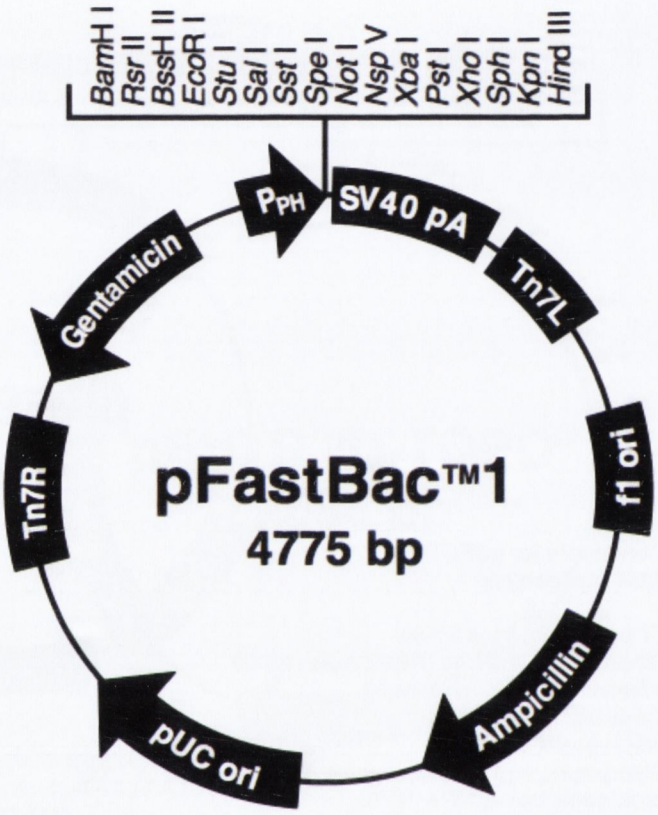

Comments for pFastBac™1
4775 nucleotides

f1 origin: bases 2-457
Ampicillin resistance gene: bases 589-1449
pUC origin: bases 1594-2267
Tn7R: bases 2511-2735
Gentamicin resistance gene: bases 2802-3335 (complementary strand)
Polyhedrin promoter (P_{PH}): bases 3904-4032
Multiple cloning site: bases 4037-4142
SV40 polyadenylation signal: bases 4160-4400
Tn7L: bases 4429-4594

Figure A4.3 - **pFastBac^{TM}1 vector map** (Source: Invitrogen life technologies. Retrieved September 30, 2011 from www.invitrogen.com).

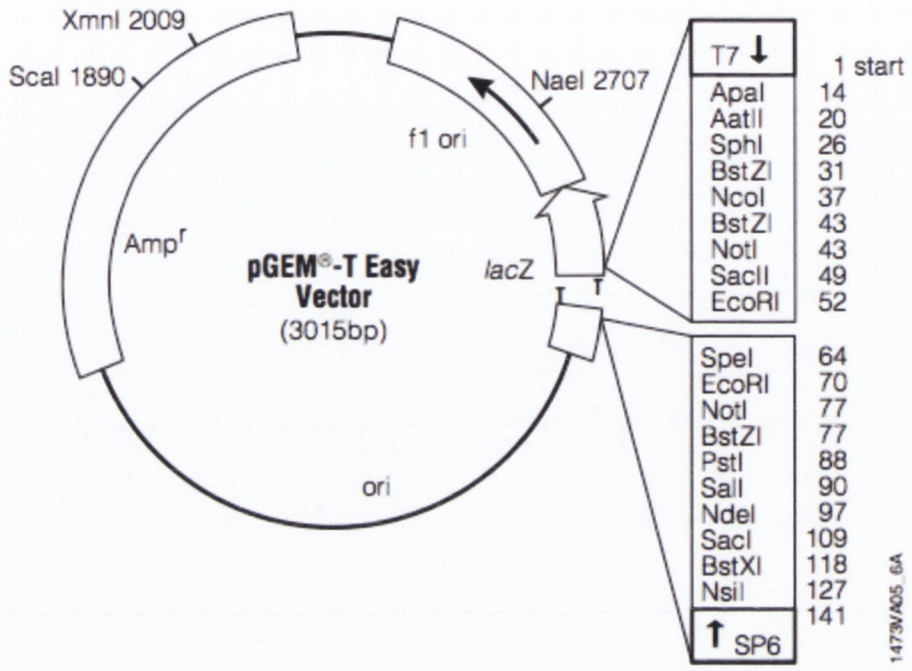

pGEM®-T Easy Vector sequence reference points:

T7 RNA polymerase transcription initiation site	1
multiple cloning region	10–128
SP6 RNA polymerase promoter (–17 to +3)	139–158
SP6 RNA polymerase transcription initiation site	141
pUC/M13 Reverse Sequencing Primer binding site	176–197
lacZ start codon	180
lac operator	200–216
β-lactamase coding region	1337–2197
phage f1 region	2380–2835
lac operon sequences	2836–2996, 166–395
pUC/M13 Forward Sequencing Primer binding site	2949–2972
T7 RNA polymerase promoter (–17 to +3)	2999–3

Figure A4.4 - **pGEM-T-easy vector map** (Source: Promega. Retrieved September 30, 2011 http://www.promega.com/).

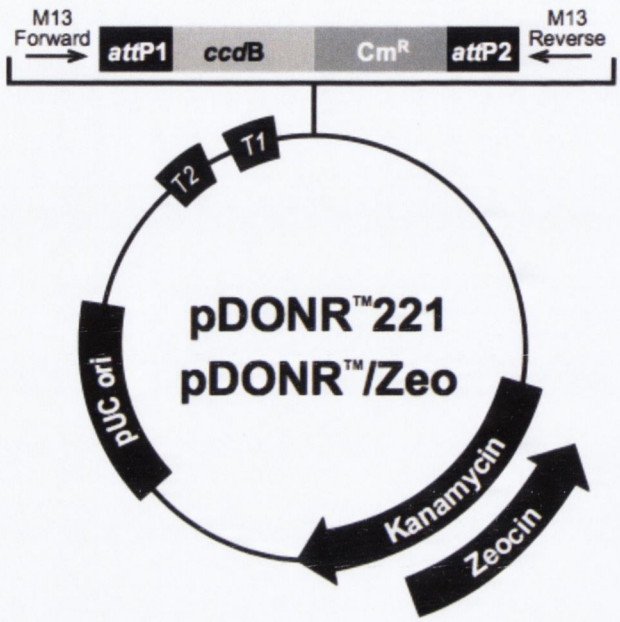

Comments for:	pDONR™221 4761 nucleotides	pDONR™/Zeo 4291 nucleotides
*rrn*B T2 transcription termination sequence (c):	268-295	268-295
rrnB T1 transcription termination sequence (c):	427-470	427-470
M13 Forward (-20) priming site:	537-552	537-552
*attP*1:	570-801	570-801
*ccd*B gene (c):	1197-1502	1197-1502
Chloramphenicol resistance gene (c):	1825-2505	1847-2506
*attP*2 (c):	2753-2984	2754-2985
M13 Reverse priming site:	3026-3042	3027-3043
Kanamycin resistance gene:	3155-3964	---
EM7 promoter (c):	---	3486-3552
Zeocin resistance gene (c):	---	3111-3485
pUC origin:	4085-4758	3615-4288

(c) = complementary strand

Figure A4.5 - **pDONR™221 vector map** (Source: Invitrogen life technologies. Retrieved September 30, 2011 from www.invitrogen.com).

Appendix 5 - M13/pUC forward and reverse primers binding sites into the bacmid

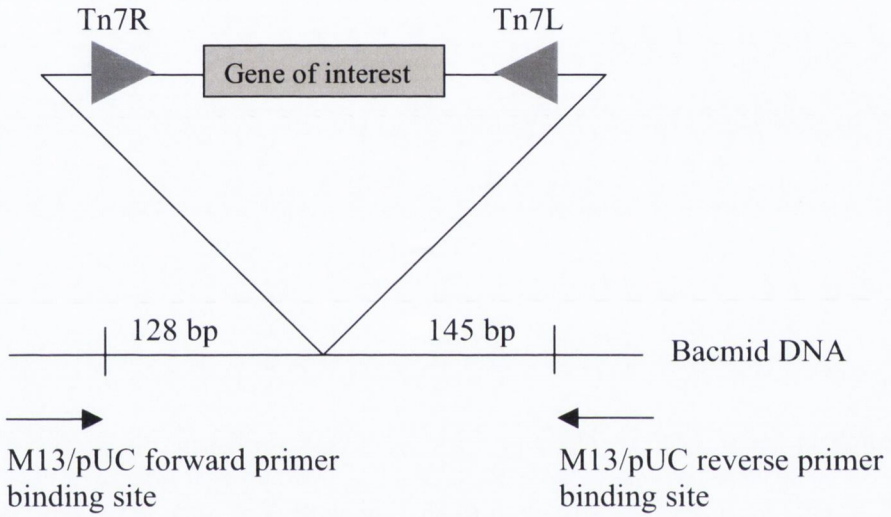

Figure A5: **M13/pUC forward and reverse primers binding sits into the bacmid**. Transposition of inserts into the bacmid is verified by PCR using the M13/pUC forward and reverse primers that bind to flanking regions of the recombination site in the bacmid The size of the amplified product generated by these primers is 2,300 bp plus the size of the insert or gene of interest. If transposition does not occur, PCR with M13/pUC primers generates a DNA band of 273 bp. Tn7R and Tn7L – recombination sites

Appendix 6 - Strategy designed for purification of *S. mansoni* Cyclophilin

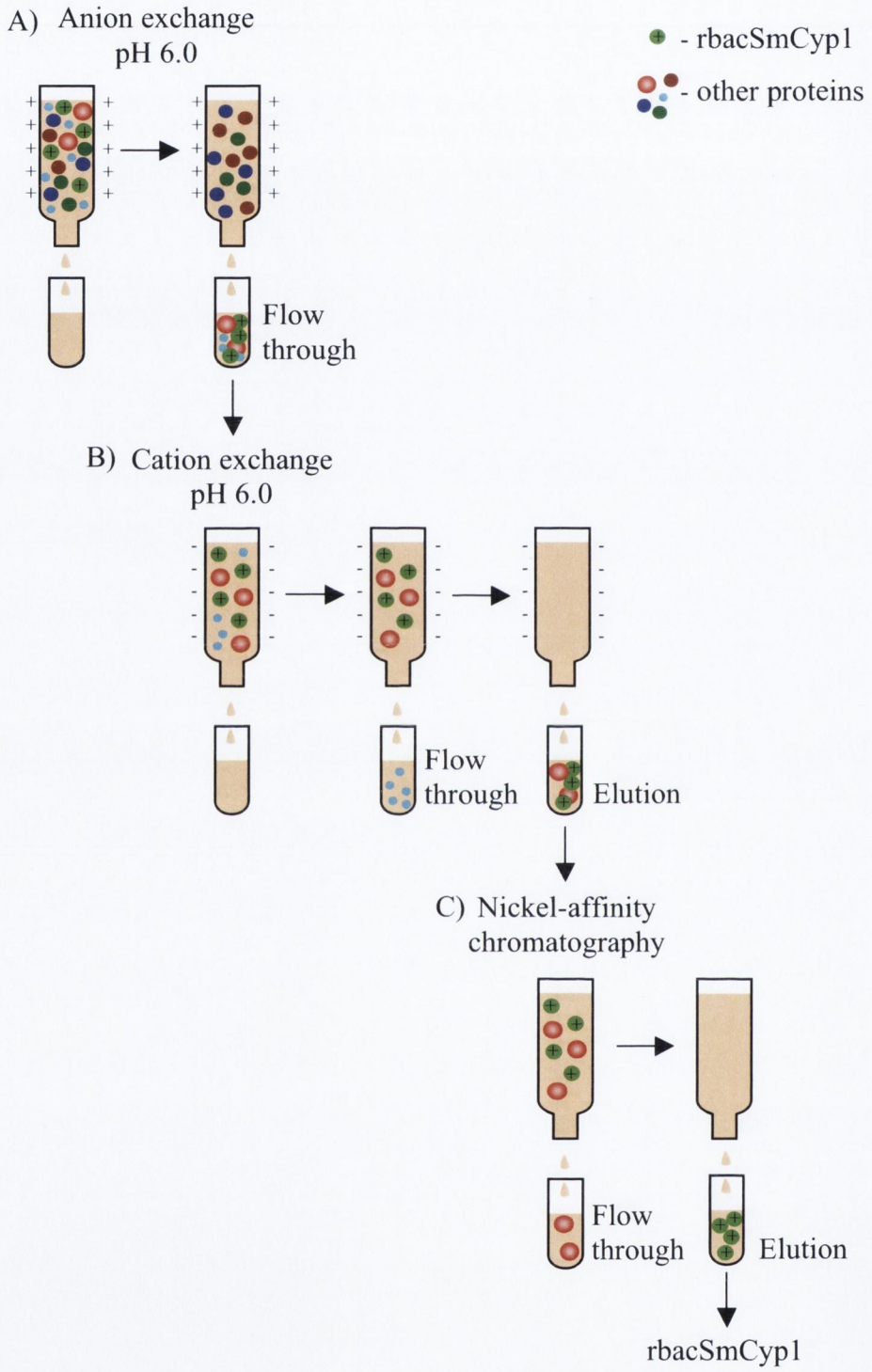

Figure A7: **Strategy designed for purification of *S. mansoni* Cyclophilin (rbacSmCyp1)**. rbacSmCyp1 would be purified in three steps: anion exchange (A), cation exchange (B) and nickel-affinity chromatography (C).